

Thesis on

**“NMR based Metabolomics of Synovial Fluid
from patient with Reactive Arthritis (ReA) for
Identifying abnormal metabolic status”**

**Submitted for the Degree of
Doctor of Philosophy
*in Biotechnology***

By

Durgesh Dubey

**BABASAHEB
BHIMRAO
AMBEDKAR
UNIVERSITY**



**• LUCKNOW •
प्रज्ञा शील करुणा
ESTABLISHED 1996**

Co- Supervisor

**Dr. Dinesh Kumar
Assistant Professor
Centre of Biomedical
Research,
SGPGIMS Campus,
*Lucknow, (U.P.) India***

Supervisor

**Prof. Dinesh Raj Modi
Head,
Department of Biotechnology,
Dean, School of Life Sciences
B.B.A. University,
*Lucknow, (U.P.) India***

Submitted to

**School for Biosciences and Biotechnology
Department of Biotechnology
Babasaheb Bhimrao Ambedkar University
Lucknow-226025, UP, INDIA
2019**

Dedicated to,

My mom,

***Prabhawati Devi, Sister Kalpana Pandey and
Sapana Pandey, and everyone who stood by me
through all walks of my life***



बाबासाहेब भीमराव अम्बेडकरविश्वविद्यालय

(केन्द्रीय विश्वविद्यालय)

विद्या विहार, रायबरेली रोड, लखनऊ-226025

BABASAHEB BHIMRAO AMBEDKAR UNIVERSITY

(A Central University)

Vidya Vihar, Rae Bareli Road, Lucknow-226025

CERTIFICATE

This is to certify that the thesis titled “NMR based Metabolomics of Synovial Fluid from patient with Reactive Arthritis (ReA) for Identifying abnormal metabolic status” submitted by **Durgesh Dubey** is an original research work and has not been previously submitted in part or full for the award of any other degree or diploma to this or other university.

The thesis submitted to Babasaheb Bhimrao Ambedkar University, Lucknow satisfies all the requirements stipulated in the Doctor of Philosophy (Ph.D.) regulations – 1999 as amended in 2008/2010/2013 and it is fit for submission and evaluation for the award of the degree of Doctor of Philosophy of the University.

Date:

Co-supervisor

Dr. Dinesh Kumar

Assistant Professor

Centre of Biomedical Research,

SGPGIMS Campus,

Lucknow, (U.P.) India

Supervisor

Prof. Dinesh Raj Modi

Head

Department of Biotechnology,

B.B.A. University,

Lucknow, (U.P.) India

Head of Department

प्रो० डी० आर० मोदी/Prof. D.R. Modi
विभागाध्यक्ष/Head

के० प्रौद्योगिकी विभाग/Biotechnology Department
बाबासाहेब भीमराव अम्बेडकर विश्वविद्यालय
Babasaheb Bhimrao Ambedkar University
लखनऊ/Lucknow-226025

CANDIDATE'S DECLARATION

I hereby declare that thesis entitled “**NMR based Metabolomics of Synovial Fluid from patient with Reactive Arthritis (ReA) for Identifying abnormal metabolic status**” is an authentic research work carried out by me under the supervision of **Prof. Dinesh Raj Modi**, Professor, Department of Biotechnology, Babasaheb Bhimrao Ambedkar University, Lucknow and the Co-Supervision of **Dr. Dinesh Kumar**, Assistant Professor, Centre of Biomedical Research, Lucknow. The research work is original, and no part of this work has been submitted for any other degree or diploma.

All the above given information is true to the best of my knowledge.

Date:

Submitted by

Durgesh Dubey

Durgesh Dubey

Enrolment No. : 1081/07

Department of Biotechnology,
Babasaheb Bhimrao Ambedkar University,
Lucknow, U.P., India



बाबासाहेब भीमराव अम्बेडकर विश्वविद्यालय
(केन्द्रीय विश्वविद्यालय)

विद्या विहार, रायबरेली रोड, लखनऊ-226025

BABASAHEB BHIMRAO AMBEDKAR UNIVERSITY

(A Central University)

Vidya Vihar, Raebareli Road, Lucknow-226025

Letter No.-.....**76**...../COE/BBAU/2015

Dated: **14/05/15**

Ph.D. Course Work Certificate

This is to certify that **Mr. Durgesh Dubey**, Enrollment No. 1081/07 Ph.D. Research Scholar, Department of Biotechnology of this University has successfully completed his Ph.D. Course work in the examination held during May, 2014.

(A.K. Maurya)

Deputy Registrar (Exam.)

Table of Contents

Content	Page No.
Abstract	i
List of Publications	ii
Acknowledgement	iv
List of Abbreviations	v
List of Figures	vii
Chapter 1: Introduction	1
Chapter 2: Review of Literature: Reactive Arthritis and NMR based Metabolomics	6
Chapter 3: Metabolite assignment of Ultra-Filtered Synovial Fluid extracted from knee joints of Reactive Arthritis patients using High Resolution NMR Spectroscopy	56
Chapter 4: NMR based serum metabolomics revealed distinctive metabolic patterns in Reactive Arthritis compared to Rheumatoid Arthritis	87
Chapter 5: Conclusion and Future Prospects	127
Appendix	130

Abstract

Reactive arthritis (ReA) is a sterile joint inflammation triggered by bacterial infection which influences the function of the whole body as well as local tissues in the joints. Currently, there are no reliable biomarkers available that can aid early differential diagnosis of ReA from other inflammatory joint diseases which makes continue to confound the clinical diagnosis and represent a clinical dilemma making treatment choices with a more personalized or generalized approach. Addressing these challenges through the approach of ‘personalised healthcare’ is of increasing interest to researchers. This has been facilitated by recent advances in metabonomic techniques. This approach involves the investigation of metabolic consequences of downstream of the disease process, including the complex interaction between host and environment. Significant consequences of inflammation are changes in metabolism. Hence, we hypothesised that inflammation alters metabolism and that the metabolic profile of an individual patient with early inflammatory arthritis predicts the subsequent course of disease. Furthermore, we suggested that differentially expressed serum metabolites would identify biomarkers in response to inflammation that constituting a unique metabolic signature of two different types of inflammatory arthritis and provide novel insights into disease mechanisms.

The main objective of the research presented in this thesis was to evaluate the use of Nuclear Magnetic Resonance (NMR) spectroscopy together with multivariate analysis based metabolomics for identifying and characterizing potential biomarkers of health-disease continuum. We derived serum and Synovial fluid metabolic profiles of ReA patients using ^1H NMR spectroscopy and subjected these to multi-parameter analyses to identify metabolic differences associated with inflammation.

This thesis has two aims:

1. To explore the abnormal human metabolic pathways affected in Reactive Arthritis (ReA) through metabolic profiling of biological samples affected in this diseased condition (i.e. serum and synovial fluid).
2. To identify and validate molecular biomarkers to aid differential diagnosis of Reactive Arthritis (ReA) conditions.

List of Publication's

1. [Dubey D](#), Kumar S, Chaurasia S, Guleria A, Ahmed S, Singh R, Kumari R, Modi DR, Misra R, Kumar D, “**NMR-Based Serum Metabolomics Revealed Distinctive Metabolic Patterns in Reactive Arthritis Compared with Rheumatoid Arthritis**”. J Proteome Res. 2018 Oct 30. doi: 10.1021/acs.jproteome.8b00439. **PMID: 30376345**
2. [Dubey D](#), Chaurasia S, Guleria A, Kumar S, Modi DR, Misra R, Kumar D, “**Metabolite assignment of ultrafiltered synovial fluid extracted from knee joints of reactive arthritis patients using high resolution NMR spectroscopy**”. Magn Reson Chem. 2018 Jun doi: 10.1002/mrc.4763. **PMID: 29907975**

Publications not included in the present thesis

1. [Dubey D](#), Arora N, Sharma M, Patel A, Guleria A, Pruthi PA, Kumar D, Pruthi V, Poluri KM, “**NMR-Based Metabolomic Approach To Elucidate the Differential Cellular Responses during Mitigation of Arsenic (III, V) in a Green Microalga**”. ACS omega. 2018 Sep 25;3(9):11847-56. **PMID: 30320279**
2. Ahmed S, [Dubey D](#), Chowdhury A, Chaurasia S, Guleria A, Kumar S, Singh R, Kumar D, Misra R “**Nuclear magnetic resonance-based metabolomics reveals similar metabolomics profiles in undifferentiated peripheral spondyloarthritis and reactive arthritis**”. Int J Rheum Dis. 2019 Feb 27. doi: 10.1111/1756-185X.13490. **PMID: 30810278**
3. Rawat A, [Dubey D](#), Guleria A, Kumar U, Keshari AK, Chaturvedi S, Prakash A, Saha S, Kumar D, “**¹H NMR-based serum metabolomics reveals erythromycin-induced liver toxicity in albino Wistar rats**”. Journal of pharmacy & bioallied sciences. 2016 Oct;8(4):327. **PMID: 28216958**
4. Guleria A, Pratap A, [Dubey D](#), Rawat A, Chaurasia S, Sukesh E, Phatak S, Ajmani S, Kumar U, Khetrpal CL, Bacon P, Misra R, Kumar D, “**NMR based serum metabolomics reveals a distinctive signature in patients with Lupus Nephritis**”. Sci Rep. 2016 Oct 14;6:35309. doi: 10.1038/srep35309. **PMID: 27739464**
5. Guleria A, Phatak S, [Dubey D](#), Kumar S, Zanzwar A, Chaurasia S, Kumar U, Gupta R, Aggarwal A, Kumar D, Misra R, “**NMR based serum metabolomics reveals reprogramming of lipid dysregulation following Cyclophosphamide based induction**”

- therapy in lupus nephritis**". J Proteome Res. 2018 Jul 6;17(7):2440-2448. doi: 10.1021/acs.jproteome.8b00192. Epub 2018 Jun 18. **PMID: 29877087**
6. Rawat A, Srivastava R K, [Dubey D](#), Guleria A, Singh S, Prakash A, Modi D R, Khetrapal C. L. , Tiwari S and Dinesh Kumar, **"Serum Metabolic Disturbances Hailing in Initial hours of Acute Myocardial Infarction elucidated by NMR based Metabolomics"**. Curr Metabolomics. 2016; 4(2). doi: 10.2174/2213235X04666160809123143.
 7. Guleria A, Misra DP, Rawat A, [Dubey D](#), Khetrapal CL, Bacon P, Misra R, Kumar D, **"NMR-Based Serum Metabolomics Discriminates Takayasu Arteritis from Healthy Individuals: A Proof-of-Principle Study"**. J Proteome Res. 2015 Aug 7;14(8):3372-81. doi: 10.1021/acs.jproteome.5b00422. **PMID: 26081138**
 8. Rawat A, Misra G, Saxena M, Tripathi S, [Dubey D](#), Saxena S, Aggarwal A, Gupta V, Khan MY, Prakash A, **"¹H NMR based serum metabolic profiling reveals differentiating biomarkers in patients with diabetes and diabetes-related complication"**. Diabetes & Metabolic Syndrome: Clinical Research & Reviews. 2019 Jan 1;13(1):290-8. **PMID: 30641714**
 9. Rawat A, Chaturvedi S, Singh AK, Guleria A, [Dubey D](#), Keshari AK, Raj V, Rai A, Prakash A, Kumar U, Kumar D, **"Metabolomics approach discriminates toxicity index of pyrazinamide and its metabolic products, pyrazinoic acid and 5-hydroxy pyrazinoic acid"**. Human & experimental toxicology. 2018 Apr;37(4):373-89. **PMID: 28425350**
 10. Kumar D, Pandey G, Bansal D, Rawat A, Kumar U, [Dubey D](#), Guleria A, Saraswat VA, **"NMR based urinary profiling of lactulose/mannitol ratio used to assess the altered intestinal permeability in acute on chronic liver failure (ACLF) patients"**. Magnetic Resonance in Chemistry. 2017 Apr;55(4):289-96. **PMID: 27623987**

Book Chapter

1. Dinesh Kumar, Atul Rawat, [Durgesh Dubey](#), Umesh Kumar, Amit K Keshari, Sudipta Saha and Anupam Guleria, **"NMR Based Metabolomics: An Emerging Tool for Therapeutic Evaluation of Traditional Herbal Medicines"**. SM-eBOOK: Nuclear Magnetic Resonance Spectroscopy (2016), June, 1-18.

Acknowledgment

First and foremost, I would like to thank all my teachers from all walks of my life, for making the individual who I am today. I would like to express my sincere gratitude to my supervisor **Professor Dinesh Raj Modi** and co-supervisor **Dr. Dinesh Kumar** and for considering me as their Ph.D. student, and for their constant belief in me, giving the privilege and pleasure of working with the very best, they continue to be a steady source of inspiration. During this course of time, I have had the pleasure to meet numerous exceptional people and most importantly learn much about science, myself and life in science.

Coming from a biotechnology background, understanding NMR was more than a task. I will always be thankful to my supervisor Dr. Dinesh who has always been very patient in teaching me the various fundamentals of NMR repeatedly. His supervision of the NMR data acquisition and provision of scripts for data analysis were of paramount importance for the success of this work in my hand.

I am also grateful to **Professor Ram Nath Misra**, HOD of Department of clinical Immunology, SGPGIMS for providing clinical samples and for his helpful comments and advice. I would like to thank all the members of the Rheumatology Research Group for all their constant support.

The work presented in this thesis was possible due to NMR facility present at the Center of Biomedical Research (CBMR) and the animal facility at the Babasaheb Bhimrao Ambedkar University (BBAU). I would like to thank **Professor C.L. Khetrpal** and **Professor Ganesh Pandey**, director CBMR for providing the excellent research facilities, and access to NMR round the clock.

Thanks' to all my co-authors and colleagues at CBMR and BBAU for creating such a brilliant environment and helping me get through the difficult times, entertainments and the caring they provided. Sincere thanks for their willingness to give feedbacks on my writing for their contributions and critical discussions, your enthusiasm, inspiration, support and valuable advice are sincerely appreciated.

I would like to thank all the patients who consented to take part in all my studies without them this work would have been just on paper without the facts, figures, and results described as such in my thesis.

I am grateful to ICMR, New Delhi for providing me the financial assistance during this study.

Sincerely,

Durgesh Dubey

List of Abbreviations

RD	Rheumatic Diseases
SSA	Seronegative spondyloarthropathy
ReA	Reactive Arthritis
uSpA	Peripheral undifferentiated spondyloarthropathy
RA	Rheumatoid arthritis
ROC	Receiver operating characteristic curve
AUROC	Area under ROC curve
HLA	Human leukocyte antigen
MHC	Major-histocompatibility-complex
CRP	C-reactive protein
ESR	Erythrocyte sedimentation rate
NC	Normal control
YNC/ENC	Young/elder normal control
IL	Interleukin
Th	T helper cell
NMR	Nuclear Magnetic Resonance
CPMG	Carr–Purcell–Meiboom–Gill
HSQC	Heteronuclear single quantum correlation spectroscopy
TOCSY	Total Correlation Spectroscopy
JRES	J-resolved NMR spectroscopy
FT	Fourier Transformation
FID	Free induction decay
MWCO	Molecular weight cut-off
PCA	Principal component analysis
PLS-DA	partial least-squares discriminant analysis
VIP	Variable importance on projection
CV	Cross validation
CI	Confidence interval
ANOVA	analysis of variance
DMARD	Disease-modifying anti-rheumatic drug

NSAIDs	Nonsteroidal anti-inflammatory drugs
SF	Synovial Fluid
HMDB	Human Metabolome Database
BMRB	Biological Magnetic Resonance Data Bank
<i>α</i>	Alpha
<i>β</i>	Beta
<i>γ</i>	Gamma
<i>δ</i>	Delta

List of Figures

Chapter	Figure No.	Figure Caption	Page No.
2	1.1	Molecular structure of HLA-B27, $\alpha 1$, $\alpha 2$, and $\alpha 3$ domain of B27 are shown in ribbon format in blue, and $\beta 2$ in green.	11
	1.2	Outline for the ReA pathogenesis. (1) The intestinal epithelium is attached and invaded with pathogenic bacteria. HLA-B27 of antigen presenting cell (APC) such as macrophages may be involved in bacterial persistence; (2) APC could present arthritogenic peptides by HLA-B27 to CD8+ T cells, or HLA-B27 itself could be recognized by killer immunoglobulin receptor (KIR)3DL2 on CD4+ T cells in mesenteric lymph node (MLN); moreover, HLA-B27 misfolding causes an unfolded protein response (UPR); (3-4) APC with bacterial antigens or with non-active bacteria and T cells circulate within peripheral blood and eventually reach the knee joint; (5), Gut-derived APC and T-cells induce an immune response with IFN- γ and IL-17 production, recruitment of other cells and induction of mesenchymal cells activation in the target joint, which enhance and sustain inflammation.	17
	1.3	Outline for a number of possible recognitions related to HLA B-27 molecules in the pathogenesis of ReA. Recreated from Reveille et al. (a) HLA-B27/b2m and peptide complex recognised by CD8+ Tcells. (b) HLA-B27/b2m and peptide complex recognised by CD4+ T cells. (c) Free HLA-B27 heavy chain alone reacting with CD4+ T cells, (d) HLA class II (DR, DQ, DP) presenting HLA-B27 restricted peptide to CD4+ T cells, (e) HLA-B27 homodimers reacting with CD4+ T cells, (f) HLA-B27 homodimers recognised by receptors on NK cells	20

	1.4	Basic principles of magnetic resonance. The figure illustrates the different spin states, energy differences and the field (B ₀) frequency relationships. Figure recreated from Shung et al	33
	1.5	Proton magnetic resonance spectra from ReA patients: Assignments of various metabolites visible in the NMR spectra are shown. The red spectrum is from Serum and the green from Synovial fluid.	35
3	2.1	(a) Generalized protocol for processing the synovial fluid (SF) samples and preparing the samples for NMR measurements (b) The typical 800 MHz 1D ¹ H CPMG NMR spectra of normal SF (in black) and ultra-filtered SF (in red) highlighting the absence of signals due to lipids and proteins in ultra-filtered SF which were present in normal SF. The peaks annotated with ‘*’ represent the resonances of metabolites which were not clearly evident or suppressed either due to the overlapping signals from high MW metabolites in the NMR spectra of intact SF or due to weak interactions between these metabolites and higher molecular weight proteins/lipoproteins present in SF.	60
	2.2A	The spectral regions showing an overlay of 1D ¹ H CPMG NMR spectra of normal SF samples recorded before and after spiking with authentic compounds. The spectral regions shown here from (a-u) represent NMR spectral spiking, respectively, with acetone, alanine, arginine, betaine, choline, citric acid, creatine, creatinine, ethanol, glutamine, glutamate, glycine, glycolate, histidine, isobutyric acid, isoleucine, leucine, methionine, phenylalanine, proline and valine.	64,65
	2.2B	An overlay of the 1D ¹ H CPMG NMR spectra of filtered SF samples recorded before and after spiking with authentic compounds (A) Citrulline, (B) Glutamate, (C) Methionine, (D) O-acetyl-L-carnitine, (E) Serine and (F) Cysteine.	66
	2.3	The stacked 1D ¹ H NMR spectra recorded on a filtered SF sample using different pulse programs as indicated: (a)	68

		zgesgp, (b) cpmgpr1d (with T ₂ filter time ~ 63.6 ms), (c) noesygprr1d (with mixing time ~10 ms) and (d) diffusion edited. All the spectra are baseline corrected using topspin “abs” command for automated baseline correction. As evident visually, the cpmgpr1d confers smooth zero baseline compared to zgesgp and noesygprr1d. No signal was evident in the diffusion edited 1D ¹ H suggesting that the ultrafiltration has removed majority of higher molecular weight metabolites including lipoproteins and protein.	
	2.4	An overlay of 1D ¹ H NMR spectra of SF samples of ReA patients recorded on Bruker 800 MHz NMR spectrometer using (a) CPMG (cpmgpr1d) and (b) NOESY (noesygprr1d) pulse programs. (c-d) represent the results of discriminatory analysis based on PLS-DA performed here to probe the spectral differences associated with CPMG and NOESY spectra. (c) The 2D score plot showing sample clustering and group separation between CPMG and NOESY spectra. (d) The model validation and performance tests (e) The VIP statistics highlighting the potential metabolic entities responsible for separation between CPMG and NOESY spectral groups.	69
	2.5	The stacked 1D ¹ H CPMG NMR spectra recorded on a filtered SF sample with different T ₂ filter time as indicated. No significant improvement is seen for CPMG spectra recorded with higher T ₂ filter time compared to that recorded with T ₂ filter time equal to 21.2 ms suggesting that the sample is completely devoid of higher MW metabolites.	70
	2.6	A typical 800 MHz (Cryoprobe) 1D CPMG ¹ H NMR spectrum of a pooled synovial fluid obtained from ReA patient after ultrafiltration using a 3 kDa filter with expanded regions from δ(0.8-1.5) ppm (a), δ(1.58-2.45) ppm (b), δ(2.46-3.15) ppm (c), δ(3.16-3.8) ppm (d), δ(3.8-4.46) ppm	71

		(e), $\delta(4.8-5.9)$ ppm (f) and $\delta(6.4-9.1)$ ppm (g) along with the annotations for all identified metabolites. Key: Arg, Arginine; Citru, Citrulline; UA, Unassigned. The ^{13}C satellite peaks of lactate are highlighted by asterisk “#”.	
	2.7	The representative 800 MHz (Cryoprobe) ^1H - ^{13}C HSQC spectrum of a pooled synovial fluid obtained from ReA patient after ultrafiltration using a 3 kDa filter showing expanded regions (A) ^1H δ 0.0-4.20 ^{13}C δ 0.0-95.0 and (B) ^1H δ 4.60 -7.60 ^{13}C δ 92.00-136.00	72
	2.8	The representative 800 MHz ^1H - ^1H TOCSY spectrum of pooled filtered (after ultrafiltration) synovial fluid samples obtained from ReA patients. Abbreviations: 2-HB: 2-Hydroxybutyric acid; 3-HB: 3-Hydroxybutyric acid; and Phe: Phenylalanine.	73
	2.9	The representative 800 MHz ^1H - ^1H J-Resolved (JRes) spectrum (A-C) with skyline F2 projection of pooled filtered (after ultrafiltration) synovial fluid samples obtained from ReA patients. Three different spectral region of the 1D ^1H Jres spectrum are expanded for improved visualization: (A) $\delta(0.8-3.1)$ ppm, (B) $\delta(3.1-4.30)$ ppm and (C) $\delta(4.60-8.40)$ ppm. Assigned peaks are annotated, whereas unassigned (UA) metabolite signals are labelled as UA.	74,75
	2.10	A typical 800 MHz 1D CPMG ^1H NMR spectrum of a normal synovial fluid obtained from ReA patient with expanded regions from $\delta(0.8-2.73)$ ppm (top panel), $\delta(2.73$ to 4.67) ppm (middle panel) and $\delta(5.18$ to 8.5) ppm (bottom panel). The abbreviations used are: 2-Hb: 2-Hydroxybutyric acid; 3-Hb: 3-Hydroxybutyric acid; Ala: Alanine; Arg: arginine; Chol: Choline; Cit: Citric acid; Citru: Citrulline; GPC: Glycerophosphocholine; α -Glc: α -Glucose; β -Glc: β -Glucose; Glu: Glutamate; Gln: Glutamine; His: Histidine; Ile: Isoleucine; Lac: Lactate; Leu: Leucine; Lys: Lysine; Pro: Proline; Val: Valine; VLDL: Very Low Density Lipoprotein;	77

		TG: Triglycerides and FA: Fatty acid.	
	2.11	The representative 800 MHz ^1H - ^{13}C HSQC spectrum of a normal synovial fluid obtained from a ReA patient showing full spectrum in its top-left panel and the zoomed spectral regions as directed showing CH cross-peak assignments for various SF metabolites.	78
	2.12	The representative 800 MHz ^1H - ^1H J-Resolved (JRes) spectrum of normal synovial fluid samples obtained from a ReA patient. Four different spectral regions of the 1D ^1H JRes spectrum are expanded for improved visualization: (a) $\delta(0.8-1.48)$ ppm, (b) $\delta(1.65-2.90)$ ppm and (c) $\delta(3.00-4.65)$ ppm and (d) $\delta(5.20-8.50)$ ppm. The labelled assignments of the metabolites are as per Table 2 (See, Appendix) .	79
	2.13	(a) The assignment of peaks in the 1D ^1H NMR spectrum of normal SF corresponding to metabolite N- α -Acetyllysine (NAAL) identified using spiking method following sequential addition of N- α -Acetyllysine solution prepared in D $_2$ O (all purchased from Sigma-Aldrich) into control serum sample. (b) The NAAL spiking experiments performed with filtered SF sample clearly revealed that the sample lack signals of NAAL.	80
4	3.1	(A,A') The 2D score plots derived from pairwise PLS-DA analysis of 1D ^1H CPMG NMR spectra of serum samples obtained from ReA and uSpA patients. (A) represents the analysis of complete data matrix generated from 1D ^1H CPMG NMR spectra, whereas (A') represent the analysis of truncated data matrix i.e. CPMG data matrix with excluded spectral regions corresponding to glucose (3.21 to 6.0) and lipid metabolites (0.6 to 0.96, 1.2 to 1.36, 1.92 to 2.04, 2.9 to 3.02). The shaded or semi-transparent areas represent the 95% confidence regions of each group as depicted by their respective colours. (B,B') represent the bar plots showing the	90

		three performance measures (prediction accuracy, multiple correlation coefficient R^2 and the explained variance in prediction Q^2) obtained after 10 fold Cross Validation analysis of complete (B) and truncated (B') CPMG data matrix, respectively. The negative Q^2 values clearly indicated that the ReA and uSpA patients lack metabolic discrimination i.e. the serum metabolic profiles of ReA and uSpA are almost similar.	
	3.2	The schematic showing the study protocol used to compare the metabolic profiles of ReA and RA with respect to normal controls.	91
	3.3	Representative 800 MHz 1D ^1H CPMG NMR spectra of serum samples selected from NC, RA and ReA study groups: (A) $\delta(0.75-4.65)$ and (B) $\delta(5.2-8.6)$. The spectral region $\delta(5.2-8.5)$ in (B) is magnified 8 times compared to spectral region $\delta(0.5-4.7)$ in (B) for the purpose of clarity. Abbreviations and notions used are: BCAA: Branched Chain Amino Acid (Isoleucine and Leucine); 3-HB: 3-Hydroxybutyrate; TMA: Trimethylamine; Lysine(P): Lysine side chains from proteins; TMA: Trimethylamine; PG: Phosphoglyceride; NDMA: N-nitroso-dimethylamine; NAG: N-acetylated glycoprotein; NAAL: N-alpha acetyl lysine; GPC: Glycerophosphocholine; LDL: Low Density Lipoprotein; VLDL: Very Low Density Lipoprotein; PUFA: Polyunsaturated Fatty Acid $-\underline{\text{C}}\underline{\text{H}}=\underline{\text{C}}\underline{\text{H}}-$; L1: $-\underline{\text{C}}\underline{\text{H}}_2-\text{CH}_2-\text{C}=\text{O}-$; L2: $-\underline{\text{C}}\underline{\text{H}}_2-\text{C}=\text{O}-$; L3: $=\text{CH}-\underline{\text{C}}\underline{\text{H}}_2-\text{CH}=\text{C}-$.	96
	3.4	The 2D score plots derived from pairwise PLS-DA analysis of 1D ^1H CPMG NMR spectra of serum samples: (A,A') ReA vs YNC, (B,B') RA vs ENC, (C) ReA vs NC and (D) RA vs NC (E,E') ReA vs RA. (A, B, C, D and E) represent the 2D score plots obtained from pairwise PLS-DA analysis of complete data matrix generated from 1D ^1H CPMG NMR spectra, whereas (A', B' and E') represent the 2D score plots obtained	98

		<p>from PLS-DA analysis of truncated data matrix generated from 1D ¹H CPMG NMR spectra. For score plots shown in (A', B' and E'), mainly the spectral regions corresponding to glucose (3.21 to 6.0) and lipid metabolites (0.6 to 0.96, 1.2 to 1.36, 1.92 to 2.04, 2.9 to 3.02) have been excluded owing to their higher serum concentration levels and thus to reveal the group discrimination based on serum metabolites present in low abundance and exhibiting relatively small difference in their quantitative profiles. The shaded or semi-transparent areas represent the 95% confidence regions of each group as depicted by their respective colors. Abbreviations used here are as per Table 3 i.e. YNC: Young normal control; ENC: Elderly normal control; RA: Rheumatoid Arthritis; ReA: Reactive Arthritis.</p>	
	3.5	<p>The 10 fold Cross Validation of pairwise PLS-DA models performed using different number of components: (A,A') ReA vs YNC, (B,B') RA vs ENC, and (C,C') ReA vs RA. The subsets (A, B and C) and (A', B' and C') represent the bar plots obtained from the analysis of complete and truncated CPMG data matrix, respectively and are showing quantitative measures of model performance for different number of components. Bar plots showing the three performance measures (prediction accuracy, multiple correlation coefficient R² and the explained variance in prediction Q²) using different number of components. The red '*' indicates the best values of the currently selected measures (Q²).</p>	99
	3.6	<p>The 2D score plots derived from combined PLS-DA (A, A') and OPLS-DA (B,B') analysis of 1D ¹H CPMG NMR spectra of all the study groups: ReA, RA and NC and the corresponding VIP score plots derived from PLS-DA modelling are shown in (C,C') for screening metabolite entities of discriminatory significance. The subsets (A, B and C) and (A', B' and C') represent the score plots obtained from</p>	100

		<p>the analysis of complete and truncated CPMG data matrix, respectively. The truncated CPMG data matrix has been generated by excluding the lipid regions (0.6 to 0.96, 1.2 to 1.36, 1.92 to 2.04, 2.9 to 3.02) and the glucose regions (3.21 to 6.0) to reveal the discriminatory importance of serum metabolites present in low abundance and exhibiting relatively small change in metabolic concentration. The colored boxes present on the right side of each VIP score plot indicate the relative concentrations of the corresponding metabolite in each group under study.</p>	
	3.7	<p>The potential discriminatory metabolite entities identified from VIP statistics based on paired PLS-DA models. The VIP score plots show the metabolite entities in decreasing order of their VIP score value. In (A, B and C), the complete NMR data matrix was used for PLS-DA modelling and resulted VIP scores for top 35 metabolite entities are shown. Most of these metabolite entities correspond to glucose, lactate and membrane/lipid metabolites. In (A', B' and C'), the truncated CPMG data matrix with excluded glucose and lipid regions (0.6 to 0.96, 1.2 to 1.36, 1.92 to 2.04, 2.9 to 3.02, 3.21 to 6.0) to reveal the discriminatory importance of serum metabolites present in low abundance and exhibiting relatively small change in metabolic concentration. In (A'', B'' and C''), the down-field spectral region from 6.1 to 8.6 ppm was used for PLS-DA modelling and revealed the discriminatory importance of aromatic amino acids like Histidine, Tyrosine and phenylalanine.</p>	102
	3.8	<p>VIP score plot analysis used to identify metabolite entities of discriminatory significance for PLS-DA analysis between (A) ReA vs NC and (B) RA vs NC. The colored boxes present on the right side of each VIP score plot indicate the relative concentrations of the corresponding metabolite in each group under study.</p>	103

	3.9	VIP score plot analysis used to identify metabolite entities of discriminatory significance for PLS-DA analysis between (A) ReA vs NC and (B) RA vs NC. The colored boxes present on the right side of each VIP score plot indicate the relative concentrations of the corresponding metabolite in each group under study.	104
	3.10	Represents the Receiver operating characteristic (ROC) curves of the metabolites discriminating G1 from G2 along with their respective box plots. AUC indicates the area under the curve and the dot refers to the cutoff value maximizing sensitivity and specificity for the given samples. For each box plot, boxes denote interquartile ranges; lines denote medians, and whiskers denote 10 th and 90 th percentiles.	105
	3.11	The ROC curves generated for six different PLS-DA models: (A,A') ReA vs YNC, (B,B') RA vs ENC, and (C,C') ReA vs RA. For ROC analysis, the predictive models were generated using top 100 features of discriminatory significance.	107
	3.12	Pearson's correlation analysis performed for serum metabolites responsible for discrimination between ReA and RA patients. Only metabolite correlations with $ R \geq 0.6$ and $p < 0.05$ were considered.	108
	3.13	Pearson correlation coefficient (R) presented as bar plot showing top 16 metabolite entities (among the selected metabolite entities responsible for discrimination between ReA and RA) correlated with LDL bin at 0.87 ppm.	109
	3.14	Representative box-cum-whisker plots showing quantitative variations for serum metabolites. These plots have been generated using binned spectral features normalized with respect to the total spectral intensity (also referred here as relative signal integrals). For presented metabolite entities, the VIP score >1 and statistical significance is at the level of $p \leq 0.05$. In the box plots, the boxes denote interquartile ranges, horizontal line inside the box denote the median, and	111

		bottom and top boundaries of boxes are 25 th and 75 th percentiles, respectively. Lower and upper whiskers are 5 th and 95 th percentiles, respectively.	
	3.15	The possible disease mechanism in ReA patients illustrated based on current metabolic disturbances and previous pathophysiological mechanistic studies.	115
	3.16	Representative 800 MHz 1D ¹ H CPMG NMR spectra of ultra-filtered serum samples selected from NC, RA and ReA study groups:(A) $\delta(0.75-4.65)$ and (B) $\delta(5.2-8.6)$. The spectral region $\delta(5.2-8.5)$ in (B) is magnified 8 times compared to spectral region $\delta(0.5-4.7)$ in (B) for the purpose of clarity. The spectral peaks corresponding to marker metabolites are labelled and also re-validated using CHENOMX software as well.	116
	3.17	The box-cum-whisker plots for marker metabolites derived from their absolute concentrations determined using ultra-filtered serum samples to achieve reliable quantitative profiling. For each shown univariate analysis, the resulted p-values are shown in orange brown text to assess the statistical significance and other parameters such as fold change and mean values are shown in Table 6, See the Appendix . For shown box-plots, the boxes denote interquartile ranges, horizontal line inside the box denote the median, and bottom and top boundaries of boxes are 25 th and 75 th percentiles, respectively. Lower and upper whiskers are 5 th and 95 th percentiles, respectively.	117
	3.18	Serum marker metabolite except pyruvate showing correlation with Synovial fluid for ReA group.	118

Chapter-1
Introduction

Introduction

Reactive arthritis is a form of heterogeneous groups of disease called as seronegative spondyloarthropathies (SSA) which is clinically related with inflammatory back pain, additive or migratory oligoarthritis, and extra-articular symptoms that typically follow a gastrointestinal or urogenital infection. The SSA group shares clinical feature like male predominance, asymmetrical lower limbs arthritis, enthesitis, sarcolitis, and strong association with HLA-B27.¹ ReA presents as acute asymmetrical lower-limb oligoarthritis with or without enthesitis, conjunctivitis or urethritis within 1-4 weeks of enteric or genitourinary infection. Enterically acquired ReA is commonly due to *Salmonella typhimurium*, *Shigella flexneri*, *Campylobacter jejuni*, *Yersinia enterocolitica* and venerally acquired ReA is due to *Chlamydia trachomatis*. Several patients who have a clinical picture like ReA, but lack history of preceding infection and do not fulfill the criteria for other well defined SSA such as AS, PsA, and IBD-A are labelled as undifferentiated spondyloarthropathy.²

ReA is an inflammatory oligoarthritis affecting less than five large joints which can follow two disease courses. The first is an acute syndrome occurring shortly after the triggering infection followed by gradual resolution of symptoms; the second begins in a similar fashion yet can progress to chronicity, sometimes years. In the former case, different joints are progressively inflamed without the earliest localizations resolving while in the latter case, new sites of arthritis become inflamed after the previous ones have recovered.³ ReA is also multiorgan disorder can be accompanied by a constellation of extraarticular findings that include symptomatology from the eyes, the genitourinary tract (urethritis in men and cervicitis in women) and the cardiovascular system.^{3,4} ReA can be selflimiting, recurrent or continuous and about 20% to 25% of the patients may progress to have chronic articular, ocular and cardiac complications (Arthritis, Reactive (Reiter Syndrome). The chronic ReA condition is characterized by sacroiliitis, periostitis, nonmarginal syndesmophytes, periosteal new bone formation, joint erosions, and joint space narrowing.⁵ Syndesmophytes and sacroiliitis are generally common in patients who have postvenereal ReA rather than in those who have postenteric ReA.⁶

The ReA incidence is estimated to be 5 - 14/100,000 patients aged 18 - 60 years, depending on the antigen frequency in a particular area.^{7,8} The aetiology of ReA is composite and the knowledge of its specific mechanisms is inconclusive but genetic and environmental factors both contribute. Demonstration of microbial components, even their DNA or RNA, in the inflamed synovium

(synovitis), synovial and in circulating blood cells in patients with ReA established the direct role of the microbes suggesting that reactive arthritis is caused by an over-stimulated autoimmune response or by bacterial antigens which deposit in the joints.^{9,10,11,12,13} The antigens that trigger reactive arthritis are Gram-negative intracellular aerobic bacteria with an LPS-containing capsule. These first invade a mucosal site that can be gastrointestinal (enteric pathogens) or urogenital.¹⁴ In addition to synovitis, a systemic inflammatory response is also seen involving changes in many systems and organs.

Systemic inflammation leads to alterations in metabolism, and several studies have investigated the resulting changes in low molecular weight metabolites in patients. Metabolomics is a comprehensive analysis of low molecular weight metabolites, which reflect the state of the human organism at a certain time point. Metabolites are the intermediates and end-products of different metabolic pathways and resemble the end result of the genotype, phenotype and environmental factors. Metabolic changes are the most proximal indicators of the disease process and drug therapy. Thus, metabolomics is an emerging area of biomedical research that may offer a better understanding of the mechanisms of underlying conditions including inflammatory arthritis.

Metabolomic methods, often focused on the information-rich analytical techniques of nuclear magnetic resonance (NMR) spectrometry and mass spectrometry (MS), is a predicting tool in the search for novel biomarkers which can be helpful in early diagnosis, response to therapy and defining disease pathogenesis in many therapeutic areas, including rheumatic diseases.^{15,16,17} Currently, NMR is the best technique for chemical structure analysis¹⁸; it demands only minimal sample preparation, and is nondestructive, inherently untargeted, and highly reproducible.^{19,20} An advantage of NMR spectroscopy is the ability to make a bridge in between vitro, ex vivo and in vivo studies by utilizing of high-resolution magic-angle spinning to profile intact tissues and magnetic resonance spectroscopic imaging for in vivo applications. NMR based metabolomics has been used to identify alterations in a broad range of different metabolites simultaneously, and from such studies several key metabolites have been identified, providing insights into the mechanisms of disease and also representing potential biomarkers which can be used to follow the disease and assess responses to therapy.^{21,22}

ReA has significant effects on metabolism, and in this thesis, I aimed to use NMR based metabolomics as a promising tool to identify potential serum/SF biomarkers that could improve early diagnosis and provide novel insights into mechanisms of disease. Many biomarkers are not

specific for the joint and there is a possibility that the concentrations of a peculiar biomarker, when evaluated in the serum, could be affected by release from alternative sites due to increased systemic inflammation. In this study, therefore, we also explored the relationship between the serum and synovial fluid concentrations of individual biomarkers, at two-time points, to determine whether measurements made in the serum reflect the concentrations observed within the signal knee.

Reference

1. Colmegna, I.; Cuchacovich, R.; Espinoza, L. R., HLA-B27-associated reactive arthritis: pathogenetic and clinical considerations. *Clinical Microbiology Reviews* **2004**, *17* (2), 348-369.
2. Kim, P. S.; Klausmeier, T. L.; Orr, D. P., Reactive arthritis: a review. *Journal of Adolescent Health* **2009**, *44* (4), 309-315.
3. Selmi, C.; Gershwin, M. E., Diagnosis and classification of reactive arthritis. *Autoimmunity reviews* **2014**, *13* (4-5), 546-549.
4. Stavropoulos, P.; Soura, E.; Kanelleas, A.; Katsambas, A.; Antoniou, C., Reactive arthritis. *Journal of the European Academy of Dermatology and Venereology* **2015**, *29* (3), 415-424.
5. Carter, J. D.; Hudson, A. P., Reactive arthritis: clinical aspects and medical management. *Rheumatic Disease Clinics* **2009**, *35* (1), 21-44.
6. Lauhio, A.; Leirisalo-Repo, M.; Lähdevirta, J.; Saikku, P.; Repo, H., Double-blind, placebo-controlled study of three-month treatment with lymecycline in reactive arthritis, with special reference to Chlamydia arthritis. *Arthritis & Rheumatism: Official Journal of the American College of Rheumatology* **1991**, *34* (1), 6-14.
7. Kvien, T.; Glennås, A.; Melby, K.; Granfors, K.; Andrup, O.; Karstensen, B.; Thoen, J., Reactive arthritis: incidence, triggering agents and clinical presentation. *The Journal of Rheumatology* **1994**, *21* (1), 115-122.
8. Hannu, T., Reactive arthritis. *Best Practice & Research Clinical Rheumatology* **2011**, *25* (3), 347-357.
9. Inman, R. D., Mechanisms of disease: infection and spondyloarthritis. *Nature Reviews Rheumatology* **2006**, *2* (3), 163.
10. Gerard, H.; Branigan, P.; Schumacher, J. H.; Hudson, A., Synovial Chlamydia trachomatis in patients with reactive arthritis/Reiter's syndrome are viable but show aberrant gene expression. *The Journal of rheumatology* **1998**, *25* (4), 734-742.
11. Granfors, K.; Merilahti-Palo, R.; Luukkainen, R.; Möttönen, T.; Lahesmaa, R.; Probst, P.; Märker-Hermann, E.; Toivanen, P., Persistence of Yersinia antigens in peripheral blood cells from patients with Yersinia enterocolitica O: 3 infection with or without reactive arthritis. *Arthritis & Rheumatism: Official Journal of the American College of Rheumatology* **1998**, *41* (5), 855-862.
12. Kuipers, J. G.; Jürgens-Saathoff, B.; Bialowons, A.; Wollenhaupt, J.; Köhler, L.; Zeidler, H., Detection of Chlamydia trachomatis in peripheral blood leukocytes of reactive arthritis patients by polymerase chain reaction. *Arthritis & Rheumatism: Official Journal of the American College of Rheumatology* **1998**, *41* (10), 1894-1895.

13. Merilahti-Palo, R.; Söderström, K.; Lahesmaa-Rantala, R.; Granfors, K.; Toivanen, A., Bacterial antigens in synovial biopsy specimens in yersinia triggered reactive arthritis. *Annals of the rheumatic diseases* **1991**, *50* (2), 87.
14. Gaston, J. H.; Lillicrap, M. S., Arthritis associated with enteric infection. *Best Practice & Research Clinical Rheumatology* **2003**, *17* (2), 219-239.
15. Guleria, A.; Misra, D. P.; Rawat, A.; Dubey, D.; Khetrpal, C. L.; Bacon, P.; Misra, R.; Kumar, D., NMR-based serum metabolomics discriminates Takayasu arteritis from healthy individuals: a proof-of-principle study. *Journal of proteome research* **2015**, *14* (8), 3372-3381.
16. Guleria, A.; Pratap, A.; Dubey, D.; Rawat, A.; Chaurasia, S.; Sukesh, E.; Phatak, S.; Ajmani, S.; Kumar, U.; Khetrpal, C. L., NMR based serum metabolomics reveals a distinctive signature in patients with Lupus Nephritis. *Scientific reports* **2016**, *6*, 35309.
17. Guleria, A.; Phatak, S.; Dubey, D.; Kumar, S.; Zanwar, A.; Chaurasia, S.; Kumar, U.; Gupta, R.; Aggarwal, A.; Kumar, D., NMR-Based Serum Metabolomics Reveals Reprogramming of Lipid Dysregulation Following Cyclophosphamide-Based Induction Therapy in Lupus Nephritis. *Journal of proteome research* **2018**, *17* (7), 2440-2448.
18. Moco, S.; Vervoort, J.; Bino, R. J.; De Vos, R. C.; Bino, R., Metabolomics technologies and metabolite identification. *TrAC Trends in Analytical Chemistry* **2007**, *26* (9), 855-866.
19. Dumas, M.-E.; Maibaum, E. C.; Teague, C.; Ueshima, H.; Zhou, B.; Lindon, J. C.; Nicholson, J. K.; Stampler, J.; Elliott, P.; Chan, Q., Assessment of analytical reproducibility of 1H NMR spectroscopy based metabonomics for large-scale epidemiological research: the INTERMAP Study. *Analytical chemistry* **2006**, *78* (7), 2199-2208.
20. Viant, M. R.; Bearden, D. W.; Bundy, J. G.; Burton, I. W.; Collette, T. W.; Ekman, D. R.; Ezernieks, V.; Karakach, T. K.; Lin, C. Y.; Rochfort, S., International NMR-based environmental metabolomics intercomparison exercise. *Environmental science & technology* **2008**, *43* (1), 219-225.
21. Brindle, J. T.; Antti, H.; Holmes, E.; Tranter, G.; Nicholson, J. K.; Bethell, H. W.; Clarke, S.; Schofield, P. M.; McKilligin, E.; Mosedale, D. E., Rapid and noninvasive diagnosis of the presence and severity of coronary heart disease using 1 H-NMR-based metabonomics. *Nature medicine* **2002**, *8* (12), 1439.
22. Sreekumar, A.; Poisson, L. M.; Rajendiran, T. M.; Khan, A. P.; Cao, Q.; Yu, J.; Laxman, B.; Mehra, R.; Lonigro, R. J.; Li, Y., Metabolomic profiles delineate potential role for sarcosine in prostate cancer progression. *Nature* **2009**, *457* (7231), 910.

Chapter-2

REVIEW OF THE LITERATURE

Contents

- 1.1 Reactive Arthritis**
 - 1.1.1 Clinical Presentation of patients with ReA**
 - 1.1.2 Epidemiology**
 - 1.1.3 Aetiology**
 - 1.1.3.1 Genetic Factors**
 - 1.1.3.2 Environmental factor**
 - 1.1.3.3 Interaction of bacteria and host in ReA**
- 1.2 Metabolism in inflammatory disease**
- 1.3 Metabolomics**
 - 1.3.1 The Metabolome**
 - 1.3.2 Metabolomics in Inflammatory Rheumatic Disease**
 - 1.3.3 Approaches to metabolomics**
 - 1.3.4 NMR based Metabolomics**
 - 1.3.4.1 NMR Spectroscopy**
 - 1.3.4.2 NMR data acquisition**
 - 1.3.5 Data Analysis**
 - 1.3.5.1 Chemometrics**
 - 1.3.5.1.1 Data Reduction**
 - 1.3.5.1.2 Normalisation**
 - 1.3.5.1.3 Scaling**
 - 1.3.5.1.4 Multivariate Analysis**
 - 1.3.5.2 Univariate Statistics**
- 1.4 Summary**
- 1.5 Aims and hypothesis**
- 1.6 References**

1.1 Reactive Arthritis

Reactive Arthritis (ReA) is defined as immune-mediated sterile synovitis triggered by a distant infection through the urogenital or gastrointestinal tract. Reactive arthritis (ReA) and undifferentiated arthritis (uSpA) belongs to the family of disease called the seronegative spondyloarthropathy (SSA). The diseases included under this umbrella are ankylosing spondylitis (AS), psoriatic arthritis (PsA), arthritis associated with inflammatory bowel disease (IBD-A), reactive arthritis (ReA) and undifferentiated spondyloarthritis (uSpA) with common clinical features such as sacroiliitis, enthesitis (insertion site of tendons and ligaments), uveitis, seronegativity for Rheumatoid factors (RF) and a strong association with HLA-B27.

ReA is the best-known examples of microbial involvement among in all inflammatory arthritis. Arthritis develops within 1-4 weeks of gastrointestinal or genitourinary infection. Patients present with the acute or subacute asymmetrical arthritis of the lower limbs of the joints with or without fever, enthesitis, dactylitis, oral ulcers, balanitis, and conjunctivitis. ReA was earlier known as Reiter's syndrome which is characterized by the classical triad of symptoms including the urethra, conjunctiva, and synovium. This terminology is dropped in favor of ReA, one of the reasons being that the urethritis characteristic could mislead to be due to a genitourinary trigger. Hans Reiter is not the first one to describe the entity; it should have been Leroy-Fiessinger. Hence, Nowadays ReA is a widely accepted term.¹ Enterically acquired ReA is induced a panel of bacteria including *Salmonella typhimurium*,² *Shigella flexineri*,³ *Compylobacter jejuni*⁴ and *Yersinia enterocolitica*⁵ while genitourinary acquired ReA develops by the infection of *Chlamydia trachomatis*. A significant proportion of the patients do not fulfill the diagnostic criteria for any of the currently established diseases in the SSA group⁶- are labelled as Undifferentiated spondyloarthritis (uSpA) implying that in the course of time they would develop symptoms of well-defined members like Ankylosing spondylitis or Psoriatic arthritis that will full fill the criteria of European Spondyloarthropathy Study Group (ESSG) like asymmetrical lower limbs arthritis or inflammatory low backache within one of the following feature: enthesitis, radiological evidence of sacroiliitis, buttock pain or a positive family history.⁷ Patients of this group closely resemble with ReA yet without any preceding history of enteric or genitourinary infection. The evidence for a microbial involvement in uSpA has been reported despite the absence of symptomatic diarrhea like in patient with enteric/genitourinary acquired

ReA. Various level of gut inflammation in intestinal biopsy specimens⁸ and the *chlamydia* DNA has been demonstrated in the synovial fluid and the synovial membrane of the patients with ReA and uSpA.⁹ Elevated serum IgA antibodies level to enteric bacteria *S. Typhimurium*, *S. flexneri* and *Y. enterocolitica* in patients with ReA as well as uSpA.¹⁰ The proliferation of SFMCs to whole enteric bacterial extract and purified membrane protein of *Salmonella* constituents in patients with ReA and uSpA^{11,12} also intimate that uSpA has similar clinical picture and immune response to microbial trigger despite the lack of preceding symptomatic infection.

1.1.1 Clinical Presentation of patients with ReA

There are no differences in the clinical manifestations in both type, i.e. venterally or enterically acquired ReA. Males are most frequently affected in case of venterally acquired ReA as male to female ratio has been estimated to be 9:1 and, however, post enteric ReA is equally found in males and females of 20-40 years of age.¹³ The onset of the disease involves a peripheral monoarthritis or asymmetric oligoarthritis is days to several weeks after the inciting infection which may be associated with malaise, fatigue, and fever.¹⁴ Lower limbs joints (knee, ankle and foot) are affected asymmetrically mimic a picture of septic arthritis. The average duration of ReA is 4 to 5 months but, however, 15% -30% of patients may develop chronic disease.¹⁵ Axial joints with the involvement of hips and spine may affecting at cervical, dorsal or lumber level manifesting with pain and limitation of movements. Asymmetric sacroiliitis can be demonstrated radiologically in 14-49% of patients with ReA, in one-third of patients with urogenital ReA and in one-tenth of patients with enterically acquired ReA.¹⁶

Enthesitis and dactylitis are two common features besides arthritis that share with other member of spondyloarthropathy. Enthesitis refers to inflammation at the transitional zone where collagenous structures, such as tendons and ligaments insert into bone and can be as painful disabling as arthritis. The commonly affected part is plantar aponeurosis and Achilles' tendon which attached to the calcaneus resulting in heel pain and difficulty in walking. Dactylitis, another common feature of ReA, typically presents diffuse swelling of an entire finger or toe ("sausage digit") in 16% of patients with ReA.^{16,17}

The most common ophthalmologic symptoms are conjunctivitis with mucopurulent discharge which has been seen in around 35% of patients in ReA. Dermatologic manifestations include circinate balanitis, and keratoderma blennorrhagica occur in 20–40% and 5–30% of patients, respectively.¹⁷ Painless oral ulcers are also seen in patients with ReA. Erythema nodosum is a well-recognized complication of *Yersinia* incited ReA which demonstrated painful nodules predominantly on the extensor surface of the arms and legs.^{18,15}

The diagnosis of ReA is based on the baseline clinical features such as raised inflammatory maker, erythrocyte sedimentation rate (ESR), C-reactive protein (CRP), complete blood count and urinalysis. In the acute phase, patients also might display other indicators of the inflammatory response, including leukocytosis or thrombocytosis. Both RF and antinuclear antibody (ANA) are measured to differentiate from other arthritis. A positive HLA-B27 result increases the likelihood of ReA, but this is neither sensitive nor specific for the condition. Therefore, it is not used for diagnosis of ReA in spite of strong association with disease. Because of *Salmonella* and *Yersinia* persist in the gut even after several weeks after resolution of diarrhea; therefore, the stool culture technique can be used to diagnose the gastrointestinal infection. For genitourinary infection, the nucleic acid amplification technique like ligase chain reaction (LCR) and PCR by using urine and swab samples obtained from urethra or vagina are preferred, as *Chlamydiae* is difficult to culture.¹

1.1.2 Epidemiology

Lack of gold standard test for the diagnosis of ReA is a major challenge in interpreting reported incidence and prevalence from the various regions. The genetic difference between populations, environmental condition, geographic distribution and prevalence of causative pathogens are influences the incidence and prevalence of disease.¹⁹

Reports based on the questionnaire survey and examination, following gastrointestinal infection with *Salmonella*, *Campylobacter*, *Yersinia* and *Shigella*, clinical ReA have been seen in 7-12% of subjects.^{20,21,22,23} Most of the epidemiological data belong from Europe. The prevalence of ReA has been estimated as 0.1%,^{24,25} with incidence rates of 4.6 to 13 per 100,000 for post-venereal ReA and 5 to 14 per 100,000 for post-enteric ReA.^{26,25} In the European population, prevalence of ReA is around 9/100,000 in most countries: Norway 9.6/100,000;²⁵ Finland

10/100,000;²⁷ and 9.3/100,000 in Czech Republic,²⁸ while in Southern Sweden it is considerably higher at 28/100,000.²⁹ The uSpA and ReA, who fulfilled ESSG criteria for spondyloarthritis, constituted 14% and 1.2% of 1379 patients, respectively, according to Spanish registry-based study of one year duration which involves 12 reference centers across the country.³⁰ Based on questionnaire survey, the prevalence of both diseases was 0.09% calculated among 2155 of respondent subjects in a central region of Italy.³¹ The estimated data from Berlin showed that prevalence of uSpA and ReA in Germany was 0.6% and 0.1%.²⁴ According to the previous two studies from Russia and Alaska, the prevalence was 0.6% and 0.1%, respectively.^{32,33} The two registry-based studies from Spain established the fact that 1.2-1.4% patients were recognized as ReA among all SSA patients,³⁰ while 25 (6.2%) were ReA out of 402 patients with SSA from Argentina.³⁴

In European countries *Y.enterocolitica* induce ReA is common in terms of the microbial-specific ReA, especially in Scandinavian countries such as Norway or Finland.³⁵ The regarding the campylobacter induce ReA, the rate of incidence was 4.3 per 100,000 case in Finland.²¹ The annual incidence of 4.6 per 100,000 case for chlamydia induced ReA, while incidence of 5 per 100,000 cases for enteric bacteria induced ReA have been reported in Norway.²⁵ The causative pathogen was identified in 29/52 (56%) patients with ReA from several rheumatology clinics across the Berlin, Germany by using tool culture and sera antibodies to various microbes, agglutination, ELISA and Immunofluorescence assay. From these, 17 were gastrointestinal infection (33% *Salmonella* and 18% *Yersinia*) induced ReA.³⁶ The clinical picture of possible ReA in 74 patients (with no symptomatic history of previous infection or uSpA), *Yersinia* (19%), *Salmonella* (12%) and *C.trachomatis* (16%) were identified as trigger pathogen in the same study.³⁶

In USA, incidence rate of ReA was estimated as 0.6-3.1/100,000 cases. According to a study from Oregon and Minnesota, USA, 6379 patients were diagnosed with the culture-confirmed enteric infection from *campylobacter jejuni*, *E.coli* O157, *S.typhimurium*, *S.flexenri* and *Y.enterocolitica*. The incidence was highest for *Compylobacter* (2.1/100,000) while far *Salmonella* it was 1.4/100,000.³⁷

1.1.3 Aetiology

The pathogenesis of ReA has been studied intensively over years, but in spite of much collected information, the picture remains elusive. ReA is definitely an infectious disease. If a genetically predisposed individual contracts a suitable infection, an immune reaction will lead to this condition. The best known predisposing factor is the HLA antigen B27, the role of which will be discussed below. The list of microbes that can trigger the disease is long and still growing.

1.1.3.1 Genetic Factors

HLA-B27 shows a strong genetic contribution to the development of ReA. The most striking association is observed for AS, 94% of patients express HLA-B27 compared with approximately 9% of the general population.³⁸ The later on, other member SSA family including ReA (Brewerton),³⁹ IBD-A,⁴⁰ and PsA⁴¹ were linked with HLA-B27. The association between HLA-B27 and ReA is well illustrated by the fact that the prevalence of disease in HLA-B27-positive individuals is five times higher than in the general population while in HLA-B27 relatives of patients with ReA, the prevalence is another 10 times greater.⁴² Direct evidence comes from transgenic animals. HLA-B27 transgenic rats develop a multi-system disease with many features resembling the human HLA-B27-associated diseases.⁴³ In addition, symptoms develop due to transfer from a specific pathogen-free environment to conventional conditions.⁴⁴ Moreover, susceptibility to disease is clearly related to the gene copy number and level of expression of HLA-B27 in transgenic animals,⁴⁵ and requires the presence of HLA-B27+ bone marrow cells⁴⁶ and T cells,⁴⁷ consistent with the features of immune mediated disease.

HLA-B27 is an MHC class I molecule, which consist of a glycosylated heavy chain (45Kda) non-covalently associated with β_2 -microglobulin (β_2m) (12Kda) (**Figure 1.1**). The class I heavy chain made up of three extracellular domains, α_1 (N-terminal), α_2 and α_3 , the transmembrane region and a cytoplasmic tail. The α_1 and α_2 domains constitute a platform of 8 anti-parallel β strands supporting 2 antiparallel α helices, which form a highly polymorphic peptide-binding cleft comprising of 6 pockets (A, B, C, D, E, F).^{49,50,51} The most distinctive structural feature of HLA-B27 is its B pocket, with a glutamic acid at its base and a cysteine residue at its mouth. This pocket is surrounded by a unique combination of residues that is found in all disease-associated HLA-B27 subtypes and confers the HLA-B27 B pocket with a strong specificity for

an arginine side chain at the second position of bound peptides.⁵² Moreover, another unique characteristic of the HLA-B27 molecule is the presence of an unpaired cysteine- 67 residue within the extracellular $\alpha 1$ domain, which facilitates adherence of the two heavy chains to each other via disulfide binding to form a “homodimer”.^{53,54,55} These unique and inherent “defects” suggest that HLA-B27 has abnormal cell biology, which may be of pathogenic significance.

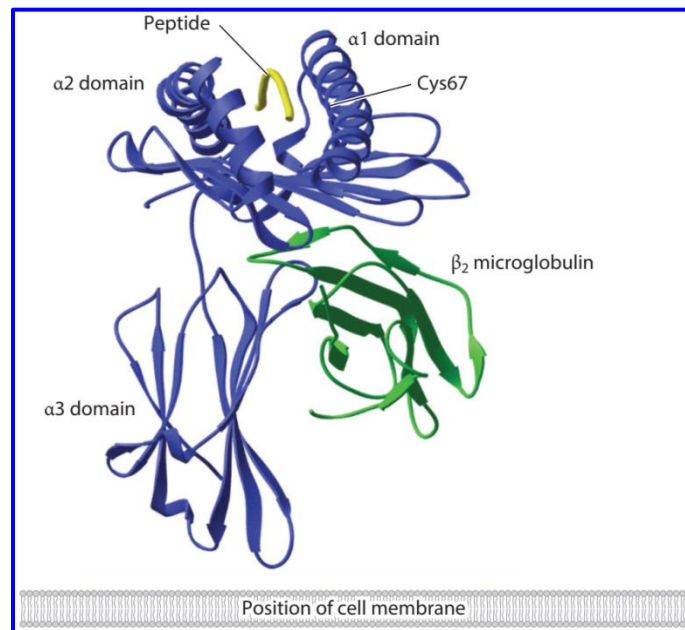


Figure 1.1: Molecular structure of HLA-B27, $\alpha 1$, $\alpha 2$, and $\alpha 3$ domain of B27 are shown in ribbon format in blue, and $\beta 2$ in green⁴⁸

Over 105 molecular subtypes of HLA-B27 have been described till date.⁵⁶ The most common subtypes (HLA-B*2705, B*2702, B*2704, B*2707) which are clearly associated with a risk of spondyloarthritis. Among them, B*2705 is the dominant subtype which is associated with spondylitis across broad ethnic and geographic boundaries.

Although HLA-B27 has remained a center of extensive research, the exact mechanism underlying the effect of HLA-B27 on disease susceptibility still has not been determined. Moreover, the reasons behind the HLA-B27-associated diseases attack certain organ systems, such as the joint, the spine, the gut, and the eye, and not others, is not clear yet. Several different hypotheses have been proposed.

The arthritogenic peptide model proposes on the basis of major function of HLA-B27 as a class I antigen in the presentation of antigenic peptides to cytotoxic lymphocytes, that the disease is the product of a cytotoxic T cell response to a peptide found only in joint tissues that can specifically be bound and presented by all HLA-B27 subtypes through their shared structural motif. However, the peptide is presented at too low levels for T-cell recognition under “normal” conditions either for clonal deletion or for initiating an immune response. During the infection, the bacteria may contain proteins with sequence motifs similar to the arthritogenic peptide. Then, infection would sensitize T cells so that they could recognise low levels of presentation of the arthritogenic peptide and initiate an anti-self response. Therefore, SpA is an autoimmune response mediated by T cells against self-antigens after a breakdown in self-tolerance by the triggering bacterial infection.⁵⁷ According to the previous report, CD4+ T cells might also be involved in class I-restricted immune recognition,⁵⁸ and consequently, SpA could involve an HLAB27-restricted CD8+ or CD4+ T cell response to microbial or self-peptides.

The hypothesis of arthritogenic peptide would require particularly strict selection of unique peptide epitopes by HLA-B27. Subtype polymorphisms influence the peptide presentation by HLAB27 within the peptide binding groove. Although subtypes of HLA-B27 differ at other key positions within the peptide binding groove except their characteristic conserve B pocket.⁵⁰ The evidence attributed to this hypothesis from the identification of HLA-B27-restricted peptides from *Chlamydia trachomatis*,⁵⁹ as well as from molecular mimicry between endogenous B27 peptides and environmental antigens.^{60,61}

Enthesitis has received more attention nowadays as the hallmark for differentiating SpA from all other arthritis.⁶² The possibility of cartilage proteoglycans versican and aggrecan and the link protein as autoantigens are being studied in SpA.⁶³ In the previous study, it was established that HLA-B27-restricted epitopes derived from human aggrecan are involved in the induction of typical inflammation of SpA (tenosynovitis) in BALB/C-B27 transgenic mice.⁶⁴

There has been substantial interest in aberrant processing especially in the folding of the heavy chain of HLA-B27. Under the normal circumstances, the cell surface HLA-B27 consist of a heavy chain bound to P2IT1 and peptide which is formed in the endoplasmic reticulum.⁶⁵ It has been recently described that, due to its unique B pocket architecture, newly synthesized HLA-

B27 is slow to fold and associate with β_2m , and has a tendency to misfold.⁶⁶ The accumulation of misfolded HLA B27 protein may result in a proinflammatory “unfolded protein response,” probably, which contribute to the pathogenesis of HLA-B27-associated disease.⁶⁷

The previous study shows that HLA-B27 itself is recognised by human CD4+ T cells isolated from SpA patients.⁶⁸ A number of molecules, including conventional HLA-B27 heterodimers, free HLA-B27 heavy chain monomers, and unconventional homodimers are involved in this unusual recognition, which also is independent of MHC II and transporter associated with antigen processing (TAP). Supporting these findings, Roddis et al. have been previously demonstrated that CD4+ and CD8+ T cell responses induced in HLA-B27 restricted TCR transgenic mice (GRb) are both functional.⁶⁹ Adoptive transfer studies have established that CD4+ T cells are more important than CD8+ T cells for evocation of arthritis.⁴⁷ Together, these findings suggest the role of unusual recognition of MHC I-restricted CD4+ T cells in the pathogenesis of SpA.

A hypothesis proposes the theory of “autodisplay” of HLA-B27 to explain the role of HLA-B27 in SpA.⁷⁰ According to this hypothesis, peptide-free heavy chains, β_2m -free, support a helix-coil transition from the α_2 domain to the α_3 domain which facilitating the rotation of backbone angles around residues 167/168, thereby occupying the peptide binding cleft of the molecule. Such auto-display of HLA-B27, occurring either within HLA-B27 molecules or between HLA-B27 molecules, might be the grounds for self-perpetuating inflammatory and immune stimulation, although experimental evidence provides the existence of such assemblies is minimal.

There is another theory which suggest the β_2m deposition.⁷¹ This is based on the observation which explains the deposition of P2IT1 in synovial fluid in the form of amyloid aggregates due to disease associated HLA-B27 subsets exhibit a higher rate of β_2m dissociation from the surface HLA-B27 complex than non-associated subsets, causing immune response against such aggregates. However, HLA-B27 itself appears incidental rather than central to the disease mechanism with this particular hypothesis. Moreover, transgenic animal studies show the opposite results that β_2m deficiency (without expression of HLA-B27) is sufficient to cause spontaneous inflammatory arthritis.⁷²

Intracellular persistence of arthritogenic microorganisms may contribute to the pathogenesis of ReA, suggesting the host/microbe interaction may be abnormal in susceptible individuals, leading to inefficient elimination of arthritogenic bacteria, fragments of them or both, after the initial infection. To support this notion, HLA-B27 expression decreases arthritogenic bacterial invasion into transfected L cells have shown in the previous study.⁶⁷ HLA-B27 also remarkably impairs the elimination of *Salmonella enteritidis* within transfected human monocytic cells in addition to invasion.⁷³ Moreover, HLA-B27-positive monocytes show less efficient capacity to kill *Salmonella* in vitro than controls, and they also show interleukin 10 (IL-10) upregulation and to a lesser extent, TNF α ,^{74,75} indicating that HLA-B27 associated modulation of cytokine response profiles may have importance in the pathogenesis of disease. From this point of view, the function of HLA-B27 may not be limited to antigen presentation. However, other studies have shown that arthritogenic bacteria does not affect HLA-B27 peptide presentation,⁷⁶ and, invasion and persistence of *Salmonella* in fibroblasts are not affected whether the cells are isolated from HLA-B27 positive or negative individuals.⁷⁷ The diverse results may reflect the properties of different cells and bacterial strains used in these studies, as both elements have a crucial effect on the outcome. Although the findings remain controversial, this theory takes account of the effects of triggering bacteria and genetic susceptibility into the pathogenesis of ReA, which is worthy of further investigation.

1.1.3.2 Environmental factors

It is well known fact that ReA is a joint inflammation that follows infections caused by certain Gram-negative bacteria, as detailed above, although the triggering infection is less clear in other diseases of the SpA family. HLA-B27 transgenic rats in a germ-free environment do not develop inflammatory pathology in the gut or the joints, and induction of arthritis following reintroduction of commensal gut flora supports the notion that such organisms play an important role in the pathogenesis of HLA-B27 associated disease.⁷⁸

1.1.3.2.1 Evidence of bacteria or their products in the joints

The evidence of *Chlamydia* as a most common causative agent for ReA in the joints has been provided using a number of different techniques. *Chlamydia* DNA, mRNA, rRNA, and intact *Chlamydia*-like cells (live but non-culturable) have been observed in synovial tissues and

peripheral blood.^{79,80,81,82,83,84} The presence of Chlamydial mRNA and rRNA (nucleic acids which have a half-life of minutes in tissues) indicates the occurrence of transcription and hence active multiplication of the bacteria.⁸⁰ The inverse relationship between the presence of Chlamydial DNA in the joint and synovial Chlamydia-specific lymphocyte proliferation has been found⁸⁵ suggests that an impaired T-cell response, possibly related to the expression of HLA-B27, which might be involved in the persistence of bacteria.

Attempts to cultivate viable *Yersinia* or *Salmonella* from affected joints have failed. In some studies, however, DNA of *Yersinia*, *Shigella*, or *Campylobacter* has been identified.^{86,87,88,16,89} Antigens related these bacteria have been demonstrated in samples of synovial tissue or synovial fluid from patients.^{87,88} Bacterial products such as lipopolysaccharide (LPS) of *Yersinia*, *Salmonella*, *Shigella*,^{87,86, 90} *Chlamydia trachomatis*⁹¹ and the YadA protein⁸⁸ and heat shock protein⁹² of *Yersinia* have been founded in the joints from ReA patients. Furthermore, LPS and heat shock protein of *Yersinia* have been detected in the synovial fluid and peripheral blood cells for up to 4 years in ReA patients,⁹² *Salmonella* LPS has been found in synovial tissue 2 years after initial infection⁸⁶ and the presence for several months of antibodies at high concentrations in serum samples from patients.⁹³ Above, all study indicates the persistence of bacteria or their products in the host after the onset of infection.

Bacteria or their components may reach the synovial tissues via blood vessels either as whole organisms that may circulate in the blood (bacteraemia) or within the cells as a part of immune complexes.^{16,86,83} It has been proposed that monocytes, including macrophages, may serve as a reservoir or as a transporter of bacteria to synovial tissue¹⁶ which is supported by approximately 50% of the cells that make up the lining layer are macrophages recruited from peripheral blood,⁹⁴ an important property of synovium. As tissue macrophages are differentiated from blood monocytes, bacteria or their components phagocytosed by the monocytes or macrophages at the site of infection (mucosa) or in the blood will inevitably find their way to the joints, with the dose being influenced by recruitment rates. Large joints and joints with some degree of inflammation due to mechanical stress would recruit greater numbers. Thereby, this factor might be account for the preferential involvement of large lower limb joints in ReA. Some experimental evidence also supports this notion, since intracellular bacterial fragments containing peripheral blood mononuclear cells are especially prone to bind to synovial high

endothelial venules and transmigrate through the endothelial cell monolayer.⁹⁵ In addition, bacteria engulfing monocytes can induce the expression of P-selectin on cultured endothelial cells, and this molecule is important for homing to the synovium.⁹⁶ However, the direct evidence is still lacking despite these findings that show monocytes/macrophages serve as transporters of bacterial antigens to the joints.

There is an also probability that these bacteria survive at an extra-articular site particularly in the mucosal membranes of the digestive system and/or the lymphocytic tissues, and are carried to the joint by monocytes, probably in a recurrent fashion.^{92,97,95} A recent study has showed the dynamic picture of invasion, degradation and persistence of *Yersinia* and *Salmonella* in synovial fluid.⁹⁸ In this study, Infection of synovial fluid with these bacteria was shown to start with the adhesion of the bacteria to synovial cell membrane and was followed by uptake of the morphologically intact bacteria into the cells. The bacteria showed very slow metabolic activity and started a process that finally led to the total disappearance of the bacterial cytosol after few hours of infection. This may help to partially explain the clinical feature of frequent recurrences in some ReA patients.

1.1.3.2.2 Common features of triggering bacteria

Environmental and genetic factors are involved and different aspects should be considered in the development of ReA including impaired elimination of causative microbes, the persistence of their antigens in the joints, host immune response and genetics factors like the presence of the molecule HLA-B27 (**Figure 1.2**).¹⁵ The ReA-triggering bacteria share certain some common biologic features: they are able to live intracellularly, they have LPS as an important component of the outer membrane, and they infect at a mucosal surface.⁹⁹ It is still unresolved how these different bacteria can lead to a similar clinical picture and have a similar association with HLA-B27. The identification of immunodominant antigens of these bacteria is of great importance to aid understanding of the pathogenesis. A common antigen shared by all bacteria has not yet been identified.

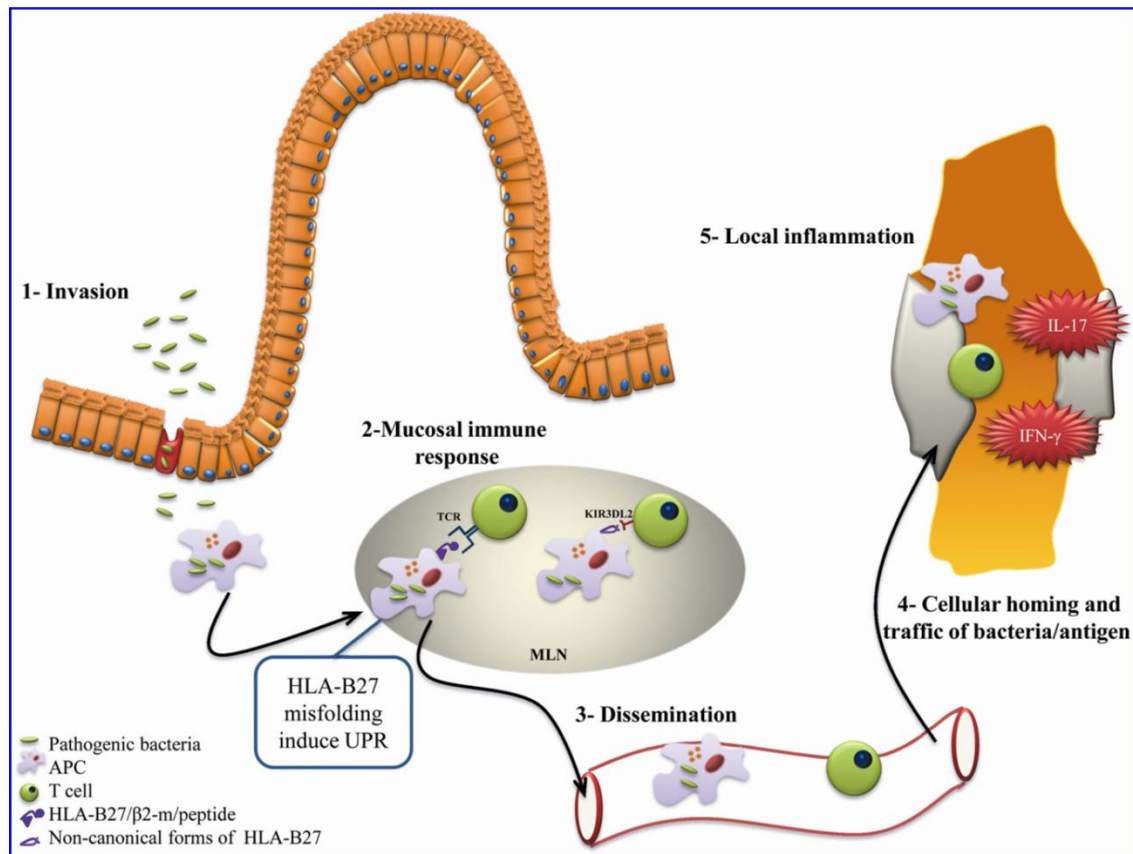


Figure 1.2: Outline for the ReA pathogenesis.¹⁵ (1) The intestinal epithelium is attached and invaded with pathogenic bacteria. HLA-B27 of antigen presenting cell (APC) such as macrophages may be involved in bacterial persistence; (2) APC could present arthritogenic peptides by HLA-B27 to CD8⁺ T cells, or HLA-B27 itself could be recognized by killer immunoglobulin receptor (KIR)3DL2 on CD4⁺ T cells in mesenteric lymph node (MLN); moreover, HLA-B27 misfolding causes an unfolded protein response (UPR); (3-4) APC with bacterial antigens or with non-active bacteria and T cells circulate within peripheral blood and eventually reach the knee joint; (5), Gut-derived APC and T-cells induce an immune response with IFN- γ and IL-17 production, recruitment of other cells and induction of mesenchymal cells activation in the target joint, which enhance and sustain inflammation.

It has been suggested that the potential immunodominant antigen has to meet four requirements: first, it needs to be expressed in the synovial microenvironment; second, it has to be conserved across several bacterial species; third, cross-reactivity must exist between human and bacterial antigens; finally, it must enable bacteria to evade the immune response.

An intensive search for the decisive arthritogenic antigen has been going on over the years and so far no one has been found. Bacterial heat shock protein (hsp)60 seems to be a major target of the T-cell response in ReA, and cross reactivity against autologous hsp60 has been discussed as a cause of autoimmunity.¹⁰⁰ However, the T cells specific for hsp60 of *Chlamydia* fail to cross-

react with hsp60 from enterobacteria.¹⁰¹ Alternative candidates have also been identified among immunodominant antigens in *Yersinia*-induced ReA, including a cationic 19-kDa urease B subunit and ribosomal protein L23. The fact that the urease subunit is highly conserved among bacteria supports the possibility that autoimmunity in ReA may be mediated by antigenic mimicry between evolutionary conserved epitopes.¹⁰²

Rather than causing autoimmunity, bacterial LPS has been documented to play an important role in the pathogenesis of ReA because it contributes greatly to the virulence of the bacteria and acts to modulate the immune system. In patients with *Salmonella* -induced ReA, the persisting humoral immune response and intra-articular antibodies are directed primarily against LPS.⁹³ In addition, LPS in synovial tissue is a potent macrophage stimulator and can induce a range of inflammatory cytokines, largely via the nuclear factor-KB (NF-kB) pathway.¹⁰³ LPS also induces the chemokine, monocyte chemoattractant protein, enhances secretion of the polymorphonuclear leukocyte chemoattractant and activating chemokine IL-8 from chondrocytes¹⁰⁴, and decreases C5aR expression on monocytes.⁸⁰ All these changes lead to the recruitment of leukocytes into the synovium and to the persistence of activated macrophages within the synovium and the ensuing chronic inflammation.

Bacterial DNA which contains more nonmethylated CpG motifs than mammalian DNA, can intensely stimulate monocytes/macrophages, and thus may also contribute to inflammation. This idea is confirmed by a study showing that experimental intra-articular injection of bacterial DNA is sufficient to induce arthritis in mice.¹⁰³

1.1.3.3 Interaction of bacteria and host in ReA

1.1.3.3.1 Humoral immune response

Although bacteria-specific antibodies are of diagnostic value, the humoral immune response does not explain the immunopathogenesis and MHC association of this disease. However, it may correlate with the severity and duration of the disease.¹⁰⁵ The production of IgM, IgG and IgA classes of antibody has been observed in *Salmonella* -triggered ReA.⁹³ The mainly humoral response is IgA (especially in enteric ReA), implying chronic stimulation of the gut mucosa.¹⁰⁶ The persistence of antibodies may indicate persistence of bacterial antigens in the arthritic patients, which also suggests an impaired cellular immunity.¹⁰⁶ Analysis of B cells isolated from

lymphoid infiltrates from synovial tissue of ReA patients suggests that B cell differentiation occurs in an antigen-driven, T cell-dependent manner.¹⁰⁷ Nevertheless, the fact that antibody responses may be absent in ReA patients indicates that they play only a secondary role in the pathogenesis of synovitis.¹⁰⁶

1.1.3.3.2 Cellular immune response

The T cells play a central role in the pathogenesis of ReA¹⁶ and antigen-specific CD4+ and CD8+ T cells have been also observed in synovial fluid of ReA patients.¹⁰⁸ The function of HLA-B27 is to present peptides to cytotoxic T cells, and HLA-B27 restricted cytotoxic T cell clones against bacterial antigens have been demonstrated in **Figure 1.3**.^{109,110,111} In addition, multiple T lymphocyte expansions are found in both the blood and synovial fluid of patients with ReA, and expansions are most commonly found in the synovial CD8+ compartment, where they appear to express both activation and memory markers.¹¹² These results suggest that HLA-B27 restricted CD8+ T cells may be pathogenic.

However, studies with HLA-B27 transgenic mice have suggested that the role of HLA-B27 in joint disease may not simply be as a restriction element for CD8+ T cells, since HLA-B27 transgenic mice lacking p2m have extremely low levels of CD8+ T cells but still develop inflammatory disease (Khare et al., 2001).¹¹³ Also induction of disease in these mice is independent of the TAP-1 gene, which is required for the loading peptide onto MHC class I molecules (Khare et al., 2001).¹¹³ In addition, adoptive transfer studies have demonstrated that CD4+ T cells are more efficient in transferring inflammatory disease than CD8+ T cells when the separate T cell subsets are transferred to nude HLA-B27+ transgenic rats.⁴⁷ These observations suggest that CD4+ T cells may be more important than CD8+ T cells in the pathogenesis of ReA. Although early studies have found predominant HLA class II restricted CD4+ responses to the triggering organisms (Figure 1.1 d),^{114,115} more recently it has been suggested that MHC II molecules are not required for disease development because MHC-II negative HLA-B27 transgenic mice still develop spontaneous disease.¹¹⁶ This raises the possibility that recognition of HLA-B27 by CD4+ T cells may be involved in disease pathogenesis. As discussed above, there is evidence that such recognition occurs as in depicted in **Figure 1.3**.^{58,68,69}

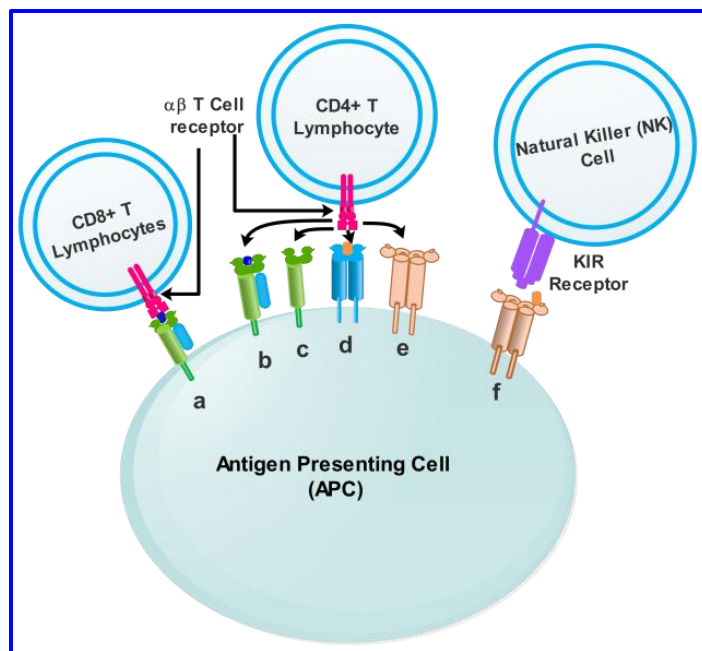


Figure 1.3: Outline for a number of possible recognitions related to HLA B-27 molecules in the pathogenesis of ReA. Recreated from Reveille et al.⁹⁹ (a) HLA-B27/b2m and peptide complex recognised by CD8+ T cells. (b) HLA-B27/b2m and peptide complex recognised by CD4+ T cells. (c) Free HLA-B27 heavy chain alone reacting with CD4+ T cells, (d) HLA class II (DR, DQ, DP) presenting HLA-B27 restricted peptide to CD4+ T cells, (e) HLA-B27 homodimers reacting with CD4+ T cells, (f) HLA-B27 homodimers recognised by receptors on NK cells

Various studies have focused on analysis of homodimers formed by free HLA-B27 heavy chain that is not associated with β_2m .^{53,54,117} Expression of these homodimers has been found on the surface of human lymphoid cell lines^{53,54} and in HLA-B27-positive patients with SpA.¹¹⁸ It has been suggested that the formation of homodimers enables the binding of an altered repertoire of antigenic peptides, or might simply resemble the MHC II molecule leading to the recognition by CD4+ T cells.⁵⁵ In addition to their classical antigen-presenting role, different forms of HLA-B27, including either classic or free heavy chain monomer or homodimers, are recognised by members of the killer immunoglobulin receptor and leukocyte immunoglobulin-like receptor families.¹¹⁹ Therefore, as the ligands for paired Ig-like receptors, which are expressed on natural killer cells, the interaction of HLA-B27 with natural killer cells has been implicated (**Figure 1.3**); exactly how this interaction contributes to the disease pathogenesis remains to be shown.

The compiled data revealed that CD4+ and CD8+ T cells might both play an essential part in the pathogenesis of ReA, while the role of HLA-B27 homodimer recognition by CD4+ T cells has drawn more recent attention.

1.1.3.3.3 Cytokines

Although in the majority of patients ReA runs a benign course, up to 15% of cases progress to chronic arthritis lasting longer than 12 months.¹²⁰ As stated before, bacterial antigens have been detected in the synovial tissues^{16,86,87} and some antigens can be found in synovial fluid and peripheral blood for up to 4 years in ReA patients.⁹² A synovial antigen-specific T cell response has been demonstrated,^{111,110} suggesting that persisting bacteria may drive the immune response locally. Another indicator for the persistence of bacteria is the high concentrations of antibodies presented in serum of ReA patients.⁹³ It is not clear why the immune system fails to eliminate these bacteria, although HLA-B27 may modulate the invasion and persistence of bacteria thus leading to the impaired immune response.¹²¹ However, secretion of the appropriate cytokines is known to be crucial for an effective immune response to eliminate bacterial infection.¹²² Among cytokines active in host defense against intracellular bacteria, Th1 and Th2 cytokines are of particular importance. Thus, the Th1 and Th2 balance have been suggested to determine the outcome of infection with the ReA-associated bacteria.¹²³ TNF- α and IFN- γ are potent antibacterial Th1 cytokines and involved in promoting cell-mediated immunity, which is required for an effective cellular immune responses against intracellular bacteria, whereas IL-4, IL-5, IL-9 and IL-13 are Th2 cytokines and more involved in the generation of humoral immunity and allergic responses. In addition, production of Th2 cytokines also has an inhibitory effect on the function of Th1 cytokines.^{124,125}

The issue of which cytokine secretion pattern predominates the milieu of synovial fluid of ReA patients is controversial. An early study showed that a Th1 cytokine pattern was predominant in synovial fluid of patients with Yersinia induced ReA,¹²⁶ which has been confirmed by another recent study.¹²⁷ High production of TNF- α and IFN- γ detected in chronic ReA supports the possible use of anti-TNF- α treatment, which has shown a promising effect in the clinic, especially for cases of chronic ReA.⁹⁹ On the contrary, impaired Th1 (TNF- α) cytokine production has also been observed to correlate with longer disease duration.¹²⁸ Concomitantly, there are some other studies suggesting that cytokines associated with Th2 subsets (such as IL-4) are prominent in the synovium of patients with ReA,^{129,122} which may delay elimination of bacteria, thus leading to persistence of the pathogen. In addition, since the disease resolves in the majority of patients with ReA (although often taking 12 months to do so),¹²⁰ another explanation

for the significance of a detectable Th2 cytokine profile in the development of disease is the appearance of anti-inflammatory Th2 cytokines, which may function to control joint inflammation.⁹⁴ This notion is supported by a study of animal models of arthritis showing that IL-4 can down regulate joint inflammation.¹³⁰ The differences in synovial tissue cytokine profiles demonstrated in the above studies are difficult to reconcile, and may relate to patient selection, sampling of the synovial tissue, or in vitro processing techniques. The underlying mechanism that determines the differentiation of T helper lymphocytes, thus resulting in a skewing of the cytokine secretion profile, is unclear. The local inflammatory milieu, the amount of IL-12 during T cell priming, differences among antigen-presenting cells (APCs) and antigen dose have been discussed as likely factors.^{131,125,132}

Another subset of CD4+ T lymphocytes producing IL-10 and TGF-p has been proposed to have a regulatory role, and an elevated level of IL-10 and TGF-p secretion has been detected in the synovial membrane of ReA patients. Whether this is a general phenomenon, and how it affects the Th1 and Th2 balance, remains to be determined.¹³³

1.2 Metabolism in inflammatory disease

1.2.1 The inflammatory process

The heat, redness, swelling and pain are classical cardinal symptoms of inflammation that characterized to acute inflammatory reaction.¹³⁴ The temporal relationships between edema, accumulation of leukocytes and accumulation of monocytes and macrophages are well established in experimental settings. These events are coupled with the release of local factors in self-limited inflammatory reactions which prevent further release of leukocytes, which allows resolution.¹³⁵ The passage from acute inflammation to chronic inflammation is widely viewed as an excess of pro-inflammatory mediators.¹³⁶

1.2.2 Metabolic consequences of inflammation

Many factors lend to the complex course of inflammatory reactions. Microbiological, immunological and toxic agents can activate the inflammatory response by activating a variety of humoral and cellular mediators. Excessive amounts of interleukins and lipid-mediators are released in the early phase of inflammation and play an important role in the pathogenesis of

organ dysfunction.¹³⁷ The membrane phospholipids release arachidonic acid (AA) during inflammatory activation which further metabolised in prostaglandins and leukotrienes. The number of strategies has been used to modulate the excessive production of lipid mediators on different levels of biochemical pathways like inhibition of phospholipase A2 which trigger the release of AA, blockade of lipoxygenase and cyclooxygenase pathways and the development of receptor antagonists against platelet activating factor and leukotrienes.¹³⁷

Some of these agents maintain protective effects in different inflammatory disorders such as septic organ failure, RA or asthma, whereas others fail to do so. Encouraging results in cardiovascular morbidity have been obtained by dietary supplementation with long chain omega-3 fatty acids like eicosapentaenoic acid (EPA).¹³⁸ EPA is released to compete with AA for enzymatic metabolism inducing the production of less inflammatory and chemotactic derivatives in an inflammatory condition.¹³⁷

During investigating the inflammation, it is crucial to take into account the many aspects of the inflammatory environment which have the potential to play a role in pathology. Hypoxia is known to be prevalent in inflammatory environments such as those associated with wounds, malignant tumors, bacterial infections, and autoimmunity.^{139,140} Enhancing hypoxia in the inflammatory site is associated with poorer disease outcome such as increased macroscopic synovitis in RA and PsA.¹⁴¹

Normal physiological oxygen levels are thought to be in between range 5-12% oxygen (compared to 21% atmospheric oxygen) but hypoxic tissue oxygen levels in pathological environments can range from as little as 0.5% oxygen to around 2.5% oxygen.¹⁴² Local hypoxia may develop as a result of either blood vessel blockage by inflamed tissues or when existing supply is insufficient for increased cellular density caused by infiltrating or proliferating inflammatory cells.¹⁴² Additionally, blockage of blood vessels by circulating phagocytes may be the reason for reducing blood flow into the inflammatory site.¹⁴³ Normal tissue structures can contribute themselves to hypoxia where they are poorly perfused, such as the synovium or the cornea. Tissue alteration associated with inflammation can lead to hypoxia by varying pressure within the blood vessels causing vessel occlusion and enhancing distances between blood vessels.^{144,145}

There is appreciable ground to support the fact that the inflamed synovium is a hypoxic environment. The tumor environment is known to be for a hypoxic condition and extensive angiogenesis reveals the requirement of the tissue to have a better oxygen supply. In RA, oxygen levels in synovial fluid have been directly measured revealing lower oxygen tensions compared with synovial fluid from osteoarthritic patients and patients with traumatic joint injuries.¹⁴⁶

The cells use an elegant cellular oxygen detection system to respond to changes in environmental oxygen. The stabilisation of the transcription factor hypoxia-inducible factor (HIF) guided by reduction of environmental oxygen which is, generally, targeted for depletion in oxygen-rich environments. HIF consists of two subunits α and β and the stability of the α subunit is regulated in an oxygen-dependent manner. Under hypoxic conditions, the HIF- α escapes degradation and dimerizes with HIF- β .¹⁴⁷ Therefore, HIF expression is implicative of hypoxic exposure which has been detected in autoimmune diseases such as RA and multiple sclerosis.^{148,149,150} HIF is known to be crucial in inflammatory development, for example, loss of HIF-1 α in macrophages is associated with impaired aggregation, motility, invasiveness and killing of bacteria.¹⁵¹

Cellular metabolism largely affected by hypoxia and HIF stabilization. By inducing the expression of glycolytic enzymes, HIF causes a preference for glycolytic metabolism over oxidative phosphorylation. This permits ATP generation to continue in the absence of sufficient oxygen albeit at a much reduced efficiency per molecule of glucose. It also accelerates the up regulation of lactate dehydrogenase A, therefore, promoting the conversion of pyruvate to lactate.¹⁵² In the case of many chronic inflammatory conditions such as in inflamed joints,^{153,154,155} multiple sclerosis,¹⁵⁶ pulmonary inflammation,¹⁵⁷ lactate has been detected and is thought to play a role in wound healing.¹⁵⁸ Conversely, an increase in lactate concentrations results in the acidosis condition and is believed to play a pathogenic role in cell transformation and autoantigen development in some inflammatory environments.¹⁵³ Hence, in metabolomics studies of disease, the detection of lactate suggests that there may be an inflammatory component to the disease being investigated which may aid future treatment and understanding. It is also generally accepted that the ReA joint is hypoxic and this may cause metabolic changes which could aid our understanding of the disease pathogenesis.

Systemic inflammation causes changes in metabolism. An indication of the strong association between metabolic processes and inflammation is seen in cachexia, the loss of cellular mass

associated with disease. The uncovering of the involvement of TNF α in this process earned it the name ‘cachexin’. TNF α is now known more generally as a mediator of inflammatory responses, thereby the ability of inflammatory cytokines to have such profound impressions on metabolic and cellular processes is informative. Rheumatoid cachexia is a consequence of chronic inflammation, and this is characterised by the preservation of fat mass and loss of muscle mass.¹⁵⁹ Classically cachexia is characterised by a low BMI. Low BMI is uncommon because of the fat mass is preserved or even increased, while muscle wasting is a common feature of RA.¹⁶⁰ Hence, RA patients may exhibit with either the classic low BMI cachexia (1-13% of RA population)¹⁶¹ or more frequently, the rheumatoid cachexia (10-20% of RA with controlled disease and 38% of patients with active RA).^{162,163}

The muscle loss that happens in rheumatoid cachexia is considered to be due to proinflammatory cytokines such as TNF, IL-1, and IL-6. TNF promotes proteolysis through the ubiquitin-proteasome pathway. The previous study has shown that cytokines may inhibit an increase in muscle protein synthesis in response to feeding (anabolic resistance).¹⁶⁴ The degree of muscle wasting is associated with the disease activity of RA in rheumatoid cachexia condition.¹⁶⁴

Low or normal levels of free testosterone are found in men and women with RA that might be contributing to rheumatoid cachexia. Population studies have revealed that obesity (particularly visceral fat accumulation) is associated with low testosterone levels. Physical activity is reduced in patients with RA, though they have a normal diet. Therefore patients with RA have a positive energy balance and tend to store fat.¹⁶⁵ This may be relevant in rheumatoid cachexia.¹⁶⁴

Metabolism is complex and is influenced by genetics and environmental factors. Systemic inflammation causes changes in metabolism and several studies have looked at individual metabolites in patients and animal models of inflammation. We therefore need to look at several metabolites together and the systemic analysis of metabolites known as metabolomics allows us to do this. Using this approach a number of metabolites have been identified in inflammatory diseases which have provided insights into the mechanisms of disease and are also potential biomarkers.

1.3 Metabolomics

Inflammation and inflammatory cytokines provoke the profound systemic and localised changes in metabolism that have been outlined above and it is not surprising that the experimental approach known as metabolomics has been used to investigate several inflammatory diseases. Metabolomics provides a ‘top down’ integrated view of complex biochemical events occurring in complex organisms by measuring the global, dynamic metabolic responses with a wide array of analytical techniques. Nuclear magnetic resonance spectroscopy (NMR) and mass spectrometry (MS) are the most commonly used analytical methods for metabolomic studies.¹⁶⁶ These techniques also help in metabolite identification by providing information on the metabolite structure.¹⁶⁷ Owing to the diversity in metabolites with different physical and chemical composition, it is practically impossible to explore the entire metabolome using a single analytical technique. Even though there is an intimate connection between genes, proteins and metabolites in a biological system, gene and protein expressions often may not directly correlate to the metabolite concentrations. This emphasise clearly the need for an additional measurement at the metabolite level and the role of metabolomics in studying gene/environment interactions.¹⁶⁸

Although classic genetics aims to relate the DNA sequences directly to the phenotype, “-omic” technologies allows to move the focus from a specific gene to the actual effect of the gene. Since it is impossible to correlate the gene or protein profiles directly to the metabolic composition, the importance of measuring small molecular weight metabolites are gaining wider attentions. By “metabolomic profiling”, it is now possible to perform quantitative and qualitative measurement of a subset of metabolites in biological samples such as body fluids and tissues. Similar to other “-omic” studies, metabolomics aims for objective and unbiased measurements of metabolite dynamics.¹⁶⁹

Metabolomic studies offer certain advantages. Being downstream in the traditional biological information cascade from genes, transcripts and proteins, metabolic perturbations will be more close to the phenotype. The metabolome is highly dynamic and changes can occur in short intervals of time (within seconds), and can thus be a rapid indicator of biological changes. Hence metabolic perturbations may have the potential for capturing early changes in clinical systems far ahead of the appearance of disease symptoms and more invasive measures are required.¹⁷⁰

A typical metabolomic study follows a common workflow.^{170,169,171} It starts with a biological question and experiment followed by sample collection. After sample preparation, appropriate analytical experiment(s) are performed to acquire data. The high density metabolic data is then subjected to pre-processing and analysis followed by biological interpretation. The analytical techniques NMR spectroscopy and MS are commonly used for metabolomics studies. Both techniques have their own advantages and disadvantages. MS is more sensitive than NMR spectroscopy while MRS is more reproducible, needs minimal sample preparation and can be performed in a non-destructive manner. Furthermore, advances in high-field clinical scanners and newer methods for in vivo NMR spectroscopy offers potential for future clinical translation of the ex vivo NMR based markers to aid in vivo diagnostics.

1.3.1 The metabolome

The complete set of small molecule chemicals found within a biological sample has been given the term “metabolome.” The term metabolome has originated as a combination of the words “metabolite” and “chromosome”. The reason for this term was to demonstrate that metabolites are indirectly encoded by genes. The term “metabolome” was first utilized in 1998 and was designed to match with existing biological terms referring to the complete set of genes (the genome), proteins (the proteome) and transcripts (the transcriptome). The study of the metabolome is called metabolomics.

We are presently unable to identify the complete set of metabolites in metabolomics unlike proteomics and genomics as identification of metabolites is still difficult and metabolite libraries cannot identify all metabolites that can presently be measured and we are presently unable to measure anything with a concentration below 5 μ M. The metabolome represents the interaction between an organism’s genome and its environment. As a result, the metabolome can act as an excellent probe of its phenotype (i.e. the product of its genotype and its environment). We are aware that genetic and environmental factors are involved in the aetiology of ReA, hence metabolomics may be a useful tool in investigating the aetiology of ReA. The rationale behind metabolomics is that changes in a disease will cause alterations in the levels of certain metabolites. To qualify as a metabolite, or to be considered to be part of the metabolome, a small molecule must typically have a molecular weight <1500 Da eg. glycolipids, polysaccharides,

short peptides and not proteins (measured by proteomics), RNA or DNA (measured by genomics).

1.3.2 Metabolomics in Inflammatory Rheumatic Disease

There is now a growing body of literature, as mentioned above, depicting metabolomic changes in inflammatory diseases, both in humans and animal models. There have been few studies looking at metabolomics in ReA. The studies looking at metabolomics in other inflammatory disease may help with our study in ReA as there appears to be several common metabolic features of inflammation. Multiple metabolites have been identified in the other inflammatory disorders using various biofluids but there is a theme of increased energy requirement with inflammation. The previous studies demonstrated that patients with RA and ReA have an increased energy requirement mainly due to the increased production of TNF.^{163,172} The studies in multiple sclerosis,¹⁷³ OA¹⁷⁴ and inflammatory lung disease¹⁵⁷ have found an increase in lactate and the studies in inflammatory eye disease¹⁷⁵ and inflammatory lung disease¹⁵⁷ have shown a reduction in glucose. The studies in RA point to the joint having a hypoxic environment^{176,177} and an association with oxidative stress.¹⁷⁸ Xanthine has been shown to distinguish RA from controls in mice¹⁷⁸ and this has also been shown in inflammatory bowel disease.¹⁷⁹

Though there are various metabolites which have been discovered in many inflammatory conditions. There are unique metabolites linked with individual disease suggesting that there may be some distinctive characteristics within the metabolic profiles of arthritis patients which may be identifiable from a metabolomic analysis and enable us to avail insights into the aetiology and pathogenesis of ReA. Metabolomics can be utilized as ‘systems medicine’ in clinical assessment with the combination of laboratory measurements through systematically and accurately identify metabolites in a meaningful manner from small quantities of biological sample. I will now discuss metabolomics in the context of inflammatory diseases in further detail.

1.3.2.1 Rheumatoid Arthritis (RA)

There are number of reasons why the inflamed synovium metabolism may be altered, namely impairment of vascularity or increased metabolic rate of the inflamed joint. Hyaluronic acid is an

essential constituent of the proteoglycan aggregate of articular cartilage which is expected for the functional integrity of the extracellular matrix. SF hyaluronate is depolymerized by the activity of reactive oxygen radical species in RA,¹⁸⁰ and hyaluronidase activity was missing in both normal and inflamed SF. Generation of reactive oxygen species plays an important role in synovial hypoxic reperfusion injury.¹⁸¹ This occurs as elevated intra-articular pressure during exercise exceeds synovial capillary perfusion pressure leading to impaired blood flow.¹⁴⁵

In 1993, the Inflammation Research Group at the London Hospital Medical College had studied the NMR profiles of RA matched SF and serum samples.¹⁷⁶ The NMR based metabolic profiles of SF were observed markedly different from their matched serum samples, and there were high levels of lactate and low levels of glucose in the SF compared to the serum. These metabolic changes were consistent with the hypoxic status of the rheumatoid joint.¹⁷⁶ Lower levels of chylomicron and very-low-density-lipoprotein associated triglycerides had been observed in all the SF samples (RA and control) compared to their matched serum samples. The SF samples also had high levels of ketone bodies compared to their matched serum samples. These results suggest that the intra-articular environment has an increased utilisation of fats for energy even though it is hypoxic.^{176,177}

Mice serum from has been used to identify a metabolite biomarker pattern associated with RA.¹⁷⁸ They found that uracil, xanthine and glycine could be used to distinguish arthritic from control animals using NMR based metabolic profiling.¹⁷⁸ The observed metabolites suggest that nucleic acid metabolism may be profoundly affected in RA and there may be an association with oxidative stress.

More recently, a research group in Denmark has worked at the plasma of RA patients.¹⁸² They found the altered metabolic profiles in RA patients compared to healthy controls and RA in remission. The identified metabolites which discriminates the active RA patients from healthy controls were cholesterol, lactate, acetylated glycoprotein and lipids. The lactate levels indicated the oxidative damage and thus indirectly reflected active inflammation. This suggests that significant changes in metabolism occurs during inflammatory processes that can be measured in the peripheral blood and metabolomics may prove useful as a measure of the extent of disease, potentially separating low disease activity states from patients in true remission.

A recent clinical study has investigated lipid profiles from patients with RA using synovial fluid.¹⁸³ They found almost 70 different lipid components which were related to anti-inflammatory and pro-resolving properties. To further categorise different types of patients with RA, traditional Chinese medicine has also been used in combination with metabolomics.¹⁸⁴ They investigated the metabolomics of urine and plasma samples and symptom profiles of patients with RA. With the combination of traditional Chinese medicine (using Cold and Heat type methodology), they have demonstrated significant biochemical differences between different subgroups of patients with RA suggesting that there are different mechanisms of disease progression and that treatments could be tailored accordingly. Metabolomic studies have also illustrated that they can predict the response to a particular treatment in RA patients.¹⁸⁵ In a study of 38 active RA patients, a significant difference of specific metabolites levels in methotrexate monotherapy response RA patients compared to non-responders was observed.¹⁸⁵

1.3.2.2 Ankylosing Spondylitis (AS)

Spondyloarthritis covers a subset of inflammatory arthritis that most notably includes ankylosing spondylitis (AS). Unfortunately, there is a considerable delay in diagnosing AS with the majority of patients who have to wait a decade from symptom onset before a diagnosis is made. According to changes in imaging results, however, MRI (magnetic resonance imaging) has successfully diagnosed. These patients could be regarded as having early AS; however, not all patients develop AS. Gao et al. were able to discriminate between a cohort of AS patients and controls.¹⁸⁶ The downregulation of vitamin D serum metabolite (23S,25R)-25-hydroxyvitamin D₃ 26,23-peroxylacetone downregulation have also shown in this study. This metabolite, downstream of 25(OH)D₃ manufacture in the kidney, may suggest an altered metabolism of vitamin D₃ with disease status but requires more investigation.¹⁸⁷

1.3.2.3 Systemic Lupus Erythematosus (SLE)

Ouyang et al. used ¹H NMR spectroscopy to discriminate the SLE (systemic lupus erythematosus) patients from RA patients and healthy controls using serum samples. They observed that the SLE serum samples were characterised by increased concentrations of N-acetyl glycoprotein, very low-density lipoprotein and low-density lipoprotein and decreased concentrations of valine, tyrosine, phenylalanine, lysine, isoleucine, histidine, glutamine, alanine, citrate, creatinine, creatine, pyruvate, high-density lipoprotein, cholesterol, glycerol, formate in

comparison with the control population. The raised levels of very low-density lipoprotein (VLDL) and low-density lipoprotein (LDL) and lower levels of high-density lipoprotein (HDL) which have been identified as the ‘lupus pattern.’ This is might be related to the inflammatory process because polyunsaturated fatty acids, such as leukotrienes or prostaglandins, are precursors of inflammatory mediators.¹⁸⁸ The decreased citrate and pyruvate levels in serum perhaps resulted from matching the energy charge in the Krebs cycle, which might suggest an increased energy demand under inflammatory conditions.

A number of researcher have further detected that lipid peroxidative damage was significantly increased in SLE,^{189,190} which is a risk factor for cardiovascular disease. These findings offer not only further insight into the pathoetiology of SLE but also highlight predicting biomarkers for diagnosis. Dai et al. demonstrated the PCA and partial least square discriminant analysis models, which are able to differentiating the SLE patients from healthy controls with a specificity and sensitivity of 97.1% and 60.9%, respectively.¹⁸⁸

1.3.3 Approaches to metabolomics

Metabolomics attempts to identify and quantify metabolites from biological samples consistently. The small molecules represent the byproduct of complex biological processes in a given cell, tissue, or organ, and thus form attractive candidates to understand disease mechanisms. Metabolites represent a various group of low molecular weight structures including lipids, amino acids, peptides, nucleic acids, and organic acids, which makes comprehensive analysis a difficult analytical challenge. The recent rapid development of a variety of analytical platforms based on NMR and mass spectrometry (MS) have enabled separation, characterization, detection, and quantification of such chemically diverse structures.

The molecular identity of metabolites cannot be derived from genomic information, unlike transcriptomics and proteomics. Thus, the identification and quantification of metabolites must depend on sophisticated instrumentation such as NMR and MS spectroscopy. Each of these technologies has its unprecedented advantages and disadvantages. Optimal selection of a particular technology relies on the specific goals of a study and is usually a compromise amongst sensitivity, selectivity, and speed.

1.3.3.1 Mass Spectrometry

MS technique has a good combination of sensitivity and selectivity. Modern MS furnishes highly specific chemical information that is directly related to the chemical and the high sensitivity of MS permits detection and measurement of very low levels of many primary and secondary metabolites. These unique advantages make MS an important tool in metabolomics.¹⁹¹

1.3.3.2 NMR spectroscopy

NMR spectroscopy was discovered in the 1940s, but with the development of higher magnetic field strengths sensitivity has improved.¹⁶⁶ NMR is non-destructive and highly selective and is generally admitted as the gold standard in metabolite structural elucidation, but it has lower sensitivity than MS. NMR is the only detection technique that does not depend on the separation of the analytes, and thereby, the sample can be recovered for further analyses.¹⁶⁶ A wide range of small molecule metabolites can be measured simultaneously hence, NMR is close to being a 'universal detector'. The primary advantages of NMR are high reproducibility and less sample preparation.¹⁹² NMR is also found to be more reliable than MS for determining concentrations of molecules.¹⁶⁶

1.6.1 NMR based Metabolomics

Nuclear Magnetic Resonance (NMR) spectroscopy is a powerful analytical technique widely used in metabolomics. By virtue of its several advantages, it is remarkably suitable for the qualitative and quantitative analysis of low molecular weight metabolites in different complex biological samples. NMR was discovered in 1946 by two independent groups of scientists: E. M. Purcell, R. V. Pound and H. C. Torrey of Harvard University and F. Bloch, W. Hansen, and M. Packard of Stanford University. The discovery first came out when it was noticed that magnetic nuclei, such as ^1H , ^{13}C and ^{31}P were able to absorb radio frequency energy when placed in a magnetic field of a strength that was specific to the nucleus. Since then, NMR has been applied to solids, liquids and gasses, kinetic and structural studies, resulting in 6 Nobel prizes being awarded in the field of chemistry.

1.6.1.1 NMR Spectroscopy

NMR Spectroscopy is an analytical technique which can detect and quantify a wide range of biochemical metabolites. All nuclei with non-zero spin have an intrinsic magnetic moment and

may be studied by NMR Spectroscopy. Spin $\frac{1}{2}$ nuclei that are commonly studied include ^1H (the most popular nucleus for NMR studies), ^{13}C , ^{19}F and ^{31}P . In contrast, the abundant isotopes of carbon and oxygen, ^{12}C and ^{16}O , have an even number of both protons and neutrons which form pairs to cancel out the individual spins and hence cannot be studied by NMR Spectroscopy. The high natural abundance of protons (^1H) in organic compounds and biological samples has made it common nuclei for magnetic resonance spectroscopy. Phosphorus NMR (^{31}P) is of particular interest for studies on phospholipid analysis and energy metabolism.¹⁹³ In the absence of an external or applied magnetic field (B_0), the nuclear spins orient randomly. However, when there is an applied magnetic field, the nuclei orient themselves with or against the larger applied field. The spin state which is parallel to the applied field has lower energy than the spin state which is antiparallel to the applied field. The energy difference ΔE between the spin states is proportional to the strength of B_0 (Figure 1.4). Spins in the lower energy states can be transferred to a higher energy state by applying an external radio frequency (RF) pulse. Following an RF pulse, spins return back to their low energy state, emitting the energy back as radio waves. This emitted energy can be detected and forms the basis of the MR signal.

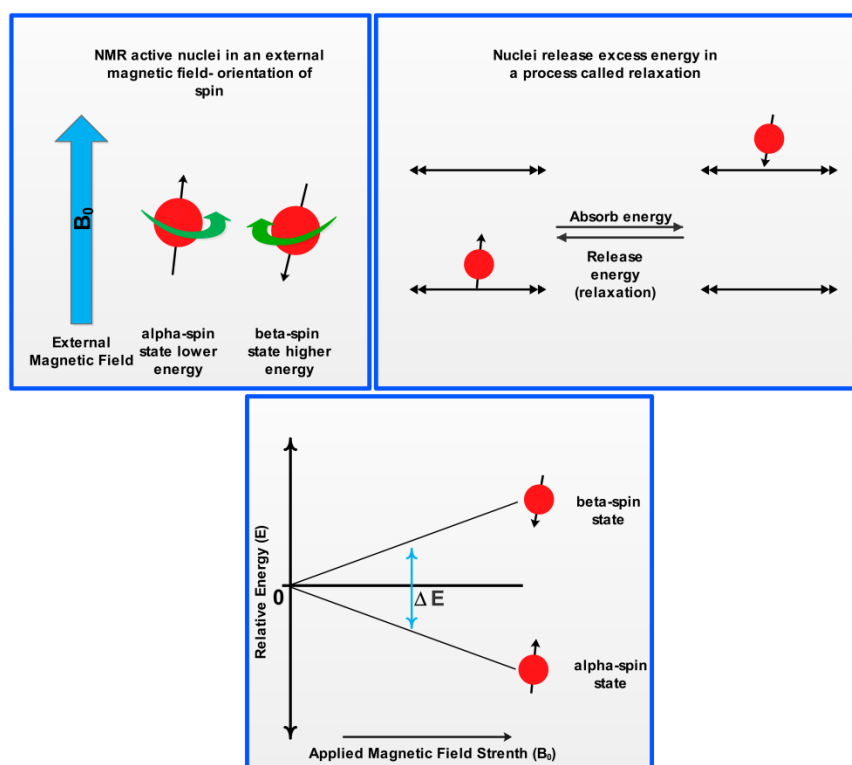


Figure 1.4: Basic principles of magnetic resonance. The figure illustrates the different spin states, energy differences and the field (B_0) frequency relationships. Figure recreated from Shung et al¹⁹⁴

A plot of intensity of MR signal versus the magnetic field frequency is known as the MR spectrum. When the spins return back to equilibrium, they go through relaxation processes characterized by two time constants called longitudinal (T1) and transverse (T2) relaxation. T1 relaxation depends on the net transfer of the energy to the environment. Larger molecules like proteins and lipids have a relatively short T1 while smaller molecules have a longer T1. The decay of transverse magnetisation (T2) depends on the dephasing of individual magnetic moments. Factors like molecular motion, viscosity, temperature, free water content, presence of paramagnetic atoms and field inhomogeneity can affect the T2. In NMR experiments, the T1 and T2 values of molecules are important in setting up the correct acquisition protocols. For obtaining accurate relative signal intensities from a sample, a recycle delay of at least five times the longest T1 has to be used, so that all nuclei can return back from their excited state to equilibrium before the subsequent excitation. Similarly large molecules have a short T2, which can be exploited to filter out the signals from macromolecules like lipids. The molecular environment around a nucleus is slightly (typically by a few parts per million) modified because of the shielding effect of the electron cloud resulting in small changes in the effective magnetic field experienced by the nucleus. This results in small changes in the resonance frequency of the given nucleus. Being very small, this shift in resonance frequency is expressed in relation to a standard reference frequency and is known as the chemical shift.

Higher magnetic field strength offers well resolved and detailed spectra of small metabolites. For example, overlapping resonances from glycerophosphocholine (GPC), phosphocholine (PCho), and free choline *in vivo*, can be studied separately at higher field strengths with *ex vivo* high-resolution NMR spectroscopy. The greater spectral resolution with increasing magnetic field strength also enhances the quantification precision.

1.3.5.2 NMR data acquisition

Metabolic data acquisition is typically performed on biofluids or tissue samples (biopsies). Typical proton spectra of filtered synovial fluid and serum from ReA patients obtained from a high resolution spectrometer (**Figure 1.5**) are comprised of sharp signals (narrow line width) from low molecular metabolites such as sugars, amino acids and small metabolites as well as broad signals from different groups of lipids and macromolecules. Most of the biological

samples contain a high proportion of water protons and the huge size of the water peak can strongly limit the dynamic range of the metabolite detection and loss of signal from low concentration substances. Hence, suppression of water signal by specialised pulse sequences that use water presaturation or excitation sculpting is commonly used to improve the signal-to-noise ratio for endogenous metabolites.¹⁹⁵ Based on the differences in spin properties of macromolecules and small metabolites, there are several spectral filtering techniques which can selectively enhance or suppress specific groups of metabolites. Macromolecules tend to have shorter T2 relaxation times and smaller diffusion coefficients than those of smaller molecules due to their longer rotational correlation times and limited translational motion. Hence it is possible to filter the MR spectra based on these properties. Smaller molecules such as endogenous metabolites present in biofluids can be observed selectively by applying spin-echo loops (Carr–Purcell–Meiboom–Gill (CPMG)), based on their longer relaxation times, prior to NMR data acquisition. This is known as T2-edited spectroscopy.¹⁹⁶

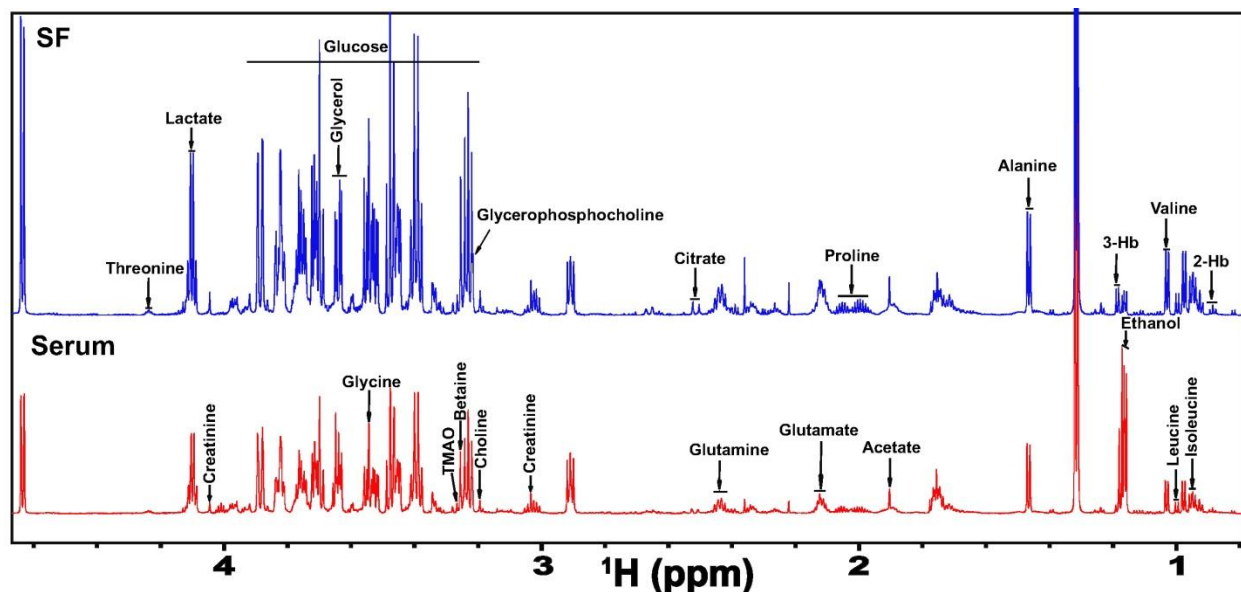


Figure 1.5: Proton magnetic resonance spectra from ReA patients: Assignments of various metabolites visible in the NMR spectra are shown. The red spectrum is from Serum and the green from Synovial fluid.

1.3.6 Data Analysis

Metabolomic experiments generate large amounts of data which needs sophisticated and powerful computational tools for proper analysis and interpretation. Multivariate data analysis techniques are able to tackle the colinearities in the NMR spectral variables and are commonly used in

metabolomic studies. Pattern recognition tools are used to analyse the large multivariate datasets. Both unsupervised and supervised techniques can be used to derive metabolic profiles.¹⁹⁷

1.3.6.2 Chemometrics

Chemometrics uses statistics and pattern recognition techniques to analyse chemical numerical data.¹⁹⁸ Metabolomics studies generate many more measured variables than there are observables (samples). Large and complex data tables are constructed that are not able to be summarised by traditional statistics.¹⁹⁹ The first stage of chemometrics involves data reduction through the process of spectral binning, whereby the spectrum is divided into smaller regions (bins) that can be compared to the bins of other spectra in the data set. For each bin, the area under the spectral curve is calculated and analysed using multivariate analysis (MVA).¹⁹⁸ Additional data processing steps, namely normalisation, and scaling, are required between data reduction and MVA to ensure fair comparisons are made.^{200,201}

1.3.6.1.1 Data Reduction

Data reduction is commonly achieved through binning (alternatively known as bucketing), whereby the spectrum is divided into smaller regions (bins) and the area under the signals contained in each bin is obtained. The binning step is required to take account of small changes in chemical shifts between samples so the same signals can be compared across spectra.

Traditionally, spectra have been divided into equal sized bins of 0.04 parts per million (ppm).^{201,202} This bin width has been used for urine because it is a good compromise between resolution and variation in peak positions.²⁰¹ All binning techniques result in a loss of information due to a reduction in the number of data points,²⁰² typically a 64k point NMR spectrum is reduced to about 250 variables (bins).²⁰³ Chemical shift variations can occur for some components, such as citrate, due to ionic strength and pH variation across the samples.²⁰¹ Variations in these factors are less prevalent for other biofluids, such as plasma and serum, but the same bin width has been conventionally adopted in many studies involving these biofluids. Some of the first studies using MVA in metabolomics used different bin widths: 0.02 ppm²⁰⁴ and 0.05 ppm.²⁰⁵ Smaller bin widths have been used in more recent studies^{206,207} because many computational limitations on data matrix sizes have been removed allowing improved

interpretation of the results by relating peaks with individual metabolites but the size is limited by peak shifting. Variable bin widths have also been employed²⁰⁸ whereby the bin width is allowed to vary by a percentage each way of a set bin width. This is aimed at accounting for small chemical shift differences by identifying local minima in the spectra and integrating a peak in a single bin²⁰⁹ which extends the advantages, and reduces the disadvantages, of smaller bin widths. However, even with adoption of variable smaller bin widths, a bin can integrate two peaks that change oppositely with, for example, disease versus control, resulting in the bin amplitude not accurately reflecting the intensity of either peak.²¹⁰

An alternative method to binning to ensure comparable signals are analysed is to perform peak alignment on the original data thus eliminating the need for data reduction and allowing full resolution data to be used in further analysis. However, the magnitude of misalignments within a single sample may not be consistent so that a simple alignment correction across an entire spectrum cannot be performed and more sophisticated computer programmes are required.²¹⁰

1.3.6.1.2 Normalisation

For each spectrum the reduced data are then normalised to accommodate concentration changes that are unrelated to the factors being investigated. Urinary volume, and hence concentration, can vary greatly whereas greater regulation occurs for plasma and serum.²⁰¹ Compared to normal urine, drug effects and food deprivation can cause dilution by a factor of ten.²¹¹ Two common normalisation procedures are constant sum and constant peak.²⁰¹ The former is the most widely employed and consists of normalising to the sum of the integrals of the whole spectrum. For every spectrum, each bin integral is divided by the total spectrum integral and the sum of all the new integrals is set to one.²¹² For all biofluids and tissues, the influence of down-regulation of certain metabolites should be approximately balanced by the up-regulation of other metabolites.²¹¹ However, this approximation can fail if certain metabolite levels change vastly, for example, the addition of a metabolite from a drug or ethanol from alcohol consumption, will cause the other peaks in the spectrum to appear to decrease because the total spectrum integral is greater.²⁰¹ Constant peak normalisation requires an internal reference compound or metabolite to be present at constant concentration. Proteins, including albumin, in plasma and serum for example, can bind nonspecifically to certain reference compounds, such as 3-

trimethylsilylpropionic acid (TSP),²¹³ and cause variation in their free concentration. An alternative method is probabilistic quotient normalisation²¹¹ whereby for each test spectrum every bin integral is divided by the integral of the same bin of a reference spectrum. The median of these quotients is calculated and the test spectrum bin integrals are divided by this value.²¹¹ This negates potential problems with highly variable metabolites that would affect constant sum normalisation.

1.3.6.1.3 Scaling

Scaling regulates the relative importance of each variable. Metabolites that have a high concentration are not always the most informative, and without scaling, variation in lower concentration metabolites would be overlooked.²¹⁴ Scaling occurs for the integral of one bin (variable) throughout the whole sample series and occurs for the variables of the entire spectrum.²⁰¹ All of the subsequent scaling methods firstly center the data to allow differences in concentrations to occur around zero instead of around the concentration mean of the metabolite resulting in the only variation being that between the samples without any offset.²¹⁵ Mean-centred scaling is just the centering process; each value of the normalised variable has the mean of the whole sample set for that normalised variable subtracted from it. Without further scaling, high concentration metabolites have a significant contribution.²¹⁶ Unit variance (UV) incorporates standard deviation into the scaling factor, whereby centered data is divided by the standard deviation of the whole sample set for that normalised variable.^{214,215} All variables have equal potential to influence the model but as a result the noise level of spectra can contribute strongly.^{216,217} The effect of pareto scaling is between that of mean centering and UV, whereby the influence of changes in the concentration of highly abundant metabolites is decreased more than that for changes in less abundant metabolites.²¹⁴ For pareto scaling, centered data is divided by the square root of the standard deviation of the whole sample set for that normalised variable.²¹⁵ Pareto scaling has been recommended for metabolomics data¹⁹⁹ but is still prone to enhancing the contribution of variables with high variance²¹⁸ and alternatives have been used.²¹⁹

1.3.6.1.4 Multivariate Analysis

MVA considers several related variables simultaneously.²²⁰ Multivariate statistical methods can be unsupervised, such as principal components analysis (PCA), or supervised, as for partial least

squares-discriminant analysis (PLS-DA). Unsupervised models are used to reveal grouping within a data set without previous knowledge of the class of individual samples, whereas supervised models use class information to produce models, from which the class of further samples can be predicted.^{221,222,223} All multivariate statistical analyses were performed using MetaboAnalyst 3.0.

1.3.6.1.4.1 Principal component analysis (PCA)

PCA is a commonly used nonsupervised technique for multivariate data exploration.²¹⁷ It reduces the dimensionality of the data and reveals the hidden structure within a dataset. The variance structure of the data is explained through linear combinations of the variables called principal components (PCs). The first PCs will be in the direction explaining most of the variance in the data set. In the score plot of the PCA, samples with a similar metabolic profile will cluster, while the corresponding loading profile displays the importance of each variable within the PC.

1.3.6.1.4.2 Partial least squares-discriminant analysis (PLS-DA)

Partial least squares is a supervised analysis method used to identify the fundamental relations between two matrices, usually the spectral data X and the clinical outcome or some other sample characteristics Y.²¹⁷ Similar to PCA, PLS is also a linear decomposition technique while it differs in the optimization problem that is solved to find a projection matrix. PLS finds projection directions for which the covariance between the data matrix or predictor variables, X, and the responses, Y is maximized. PLS models can be interpreted in a similar way as PCA models using the scores and loadings plots. PLS Discriminant Analysis (PLS-DA) consists of a classical PLS regression where the response variable is a categorical one and expresses the class memberships.

1.3.6.2 Univariate Statistics

The role of univariate analysis in metabolomics is mainly of a targeted nature. An example would be where metabolites of interest have been identified by MVSA, and detailed analysis of statistical significance of the individual metabolites is desired. Basic univariate methods can be used to analyze whether or not individual metabolites are significantly different between two classes. However, as with any statistical analysis, the distribution of the data determines the type

of analysis used. If the data are normally distributed, t-tests, z-tests, and analysis of variance (ANOVA) may be used.

The appropriate test to be used for generation of a p-value depends on the distribution of the data in the two groups that are compared. The Shapiro-Wilk test ascertains whether the values of an integral are normally distributed within each 24 groups.²²⁴ For this test, H_0 is that the data distribution is normal and H_1 is that the data distribution is not normal.

If both groups are independent and the data distribution is normal the Student's t-test can be used. This test assumes that the variances of the two groups are equal, which can be determined by the Levene's test.²²⁵ If the variances are not equal the Welch-Aspin test²²⁶ is used, a modification of the Student's t-test. If the data distribution is non-normal for one or both independent groups, the Mann-Whitney U test can be applied. The median integral values are compared instead of the means to reduce the effect of any outliers that cause the data to be non-normally distributed. If the two groups are not independent, for example, if the groups are measurements of the same patients taken from two different sample types or at two different time points, the paired samples t-test is required for normally distributed data and the Wilcoxon Matched-Pair test for non-normally distributed data.²²⁵

1.4 Summary

ReA involves a complex interaction between genes and the environment with a significant effect on systemic metabolism. As metabolism is influenced by both genetics and lifestyle analysis of metabolites may provide novel insights into the early stages of inflammatory disease.

1.5 References

1. Gaston, J. H., Reactive arthritis and undifferentiated spondyloarthritis. In *Kelley's Textbook of Rheumatology (Ninth Edition)*, Elsevier: 2013; pp 1221-1231.
2. VARTIAINEN, J.; HURRI, L., Arthritis Due to Salmonella Typhimurium: Report of 12 Cases of Migratory Arthritis in Association with Salmonella Typhimurium Infection. *Acta Medica Scandinavica* **1964**, *175* (6), 771-776.
3. Paronen, I., Reiter's Disease. A Study of 344 Cases Observed, in Finland. *Acta Medica Scandinavica* **1948**, *131* (Suppl. 212).
4. Pönkä, A.; Martio, J.; Kosunen, T., Reiter's syndrome in association with enteritis due to *Campylobacter fetus* ssp. *jejuni*. *Annals of the rheumatic diseases* **1981**, *40* (4), 414.
5. Ahvonen, P.; Sievers, K.; Aho, K., Arthritis associated with *Yersinia enterocolitica* infection. *Acta rheumatologica scandinavica* **1969**, *15* (1-4), 232-253.
6. Zeidler, H.; Mau, W.; Khan, M. A., Undifferentiated spondyloarthropathies. *Rheumatic diseases clinics of North America* **1992**, *18* (1), 187-202.
7. Dougados, M.; Linden, S. V. D.; Juhlin, R.; Huitfeldt, B.; Amor, B.; Calin, A.; Cats, A.; Dijkmans, B.; Olivieri, I.; Pasero, G., The European Spondylarthropathy Study Group preliminary criteria for the classification of spondylarthropathy. *Arthritis & Rheumatism: Official Journal of the American College of Rheumatology* **1991**, *34* (10), 1218-1227.
8. Porzio, V.; Biasi, G.; Corrado, A.; De Santi, M.; Vindigni, C.; Vrti, S.; Bayeli, P.; Marcolongo, R., Intestinal histological and ultrastructural inflammatory changes in spondyloarthropathy and rheumatoid arthritis. *Scandinavian journal of rheumatology* **1997**, *26* (2), 92-98.
9. Bas, S.; Kvien, T.; Buchs, N.; Fulpius, T.; Gabay, C., Lower level of synovial fluid interferon- γ in HLA-B27-positive than in HLA-B27-negative patients with *Chlamydia trachomatis* reactive arthritis. *Rheumatology* **2003**, *42* (3), 461-467.
10. Aggarwal, A.; Misra, R.; Chandrasekhar, S.; Prasad, K.; Dayal, R.; Ayyagari, A., Is undifferentiated seronegative spondyloarthropathy a forme fruste of reactive arthritis? *British journal of rheumatology* **1997**, *36* (9), 1001-1004.
11. Sinha, R.; Aggarwal, A.; Prasad, K.; Misra, R., Sporadic enteric reactive arthritis and undifferentiated spondyloarthropathy: evidence for involvement of *Salmonella typhimurium*. *The Journal of Rheumatology* **2003**, *30* (1), 105-113.
12. Singh, R.; Shasany, A.; Aggarwal, A.; Sinha, S.; Sisodia, B.; Khanuja, S.; Misra, R., Low molecular weight proteins of outer membrane of *Salmonella typhimurium* are immunogenic in *Salmonella* induced reactive arthritis revealed by proteomics. *Clinical & Experimental Immunology* **2007**, *148* (3), 486-493.
13. Carter, J. D.; Hudson, A. P., Reactive arthritis: clinical aspects and medical management. *Rheumatic Disease Clinics* **2009**, *35* (1), 21-44.
14. Kim, P. S.; Klausmeier, T. L.; Orr, D. P., Reactive arthritis: a review. *Journal of Adolescent Health* **2009**, *44* (4), 309-315.
15. Di Genaro, M. S.; Cargnelutti, E., Reactive arthritis: from clinical features to pathogenesis. **2013**.
16. Colmegna, I.; Cuchacovich, R.; Espinoza, L. R., HLA-B27-associated reactive arthritis: pathogenetic and clinical considerations. *Clinical Microbiology Reviews* **2004**, *17* (2), 348-369.
17. Kwiatkowska, B.; Filipowicz-Sosnowska, A., Reactive arthritis. *Pol Arch Med Wewn* **2009**, *119* (1-2), 60-65.

18. Rosner, B. M.; Werber, D.; Höhle, M.; Stark, K., Clinical aspects and self-reported symptoms of sequelae of *Yersinia enterocolitica* infections in a population-based study, Germany 2009–2010. *BMC infectious diseases* **2013**, *13* (1), 236.
19. Braun, J.; Kingsley, G.; Sieper, J., On the difficulties of establishing a consensus on the definition of and diagnostic investigations for reactive arthritis. Results and discussion of a questionnaire prepared for the 4th International Workshop on Reactive Arthritis, Berlin, Germany, July 3-6, 1999. *The Journal of rheumatology* **2000**, *27* (9), 2185-2192.
20. Hannu, T.; Mattila, L.; Nuorti, J.; Ruutu, P.; Mikkola, J.; Siitonen, A.; Leirisalo-Repo, M., Reactive arthritis after an outbreak of *Yersinia pseudotuberculosis* serotype O: 3 infection. *Annals of the rheumatic diseases* **2003**, *62* (9), 866-869.
21. Hannu, T.; Mattila, L.; Rautelin, H.; Pelkonen, P.; Lahdenne, P.; Siitonen, A.; Leirisalo-Repo, M., *Campylobacter*-triggered reactive arthritis: a population-based study. *Rheumatology* **2002**, *41* (3), 312-318.
22. Hannu, T.; Mattila, L.; Siitonen, A.; Leirisalo-Repo, M., Reactive arthritis following an outbreak of *Salmonella typhimurium* phage type 193 infection. *Annals of the rheumatic diseases* **2002**, *61* (3), 264-266.
23. Hannu, T.; Mattila, L.; Siitonen, A.; Leirisalo-Repo, M., Reactive arthritis attributable to *Shigella* infection: a clinical and epidemiological nationwide study. *Annals of the rheumatic diseases* **2005**, *64* (4), 594-598.
24. Braun, J.; Bollow, M.; Remlinger, G.; Eggens, U.; Rudwaleit, M.; Distler, A.; Sieper, J., Prevalence of spondylarthropathies in HLA-B27 positive and negative blood donors. *Arthritis & Rheumatism: Official Journal of the American College of Rheumatology* **1998**, *41* (1), 58-67.
25. Kvien, T.; Glennås, A.; Melby, K.; Granfors, K.; Andrup, O.; Karstensen, B.; Thoen, J., Reactive arthritis: incidence, triggering agents and clinical presentation. *The Journal of Rheumatology* **1994**, *21* (1), 115-122.
26. Isomäki, H.; Raunio, J.; Von Essen, R.; Hämeenkorpi, R., Incidence of inflammatory rheumatic diseases in Finland. *Scandinavian journal of rheumatology* **1978**, *7* (3), 188-192.
27. Savolainen, E.; Kaipainen-Seppänen, O.; Kröger, L.; Luosujärvi, R., Total incidence and distribution of inflammatory joint diseases in a defined population: results from the Kuopio 2000 arthritis survey. *The Journal of Rheumatology* **2003**, *30* (11), 2460-2468.
28. Hanova, P.; Pavelka, K.; Holcatova, I.; Pikhart, H., Incidence and prevalence of psoriatic arthritis, ankylosing spondylitis, and reactive arthritis in the first descriptive population-based study in the Czech Republic. *Scandinavian journal of rheumatology* **2010**, *39* (4), 310-317.
29. Söderlin, M. K.; Börjesson, O.; Kautiainen, H.; Skogh, T.; Leirisalo-Repo, M., Annual incidence of inflammatory joint diseases in a population based study in southern Sweden. *Annals of the rheumatic diseases* **2002**, *61* (10), 911-915.
30. Collantes, E.; Zarco, P.; Muñoz, E.; Juanola, X.; Mulero, J.; Fernández-Sueiro, J.; Torre-Alonso, J.; Gratacós, J.; González, C.; Batlle, E., Disease pattern of spondyloarthropathies in Spain: description of the first national registry (REGISPONSER). *Rheumatology* **2007**, *46* (8), 1309-1315.
31. De Angelis, R.; Salaffi, F.; Grassi, W.; study, o. b. o. t. M. P. P. I. G., Prevalence of spondyloarthropathies in an Italian population sample: a regional community-based study. *Scandinavian journal of rheumatology* **2007**, *36* (1), 14-21.

32. Alexeeva, L.; Krylov, M.; Vturin, V.; Mylov, N.; Erdesz, S.; Benevolenskaya, L., Prevalence of spondyloarthropathies and HLA-B27 in the native population of Chukotka, Russia. *The Journal of rheumatology* **1994**, *21* (12), 2298-2300.
33. Boyer, G.; Templin, D.; Cornoni-Huntley, J.; Everett, D.; Lawrence, R.; Heyse, S.; Miller, M.; Goring, W., Prevalence of spondyloarthropathies in Alaskan Eskimos. *The Journal of rheumatology* **1994**, *21* (12), 2292-2297.
34. Buschiazzo, E.; Maldonado-Cocco, J. A.; Arturi, P.; Citera, G.; Berman, A.; Nitsche, A.; Rillo, O. L., Epidemiology of spondyloarthritis in Argentina. *The American journal of the medical sciences* **2011**, *341* (4), 289-292.
35. Leirisalo-Repo, M.; Suoranta, H., Ten-year followup study of patients with Yersinia arthritis. *Arthritis & Rheumatism* **1988**, *31* (4), 533-537.
36. Fendler, C.; Laitko, S.; Sörensen, H.; Gripenberg-Lerche, C.; Groh, A.; Uksila, J.; Granfors, K.; Braun, J.; Sieper, J., Frequency of triggering bacteria in patients with reactive arthritis and undifferentiated oligoarthritis and the relative importance of the tests used for diagnosis. *Annals of the rheumatic diseases* **2001**, *60* (4), 337-343.
37. Townes, J. M.; Deodhar, A. A.; Laine, E. S.; Smith, K.; Krug, H. E.; Barkhuizen, A.; Thompson, M. E.; Cieslak, P. R.; Sobel, J., Reactive arthritis following culture-confirmed infections with bacterial enteric pathogens in Minnesota and Oregon: a population-based study. *Annals of the Rheumatic Diseases* **2008**, *67* (12), 1689-1696.
38. Brown, M. A.; Pile, K. D.; Kennedy, L. G.; Calin, A.; Darke, C.; Bell, J.; Wordsworth, B. P.; Cornelis, F., HLA class I associations of ankylosing spondylitis in the white population in the United Kingdom. *Annals of the rheumatic diseases* **1996**, *55* (4), 268.
39. Brewerton, D.; Hart, F. D.; Nicholls, A.; Caffrey, M.; James, D.; Sturrock, R., Ankylosing spondylitis and HL-A 27. *The Lancet* **1973**, *301* (7809), 904-907.
40. Mallas, E. G.; Mackintosh, P.; Asquith, P.; Cooke, W., Histocompatibility antigens in inflammatory bowel disease. Their clinical significance and their association with arthropathy with special reference to HLA-B27 (W27). *Gut* **1976**, *17* (11), 906-910.
41. Feldmann JL, A. B., Cazalis P, Dryll A, Hors J, Hacquart B., HL-A antigens in patients with psoriatic rheumatism. *Nouv Presse Med.* **1976**
42. Feltkamp, T., Factors involved in the pathogenesis of HLA-B27 associated arthritis. *Scandinavian Journal of Rheumatology* **1995**, *24* (sup101), 213-217.
43. Hammer, R. E.; Maika, S. D.; Richardson, J. A.; Tang, J.-P.; Taurog, J. D., Spontaneous inflammatory disease in transgenic rats expressing HLA-B27 and human β 2m: an animal model of HLA-B27-associated human disorders. *Cell* **1990**, *63* (5), 1099-1112.
44. Khare, S. D.; Luthra, H. S.; David, C. S., Spontaneous inflammatory arthritis in HLA-B27 transgenic mice lacking beta 2-microglobulin: a model of human spondyloarthropathies. *Journal of Experimental Medicine* **1995**, *182* (4), 1153-1158.
45. Taurog, J. D.; Maika, S. D.; Simmons, W. A.; Breban, M.; Hammer, R., Susceptibility to inflammatory disease in HLA-B27 transgenic rat lines correlates with the level of B27 expression. *The Journal of Immunology* **1993**, *150* (9), 4168-4178.
46. Breban, M.; Hammer, R. E.; Richardson, J. A.; Taurog, J. D., Transfer of the inflammatory disease of HLA-B27 transgenic rats by bone marrow engraftment. *Journal of Experimental Medicine* **1993**, *178* (5), 1607-1616.

47. Breban, M.; Fernandez-Sueiro, J. L.; Richardson, J. A.; Hadavand, R.; Maika, S. D.; Hammer, R. E.; Taurog, J. D., T cells, but not thymic exposure to HLA-B27, are required for the inflammatory disease of HLA-B27 transgenic rats. *The Journal of Immunology* **1996**, *156* (2), 794-803.
48. Bowness, P., HLA-B27. *Annual review of immunology* **2015**, *33*, 29-48.
49. Bjorkman, P. J.; Saper, M.; Samraoui, B.; Bennett, W. S.; Strominger, J. t.; Wiley, D., Structure of the human class I histocompatibility antigen, HLA-A2. *Nature* **1987**, *329* (6139), 506.
50. Madden, D.; Gorga, J.; Strominger, J.; Wiley, D., The structure of HLA-B27 reveals nonamer self-peptides bound in an extended conformation. *Nature* **1991**, *353* (6342), 321.
51. Madden, D. R.; Gorga, J. C.; Strominger, J. L.; Wiley, D. C., The three-dimensional structure of HLA-B27 at 2.1 Å resolution suggests a general mechanism for tight peptide binding to MHC. *Cell* **1992**, *70* (6), 1035-1048.
52. Colbert, R. A.; Rowland-Jones, S. L.; McMichael, A. J.; Frelinger, J. A., Differences in peptide presentation between B27 subtypes: The importance of the P1 side chain in maintaining high affinity peptide binding to B★ 2703. *Immunity* **1994**, *1* (2), 121-130.
53. Allen, R. L.; O'Callaghan, C. A.; McMichael, A. J.; Bowness, P., Cutting edge: HLA-B27 can form a novel β 2-microglobulin-free heavy chain homodimer structure. *The Journal of Immunology* **1999**, *162* (9), 5045-5048.
54. Bird, L. A.; Peh, C. A.; Kollnberger, S.; Elliott, T.; McMichael, A. J.; Bowness, P., Lymphoblastoid cells express HLA-B27 homodimers both intracellularly and at the cell surface following endosomal recycling. *European journal of immunology* **2003**, *33* (3), 748-759.
55. Bowness, P.; Zaccari, N.; Bird, L.; Jones, E. Y., HLA-B27 and disease pathogenesis: new structural and functional insights. *Expert reviews in molecular medicine* **1999**, *1* (16), 1-10.
56. Khan, M. A., Polymorphism of HLA-B27: 105 subtypes currently known. *Current rheumatology reports* **2013**, *15* (10), 362.
57. Benjamin, R.; Parham, P., Guilt by association: HLA-B27 and ankylosing spondylitis. *Immunology today* **1990**, *11*, 137-142.
58. Boyle, L. H.; Goodall, J. C.; Gaston, J., The recognition of abnormal forms of HLA-B27 by CD4+ T cells. *Current molecular medicine* **2004**, *4* (1), 51-58.
59. Kuon, W.; Holzhütter, H.-G.; Appel, H.; Grolms, M.; Kollnberger, S.; Traeder, A.; Henklein, P.; Weiss, E.; Thiel, A.; Lauster, R., Identification of HLA-B27-restricted peptides from the Chlamydia trachomatis proteome with possible relevance to HLA-B27-associated diseases. *The Journal of Immunology* **2001**, *167* (8), 4738-4746.
60. Dulphy, N.; Peyrat, M.-A.; Tieng, V.; Douay, C.; Rabian, C.; Tamouza, R.; Laoussadi, S.; Berenbaum, F.; Chabot, A.; Bonneville, M., Common intra-articular T cell expansions in patients with reactive arthritis: identical β -chain junctional sequences and cytotoxicity toward HLA-B27. *The Journal of Immunology* **1999**, *162* (7), 3830-3839.
61. Fiorillo, M. T.; Maragno, M.; Butler, R.; Dupuis, M. L.; Sorrentino, R., CD8+ T-cell autoreactivity to an HLA-B27-restricted self-epitope correlates with ankylosing spondylitis. *The Journal of clinical investigation* **2000**, *106* (1), 47-53.
62. Granfors, K.; Märker-Hermann, E.; De Keyser, F.; Khan, M. A.; Veys, E. M.; Yu, D. T., The cutting edge of spondylarthropathy research in the millennium. *Arthritis & Rheumatism* **2002**, *46* (3), 606-613.
63. Khan, M. A., Update on spondyloarthropathies. *Annals of Internal Medicine* **2002**, *136* (12), 896-907.

64. Kuon, W.; Kuhne, M.; Busch, D. H.; Atagunduz, P.; Seipel, M.; Wu, P.; Morawietz, L.; Fernahl, G.; Appel, H.; Weiss, E. H., Identification of novel human aggrecan T cell epitopes in HLA-B27 transgenic mice associated with spondyloarthritis. *The Journal of Immunology* **2004**, *173* (8), 4859-4866.
65. Pamer, E.; Cresswell, P., Mechanisms of MHC class I-restricted antigen processing. *Annual review of immunology* **1998**, *16* (1), 323-358.
66. Ortman, B.; Copeman, J.; Lehner, P. J.; Sadasivan, B.; Herberg, J. A.; Grandea, A. G.; Riddell, S. R.; Tampe, R.; Spies, T.; Trowsdale, J., A critical role for tapasin in the assembly and function of multimeric MHC class I-TAP complexes. *Science* **1997**, *277* (5330), 1306-1309.
67. Mear, J. P.; Schreiber, K. L.; Münz, C.; Zhu, X.; Stevanović, S.; Rammensee, H.-G.; Rowland-Jones, S. L.; Colbert, R. A., Misfolding of HLA-B27 as a result of its B pocket suggests a novel mechanism for its role in susceptibility to spondyloarthropathies. *The Journal of Immunology* **1999**, *163* (12), 6665-6670.
68. Boyle, L. H.; Goodall, J. C.; Opat, S. S.; Gaston, J. H., The recognition of HLA-B27 by human CD4+ T lymphocytes. *The Journal of Immunology* **2001**, *167* (5), 2619-2624.
69. Roddis, M.; Carter, R. W.; Sun, M.-Y.; Weissensteiner, T.; McMichael, A. J.; Bowness, P.; Bodmer, H. C., Fully functional HLA B27-restricted CD4+ as well as CD8+ T cell responses in TCR transgenic mice. *The Journal of Immunology* **2004**, *172* (1), 155-161.
70. Luthra-Guptasarma, M.; Singh, B., HLA-B27 lacking associated β 2-microglobulin rearranges to auto-display or cross-display residues 169–181: a novel molecular mechanism for spondyloarthropathies. *FEBS letters* **2004**, *575* (1-3), 1-8.
71. Uchanska-Ziegler, B.; Ziegler, A., Ankylosing spondylitis: a β 2m–deposition disease? *TRENDS in Immunology* **2003**, *24* (2), 73-76.
72. Kingsbury, D. J.; Mear, J. P.; Witte, D. P.; Taurog, J. D.; Roopenian, D. C.; Colbert, R. A., Development of spontaneous arthritis in β 2-microglobulin–deficient mice without expression of HLA–B27: Association with deficiency of endogenous major histocompatibility complex class I expression. *Arthritis & Rheumatism: Official Journal of the American College of Rheumatology* **2000**, *43* (10), 2290-2296.
73. Laitio, P.; Virtala, M.; Salmi, M.; Pelliniemi, L. J.; Yu, D. T.; Granfors, K., HLA-B27 modulates intracellular survival of *Salmonella enteritidis* in human monocytic cells. *European journal of immunology* **1997**, *27* (6), 1331-1338.
74. Ekman, P.; Saarinen, M.; He, Q.; Gripenberg-Lerche, C.; Grönberg, A.; Arvilommi, H.; Granfors, K., HLA-B27-transfected (*Salmonella* permissive) and HLA-A2-transfected (*Salmonella* nonpermissive) human monocytic U937 cells differ in their production of cytokines. *Infection and immunity* **2002**, *70* (3), 1609-1614.
75. Inman, R. D.; Payne, U., Determinants of synovial clearance of arthritogenic bacteria. *The Journal of rheumatology* **2003**, *30* (6), 1291-1297.
76. Ringrose, J. H.; Meiring, H. D.; Speijer, D.; Feltkamp, T. E.; Van Els, C. A.; De Jong, A. P.; Dankert, J., Major histocompatibility complex class I peptide presentation after *Salmonella enterica* serovar typhimurium infection assessed via stable isotope tagging of the B27-presented peptide repertoire. *Infection and immunity* **2004**, *72* (9), 5097-5105.
77. Huppertz, H.-I.; Heesemann, J., Invasion and persistence of *Salmonella* in human fibroblasts positive or negative for endogenous HLA B27. *Annals of the rheumatic diseases* **1997**, *56* (11), 671-676.

78. Taurog, J. D.; Richardson, J. A.; Croft, J.; Simmons, W. A.; Zhou, M.; Fernández-Sueiro, J. L.; Balish, E.; Hammer, R. E., The germfree state prevents development of gut and joint inflammatory disease in HLA-B27 transgenic rats. *Journal of Experimental Medicine* **1994**, *180* (6), 2359-2364.
79. Bas, S.; Griffais, R.; Kvien, T. K.; Glennås, A.; Melby, K.; Vischer, T. L., Amplification of plasmid and chromosome Chlamydia DNA in synovial fluid of patients with reactive arthritis and undifferentiated seronegative oligoarthritis. *Arthritis & Rheumatism: Official Journal of the American College of Rheumatology* **1995**, *38* (7), 1005-1013.
80. Gerard, H.; Branigan, P.; Schumacher, J. H.; Hudson, A., Synovial Chlamydia trachomatis in patients with reactive arthritis/Reiter's syndrome are viable but show aberrant gene expression. *The Journal of rheumatology* **1998**, *25* (4), 734-742.
81. Hammer, M.; Nettelbreker, E.; Hopf, S.; Schmitz, E.; Pörschke, K.; Zeidler, H., Chlamydial rRNA in the joints of patients with Chlamydia-induced arthritis and undifferentiated arthritis. *Clinical and experimental rheumatology* **1992**, *10* (1), 63-66.
82. Kuipers, J. G.; Jürgens-Saathoff, B.; Bialowons, A.; Wollenhaupt, J.; Köhler, L.; Zeidler, H., Detection of Chlamydia trachomatis in peripheral blood leukocytes of reactive arthritis patients by polymerase chain reaction. *Arthritis & Rheumatism: Official Journal of the American College of Rheumatology* **1998**, *41* (10), 1894-1895.
83. Schumacher, J. H.; Magge, S.; Cherian, P.; Sleckman, J.; Rothfuss, S.; Clayburne, G.; Sieck, M., Light and electron microscopic studies on the synovial membrane in Reiter's syndrome. Immunocytochemical identification of chlamydial antigen in patients with early disease. *Arthritis and rheumatism* **1988**, *31* (8), 937-946.
84. Taylor-Robinson, D.; Gilroy, C.; Thomas, B.; Keat, A., Detection of Chlamydia trachomatis DNA in joints of reactive arthritis patients by polymerase chain reaction. *The Lancet* **1992**, *340* (8811), 81-82.
85. Sieper, J.; Fendler, C.; Laitko, S.; Sörensen, H.; Gripenberg-Lerche, C.; Hiepe, F.; Alten, R.; Keitel, W.; Groh, A.; Uksila, J., No benefit of long-term ciprofloxacin treatment in patients with reactive arthritis and undifferentiated oligoarthritis: a three-month, multicenter, double-blind, randomized, placebo-controlled study. *Arthritis & Rheumatism: Official Journal of the American College of Rheumatology* **1999**, *42* (7), 1386-1396.
86. Granfors, K.; Jalkanen, S.; Mäki-Ikola, O.; Lahesmaa-Rantala, R.; Saario, R.; Toivanen, A.; Lindberg, A.; von Essen, R.; Isomäki, H.; Arnold, W., Salmonella lipopolysaccharide in synovial cells from patients with reactive arthritis. *The Lancet* **1990**, *335* (8691), 685-688.
87. Granfors, K.; Jalkanen, S.; von Essen, R.; Lahesmaa-Rantala, R.; Isomäki, O.; Pekkola-Heino, K.; Merilahti-Palo, R.; Saario, R.; Isomäki, H.; Toivanen, A., Yersinia antigens in synovial-fluid cells from patients with reactive arthritis. *New England Journal of Medicine* **1989**, *320* (4), 216-221.
88. Hammer, M.; Zeidler, H.; Klimsa, S.; Heesemann, J., Yersinia enterocolitica in the synovial membrane of patients with Yersinia-induced arthritis. *Arthritis & Rheumatism: Official Journal of the American College of Rheumatology* **1990**, *33* (12), 1795-1800.
89. Sibia, J.; Limbach, F., Reactive arthritis or chronic infectious arthritis? *Annals of the rheumatic diseases* **2002**, *61* (7), 580-587.
90. Granfors, K.; Jalkanen, S.; Toivanen, P.; Koski, J.; Lindberg, A., Bacterial lipopolysaccharide in synovial fluid cells in Shigella triggered reactive arthritis. *The Journal of rheumatology* **1992**, *19* (3), 500-500.

91. Jendro, M. C.; Deutsch, T.; Körber, B.; Köhler, L.; Kuipers, J. G.; Krause-Opatz, B.; Westermann, J.; Raum, E.; Zeidler, H., Infection of human monocyte-derived macrophages with *Chlamydia trachomatis* induces apoptosis of T cells: a potential mechanism for persistent infection. *Infection and immunity* **2000**, *68* (12), 6704-6711.
92. Granfors, K.; Merilahti-Palo, R.; Luukkainen, R.; Möttönen, T.; Lahesmaa, R.; Probst, P.; Märker-Hermann, E.; Toivanen, P., Persistence of *Yersinia* antigens in peripheral blood cells from patients with *Yersinia enterocolitica* O: 3 infection with or without reactive arthritis. *Arthritis & Rheumatism: Official Journal of the American College of Rheumatology* **1998**, *41* (5), 855-862.
93. Mäki-Ikola, O., Salmonella-triggered reactive arthritis: serological diagnosis and pathogenesis [thesis]. *Turku: Univ. of Turku* **1991**.
94. Gaston, J., Role of T-cells in the development of arthritis. *Clinical Science* **1998**, *95* (1), 19-31.
95. Kirveskari, J.; Jalkanen, S.; Mäki-Ikola, O.; Granfors, K., Increased synovial endothelium binding and transendothelial migration of mononuclear cells during *Salmonella* infection. *Arthritis & Rheumatism: Official Journal of the American College of Rheumatology* **1998**, *41* (6), 1054-1063.
96. Salmi, M.; Jalkanen, S., Human leukocyte subpopulations from inflamed gut bind to joint vasculature using distinct sets of adhesion molecules. *The Journal of Immunology* **2001**, *166* (7), 4650-4657.
97. Kirveskari, J.; He, Q.; Holmström, T.; Leirisalo-Repo, M.; Wuorela, M.; Mertsola, J.; Granfors, K., Modulation of peripheral blood mononuclear cell activation status during salmonella-triggered reactive arthritis. *Arthritis & Rheumatism: Official Journal of the American College of Rheumatology* **1999**, *42* (10), 2045-2054.
98. Meyer-Bahlburg, A.; Brinkhoff, J.; Krenn, V.; Trebesius, K.; Heesemann, J.; Huppertz, H.-I., Infection of synovial fibroblasts in culture by *Yersinia enterocolitica* and *Salmonella enterica* serovar Enteritidis: ultrastructural investigation with respect to the pathogenesis of reactive arthritis. *Infection and immunity* **2001**, *69* (12), 7915-7921.
99. Reveille, J. D.; Arnett, F. C., Spondyloarthritis: update on pathogenesis and management. *The American journal of medicine* **2005**, *118* (6), 592-603.
100. Sieper, J.; Braun, J.; Kingsley, G. H., Report on the Fourth International Workshop on Reactive Arthritis. *Arthritis and rheumatism* **2000**, *43* (4), 720-734.
101. Deane, K.; Jecock, R.; Pearce, J.; Gaston, J., Identification and characterization of a DR4-restricted T cell epitope within chlamydia heat shock protein 60. *Clinical & Experimental Immunology* **1997**, *109* (3), 439-445.
102. Mertz, A. K.; Daser, A.; Skurnik, M.; Wiesmüller, K.-H.; Braun, J.; Appel, H.; Batsford, S.; Wu, P.; Distler, A.; Sieper, J., The evolutionarily conserved ribosomal protein L23 and the cationic urease β -subunit of *Yersinia enterocolitica* O: 3 belong to the immunodominant antigens in *Yersinia*-triggered reactive arthritis: Implications for autoimmunity. *Molecular Medicine* **1994**, *1* (1), 44-55.
103. Deng, G.-M.; Nilsson, M.; Verdrengh, M.; Collins, L. V.; Tarkowski, A., Intra-articularly localized bacterial DNA containing CpG motifs induces arthritis. *Nature medicine* **1999**, *5* (6), 702.
104. Hill Gaston, J.; Cox, C.; Granfors, K., Clinical and experimental evidence for persistent *Yersinia* infection in reactive arthritis. *Arthritis & Rheumatism: Official Journal of the American College of Rheumatology* **1999**, *42* (10), 2239-2242.
105. Thomson, G. T.; DeRubeis, D. A.; Hodge, M. A.; Rajanayagam, C.; Inman, R. D., Post-Salmonella reactive arthritis: late clinical sequelae in a point source cohort. *The American journal of medicine* **1995**, *98* (1), 13-21.

106. Kingsley, G.; Panayi, G., Antigenic responses in reactive arthritis. *Rheumatic diseases clinics of North America* **1992**, *18* (1), 49-66.
107. Schröder, A. E.; Sieper, J.; Berek, C., Antigen-dependent B cell differentiation in the synovial tissue of a patient with reactive arthritis. *Molecular Medicine* **1997**, *3* (4), 260-272.
108. Beacock-Sharp, H.; Young, J. L.; Gaston, J. H., Analysis of T cell subsets present in the peripheral blood and synovial fluid of reactive arthritis patients. *Annals of the rheumatic diseases* **1998**, *57* (2), 100-106.
109. Hermann, E.; zum Büschenfelde, K. M.; Fleischer, B.; Yu, D., HLA-B27-restricted CD8 T cells derived from synovial fluids of patients with reactive arthritis and ankylosing spondylitis. *The Lancet* **1993**, *342* (8872), 646-650.
110. Ugrinovic, S.; Mertz, A.; Wu, P.; Braun, J.; Sieper, J., A single nonamer from the Yersinia 60-kDa heat shock protein is the target of HLA-B27-restricted CTL response in Yersinia-induced reactive arthritis. *The Journal of Immunology* **1997**, *159* (11), 5715-5723.
111. Appel, H.; Kuon, W.; Kuhne, M.; Wu, P.; Kuhlmann, S.; Kollnberger, S.; Thiel, A.; Bowness, P.; Sieper, J., Use of HLA-B27 tetramers to identify low-frequency antigen-specific T cells in Chlamydia-triggered reactive arthritis. *Arthritis Res Ther* **2004**, *6* (6), R521.
112. Allen, R.; Gillespie, G.; Hall, F.; Edmonds, S.; Hall, M.; Wordsworth, B.; McMichael, A.; Bowness, P., Multiple T cell expansions are found in the blood and synovial fluid of patients with reactive arthritis. *The Journal of rheumatology* **1997**, *24* (9), 1750-1757.
113. Khare, S. D.; Lee, S.; Bull, M.; Hanson, J.; Luthra, H.; David, C., Spontaneous inflammatory disease in HLA-B27 transgenic mice does not require transporter of antigenic peptides. *Clinical Immunology* **2001**, *98* (3), 364-369.
114. Hassell, A.; Reynolds, D.; Deacon, M.; Gaston, J.; Pearce, J., Identification of T-cell stimulatory antigens of Chlamydia trachomatis using synovial fluid-derived T-cell clones. *Immunology* **1993**, *79* (4), 513.
115. Sieper, J.; Braun, J.; Wu, P.; Kingsley, G., T cells are responsible for the enhanced synovial cellular immune response to triggering antigen in reactive arthritis. *Clinical & Experimental Immunology* **1993**, *91* (1), 96-102.
116. Khare, S. D.; Bull, M. J.; Hanson, J.; Luthra, H. S.; David, C. S., Spontaneous inflammatory disease in HLA-B27 transgenic mice is independent of MHC class II molecules: a direct role for B27 heavy chains and not B27-derived peptides. *The Journal of Immunology* **1998**, *160* (1), 101-106.
117. Kollnberger, S.; Bird, L. A.; Roddis, M.; Hacquard-Bouder, C.; Kubagawa, H.; Bodmer, H. C.; Breban, M.; McMichael, A. J.; Bowness, P., HLA-B27 heavy chain homodimers are expressed in HLA-B27 transgenic rodent models of spondyloarthritis and are ligands for paired Ig-like receptors. *The Journal of Immunology* **2004**, *173* (3), 1699-1710.
118. Kollnberger, S.; Bird, L.; Sun, M. Y.; Retiere, C.; Braud, V. M.; McMichael, A.; Bowness, P., Cell-surface expression and immune receptor recognition of HLA-B27 homodimers. *Arthritis & Rheumatism: Official Journal of the American College of Rheumatology* **2002**, *46* (11), 2972-2982.
119. Allen, R. L.; Raine, T.; Haude, A.; Trowsdale, J.; Wilson, M. J., Cutting edge: Leukocyte receptor complex-encoded immunomodulatory receptors show differing specificity for alternative HLA-B27 structures. *The Journal of Immunology* **2001**, *167* (10), 5543-5547.
120. Kohnke, S. J., Reactive Arthritis: A Clinical Approach. *Orthopaedic Nursing* **2004**, *23* (4), 274-280.

121. Saarinen, M.; Ekman, P.; Ikeda, M.; Virtala, M.; Grönberg, A.; Yu, D.; Arvilommi, H.; Granfors, K., Invasion of Salmonella into human intestinal epithelial cells is modulated by HLA-B27. *Rheumatology* **2002**, *41* (6), 651-657.
122. Yin, Z.; Braun, J.; Neure, L.; Wu, P.; Liu, L.; Eggens, U.; Sieper, J., Crucial role of interleukin-10/interleukin-12 balance in the regulation of the type 2 T helper cytokine response in reactive arthritis. *Arthritis & Rheumatism* **1997**, *40* (10), 1788-1797.
123. Yin, Z.; Braun, J.; Neure, L.; Wu, P.; Eggens, U.; Krause, A.; Kamradt, T.; Sieper, J., T cell cytokine pattern in the joints of patients with Lyme arthritis and its regulation by cytokines and anticytokines. *Arthritis & Rheumatism: Official Journal of the American College of Rheumatology* **1997**, *40* (1), 69-79.
124. Hitchon, C. A.; El-Gabalawy, H. S., Immune features of seronegative and seropositive arthritis in early synovitis studies. *Current opinion in rheumatology* **2002**, *14* (4), 348-353.
125. Paul, W. E.; Seder, R. A., Lymphocyte responses and cytokines. *Cell* **1994**, *76* (2), 241-251.
126. Schlaak, J.; Hermann, E.; Ringhoffer, M.; Probst, P.; Gallati, H.; zum Büschenfelde, K. H. M.; Fleischer, B., Predominance of Th1-type T cells in synovial fluid of patients with Yersinia-induced reactive arthritis. *European journal of immunology* **1992**, *22* (11), 2771-2776.
127. Butrimiene, I.; Jarmalaite, S.; Ranceva, J.; Venalis, A.; Jasiuleviciute, L.; Zvirbliene, A., Different cytokine profiles in patients with chronic and acute reactive arthritis. *Rheumatology* **2004**, *43* (10), 1300-1304.
128. Braun, J.; Sieper, J., Cytokines and the immunopathology of the spondyloarthropathies. *Current rheumatology reports* **1999**, *1* (1), 67-77.
129. Simon, A. K.; Seipelt, E.; Sieper, J., Divergent T-cell cytokine patterns in inflammatory arthritis. *Proceedings of the National Academy of Sciences* **1994**, *91* (18), 8562-8566.
130. Joosten, L. A.; Lubberts, E.; Durez, P.; Helsen, M. M.; Jacobs, M. J.; Goldman, M.; Van Den Berg, W. B., Role of interleukin-4 and interleukin-10 in murine collagen-induced arthritis. Protective effect of interleukin-4 and interleukin-10 treatment on cartilage destruction. *Arthritis & Rheumatism: Official Journal of the American College of Rheumatology* **1997**, *40* (2), 249-260.
131. Moser, M.; Murphy, K. M., Dendritic cell regulation of T H 1-T H 2 development. *Nature immunology* **2000**, *1* (3), 199.
132. Sher, A.; Coffman, R., Regulation of immunity to parasites by T cells and T cell-derived cytokines. *Annual review of immunology* **1992**, *10* (1), 385-409.
133. Appel, H.; Neure, L.; Kuhne, M.; Braun, J.; Rudwaleit, M.; Sieper, J., An elevated level of IL-10 and TGF β -secreting T cells, B cells and macrophages in the synovial membrane of patients with reactive arthritis compared to rheumatoid arthritis. *Clinical rheumatology* **2004**, *23* (5), 435-440.
134. Tracy, R. P., The five cardinal signs of inflammation: calor, dolor, rubor, tumor... and penuria (apologies to Aulus Cornelius Celsus, De medicina, c. AD 25). *The Journals of Gerontology Series A: Biological Sciences and Medical Sciences* **2006**, *61* (10), 1051-1052.
135. Serhan, C., Systems approach to inflammation resolution: identification of novel anti-inflammatory and pro-resolving mediators. *Journal of Thrombosis and Haemostasis* **2009**, *7*, 44-48.
136. Burger, D.; Dayer, J.-M., Inhibitory cytokines and cytokine inhibitors. *Neurology* **1995**, *45* (6 Suppl 6), S39-S43.
137. Heller, A.; Koch, T.; Schmeck, J.; van Ackern, K., Lipid mediators in inflammatory disorders. *Drugs* **1998**, *55* (4), 487-496.

138. Calder, P. C.; Yaqoob, P., Understanding omega-3 polyunsaturated fatty acids. *Postgraduate medicine* **2009**, *121* (6), 148-157.
139. Eltzschig, H. K.; Carmeliet, P., Hypoxia and inflammation. *New England Journal of Medicine* **2011**, *364* (7), 656-665.
140. Murdoch, C.; Muthana, M.; Lewis, C. E., Hypoxia regulates macrophage functions in inflammation. *The Journal of Immunology* **2005**, *175* (10), 6257-6263.
141. Ng, C.; Biniiecka, M.; Kennedy, A.; McCormick, J.; Fitzgerald, O.; Bresnihan, B.; Buggy, D.; Taylor, C.; O'sullivan, J.; Fearon, U., Synovial tissue hypoxia and inflammation in vivo. *Annals of the rheumatic diseases* **2010**, *69* (7), 1389-1395.
142. Biniiecka, M.; Kennedy, A.; Fearon, U.; Ng, C. T.; Veale, D. J.; O'sullivan, J. N., Oxidative damage in synovial tissue is associated with in vivo hypoxic status in the arthritic joint. *Annals of the rheumatic diseases* **2010**, *69* (6), 1172-1178.
143. Sitkovsky, M.; Lukashev, D., Regulation of immune cells by local-tissue oxygen tension: HIF1 α and adenosine receptors. *Nature Reviews Immunology* **2005**, *5* (9), 712.
144. Jawed, S.; Gaffney, K.; Blake, D. R., Intra-articular pressure profile of the knee joint in a spectrum of inflammatory arthropathies. *Annals of the rheumatic diseases* **1997**, *56* (11), 686-689.
145. Mapp, P.; Grootveld, M.; Blake, D., Hypoxia, oxidative stress and rheumatoid arthritis. *British medical bulletin* **1995**, *51* (2), 419-436.
146. Lund-Olesen, K., Oxygen tension in synovial fluids. *Arthritis & Rheumatism: Official Journal of the American College of Rheumatology* **1970**, *13* (6), 769-776.
147. Aro, E.; Khatri, R.; Gerard-O'Riley, R.; Mangiavini, L.; Myllyharju, J.; Schipani, E., Hypoxia-inducible factor-1 (HIF-1) but not HIF-2 is essential for hypoxic induction of collagen prolyl 4-hydroxylases in primary newborn mouse epiphyseal growth plate chondrocytes. *Journal of Biological Chemistry* **2012**, *287* (44), 37134-37144.
148. Gaber, T.; Häupl, T.; Sandig, G.; Tykwinska, K.; Fangradt, M.; Tschirschmann, M.; Hahne, M.; Dziurla, R.; Erekul, K.; Lautenbach, M., Adaptation of human CD4+ T cells to pathophysiological hypoxia: a transcriptome analysis. *The Journal of rheumatology* **2009**, *36* (12), 2655-2669.
149. Hollander, A. P.; Corke, K. P.; Freemont, A. J.; Lewis, C. E., Expression of hypoxia-inducible factor 1 α by macrophages in the rheumatoid synovium: implications for targeting of therapeutic genes to the inflamed joint. *Arthritis & Rheumatism: Official Journal of the American College of Rheumatology* **2001**, *44* (7), 1540-1544.
150. Lassmann, H., Hypoxia-like tissue injury as a component of multiple sclerosis lesions. *Journal of the neurological sciences* **2003**, *206* (2), 187-191.
151. Cramer, T.; Yamanishi, Y.; Clausen, B. E.; Förster, I.; Pawlinski, R.; Mackman, N.; Haase, V. H.; Jaenisch, R.; Corr, M.; Nizet, V., HIF-1 α is essential for myeloid cell-mediated inflammation. *Cell* **2003**, *112* (5), 645-657.
152. Wheaton, W. W.; Chandel, N. S., Hypoxia regulates cell metabolism. *American Journal of Physiology-Cell Physiology* **2010**.
153. Chang, X.; Chao, W., Glycolysis and rheumatoid arthritis. *International journal of rheumatic diseases* **2011**, *14* (3), 217-222.
154. Treuhart, P. S.; McCarty, D. J., Synovial fluid pH, lactate, oxygen and carbon dioxide partial pressure in various joint diseases. *Arthritis & Rheumatism: Official Journal of the American College of Rheumatology* **1971**, *14* (4), 475-484.

155. Kortekangas, P.; Peltola, O.; Toivanen, A.; Aro, H., Synovial fluid L-lactic acid in acute arthritis of the adult knee joint. *Scandinavian journal of rheumatology* **1995**, *24* (2), 98-101.
156. Reinke, S.; Broadhurst, D.; Sykes, B.; Baker, G.; Catz, I.; Warren, K.; Power, C., Metabolomic profiling in multiple sclerosis: insights into biomarkers and pathogenesis. *Multiple Sclerosis Journal* **2014**, *20* (10), 1396-1400.
157. Serkova, N. J.; Van Rheen, Z.; Tobias, M.; Pitzer, J. E.; Wilkinson, J. E.; Stringer, K. A., Utility of Magnetic Resonance Imaging and Nuclear Magnetic Resonance-Based Metabolomics for the Quantitation of Inflammatory Lung Injury. *American Journal of Physiology-Lung Cellular and Molecular Physiology* **2008**.
158. Trabold, O.; Wagner, S.; Wicke, C.; Scheuenstuhl, H.; Hussain, M. Z.; Rosen, N.; Seremetiev, A.; Becker, H. D.; Hunt, T. K., Lactate and oxygen constitute a fundamental regulatory mechanism in wound healing. *Wound Repair and Regeneration* **2003**, *11* (6), 504-509.
159. Evans, W. J.; Morley, J. E.; Argilés, J.; Bales, C.; Baracos, V.; Guttridge, D.; Jatoi, A.; Kalantar-Zadeh, K.; Lochs, H.; Mantovani, G., Cachexia: a new definition. *Clinical nutrition* **2008**, *27* (6), 793-799.
160. Summers, G.; Deighton, C.; Rennie, M.; Booth, A., Rheumatoid cachexia: a clinical perspective. *Rheumatology* **2008**, *47* (8), 1124-1131.
161. Munro, R.; Capell, H., Prevalence of low body mass in rheumatoid arthritis: association with the acute phase response. *Annals of the rheumatic diseases* **1997**, *56* (5), 326-329.
162. Engvall, I. L.; Elkan, A. C.; Tengstrand, B.; Cederholm, T.; Brismar, K.; Hafström, I., Cachexia in rheumatoid arthritis is associated with inflammatory activity, physical disability, and low bioavailable insulin-like growth factor. *Scandinavian journal of rheumatology* **2008**, *37* (5), 321-328.
163. Metsios, G. S.; Stavropoulos-Kalinoglou, A.; Nevill, A. M.; Douglas, K. M.; Koutedakis, Y.; Kitas, G. D., Cigarette smoking significantly increases basal metabolic rate in patients with rheumatoid arthritis. *Annals of the Rheumatic Diseases* **2008**, *67* (1), 70-73.
164. Summers, G. D.; Metsios, G. S.; Stavropoulos-Kalinoglou, A.; Kitas, G. D., Rheumatoid cachexia and cardiovascular disease. *Nature Reviews Rheumatology* **2010**, *6* (8), 445.
165. Metsios, G. S.; Stavropoulos-Kalinoglou, A.; Veldhuijzen van Zanten, J.; Treharne, G.; Panoulas, V. F.; Douglas, K. M.; Koutedakis, Y.; Kitas, G. D., Rheumatoid arthritis, cardiovascular disease and physical exercise: a systematic review. *Rheumatology* **2007**, *47* (3), 239-248.
166. Nicholson, J. K.; Lindon, J. C., Systems biology: metabonomics. *Nature* **2008**, *455* (7216), 1054.
167. Saito, K.; Matsuda, F., Metabolomics for functional genomics, systems biology, and biotechnology. *Annual review of plant biology* **2010**, *61*, 463-489.
168. Mayr, M., Metabolomics: ready for the prime time? *Circulation: Cardiovascular Genetics* **2008**, *1* (1), 58-65.
169. Mamas, M.; Dunn, W. B.; Neyses, L.; Goodacre, R., The role of metabolites and metabolomics in clinically applicable biomarkers of disease. *Archives of toxicology* **2011**, *85* (1), 5-17.
170. Dunn, W. B.; Broadhurst, D. I.; Atherton, H. J.; Goodacre, R.; Griffin, J. L., Systems level studies of mammalian metabolomes: the roles of mass spectrometry and nuclear magnetic resonance spectroscopy. *Chemical Society Reviews* **2011**, *40* (1), 387-426.
171. Brown, M.; Dunn, W. B.; Ellis, D. I.; Goodacre, R.; Handl, J.; Knowles, J. D.; O'Hagan, S.; Spasić, I.; Kell, D. B., A metabolome pipeline: from concept to data to knowledge. *Metabolomics* **2005**, *1* (1), 39-51.

172. Saxne, T.; Palladino Jr, M.; Heinegard, D.; Talal, N.; Wollheim, F., Detection of tumor necrosis factor α but not tumor necrosis factor β in rheumatoid arthritis synovial fluid and serum. *Arthritis & Rheumatism: Official Journal of the American College of Rheumatology* **1988**, *31* (8), 1041-1045.
173. Nicoli, F.; Vion-Dury, J.; Confort-Gouny, S.; Maillet, S.; Gastaut, J.-L.; Cozzone, P. J., Cerebrospinal fluid metabolic profiles in multiple sclerosis and degenerative dementias obtained by high resolution proton magnetic resonance spectroscopy. *Comptes rendus de l'Academie des sciences. Serie III, Sciences de la vie* **1996**, *319* (7), 623-631.
174. Damyanovich, A.; Staples, J.; Chan, A.; Marshall, K., Comparative study of normal and osteoarthritic canine synovial fluid using 500 MHz ^1H magnetic resonance spectroscopy. *Journal of Orthopaedic Research* **1999**, *17* (2), 223-231.
175. Young, S. P.; Nessim, M.; Falciani, F.; Trevino, V.; Banerjee, S. P.; Scott, R. A.; Murray, P. I.; Wallace, G. R., Metabolomic analysis of human vitreous humor differentiates ocular inflammatory disease. *Molecular vision* **2009**, *15*, 1210.
176. Naughton, D.; Whelan, M.; Smith, E. C.; Williams, R.; Blake, D. R.; Grootveld, M., An investigation of the abnormal metabolic status of synovial fluid from patients with rheumatoid arthritis by high field proton nuclear magnetic resonance spectroscopy. *FEBS letters* **1993**, *317* (1-2), 135-138.
177. Naughton, D. P.; Haywood, R.; Blake, D. R.; Edmonds, S.; Hawkes, G. E.; Grootveld, M., A comparative evaluation of the metabolic profiles of normal and inflammatory knee-joint synovial fluids by high resolution proton NMR spectroscopy. *FEBS letters* **1993**, *332* (3), 221-225.
178. Weljie, A. M.; Dowlatbadi, R.; Miller, B. J.; Vogel, H. J.; Jirik, F. R., An inflammatory arthritis-associated metabolite biomarker pattern revealed by ^1H NMR spectroscopy. *Journal of proteome research* **2007**, *6* (9), 3456-3464.
179. Schicho, R.; Shaykhutdinov, R.; Ngo, J.; Nazyrova, A.; Schneider, C.; Panaccione, R.; Kaplan, G. G.; Vogel, H. J.; Storr, M., Quantitative metabolomic profiling of serum, plasma, and urine by ^1H NMR spectroscopy discriminates between patients with inflammatory bowel disease and healthy individuals. *Journal of proteome research* **2012**, *11* (6), 3344-3357.
180. Parkes, H. G.; Grootveld, M. C.; Henderson, E. B.; Farrell, A.; Blake, D. R., Oxidative damage to synovial fluid from the inflamed rheumatoid joint detected by ^1H NMR spectroscopy. *Journal of pharmaceutical and biomedical analysis* **1991**, *9* (1), 75-82.
181. Farrell, A. J.; Williams, R. B.; Stevens, C. R.; Lawrie, A.; Cox, N.; Blake, D., Exercise induced release of von Willebrand factor: evidence for hypoxic reperfusion microvascular injury in rheumatoid arthritis. *Annals of the rheumatic diseases* **1992**, *51* (10), 1117-1122.
182. Lauridsen, M. B.; Bliddal, H.; Christensen, R.; Danneskiold-Samsøe, B.; Bennett, R.; Keun, H.; Lindon, J. C.; Nicholson, J. K.; Dorff, M. H.; Jaroszewski, J. W., ^1H NMR spectroscopy-based interventional metabolic phenotyping: a cohort study of rheumatoid arthritis patients. *Journal of proteome research* **2010**, *9* (9), 4545-4553.
183. Giera, M.; Ioan-Facsinay, A.; Toes, R.; Gao, F.; Dalli, J.; Deelder, A. M.; Serhan, C. N.; Mayboroda, O. A., Lipid and lipid mediator profiling of human synovial fluid in rheumatoid arthritis patients by means of LC-MS/MS. *Biochimica et Biophysica Acta (BBA)-Molecular and Cell Biology of Lipids* **2012**, *1821* (11), 1415-1424.
184. van Wietmarschen, H. A.; Dai, W.; van der Kooij, A. J.; Reijmers, T. H.; Schroen, Y.; Wang, M.; Xu, Z.; Wang, X.; Kong, H.; Xu, G., Characterization of rheumatoid arthritis subtypes using symptom profiles, clinical chemistry and metabolomics measurements. *PloS one* **2012**, *7* (9), e44331.

185. Wang, Z.; Chen, Z.; Yang, S.; Wang, Y.; Yu, L.; Zhang, B.; Rao, Z.; Gao, J.; Tu, S., ¹H NMR-based metabolomic analysis for identifying serum biomarkers to evaluate methotrexate treatment in patients with early rheumatoid arthritis. *Experimental and therapeutic medicine* **2012**, *4* (1), 165-171.
186. Gao, P.; Lu, C.; Zhang, F.; Sang, P.; Yang, D.; Li, X.; Kong, H.; Yin, P.; Tian, J.; Lu, X., Integrated GC-MS and LC-MS plasma metabonomics analysis of ankylosing spondylitis. *Analyst* **2008**, *133* (9), 1214-1220.
187. Fischer, R.; Trudgian, D. C.; Wright, C.; Thomas, G.; Bradbury, L. A.; Brown, M. A.; Bowness, P.; Kessler, B. M., Discovery of candidate serum proteomic and metabolomic biomarkers in ankylosing spondylitis. *Molecular & cellular proteomics* **2012**, *11* (2), M111. 013904.
188. Ouyang, X.; Dai, Y.; Wen, J.; Wang, L., ¹H NMR-based metabolomic study of metabolic profiling for systemic lupus erythematosus. *Lupus* **2011**, *20* (13), 1411-1420.
189. Michel, P.; Eggert, W.; Albrecht-Nebe, H.; Grune, T., Increased lipid peroxidation in children with autoimmune diseases. *Acta Paediatrica* **1997**, *86* (6), 609-612.
190. Serban, M.; Tănăseanu, S., Lipid peroxidation in autoimmune systemic vasculitides. Effect of corticoid treatment on lipid peroxidation. Antioxidant protection with vitamin E. *Romanian journal of internal medicine= Revue roumaine de medecine interne* **1994**, *32* (2), 137-142.
191. Lei, Z.; Huhman, D. V.; Sumner, L. W., Mass spectrometry strategies in metabolomics. *Journal of Biological Chemistry* **2011**, *286* (29), 25435-25442.
192. Beckonert, O.; Keun, H. C.; Ebbels, T. M.; Bundy, J.; Holmes, E.; Lindon, J. C.; Nicholson, J. K., Metabolic profiling, metabolomic and metabonomic procedures for NMR spectroscopy of urine, plasma, serum and tissue extracts. *Nature protocols* **2007**, *2* (11), 2692.
193. Louis, D. N.; Ohgaki, H.; Wiestler, O. D.; Cavenee, W. K.; Burger, P. C.; Jouvett, A.; Scheithauer, B. W.; Kleihues, P., The 2007 WHO classification of tumours of the central nervous system. *Acta neuropathologica* **2007**, *114* (2), 97-109.
194. Shung, K. K.; Smith, M.; Tsui, B. M., *Principles of medical imaging*. Academic Press: 2012.
195. Beckonert, O.; Coen, M.; Keun, H. C.; Wang, Y.; Ebbels, T. M.; Holmes, E.; Lindon, J. C.; Nicholson, J. K., High-resolution magic-angle-spinning NMR spectroscopy for metabolic profiling of intact tissues. *Nature protocols* **2010**, *5* (6), 1019.
196. Meiboom, S.; Gill, D., Modified spin-echo method for measuring nuclear relaxation times. *Review of scientific instruments* **1958**, *29* (8), 688-691.
197. Griffin, J. L.; Shockcor, J. P., Metabolic profiles of cancer cells. *Nature reviews cancer* **2004**, *4* (7), 551.
198. Wishart, D. S., Quantitative metabolomics using NMR. *TrAC trends in analytical chemistry* **2008**, *27* (3), 228-237.
199. Trygg, J.; Holmes, E.; Lundstedt, T., Chemometrics in metabonomics. *Journal of proteome research* **2007**, *6* (2), 469-479.
200. Hollywood, K.; Brison, D. R.; Goodacre, R., Metabolomics: current technologies and future trends. *Proteomics* **2006**, *6* (17), 4716-4723.
201. Craig, A.; Cloarec, O.; Holmes, E.; Nicholson, J. K.; Lindon, J. C., Scaling and normalization effects in NMR spectroscopic metabonomic data sets. *Analytical chemistry* **2006**, *78* (7), 2262-2267.
202. Anderson, P. E.; Reo, N. V.; DelRaso, N. J.; Doom, T. E.; Raymer, M. L., Gaussian binning: a new kernel-based method for processing NMR spectroscopic data for metabolomics. *Metabolomics* **2008**, *4* (3), 261-272.

203. Weljie, A. M.; Newton, J.; Mercier, P.; Carlson, E.; Slupsky, C. M., Targeted profiling: quantitative analysis of 1H NMR metabolomics data. *Analytical chemistry* **2006**, 78 (13), 4430-4442.
204. Holmes, E.; Foxall, P.; Nicholson, J.; Neild, G.; Brown, S.; Beddell, C.; Sweatman, B.; Rahr, E.; Lindon, J.; Spraul, M., Automatic data reduction and pattern recognition methods for analysis of 1H nuclear magnetic resonance spectra of human urine from normal and pathological states. *Analytical biochemistry* **1994**, 220 (2), 284-296.
205. Spraul, M.; Neidig, P.; Klauck, U.; Kessler, P.; Holmes, E.; Nicholson, J.; Sweatman, B.; Salman, S.; Farrant, R.; Rahr, E., Automatic reduction of NMR spectroscopic data for statistical and pattern recognition classification of samples. *Journal of pharmaceutical and biomedical analysis* **1994**, 12 (10), 1215-1225.
206. Loo, R. L.; Coen, M.; Ebbels, T.; Cloarec, O.; Maibaum, E.; Bictash, M.; Yap, I.; Elliott, P.; Stamler, J.; Nicholson, J. K., Metabolic profiling and population screening of analgesic usage in nuclear magnetic resonance spectroscopy-based large-scale epidemiologic studies. *Analytical chemistry* **2009**, 81 (13), 5119-5129.
207. Teahan, O.; Gamble, S.; Holmes, E.; Waxman, J.; Nicholson, J. K.; Bevan, C.; Keun, H. C., Impact of analytical bias in metabolomic studies of human blood serum and plasma. *Analytical chemistry* **2006**, 78 (13), 4307-4318.
208. Salek, R. M.; Maguire, M. L.; Bentley, E.; Rubtsov, D. V.; Hough, T.; Cheeseman, M.; Nunez, D. J.; Sweatman, B. C.; Haselden, J. N.; Cox, R., A metabolomic comparison of urinary changes in type 2 diabetes in mouse, rat and man. *Physiological genomics* **2007**.
209. Beger, R. D.; Schnackenberg, L. K.; Holland, R. D.; Li, D.; Dragan, Y., Metabolomic models of human pancreatic cancer using 1D proton NMR spectra of lipids in plasma. *Metabolomics* **2006**, 2 (3), 125-134.
210. Jahns, G. L.; Kent, M. N.; Burgoon, L. D.; DelRaso, N.; Zacharewski, T. R.; Reo, N. V., Development of analytical methods for NMR spectra and application to a 13 C toxicology study. *Metabolomics* **2009**, 5 (2), 253-262.
211. Dieterle, F.; Ross, A.; Schlotterbeck, G.; Senn, H., Probabilistic quotient normalization as robust method to account for dilution of complex biological mixtures. Application in 1H NMR metabolomics. *Analytical chemistry* **2006**, 78 (13), 4281-4290.
212. Webb-Robertson, B.-J. M.; Lowry, D. F.; Jarman, K. H.; Harbo, S. J.; Meng, Q. R.; Fuciarelli, A. F.; Pounds, J. G.; Lee, K. M., A study of spectral integration and normalization in NMR-based metabolomic analyses. *Journal of pharmaceutical and biomedical analysis* **2005**, 39 (3-4), 830-836.
213. Sheedy, J. R.; Ebeling, P. R.; Gooley, P. R.; McConville, M. J., A sample preparation protocol for 1H nuclear magnetic resonance studies of water-soluble metabolites in blood and urine. *Analytical biochemistry* **2010**, 398 (2), 263-265.
214. Keun, H. C.; Ebbels, T. M.; Antti, H.; Bollard, M. E.; Beckonert, O.; Holmes, E.; Lindon, J. C.; Nicholson, J. K., Improved analysis of multivariate data by variable stability scaling: application to NMR-based metabolic profiling. *Analytica chimica acta* **2003**, 490 (1-2), 265-276.
215. van den Berg, R. A.; Hoefsloot, H. C.; Westerhuis, J. A.; Smilde, A. K.; van der Werf, M. J., Centering, scaling, and transformations: improving the biological information content of metabolomics data. *BMC genomics* **2006**, 7 (1), 142.
216. Holmes, E.; Cloarec, O.; Nicholson, J., Probing latent biomarker signatures and in vivo pathway activity in experimental disease states via statistical total correlation spectroscopy (STOCSY) of biofluids: application to HgCl₂ toxicity. *Journal of proteome research* **2006**, 5 (6), 1313-1320.

217. Constantinou, M. A.; Papakonstantinou, E.; Spraul, M.; Sevastiadou, S.; Costalos, C.; Koupparis, M. A.; Shulpis, K.; Tsantili-Kakoulidou, A.; Mikros, E., 1H NMR-based metabonomics for the diagnosis of inborn errors of metabolism in urine. *Analytica Chimica Acta* **2005**, *542* (2), 169-177.
218. Cloarec, O.; Dumas, M. E.; Trygg, J.; Craig, A.; Barton, R. H.; Lindon, J. C.; Nicholson, J. K.; Holmes, E., Evaluation of the orthogonal projection on latent structure model limitations caused by chemical shift variability and improved visualization of biomarker changes in 1H NMR spectroscopic metabonomic studies. *Analytical chemistry* **2005**, *77* (2), 517-526.
219. Parsons, H. M.; Ludwig, C.; Günther, U. L.; Viant, M. R., Improved classification accuracy in 1- and 2-dimensional NMR metabolomics data using the variance stabilising generalised logarithm transformation. *BMC bioinformatics* **2007**, *8* (1), 234.
220. Manly, B. F., *Randomization, bootstrap and Monte Carlo methods in biology*. Chapman and Hall/CRC: 2006.
221. Westerhuis, J. A.; Hoefsloot, H. C.; Smit, S.; Vis, D. J.; Smilde, A. K.; van Velzen, E. J.; van Duijnhoven, J. P.; van Dorsten, F. A., Assessment of PLSDA cross validation. *Metabolomics* **2008**, *4* (1), 81-89.
222. Brindle, J. T.; Nicholson, J. K.; Schofield, P. M.; Grainger, D. J.; Holmes, E., Application of chemometrics to 1 H NMR spectroscopic data to investigate a relationship between human serum metabolic profiles and hypertension. *Analyst* **2003**, *128* (1), 32-36.
223. Lee, K. R.; Lin, X.; Park, D. C.; Eslava, S., Megavariate data analysis of mass spectrometric proteomics data using latent variable projection method. *Proteomics* **2003**, *3* (9), 1680-1686.
224. Shapiro, S. S.; Wilk, M. B., An analysis of variance test for normality (complete samples). *Biometrika* **1965**, *52* (3/4), 591-611.
225. Bland, M., *An introduction to medical statistics*. Oxford University Press (UK): 2015.
226. Aspin, A. A.; Welch, B., Tables for use in comparisons whose accuracy involves two variances, separately estimated. *Biometrika* **1949**, *36* (3/4), 290-296.

Chapter-3

Metabolite assignment of Ultra-Filtered Synovial Fluid extracted from knee joints of Reactive Arthritis patients using High Resolution NMR Spectroscopy

Durgesh Dubey, Smriti Chaurasia, Anupam Guleria, Sandeep Kumar, Dinesh Raj Modi,

Ramnath Misra and Dinesh Kumar

Magn Reson Chem. 2018;1–14.

CONTENTS-

2.1 Abstract

2.2 Introduction

2.3 Materials and Method

2.3.1 Sample Collection

2.3.2 NMR Spectroscopy

2.3.3 Multivariate analysis

2.3.4 Identification of Metabolites in SF Samples

2.4 Result and discussion

2.5 Concluding remarks

2.6 Acknowledgment

2.7 References

2.1 Abstract

Currently, there are no reliable clinical biomarkers available that can aid early differential diagnosis of reactive arthritis (ReA) from other inflammatory joint diseases. Metabolic profiling of synovial fluid (SF) –obtained from joints affected in ReA- holds great promise in this regard and will further aid monitoring treatment and improving our understanding about disease mechanism. As a first step in this direction, we report here the metabolite specific assignment of ^1H and ^{13}C resonances detected in the NMR spectra of SF samples extracted from human patients with established ReA. The metabolite characterization has been carried out on both normal as well as on ultra-filtered (deproteinized) SF samples of eight ReA patients (n=8) using high resolution (800 MHz) ^1H and ^1H - ^{13}C NMR spectroscopy methods such as one-dimensional (1D) ^1H CPMG and two-dimensional (2D) J-resolved ^1H NMR and homonuclear ^1H - ^1H TOCSY and heteronuclear ^1H - ^{13}C HSQC correlation spectra. Compared to normal SF samples, several distinctive ^1H NMR signals were identified and assigned to metabolites in the ^1H NMR spectra of ultra-filtered SF samples. Overall, we assigned 53 metabolites in normal filtered SF and 64 metabolites in filtered pooled SF sample compared to non-filtered SF samples for which only 48 metabolites (including lipid/membrane metabolites as well) have been identified. The established NMR characterization of SF metabolites will serve to guide future metabolomics studies aiming to identify/evaluate the SF based metabolic biomarkers of diagnostic/prognostic potential or seeking biochemical insights into disease mechanisms in a clinical perspective.

2.2 Introduction:

Differential biomarkers are becoming clinically essential for timely diagnosis and predicting prognosis of rheumatic diseases and subsequent treatment monitoring.¹ Reactive arthritis (ReA) is an autoimmune rheumatic condition that develops in response to an infection by certain bacteria in the genitals (especially with *Chlamydia trachomatis*) or gastrointestinal (GI) infections with *Campylobacter*, *Salmonella*, *Shigella* and *Yersinia*.²⁻⁶ The diagnosis is largely based on few clinical symptoms (including positive serological demonstration of antibodies directed against specific bacteria), but the clinical picture is mainly dominated by Rheumatoid arthritis (RA) like features.^{2,7} Currently, there are no reliable biomarkers in the serum available to differentiate ReA from RA and other inflammatory joint conditions. Therefore, there is an immense interest to discover molecular biomarkers for rapid differential diagnosis of ReA from RA and to further use them for treatment monitoring.

Metabolomics –an analytical approach used to reveal altered metabolism- is becoming a mutually complementary technique to genomics, transcriptomics and proteomics for comprehensive analysis of biological systems in health and disease.⁸⁻¹² Recent, developments in analytical hardware technology and softwares have turned it into an extremely powerful laboratory methodology that has increasingly been used virtually in all aspects of biomedical and clinical research today. Currently, the most information-rich techniques used in metabolomics studies are Liquid chromatography Mass spectrometry (LC-MS), Gas chromatography Mass spectrometry (GC-MS) and nuclear magnetic resonance (NMR); each brings its own advantages and limitations.¹³ Of them, NMR based metabolomics approach has shown considerable promise in disease diagnosis and biomarker discovery because it is particularly very simple (as it requires little or no sample preparation), non-destructive and provides highly reproducible results. Therefore, it has extensively been used in the recent past for disease metabotyping of various rheumatic diseases involving joint inflammation.¹⁴⁻³³ The metabolomics studies often involve both quantitative and comparative analysis of essentially all low molecular weight metabolites and their intermediates in affected biological systems (typically urine, blood plasma/serum, cell lysates, or tissue extracts).^{12, 34-36}

For majority of ReA and RA patients involving articular cartilage/joint inflammation, the extraction of synovial fluid (SF) remains a part of clinical procedure due to SF accumulation in the joints. As SF remains in direct contact with the cartilage and other connective tissues affected in RDs, therefore, it is very likely that the disease related metabolic changes will first accumulate

in the SF before they can be detected in the serum. In other words, the metabolic profiling of SF reflects directly what is happening in a joint and thus is most relevant for disease metabotyping. Based on this assumption, a number of metabolomics studies involving SF samples have been carried out in the past to identify and appraise the clinical utility of metabolic biomarkers.^{1, 14, 19, 20, 22-28, 30, 32, 37} However, so far, no studies have been performed to establish the metabolic patterns of SF in ReA patients and if they differ from those in RA. The distinctive SF metabolic patterns of ReA and RA are important not only to improve the differential diagnosis of ReA and RA, but further to elaborate our understanding about pathophysiological processes dominating in septic and non-septic arthritis conditions. Overall, the metabolomics analysis of synovial fluid holds a great promise to identify disease specific metabolic signatures. Currently, in our lab, we are involved in disease metabotyping of ReA using NMR based metabolomics of SF samples and the present study is a part of this endeavour. The 1D proton (¹H) Nuclear magnetic resonance (NMR) spectroscopy is one of the two most widely used analytical platforms -other being the mass spectrometry (MS)- for metabolic profiling of biological fluids affected in diseased conditions such as blood, urine, bile, cerebrospinal fluid, , synovial fluid, and biopsied/surgical tissue or cell extracts. Specifically, the SF samples can be analysed by NMR either directly in their nearly native condition or after filtering out the proteins (deproteinization) and other higher molecular weight species (like lipoproteins and fats). Though the Carr-Purcell-Meiboom-Gill (CPMG) echo-train acquisition of NMR spectra obviates the need for prior deproteinization by attenuating signals from proteins and other macromolecules based on their short T2 relaxation times,^{38, 39} however, the concentration values of metabolites measured for normal SF may not necessarily reflect total or free metabolite content.⁴⁰ Further from the CPMG NMR spectra of normal SF samples, it becomes very difficult to discern the precise quantitative information about many clinically relevant and important metabolites either due to overlap/disappearance of peaks under the dominant residual signals of proteins and lipid metabolites. On the other hand, the filtering of proteins/lipids helps to improve NMR detection of low molecular weight metabolites; however, it results in the loss of information about lipid/membrane metabolites. Further, it is well known that both the NMR chemical shifts and NMR signals are sensitive to altered sample conditions, therefore, the present study has been carried out as a guide for future NMR based metabolomics studies through providing comprehensive peak annotations for normal and filtered SF samples.

2.3 Materials and Method:

2.3.1 Sample Collection:

Synovial fluids were obtained from ReA (n=8) patients attending the Department of Clinical Immunology at SGPGIMS, Lucknow, India and NMR experiments were executed at Centre of Biomedical Research (CBMR), Lucknow, India. The study protocol was approved by the Institutional Research Ethics Committee, SGPGIMS, Lucknow and written informed consents were obtained from all the patients before enrolment in study. Standard sterile knee aspiration technique was used to collect the synovial fluid from the ReA patients and subsequently placed in plastic tubes and transported to laboratory. The SF samples were centrifuged (2,000 rpm, 10 min) to remove cellular debris and then frozen immediately using liquid Nitrogen (N₂) and stored at a temperature of -80 °C, until the NMR measurements were performed.

For NMR experiments, the SF samples were prepared as described in [Figure 2.1a](#). Prior to NMR experiments, the stored SF samples were thawed at room temperature, vortexed and centrifuged at relative centrifugal force (rcf) of 16278 for 5 minutes at 4 °C to remove precipitates if any. The aliquots of 300 µL of SF were then added with additional 300 µL of 0.9% saline sodium phosphate buffer (of strength 20 mM and pH 7.4 prepared in 100% D₂O) to minimise the variation in pH. The buffer also contained 1.0 mM d6-DSS (i.e. 2,2-Dimethyl- 2-silapentane- 5-sulfonate sodium salt) which served as an internal standard reference for chemical shift to aid NMR identification of metabolites based on their specific chemical shift pattern in CHENOMX. The deuterium oxide (D-99%) was purchased from Cambridge Isotop Laboratories (CIL), Inc., 3 Highwood Drive, Tewksbury, MA 01876; whereas all other buffer reagents (of analytical grade) as well as d6-DSS were purchased from Sigma-Aldrich (St. Louis, MI, USA). Buffer mixed SF samples were vortexed and a 550 µL of sample was transferred into a 5 mm NMR tube (Wilmad Glass, USA) for NMR experiments.

For improved metabolite identification, the SF samples were subjected to ultra-centrifugation to remove protein and lipid metabolites. The samples were filtered using centrifugal filter units (Amicon Ultra 0.5 Centrifugal filter; Merck USA) of 3 kDa molecular-weight-cut-off (MWCO). Before ultrafiltration, the filter units were washed with milli-Q water and centrifuged with 450µL of water at 14000 rcf for 10 min and the process is repeated thrice. For ultra-filtration, the buffer mixed SF sample (prepared as described above) was transferred to the filter units and centrifuged for 30 min at 14000 rcf (400 µL in two steps). In each case, total 800 µL of buffer mixed SF was subjected to ultra-filtration and resulted in > 600 µL of filtrate. From resulted filtrate, the 550 µL was transferred to 5 mm NMR tube for experiments. Additionally, we also prepared a pooled SF

sample for recording a representative NMR spectrum of filtered SF (shown here in the main paper). The pooled SF sample was prepared by mixing 100 μL of filtered SF from each individual sample. The collected 800 μL of pooled SF from eight individual samples was transferred to a 1.5 ml of microcentrifuge tube (MCT) and lyophilized in a freeze-dryer system (**Make** Heto; **Model**: Lyolab 3000). Finally, the dried filtrate was dissolved in 550 μL D_2O and used for NMR measurements.

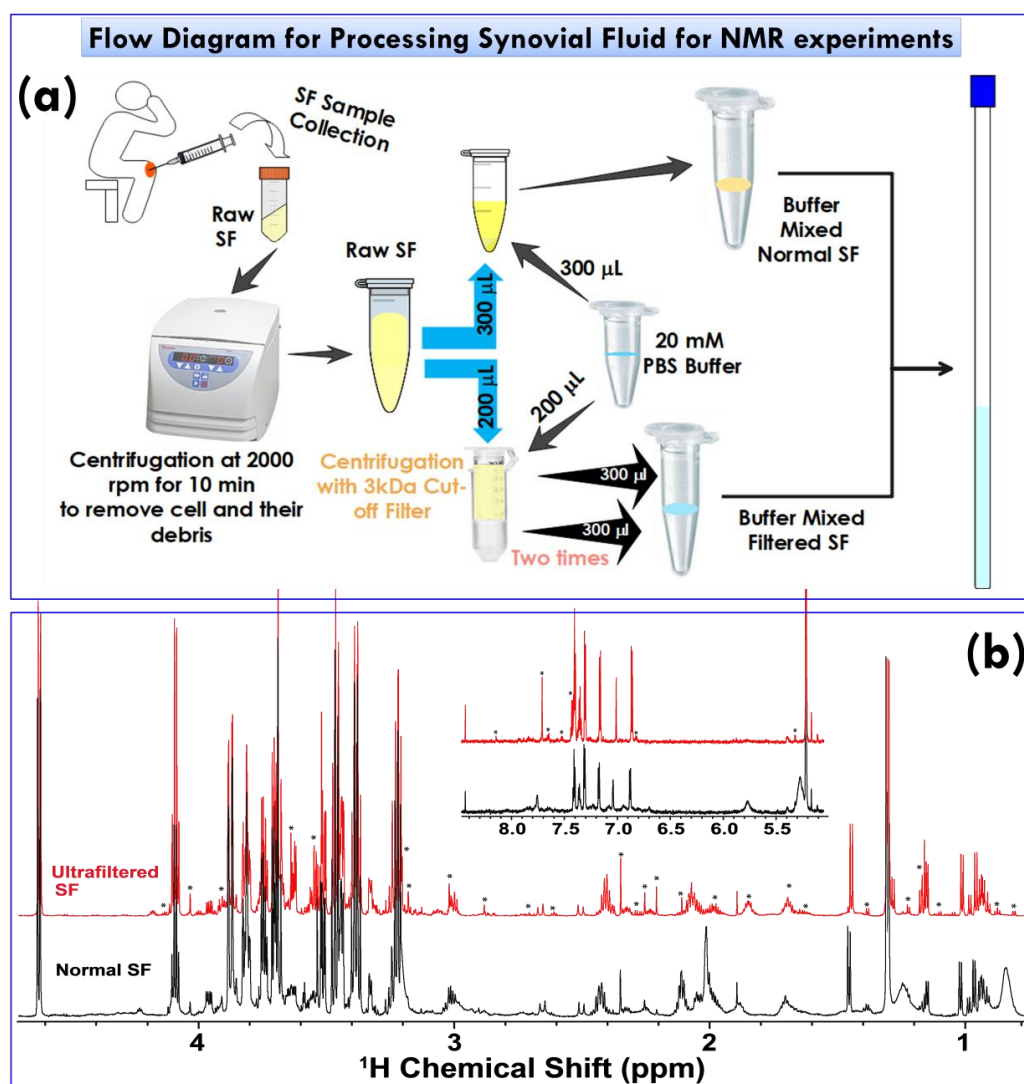


Figure 2.1:(a) Generalized protocol for processing the synovial fluid (SF) samples and preparing the samples for NMR measurements (b) The typical 800 MHz 1D ^1H CPMG NMR spectra of normal SF (in black) and ultra-filtered SF (in red) highlighting the absence of signals due to lipids and proteins in ultra-filtered SF which were present in normal SF. The peaks annotated with '*' represent the resonances of metabolites which were not clearly evident or suppressed either due to the overlapping signals from high MW metabolites in the NMR spectra of intact SF or due to weak interactions between these metabolites and higher molecular weight proteins/lipoproteins present in SF.

2.3.2 NMR Spectroscopy:

For metabolite characterization, the NMR spectra were recorded at 300 K for all the normal and filtered SF samples on high-resolution 800 MHz NMR spectrometer (Bruker, Avance III,

equipped with Cryoprobe, Website: www.bruker.com). The various spectra were recorded using the Bruker's standard pulse program library sequences. The performance of both 1D-NOESY-presat sequence (noesy1dgprr) and CPMG (Carr–Purcell–Meiboom–Gill) relaxation-editing sequence with pre-saturation (cpmgpr1D) was tested for selecting better option for future experiments.

For comparing the spectral features, both NOESY and CPMG spectra were recorded with pre-saturation of the water peak during recycle delay (RD) of 5.0 sec.⁴¹ Other acquisition parameters used for 1D ¹H CPMG pulse sequence were as follows: flip angle of radio frequency pulse: 90°; number of scans: 128; spectral sweep width: 12 ppm; and sampling data points: 32 K. For suppressing the signals of proteins and higher MW lipid or lipoprotein metabolites in the CPMG spectra, the T_2 filtering was obtained with an echo time of 200 μ s repeated 300 times, resulting in a total duration of effective echo time of 60 ms. Contrary to this, we used a mixing time of 80 ms for 1D NOESY experiment.⁴² The raw NMR data were processed using standard Fourier Transformation (FT) procedure in Bruker software Topspin-v2.1 (Bruker-BioSpin GmbH, Silberstreifen 4 76287 Rheinstetten, Germany) followed by manual phase and baseline correction. Prior to FT, each free induction decay (FID) was zero-filled to 64 k data points, multiplied by an exponential window function and a line broadening function of 0.3 Hz was applied. After FT, the chemical shifts values were internally calibrated to the DSS peak at 0.0 ppm.

2.3.3 Multivariate analysis:

For multivariate analysis, all the CPMG and NOESY spectra of filtered SF samples (in the chemical shift region δ 0.80–8.45 ppm) were binned into spectral regions of 0.01 ppm width using free multivariate data analysis toolbox named PATHOMX.⁴³ The spectral region of δ 4.34–5.2 that contained the resonance from residual water was excluded. The resulted data matrix generated with AMIX software was then exported into Microsoft Office Excel 2010, converted into CSV (comma-separated values) format, added with sample and class information. Then, integrated NMR spectral bin data was imported into metabolomics data processing server MetaboAnalyst 3.0 (<http://www.metaboanalyst.ca>) for multivariate analysis.^{8,44} Specifically, the supervised partial least-squares discriminant analysis (PLS-DA) was used to visualize the metabolic differences. To remove possible bias due to sample variability and preparation, the data matrix was Pareto-scaled before PLS-DA analysis.⁴⁵ The PLS-DA model was validated by default 10-fold cross-validation procedure using R^2 and Q^2 parameters, where R^2 provides a

measure for how much variation is represented by the model and Q^2 for the goodness of prediction and 100 random permutations test was performed to check over fitting of the PLS-DA models. After building the PLS-DA model, variable importance in projection (VIP) score was used in the identification of distinctive features of the metabolite that responsible for group differentiation. Metabolite with VIP score >1 was selected as discriminatory significance. The Student's *t* test or Wilcoxon (Mann–Whitney) test was applied to measure the statically significance of each metabolite (univariate analysis). Metabolites with both multivariate and univariate statistical significance (VIP >1.5 and $p < 0.05$) were considered to be responsible for the differentiation in CPMG and NOESY spectra.

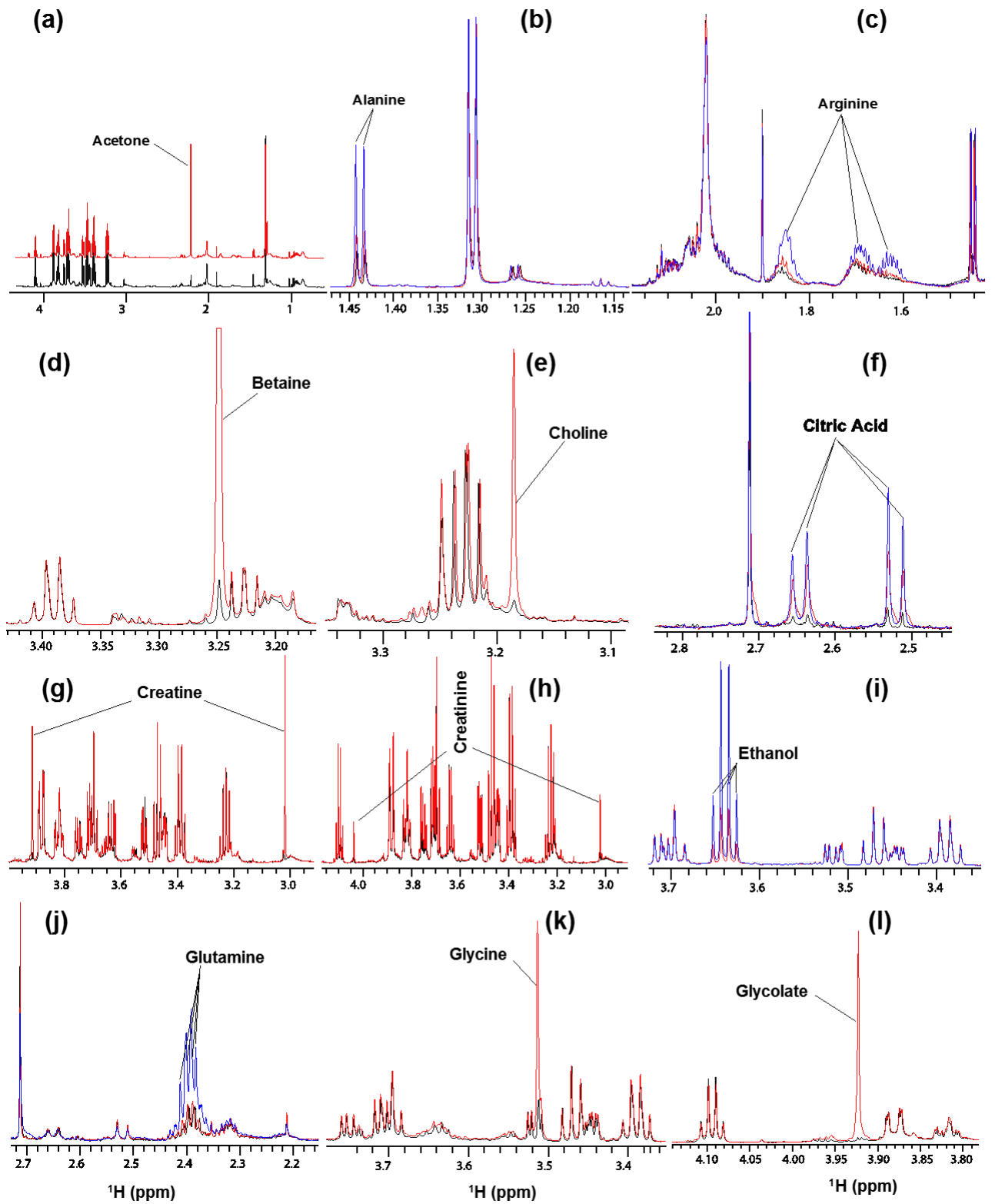
2.3.4 Identification of Metabolites in SF Samples:

The metabolite resonances in 1D ^1H CPMG NMR spectra were assigned as much as possible using NMR Suite of commercial software CHENOMX (form Chenomx Inc. v8.1, Edmonton, AB, Canada). The spectral resonances were identified and assigned by comparing them with the chemical shifts available in the database library of CHENOMX Profiler using 800 MHz chemical shift database. The obtained resonance assignments were further validated based on their specific patterns of CH correlations, HH correlations and ^1H - ^1H scalar coupling constants, respectively, in the two-dimensional (2D) ^1H - ^{13}C HSQC (single-quantum correlation spectroscopy), homonuclear ^1H - ^1H TOCSY (total correlation spectroscopy) and 2D *J*-resolved (JRES) NMR spectra.

Unambiguous assignments of various metabolites were obtained using two-dimensional *J*-resolved (JRES), TOCSY (total proton-proton correlation spectroscopy) and HSQC (heteronuclear single quantum correlation) spectra (acquired on two-to-three SF samples) and spiking experiments using standard chemicals. Homonuclear 2D *J*-resolved spectra (jresgpprqf) were recorded in magnitude mode using quadrature phase (QF)- with water pre-saturation during recycle delay (RD) of 2 sec. 16K data points were collected along direct proton (F_2) dimension with spectral width of 16 ppm, whereas, along indirect *J*- Couplings (F_1) dimension, 80 points (increments) corresponding to spectral width of 78 Hz (~ 0.0976 ppm) were collected and for each F_1 increment, 16 transients were acquired. Prior to Fourier transform, free induction decay (FID) signals were weighted in both dimensions by a sine-bell function and zero-filled in the F_1 dimension to 256 data points. The spectra were tilted by 45° to provide orthogonality of the chemical shift and coupling constant axes and subsequently symmetrized about the F_1 axis.

Two-dimensional ^1H - ^1H TOCSY (dipsi2esgpph) and sensitivity enhanced ^1H - ^{13}C HSQC (hsqctetgp) spectra were acquired in phase sensitive mode using time proportional phase incrementation (TPPI). 2D TOCSY spectrum was recorded using 2048 data points along direct dimension (F_2) and 512 increments along indirect dimension (F_1) with 16 transients per increment and a spectral width of 12 ppm in both dimensions. The FIDs were weighted using a sine-bell-squared function in both dimensions and zero filled to 2048 and 4096 data points, respectively, in the F_1 and F_2 dimensions prior to FT. For COSY experiment, the RD between successive pulse sequence cycles was 1.5 sec, while for TOCSY experiment (with mixing time of 80 ms), the RD between successive pulse cycles was 3.0 sec. Spin-lock was achieved by a DIPSI2 pulse sequence train during the TOCSY mixing time. 2D HSQC spectrum was recorded with inverse ^{13}C detection and using ^{13}C decoupling during acquisition using GARP-1. A RD of 2.0 sec was used between successive pulse sequence cycles and a refocusing delay equal to $1/(4*^1J_{\text{C-H}}=1.75\text{ ms})$ was employed. 2048 x 256 complex t_2 (^1H) and t_1 (^{13}C) data points with 96 scans per increment were acquired with spectral widths of 12 and 165 ppm, respectively, in the ^1H and ^{13}C dimensions. The FIDs were weighted using a sine-bell-squared function in both dimensions and zero filled to 4096 and 2048 data points, respectively, in the F_2 and F_1 dimensions prior to FT. After FT, the final spectrum was manually phase corrected and ^1H and ^{13}C dimensions were referenced to lactate methyl protons and carbon, respectively, at 1.31 and 22.5 ppm. After spectral processing, the $^1\text{H}/^{13}\text{C}$ chemical shifts in various 1D and 2D spectra were referenced internally with respect to the methyl (CH_3) group of DSS at 0 ppm. The validation analysis through HSQC and TOCSY was performed using freely available software MetaboMiner with tolerances of 0.02 ppm (^1H) and 0.5 ppm (^{13}C).⁴⁶ The unambiguous metabolite peaks were assigned by performing spiking experiments using standard chemicals (see [Figure 2.2A and 2.2B](#)).

Some left over peaks were also assigned by comparing them with the metabolite assignments reported previously in the literature^{38, 47-52} or those available with BMRB database (Biological Magnetic Resonance Data Bank) and HMDB (The Human Metabolome Database) with tolerances of 0.02 ppm (^1H) and 0.5 ppm (^{13}C). Identification was achieved if there was only one candidate in the database within the specified tolerances for an observed peak and its correlated shifts.



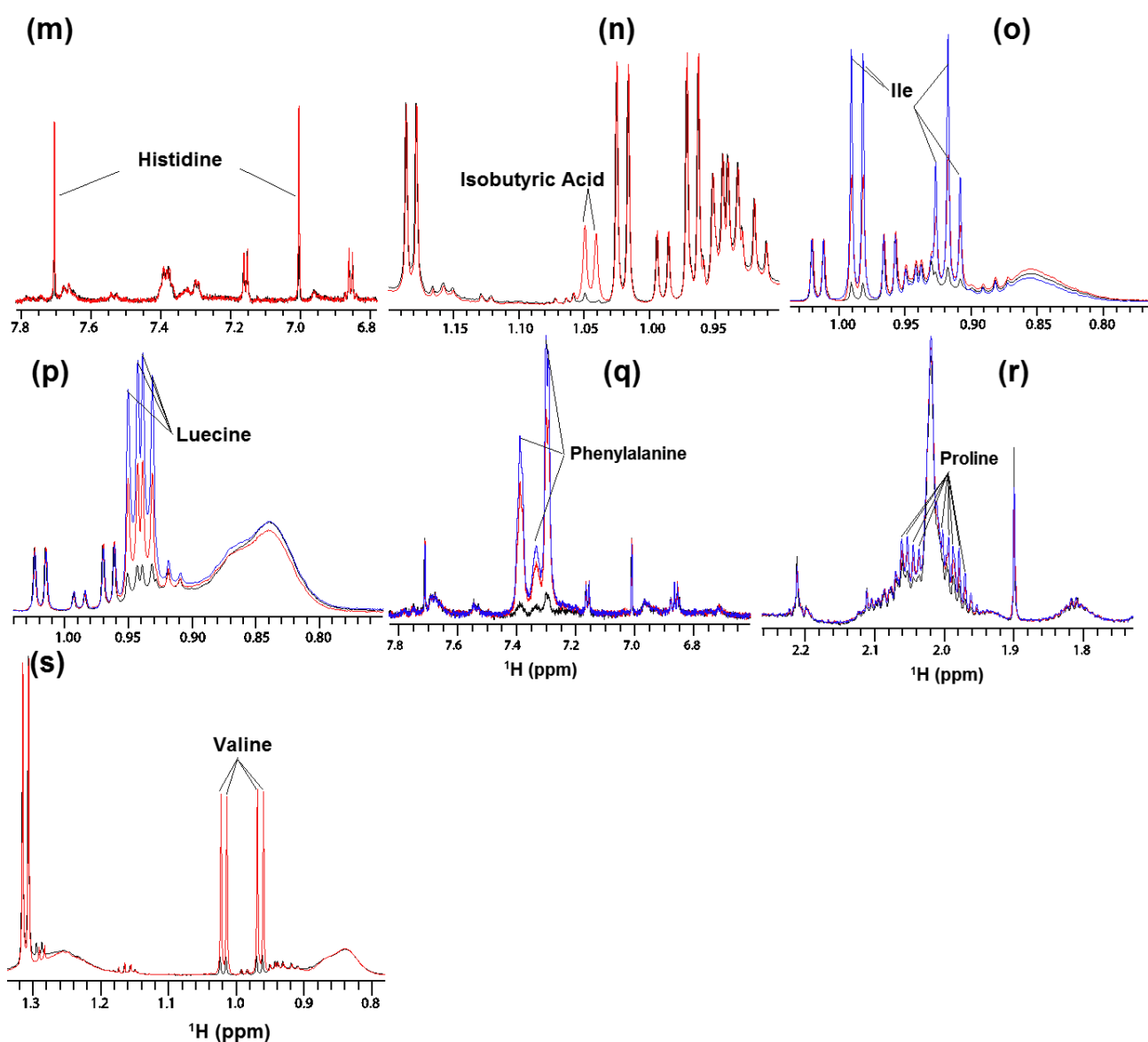


Figure 2.2A: The spectral regions showing an overlay of 1D ^1H CPMG NMR spectra of normal SF samples recorded before and after spiking with authentic compounds. The spectral regions shown here from (a-u) represent NMR spectral spiking, respectively, with acetone, alanine, arginine, betaine, choline, citric acid, creatine, creatinine, ethanol, glutamine, glutamate, glycine, glycolate, histidine, isobutyric acid, isoleucine, leucine, methionine, phenylalanine, proline and valine.

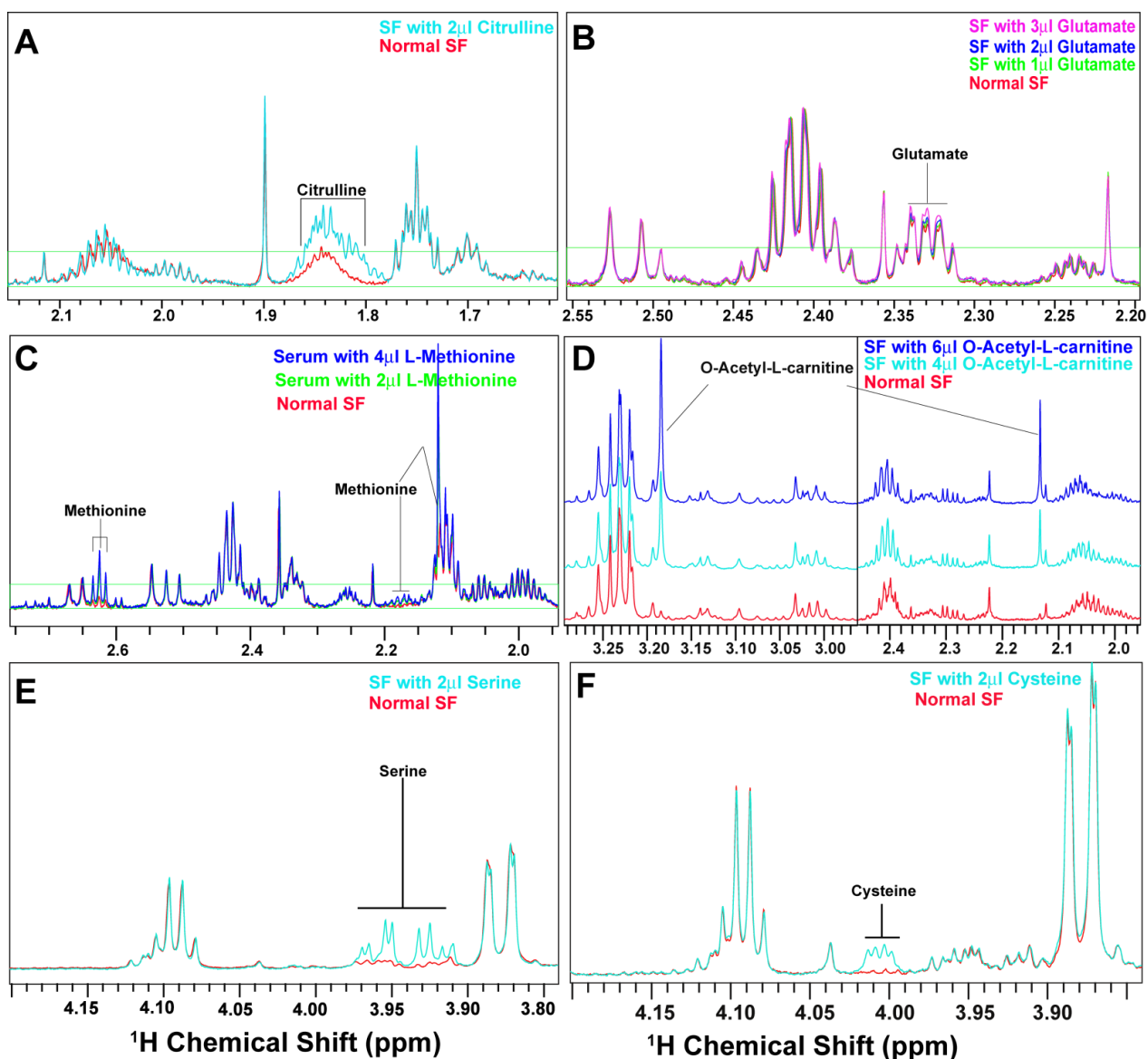


Figure 2.2B: An overlay of the 1D ^1H CPMG NMR spectra of filtered SF samples recorded before and after spiking with authentic compounds (A) Citrulline, (B) Glutamate, (C) Methionine, (D) O-acetyl-L-carnitine, (E) Serine and (F) Cysteine.

2.4 Result and discussion:

Like blood serum/plasma, the synovial fluid samples are invariably present with proteins which interfere with the quantitative and qualitative analysis of their metabolites by NMR. Often, the protein interference is alleviated by suppressing their signals based on their short T_2 relaxation times using the Carr–Purcell–Meiboom–Gill (CPMG) experiment.³⁸ The limitation of this approach is that many metabolites that exhibit binding affinity to proteins make them either invisible or significantly attenuated in the resulting NMR spectra (e.g. several aromatic amino acids).³⁸ Both these issues can be circumvented by removing proteins either by protein-precipitation or by ultrafiltration.^{38, 39} Here, we employed the ultra-centrifugation method to filter

out the proteins and higher MW lipid metabolites which resulted in significant improvement of spectral resolution and made possible to detect a number of metabolite peaks. The effectiveness of protein and lipid removal has been illustrated in **Figure 2.1B** showing the comparison of 1D ^1H CPMG NMR spectra of normal and filtered SF samples. As clearly evident, the protein filtering has greatly alleviated the peak attenuation problem and highlighted the signals from low molecular weight (MW) metabolites in the presence of higher MW species (**Figure 2.1B**). In addition to sample handling, the data acquisition remains equally important to ensure the reproducibility in metabolomics research. Though, 1D ^1H CPMG experiment is preferred for quantitative metabolic profiling of serum, however, it is the NOESY presat pulse sequence (noesygprr1d on Bruker spectrometers) is the leading choice for reliable metabolite quantitation of urine samples.⁵³⁻⁵⁵ One of the main reasons for the success of noesygprr1d is its ability to greatly suppress the water peak without intensity attenuation for most of the other peaks (except those close to the water resonance, like urea, glucose and carnitine).⁴² Unlike serum, the urine samples lack higher molecular weight species such as proteins, lipoproteins and fats except for under some pathological conditions. As the ultra-filtered SF sample also lacks the higher MW species (**Figure 2.1B**), the 1D NOESY practically seems to be a better choice for reliable concentration profiling of metabolites in filtered SF. To evaluate this point, the CPMG spectra recorded on filtered SF samples were overlaid (**Figure 2.4a**) compared to NOESY spectra (**Figure 2.4b**) visually as well as employing multivariate analysis approach. The results of this comparative evaluation are summarized in **Figure 2.4**. Both the CPMG and NOESY spectra are acquired using same recycle delay of 4.0 sec. As evident from **Figure 2.4a**, the baseline of 1D CPMG NMR spectra lies close to zero; whereas the baseline in 1D NOESY spectra is slightly and variably elevated along 0.8 to 4.4 ppm. The other versions of 1D ^1H NMR spectra (i.e. ZGESGP and diffusion edited) were also recorded on filtered SF samples and compared to CPMG and NOESY spectra (see the, **Figure 2.3**). As evident, the NOESY spectrum shares almost the same baseline feature as ZGESGP spectrum, however, ZGESGP spectrum additionally contains NMR signals of urea (at 5.73 ppm, which probably saturate in NOESY spectrum due to water presaturation pulse effect).

Next, the NMR spectral profiles of CPMG and NOESY were subjected to discriminatory analysis employing multivariate PLS-DA method (**Figure 2.4c-2.4e**). The 2D score plot showed well separated CPMG spectra from NOESY spectra suggesting subtle variations in metabolic profiles measured through two different methods. The higher values of model validation parameters R^2 (>0.8) and Q^2 (>0.67) is suggestive of significant different metabolic profiles (**Figure 2.4d**). The potential metabolic entities responsible for this exquisite separation are

evident from VIP score plot shown in **Figure 2.4e**. As evident, the discrimination is mainly because of decreased levels of Glucose and lactate in the NOESY group (**Figure 2.4e**). For discriminatory analysis, the binned spectral data has been used and for each spectrum, the bins were normalized w.r.t. the total spectral intensity. Possibly, this could be the reason for the under-estimated SF levels of metabolites in NOESY group where the presence of baseline humps additionally contributes to total spectral intensity. This is well reflected from the VIP score plot also where the spectral bins corresponding to hump regions (e.g. 1.5 to 1.7 ppm region) of NOESY spectra are elevated (**Figure 2.4e**). The over dispersed NOESY spectral points in 2D score plot of PLS-DA can also attributed to these spectral humps, whereas the CPMG spectral points are well clustered together in the 2D score plot (**Figure 2.4c**).

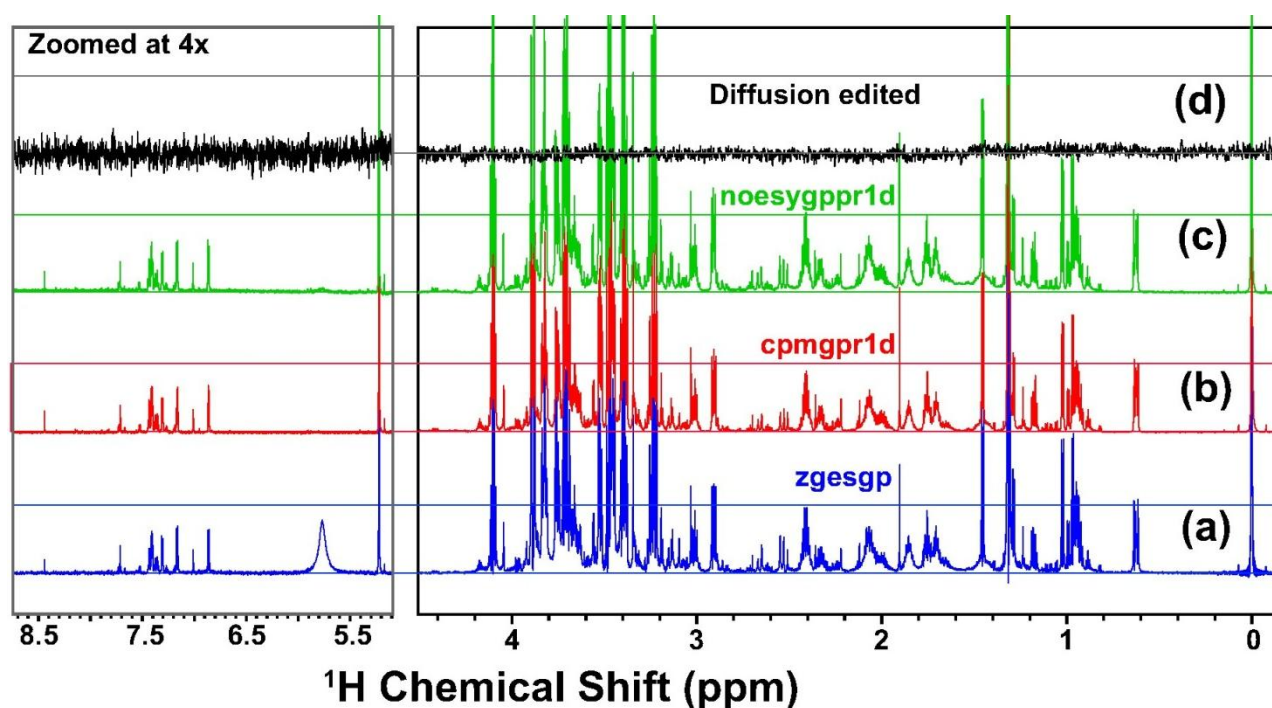


Figure 2.3: The stacked 1D ^1H NMR spectra recorded on a filtered SF sample using different pulse programs as indicated: (a) zgesgp, (b) cpmgrp1d (with T_2 filter time ~ 63.6 ms), (c) noesygp1d (with mixing time ~ 10 ms) and (d) diffusion edited. All the spectra are baseline corrected using topspin “abs” command for automated baseline correction. As evident visually, the cpmgrp1d confers smooth zero baseline compared to zgesgp and noesygp1d. No signal was evident in the diffusion edited 1D ^1H suggesting that the ultrafiltration has removed majority of higher molecular weight metabolites including lipoproteins and protein.

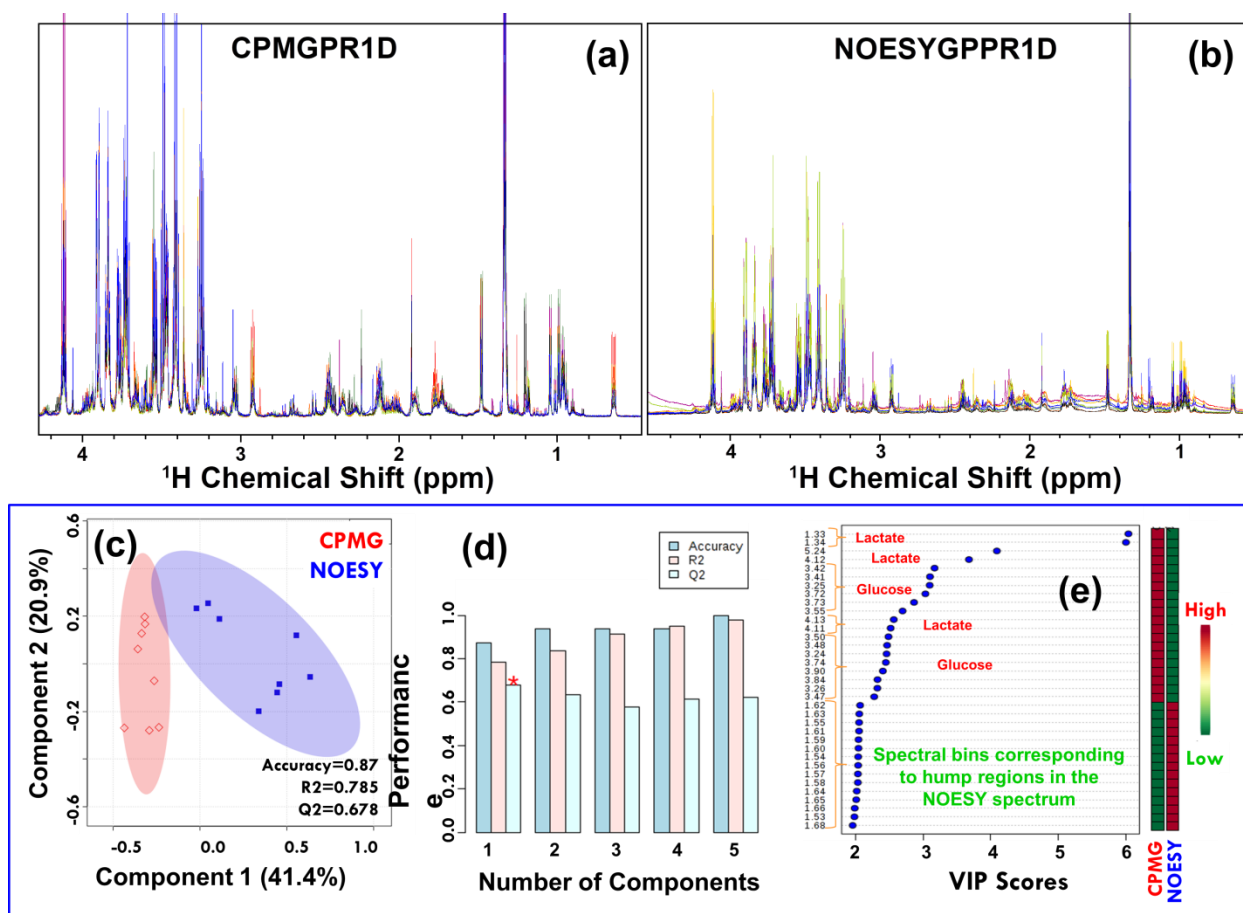


Figure 2.4: An overlay of 1D ^1H NMR spectra of SF samples of ReA patients recorded on Bruker 800 MHz NMR spectrometer using (a) CPMG (cpmgrp1d) and (b) NOESY (noesygp1d) pulse programs. (c-d) represent the results of discriminatory analysis based on PLS-DA performed here to probe the spectral differences associated with CPMG and NOESY spectra (c) The 2D score plot showing sample clustering and group separation between CPMG and NOESY spectra. (d) The model validation and performance tests (e) The VIP statistics highlighting the potential metabolic entities responsible for separation between CPMG and NOESY spectral groups.

Overall, based upon relatively better baseline features and exquisite sample clustering, the use of CPMG spectra seems to be well apposite for future NMR studies on filtered SF samples involving comparison of the relative peak intensities between different groups of samples. We further evaluated the baseline features of CPMG experiments as a function of T_2 filter time (varied from 21.2 ms to 106 ms in steps of 21.2 ms, where the spin-echo time in each case was 100 μs and recycle delays was 4.0 sec) and the results are shown in (Figure 2.5). As evident, the baseline position w.r.t. to zero was almost invariable for different T_2 filter times suggesting that there is no attenuation of metabolite signals in the filtered SF (which is otherwise posed by the interference of proteins); therefore the use of CPMG experiment with shortest possible T_2 filter time is adequate for metabolic profiling of filtered SF.

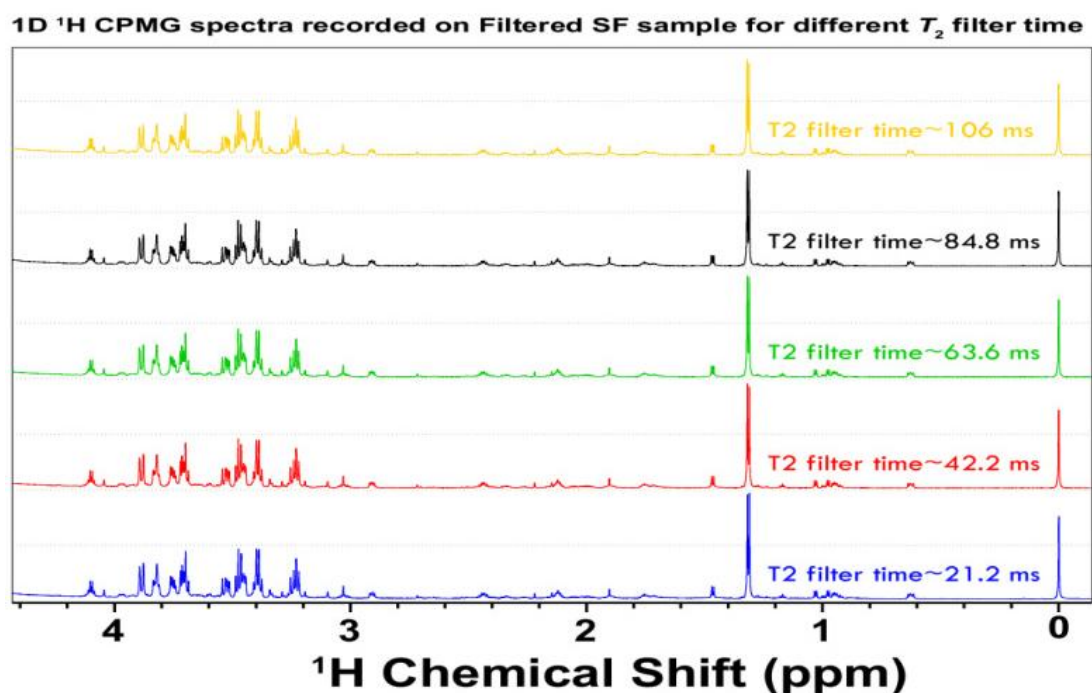


Figure 2.5: The stacked 1D ¹H CPMG NMR spectra recorded on a filtered SF sample with different T₂ filter time as indicated. No significant improvement is seen for CPMG spectra recorded with higher T₂ filter time compared to that recorded with T₂ filter time equal to 21.2 ms suggesting that the sample is completely devoid of higher MW metabolites.

Following preliminary optimizations of experimental parameters, the metabolite assignment of spectral peaks of in the 1D ¹H NMR spectra of ultra-filtered SF was established through the composite use of various 1D and 2D NMR experiments such as 1D ¹H CPMG, 2D ¹H-¹H JRES, ¹H-¹³C HSQC, ¹H-¹H TOCSY. Prior to resonance assignments, all the 1D and 2D NMR spectra were referenced with respect to the methyl (CH₃) group of DSS at 0 ppm both for ¹H and ¹³C chemical shift axis. In order to further confirm the identity of ambiguous peaks, spectral spiking method was employed using authentic compounds (Figure 2.2A-2.2B) and finally the assignment was validated in CHENOMX profiler (through comparing the spin-spin coupling constant and peak multiplicity patterns). Figure 2.6 demonstrates a comprehensively characterized and analysed 1D ¹H CPMG NMR spectrum of ultra-filtered synovial fluid along with annotations of characteristic peaks of the identified metabolites. Compared to the spectra of intact synovial fluid, the ¹H NMR spectra of ultra-filtered SF provided well resolved peaks and allowed the detection of significantly higher number of metabolites as evident from expanded NMR spectral regions shown in Figure 2.6. The improved peak resolution (sharpness) and baseline properties led to the identification of 64 metabolites. The complete list of identified metabolites in filtered SF along with their ¹H and ¹³C chemical shift, spin-spin coupling constant and peak multiplicity has been tabulated in Table 1 (See, Appendix). As evident, the SF

The elimination of signals originating from proteins as well as lipids in this low frequency region particularly at around 0.83, 1.20, 2.00, 2.25, 2.75 ppm leads to the appearance of numerous metabolite peaks in the CPMG NMR spectra of filtered SF samples. The spectral congestion as observed in ppm range 3.0 to 4.0 ppm because of glucose resonances has been resolved with the help of 2D NMR HSQC spectra owing to better dispersion of chemical shifts in the ^{13}C dimension and TOCSY spectra which aided in the identification of many coupled spin systems and thus facilitated the assignment several metabolites which were otherwise hidden by superimposed peaks in one-dimensional spectra.

Figure 2.7 shows the annotated CH correlation peaks in the ^{13}C HSQC spectrum assigned through matching the peak patterns in Metabominer software; whereas the assignment of resonances of SF metabolites in the 2D ^1H - ^1H TOCSY spectrum has been shown in **Figure 2.8**.

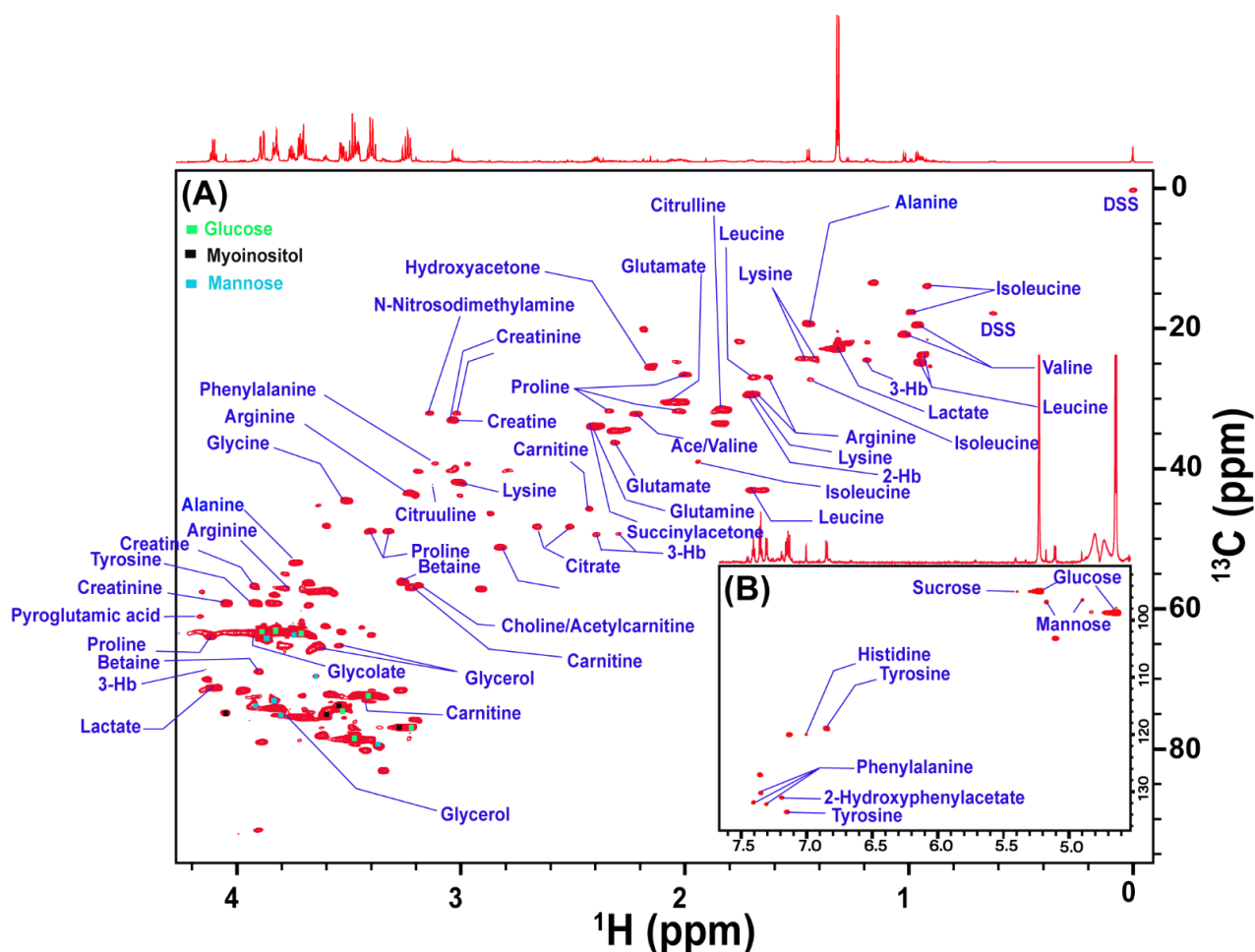


Figure 2.7: The representative 800 MHz (Cryoprobe) ^1H - ^{13}C HSQC spectrum of a pooled synovial fluid obtained from ReA patient after ultrafiltration using a 3 kDa filter showing expanded regions (A) ^1H δ 0.0-4.20 ^{13}C δ 0.0-95.0 and (B) ^1H δ 4.60 -7.60 ^{13}C δ 92.00-136.00

With the help of ^1H - ^{13}C HSQC spectra, we were able to assign many complex multiplet resonances of metabolites including arginine, lysine, citrulline, proline, carnitine, leucine and isoleucine etc. from the overlapped area of low-frequency region. Further, the singlet peaks

arising from acetate, acetone, hydroxyacetone, acetoacetate, pyruvate, creatine, creatinine and NDMA were also confirmed by 2D ^1H - ^{13}C HSQC spectra as they were not observed as off diagonal cross peaks in TOCSY.

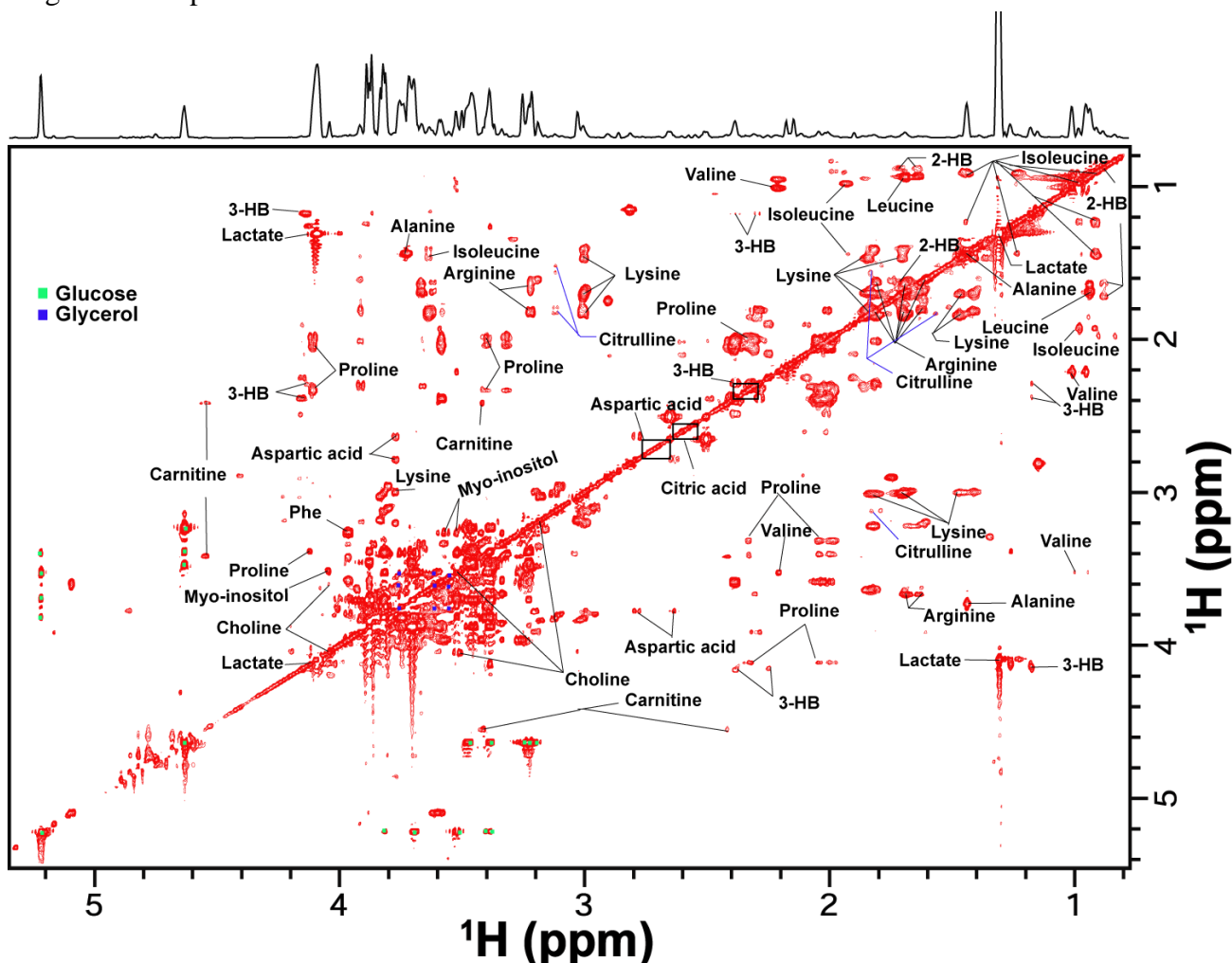
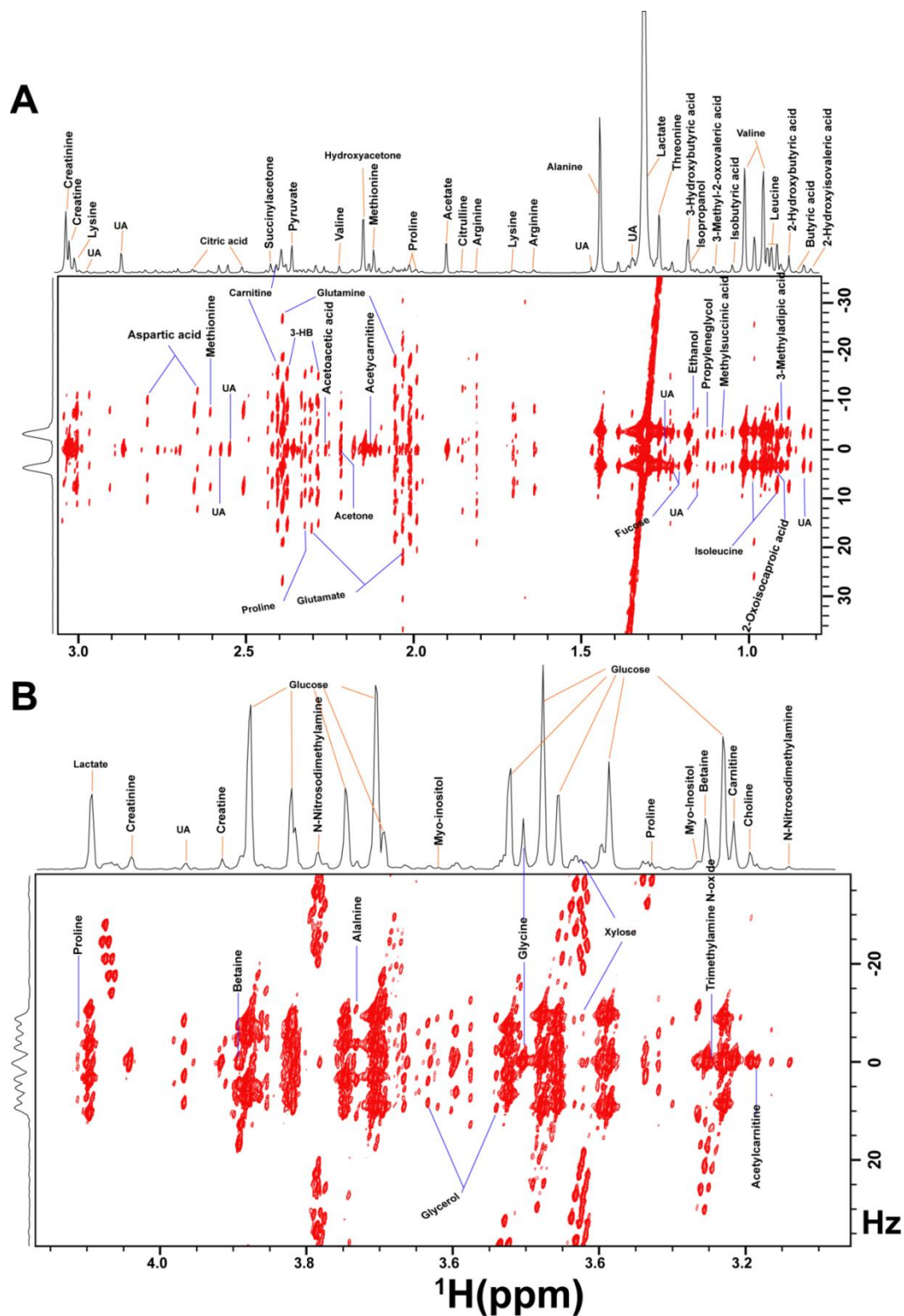


Figure 2.8: The representative 800 MHz ^1H - ^1H TOCSY spectrum of pooled filtered (after ultrafiltration) synovial fluid samples obtained from ReA patients. **Abbreviations:** 2-HB: 2-Hydroxybutyric acid; 3-HB: 3-Hydroxybutyric acid; and Phe: Phenylalanine.

The splitting pattern of the assigned metabolites has been shown in the 2D ^1H - ^1H JRES spectral expansions presented in [Figure 2.9](#). As can be seen from the 2D JRES NMR spectrum, overlapped multiplet signals are completely resolved from one another and the proton-decoupled 1D spectrum obtained from the skyline projection along the chemical shift dimension facilitates the metabolite assignments by separation of the signals in crowded regions. The J-coupling constants were also determined (as tabulated in [Table 1, See, Appendix](#)) which aid in metabolite identifications as the J-couplings are insensitive to physiological factors (such as temperature or pH value).⁵⁶ Further, the HSQC and TOCSY spectra in combination with J-resolved NMR spectra also enabled us to unambiguously assign several resonances in the up-field spectral region of filtered SF samples such as 2-Hydroxyisovaleric acid, methylsuccinate, propylene glycol, isopropanol, threonine, arginine, citrulline, methionine, aspartic acid,

acetylcarnitine and carnitine etc. The complex multiplet resonances attributed from non-equivalent CH₂ proton of glutamate and glutamine were confirmed by well dispersed ¹³C chemical shifts in the HSQC spectra (Figure 2.7). The mid-frequency region (3.15–4.58 ppm) consists of many complex and severely overlapped resonances which were well resolved in the 2D HSQC NMR spectra.



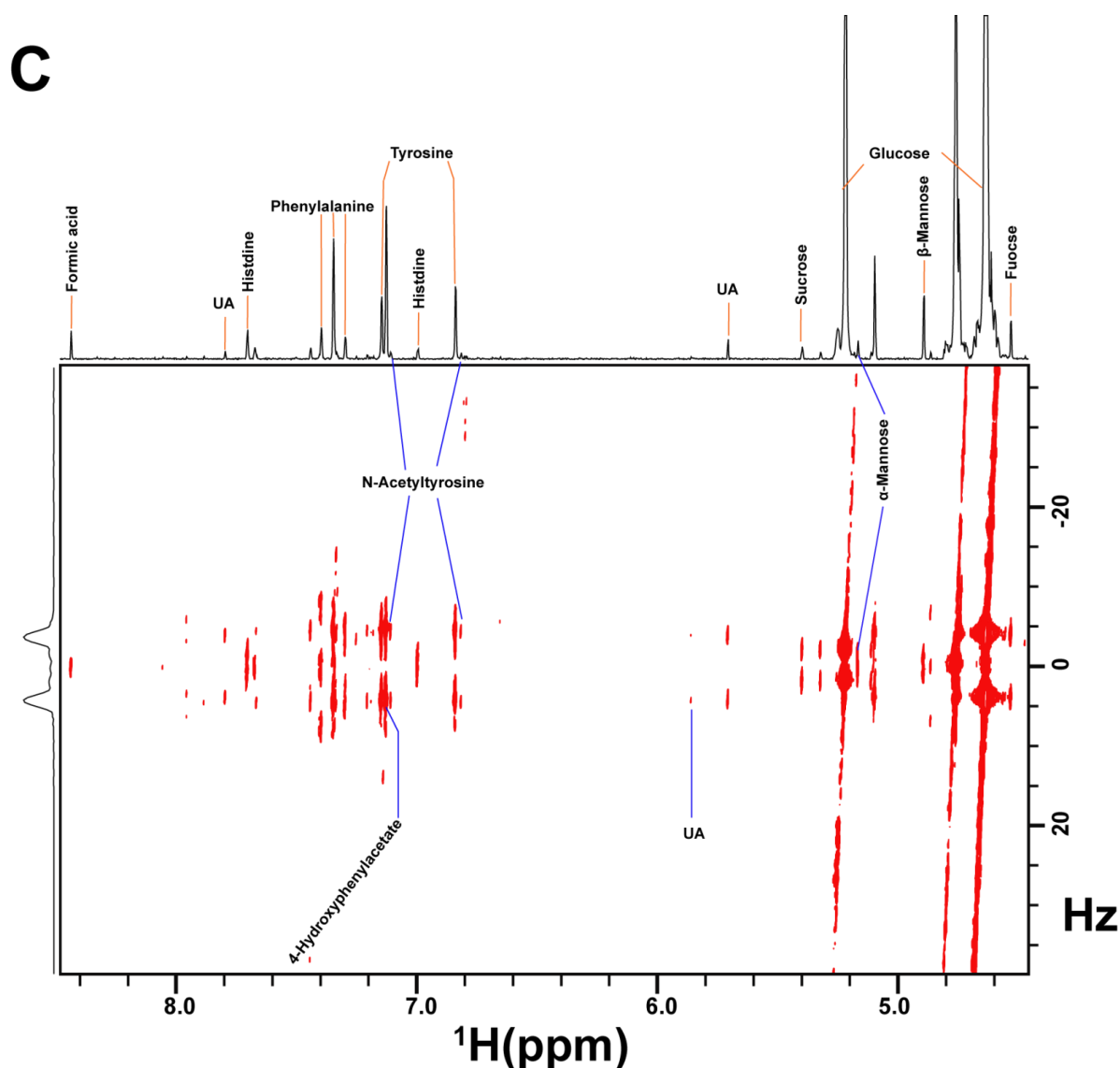


Figure 2.9: The representative 800 MHz ^1H - ^1H J-Resolved (JRes) spectrum (A-C) with skyline F2 projection of pooled filtered (after ultrafiltration) synovial fluid samples obtained from ReA patients. Three different spectral regions of the 1D ^1H JRes spectrum are expanded for improved visualization: (A) $\delta(0.8-3.1)$ ppm, (B) $\delta(3.1-4.30)$ ppm and (C) $\delta(4.60-8.40)$ ppm. Assigned peaks are annotated, whereas unassigned (UA) metabolite signals are labelled as UA.

The most of the multiplets observed between 3.2 – 3.9 ppm were assigned to α - and β - glucose followed by a quartet due to CH group of lactate at 4.11 ppm and intense doublet's due to C_1H group of β -, α - glucose at 4.64 ppm and 5.23 ppm, respectively. Other resonances evident in the spectra were: singlets due to CH_2 group of glycine (~ 3.51 ppm), creatine (~ 3.91 ppm), creatinine (~ 4.04 ppm) and due to the $\text{N}^+(\text{CH}_3)_3$ groups of carnitine, betaine and trimethylamine-N-oxide, which overlapped with glucose resonance between 3.21-3.27 ppm and were distinguished based on the HSQC spectra. The intense singlet peak of Choline at 3.19 ppm

arising from $\text{N}^+(\text{CH}_3)_3$ group was also ascribed through the ^{13}C chemical shift in HSQC spectra and the cross peaks pattern observed at 3.52, 4.05 ppm due to the corresponding α -, β - CH_2 group, respectively in TOCSY spectra. The sparse resonance from $\text{N}^+(\text{CH}_3)_3$ group of acetylcarnitine was fused with intense resonance of choline and unambiguously assigned with the help of HSQC spectra based on the chemical shift resonating at 3.19 ppm in the ^1H dimension (**Figure 2.7**). The triplet resonances from the CH group of myo-inositol at 3.27 and 3.62 ppm were well resolved in the JRES spectra of filtered SF which were unequivocally assigned with specific J-coupling in JRES spectra, ^{13}C chemical shift in HSQC spectra and diagonal cross peaks of TOCSY spectra.

The assignment of glycerol resonances –which was not possible in the 1D ^1H CPMG NMR spectra of filtered SF samples due to spectral congestion and overlap- were assigned with the help of JRES spectra at 3.54, 3.64 and 3.77 ppm and further confirmed on the basis of specific pattern of its CH and HH cross-peaks in the HSQC and TOCSY spectra, respectively. Further, the mannose anomers (α and β) were distinctively identified at 5.17 and 4.90 ppm with the corresponding ^{13}C chemical shift at 96.80 ppm and 96.40 ppm in HSQC spectra as depicted in **Figure 2.7B**. A triplet resonance due CH group of xylose was observed at 3.43 ppm confirmed through their J-coupling constant of 9.27 Hz. The high-frequency (4.87–9.19 ppm) region of the spectra contains weak signals arising from tyrosine, phenylalanine, histidine and formate as annotated in **Figure 2.6f -2.6g**. The doublet resonances originated from CH group of tyrosine and N-acetyltyrosine observed at 6.84, 7.15 ppm and 6.82 ppm, 7.12 ppm, respectively, were confirmed by CH and HH correlation peaks (**Figure 2.7B** and **Fig. 2.9C**). The resonances arising due to the aromatic compound rings of phenylalanine at 7.30, 7.35 and 7.42 ppm were confirmed with the help of HSQC and TOCSY spectra. The histidine molecule exhibit a CH doublet at 7.00 ppm with the corresponding ^{13}C shift at 119.99 ppm and 1.40 Hz J-coupling constant and another correlated doublet at 7.71 ppm. A number of phenylacetate derivative resonances such as multiplets and doublets from CH group at 7.19 ppm (2-hydroxyphenylacetate) and 7.14 ppm (4-hydroxyphenylacetate), respectively, were observed and unequivocally confirmed by 2D HSQC and JRES spectra (**Figure 2.7B** and **Figure 2.9C**) which were, probably, originated from the gut microflora metabolites or co-metabolism between host and gut microbiota. The doublet resonances observed at 6.66 ppm and 7.44 ppm in 1D ^1H NMR spectra (**Figure 2.6g**), respectively, were assigned as 6-hydroxynicotinic and melatonin by J-coupling constant of ^1H - ^1H JRES spectra as tabulated in **Table 1 (See, Appendix)**.

To be mentioned here is that we have also assigned the metabolite resonances in the 1D ^1H CPMG NMR spectra of normal SF samples and the resulted assignments have been shown in

Figure 2.10. The corresponding peaks assigned in the HSQC and JRES NMR spectra have also been shown in the **Figure 2.11** and **2.12**. For normal synovial fluid samples, we were able to identify a total of 48 metabolites and the complete list of identified metabolites in normal SF along with their ^1H and ^{13}C chemical shifts, spin-spin coupling constants and peak multiplicity has been tabulated in **Table 2** (See, **Appendix**). An important add up by this study is that for the first time the resonances of N-alpha acetyl lysine (NAAL) have been assigned in the 1D ^1H NMR spectrum of normal SF (**Figure 2.13a**). However, the corresponding signals of NAAL were not discerned in filtered SF (**Figure 2.13b**) suggesting the presence of acetylated proteins in the SF.

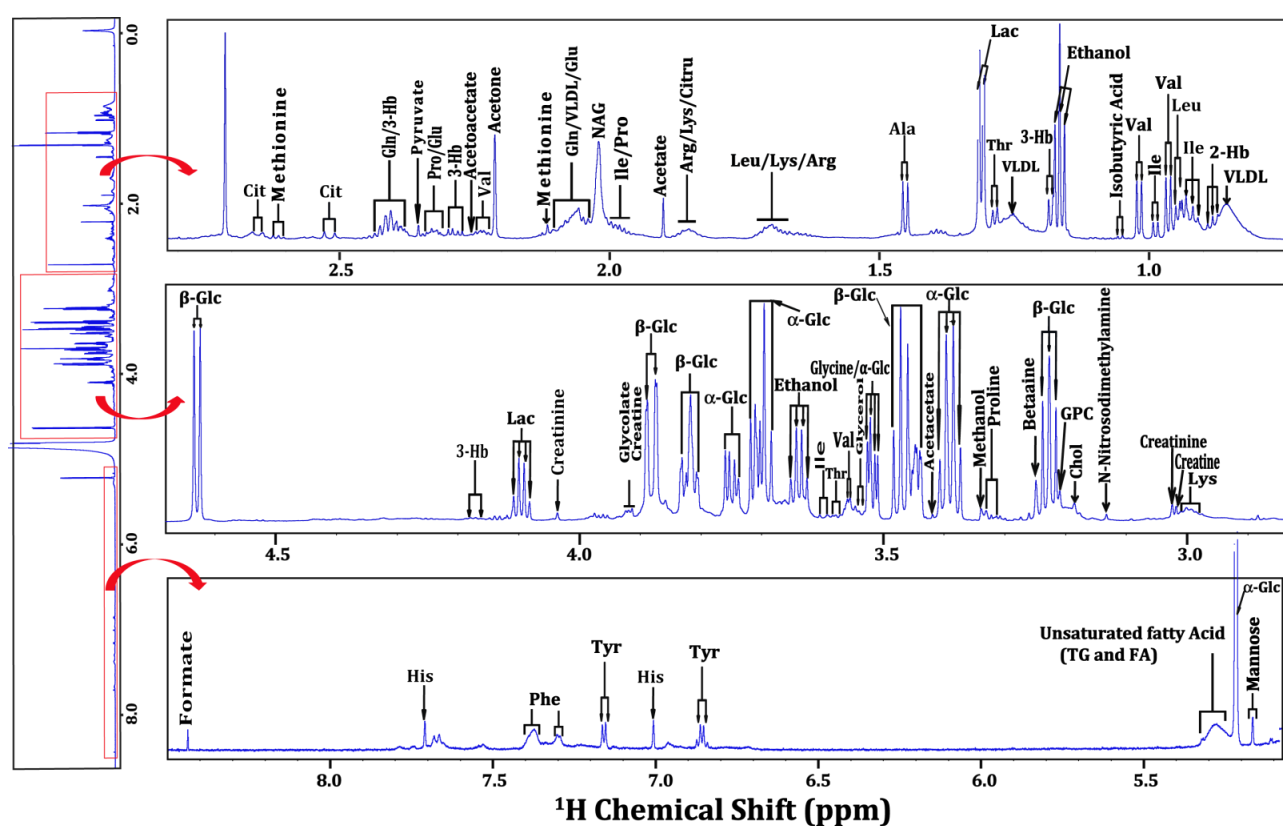


Figure 2.10: A typical 800 MHz 1D CPMG ^1H NMR spectrum of a normal synovial fluid obtained from ReA patient with expanded regions from $\delta(0.8\text{-}2.73)$ ppm (top panel), $\delta(2.73\text{ to }4.67)$ ppm (middle panel) and $\delta(5.18\text{ to }8.5)$ ppm (bottom panel). The abbreviations used are: 2-Hb: 2-Hydroxybutyric acid; 3-Hb: 3-Hydroxybutyric acid; Ala: Alanine; Arg: arginine; Chol: Choline; Cit: Citric acid; Citru: Citrulline; GPC: Glycerophosphocholine; α -Glc: α -Glucose; β -Glc: β -Glucose; Glu: Glutamate; Gln: Glutamine; His: Histidine; Ile: Isoleucine; Lac: Lactate; Leu: Leucine; Lys: Lysine; Pro: Proline; Val: Valine; VLDL: Very Low Density Lipoprotein; TG: Triglycerides and FA: Fatty acid.

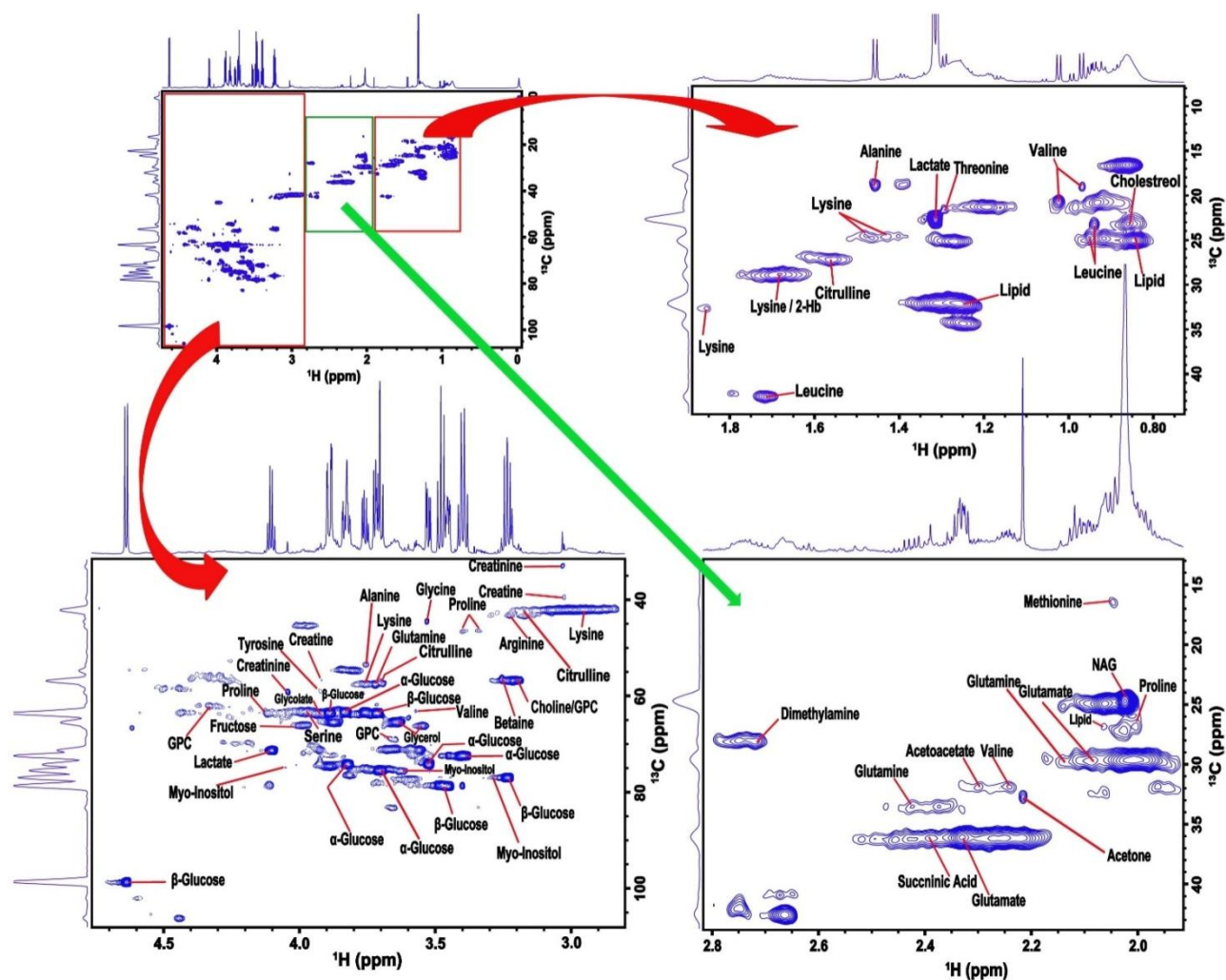


Figure 2.11: The representative 800 MHz ^1H - ^{13}C HSQC spectrum of a normal synovial fluid obtained from a ReA patient showing full spectrum in its top-left panel and the zoomed spectral regions as directed showing CH cross-peak assignments for various SF metabolites.

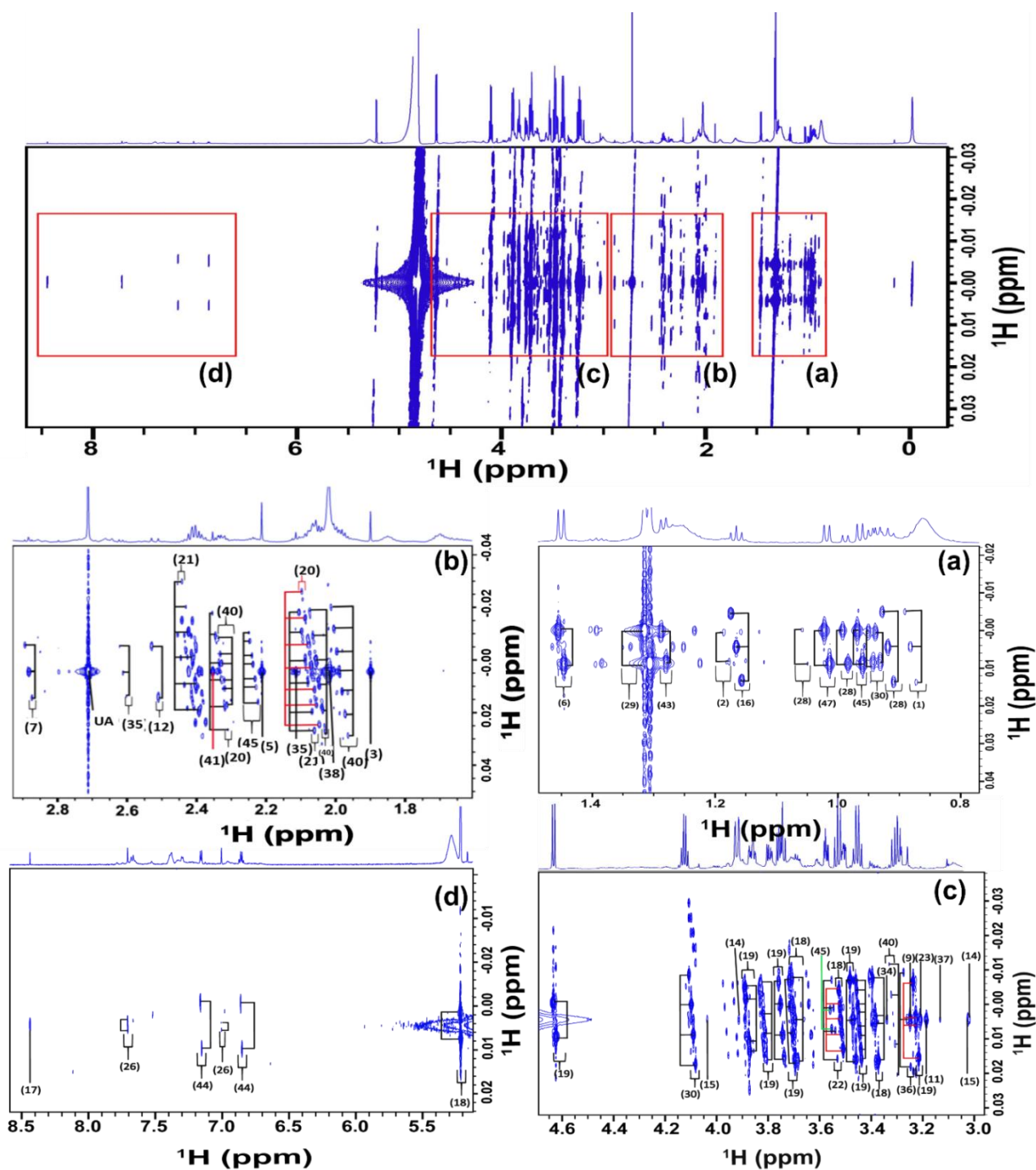


Figure 2.12: The representative 800 MHz ^1H - ^1H J-Resolved (JRes) spectrum of normal synovial fluid samples obtained from a ReA patient. Four different spectral regions of the 1D ^1H JRes spectrum are expanded for improved visualization: (a) $\delta(0.8-1.48)$ ppm, (b) $\delta(1.65-2.90)$ ppm and (c) $\delta(3.00-4.65)$ ppm and (d) $\delta(5.20-8.50)$ ppm. The labelled assignments of the metabolites are as per Table 2 (See, Appendix).

Previously, the altered acetylation of proteins in patients with rheumatoid arthritis has been revealed by acetyl-proteomics.⁵⁷ Thus, we believe that the quantitative and comparative analysis of NAAL signals by NMR would have important future implications in determining the load of acetylated proteins in the synovial fluid for its possible use in clinical diagnosis and surveillance of rheumatic conditions involving synovitis.

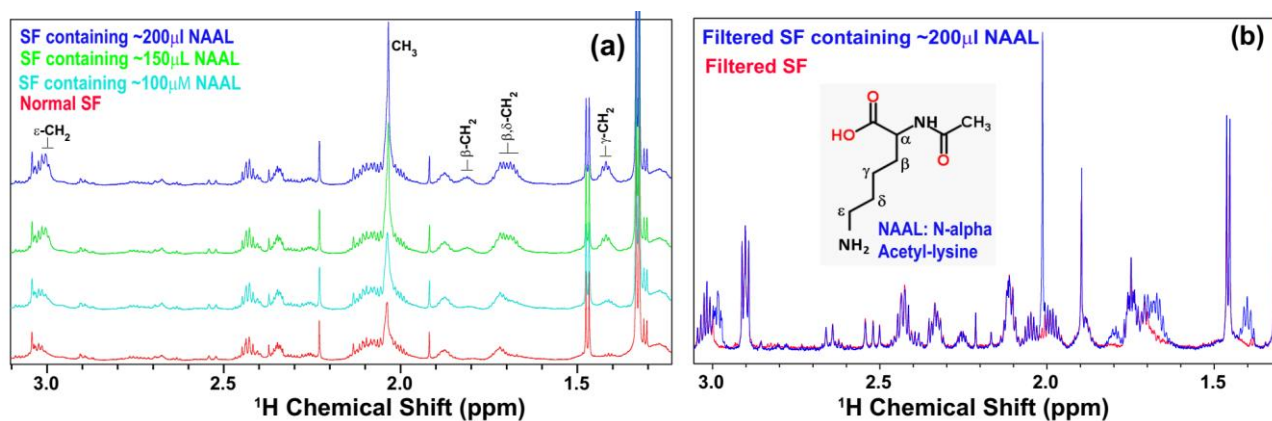


Figure 2.13: (a) The assignment of peaks in the 1D ^1H NMR spectrum of normal SF corresponding to metabolite N- α -Acetyllysine (NAAL) identified using spiking method following sequential addition of N- α -Acetyllysine solution prepared in D_2O (all purchased from Sigma-Aldrich) into control serum sample. (b) The NAAL spiking experiments performed with filtered SF sample clearly revealed that the sample lack signals of NAAL.

2.5 Concluding remarks:

Synovial fluid is a viscous body fluid found in the articular joint cavities and is the direct medium for the pathological products including metabolic changes.⁵⁸ As synovitis -i.e. inflammation in the joint and subsequent accumulation of synovial fluid- remains a common clinical manifestation of several autoimmune rheumatic diseases, thus it is very likely that the breakdown products of articular cartilage will first accumulate in the SF before they can be detected in serum. Therefore it is legitimate to consider for rheumatic diseases involving synovitis that the concentration profiles of disease specific metabolites would be significantly altered in SF compared to serum, which increases the likelihood of reliable early detection of underlying rheumatic condition. The combination of ultrafiltration and high resolution ^1H NMR analysis is a particularly powerful method for concentration profiling of low molecular weight metabolites. Ultrafiltration also serves to free metabolic components that are otherwise bound to proteins through weak interactions as well as to reveal those hidden by more dominant resonances. However, the majority of NMR-based metabolomics studies carried out in past with synovial fluid utilized intact SF and suffers with numerous challenges such as the limited resolution, low metabolite identification, and the adverse effects of ample proteins.

To the best of our knowledge, this is the first attempt where the rigorous analysis and detailed characterization of the low molecular weight metabolites present in the SF has been carried out on ultra-filtered SF by the composite use of 800 MHz 1D ^1H CPMG NMR and 2D J-resolved spectroscopy, homonuclear ^1H - ^1H TOCSY and heteronuclear ^1H - ^{13}C HSQC correlation methods. In total, we were able to identify 64 small endogenous metabolites (including many complex coupled spin systems) in ultra-filtered SF representing several metabolic pathways including those relevant in the context of energy metabolism, amino acid metabolism, lipid metabolism, inflammation and oxidative stress conditions. Also for the first time, we assigned the resonances of N-alpha acetyl lysine in the 1D ^1H NMR spectrum of normal SF, whereas these signals were not discerned in filtered SF suggesting the presence of acetylated proteins in the SF. We foresee that the characteristic spectral fingerprints of various metabolites present in the ultra-filtered SF samples will form the basis of future metabolomics studies aiming to identify SF based metabolic biomarkers for the diagnosis/prognosis, treatment response, or to provide valuable insights into the underlying biochemical processes and thus to aid in the pathogenesis of the inflammatory joint diseases such as Reactive arthritis.

2.6 Acknowledgment:

We greatly acknowledge the Department of Medical Education, Government of Uttar Pradesh, for supporting the high-field NMR facility at the Centre of Biomedical Research, Lucknow, India. DD acknowledges the ICMR, India for his PhD research fellowship.

2.7 References:

1. Guma, M.; Tiziani, S.; Firestein, G. S., Metabolomics in rheumatic diseases: desperately seeking biomarkers. *Nature Reviews Rheumatology* **2016**, 12, (5), 269-281.
2. Smeets, T. J. M.; Dolhain, R. J. E. M.; Breedveld, F. C.; Tak, P. P., Analysis of the cellular infiltrates and expression of cytokines in synovial tissue from patients with rheumatoid arthritis and reactive arthritis. *The Journal of pathology* **1998**, 186, (1), 75-81.
3. Kvien, T. K.; Glennas, A.; Melby, K.; Granfors, K.; Andrup, O.; Karstensen, B.; Thoen, J. E., Reactive arthritis: incidence, triggering agents and clinical presentation. *The Journal of Rheumatology* **1994**, 21, (1), 115-122.
4. Kekow, J. r.; Thiesen, H.-J. r.; Glocker, M. O., Mass spectrometric proteome analyses of synovial fluids and plasmas from patients suffering from rheumatoid arthritis and comparison to reactive arthritis or osteoarthritis. *Electrophoresis* **2002**, 23, 3445-3456.
5. Keat, A.; Dixey, J.; Sonnex, C.; Thomas, B.; Osborn, M.; Taylor-Robinson, D., Chlamydia trachomatis and reactive arthritis: the missing link. *The Lancet* **1987**, 329, (8524), 72-74.
6. Granfors, K.; Jalkanen, S.; von Essen, R.; Lahesmaa-Rantala, R.; Isomaki, O.; Pekkola-Heino, K.; Merilahti-Palo, R.; Saario, R.; Isomaki, H.; Toivanen, A., Yersinia antigens in synovial-fluid cells from patients with reactive arthritis. *New England Journal of Medicine* **1989**, 320, (4), 216-221.
7. Saxne, T.; Wollheim, F.; Heinegård, D.; Pettersson, H., Difference in cartilage proteoglycan level in synovial fluid in early rheumatoid arthritis and reactive arthritis. *The Lancet* **1985**, 326, (8447), 127-128.
8. Xia, J.; Sinelnikov, I. V.; Han, B.; Wishart, D. S., MetaboAnalyst 3.0-making metabolomics more meaningful. *Nucleic acids research* **2015**, 43, (W1), W251-W257.
9. Nicholson, J. K.; Lindon, J. C., Systems biology: metabonomics. *Nature* **2008**, 455, (7216), 1054-1056.
10. Nicholson, J. K.; Connelly, J.; Lindon, J. C.; Holmes, E., Metabonomics: a platform for studying drug toxicity and gene function. *Nature reviews Drug discovery* **2002**, 1, (2), 153-161.
11. Gowda, G. A. N.; Zhang, S.; Gu, H.; Asiago, V.; Shanaiah, N.; Raftery, D., Metabolomics-based methods for early disease diagnostics. *Expert review of molecular diagnostics* **2008**, 8, (5), 617-633.
12. Beckonert, O.; Keun, H. C.; Ebbels, T. M. D.; Bundy, J.; Holmes, E.; Lindon, J. C.; Nicholson, J. K., Metabolic profiling, metabolomic and metabonomic procedures for NMR spectroscopy of urine, plasma, serum and tissue extracts. *Nature protocols* **2007**, 2, (11), 2692-2703.
13. Emwas, A.-H. M., The strengths and weaknesses of NMR spectroscopy and mass spectrometry with particular focus on metabolomics research. *Metabonomics: Methods and Protocols* **2015**, 161-193.
14. Zhang, W.; Sun, G.; Likhodii, S.; Aref-Eshghi, E.; Harper, P. E.; Randell, E.; Green, R.; Martin, G.; Furey, A.; Rahman, P., Metabolomic analysis of human synovial fluid and plasma reveals that phosphatidylcholine metabolism is associated with both osteoarthritis and diabetes mellitus. *Metabolomics* **2016**, 12, (2), 24.

15. Zhang, W.; Likhodii, S.; Zhang, Y.; Aref-Eshghi, E.; Harper, P. E.; Randell, E.; Green, R.; Martin, G.; Furey, A.; Sun, G., Classification of osteoarthritis phenotypes by metabolomics analysis. *BMJ open* **2014**, 4, (11), e006286.
16. Zhang, Q.; Li, H.; Zhang, Z.; Yang, F.; Chen, J., Serum metabolites as potential biomarkers for diagnosis of knee osteoarthritis. *Disease markers* **2015**, Article ID 684794.
17. Young, S. P.; Kapoor, S. R.; Viant, M. R.; Byrne, J. J.; Filer, A.; Buckley, C. D.; Kitas, G. D.; Raza, K., The impact of inflammation on metabolomic profiles in patients with arthritis. *Arthritis & Rheumatology* **2013**, 65, (8), 2015-2023.
18. van Wietmarschen, H. A.; Dai, W.; van der Kooij, A. J.; Reijmers, T. H.; Schroën, Y.; Wang, M.; Xu, Z.; Wang, X.; Kong, H.; Xu, G., Characterization of rheumatoid arthritis subtypes using symptom profiles, clinical chemistry and metabolomics measurements. *PloS one* **2012**, 7, (9), e44331.
19. Smolenska, Z.; Zdrojewski, Z., Metabolomics and its potential in diagnosis, prognosis and treatment of rheumatic diseases. *Reumatologia* **2015**, 53, (3), 152.
20. Semerano, L.; Romeo, P.-H.; Boissier, M.-C., Metabolomics for rheumatic diseases: has the time come? In BMJ Publishing Group Ltd: 2015.
21. Scrivo, R.; Casadei, L.; Valerio, M.; Priori, R.; Valesini, G.; Manetti, C., Metabolomics approach in allergic and rheumatic diseases. *Current allergy and asthma reports* **2014**, 14, (6), 445.
22. Parkes, H. G.; Grootveld, M. C.; Henderson, E. B.; Farrell, A.; Blake, D. R., Oxidative damage to synovial fluid from the inflamed rheumatoid joint detected by ¹H NMR spectroscopy. *Journal of pharmaceutical and biomedical analysis* **1991**, 9, (1), 75-82.
23. Naughton, D. P.; Haywood, R.; Blake, D. R.; Edmonds, S.; Hawkes, G. E.; Grootveld, M., A comparative evaluation of the metabolic profiles of normal and inflammatory knee-joint synovial fluids by high resolution proton NMR spectroscopy. *FEBS letters* **1993**, 332, (3), 221-225.
24. Naughton, D.; Whelan, M.; Smith, E. C.; Williams, R.; Blake, D. R.; Grootveld, M., An investigation of the abnormal metabolic status of synovial fluid from patients with rheumatoid arthritis by high field proton nuclear magnetic resonance spectroscopy. *FEBS letters* **1993**, 317, (1-2), 135-138.
25. Mickiewicz, B.; Kelly, J. J.; Ludwig, T. E.; Weljie, A. M.; Wiley, J. P.; Schmidt, T. A.; Vogel, H. J., Metabolic analysis of knee synovial fluid as a potential diagnostic approach for osteoarthritis. *Journal of Orthopaedic Research* **2015**, 33, (11), 1631-1638.
26. Mickiewicz, B.; Heard, B. J.; Chau, J. K.; Chung, M.; Hart, D. A.; Shrive, N. G.; Frank, C. B.; Vogel, H. J., Metabolic profiling of synovial fluid in a unilateral ovine model of anterior cruciate ligament reconstruction of the knee suggests biomarkers for early osteoarthritis. *Journal of Orthopaedic Research* **2015**, 33, (1), 71-77.
27. Kokebie, R.; Aggarwal, R.; Lidder, S.; Hakimiyan, A. A.; Rueger, D. C.; Block, J. A.; Chubinskaya, S., The role of synovial fluid markers of catabolism and anabolism in osteoarthritis, rheumatoid arthritis and asymptomatic organ donors. *Arthritis research & therapy* **2011**, 13, (2), R50.

28. Kim, S.; Hwang, J.; Xuan, J.; Jung, Y. H.; Cha, H.-S.; Kim, K. H., Global metabolite profiling of synovial fluid for the specific diagnosis of rheumatoid arthritis from other inflammatory arthritis. *PLoS one* **2014**, 9, (6), e97501.
29. Kapoor, S.; Fitzpatrick, M.; Clay, E.; Bayley, R.; Wallace, G. R.; Young, S. P., *Metabolomics in the analysis of inflammatory diseases*. Intech: 2017.
30. Hugle, T.; Kovacs, H.; Heijnen, I. A.; Daikeler, T.; Baisch, U.; Hicks, J. M.; Valderrabano, V., Synovial fluid metabolomics in different forms of arthritis assessed by nuclear magnetic resonance spectroscopy. *Clin Exp Rheumatol* **2012**, 30, (2), 240-5.
31. Grootveld, M.; Henderson, E. B.; Farrell, A.; Blake, D. R.; Parkes, H. G.; Haycock, P., Oxidative damage to hyaluronate and glucose in synovial fluid during exercise of the inflamed rheumatoid joint. Detection of abnormal low-molecular-mass metabolites by proton-nmr spectroscopy. *Biochemical Journal* **1991**, 273, (2), 459-467.
32. Adams, S. B.; Setton, L. A.; Kensicki, E.; Bolognesi, M. P.; Toth, A. P.; Nettles, D. L., Global metabolic profiling of human osteoarthritic synovium. *Osteoarthritis and cartilage* **2012**, 20, (1), 64-67.
33. Adams Jr, S. B.; Setton, L. A.; Nettles, D. L., The role of metabolomics in osteoarthritis research. *The Journal of the American Academy of Orthopaedic Surgeons* **2013**, 21, (1), 63.
34. Nicholson, J. K.; Lindon, J. C.; Holmes, E., 'Metabonomics': understanding the metabolic responses of living systems to pathophysiological stimuli via multivariate statistical analysis of biological NMR spectroscopic data. *Xenobiotica* **1999**, 29, (11), 1181-1189.
35. Lindon, J. C.; Nicholson, J. K.; Holmes, E.; Everett, J. R., Metabonomics: metabolic processes studied by NMR spectroscopy of biofluids. *Concepts in Magnetic Resonance Part A* **2000**, 12, (5), 289-320.
36. Kumar, D.; Rawat, A.; Dubey, D.; Kumar, U.; Keshari, A. K.; Saha, S.; Guleria, A., NMR Based Metabolomics: An Emerging Tool for Therapeutic Evaluation of Traditional Herbal Medicines. *SM-eBOOK: Nuclear Magnetic Resonance Spectroscopy* **2016**, 1-18.
37. Weljie, A. M.; Dowlatabadi, R.; Miller, B. J.; Vogel, H. J.; Jirik, F. R., An inflammatory arthritis-associated metabolite biomarker pattern revealed by ¹H NMR spectroscopy. *Journal of proteome research* **2007**, 6, (9), 3456-3464.
38. Gowda, G. A. N.; Raftery, D., Quantitating metabolites in protein precipitated serum using NMR spectroscopy. *Analytical chemistry* **2014**, 86, (11), 5433-5440.
39. Daykin, C. A.; Foxall, P. J. D.; Connor, S. C.; Lindon, J. C.; Nicholson, J. K., The comparison of plasma deproteinization methods for the detection of low-molecular-weight metabolites by ¹H nuclear magnetic resonance spectroscopy. *Analytical Biochemistry* **2002**, 304, (2), 220-230.
40. Wallmeier, J.; Samol, C.; Ellmann, L.; Zacharias, H. U.; Vogl, F. C.; Garcia, M.; Dettmer, K.; Oefner, P. J.; Gronwald, W.; Investigators, G. S., Quantification of Metabolites by NMR Spectroscopy in the Presence of Protein. *Journal of proteome research* **2017**, 16, (4), 1784-1796.

41. Wishart, D. S., Quantitative metabolomics using NMR. *TrAC Trends in Analytical Chemistry* **2008**, 27, (3), 228-237.
42. McKay, R. T., How the 1D-NOESY suppresses solvent signal in metabonomics NMR spectroscopy: An examination of the pulse sequence components and evolution. *Concepts in Magnetic Resonance Part A* **2011**, 38, (5), 197-220.
43. Fitzpatrick, M. A.; McGrath, C. M.; Young, S. P., Pathomx: an interactive workflow-based tool for the analysis of metabolomic data. *BMC bioinformatics* **2014**, 15, (1), 396.
44. Xia, J.; Psychogios, N.; Young, N.; Wishart, D. S., MetaboAnalyst: a web server for metabolomic data analysis and interpretation. *Nucleic acids research* **2009**, 37, (suppl_2), W652-W660.
45. Worley, B.; Powers, R., Multivariate analysis in metabolomics. *Current Metabolomics* **2013**, 1, (1), 92-107.
46. Xia, J.; Bjorndahl, T. C.; Tang, P.; Wishart, D. S., MetaboMiner-semi-automated identification of metabolites from 2D NMR spectra of complex biofluids. *BMC bioinformatics* **2008**, 9, (1), 507.
47. Wishart, D. S.; Jewison, T.; Guo, A. C.; Wilson, M.; Knox, C.; Liu, Y.; Djoumbou, Y.; Mandal, R.; Aziat, F.; Dong, E., HMDB 3.0-the human metabolome database in 2013. *Nucleic acids research* **2013**, 41, (D1), D801-D807.
48. Nicholson, J. K.; Foxall, P. J. D.; Spraul, M.; Farrant, R. D.; Lindon, J. C., 750 MHz ¹H and ¹H-¹³C NMR spectroscopy of human blood plasma. *Analytical chemistry* **1995**, 67, (5), 793-811.
49. Nagana Gowda, G. A.; Gowda, Y. N.; Raftery, D., Expanding the limits of human blood metabolite quantitation using NMR spectroscopy. *Analytical chemistry* **2014**, 87, (1), 706-715.
50. Merrifield, C. A.; Lewis, M.; Claus, S. P.; Beckonert, O. P.; Dumas, M.-E.; Duncker, S.; Kochhar, S.; Rezzi, S.; Lindon, J. C.; Bailey, M., A metabolic system-wide characterisation of the pig: a model for human physiology. *Molecular BioSystems* **2011**, 7, (9), 2577-2588.
51. Govindaraju, V.; Young, K.; Maudsley, A. A., Proton NMR chemical shifts and coupling constants for brain metabolites. *NMR in Biomedicine* **2000**, 13, (3), 129-153.
52. Duarte, I. F.; Legido-Quigley, C.; Parker, D. A.; Swann, J. R.; Spraul, M.; Braumann, U.; Gil, A. M.; Holmes, E.; Nicholson, J. K.; Murphy, G. M., Identification of metabolites in human hepatic bile using 800 MHz ¹H NMR spectroscopy, HPLC-NMR/MS and UPLC-MS. *Molecular BioSystems* **2009**, 5, (2), 180-190.
53. Wang, L.; Tang, Y.; Liu, S.; Mao, S.; Ling, Y.; Liu, D.; He, X.; Wang, X., Metabonomic profiling of serum and urine by ¹H NMR-based spectroscopy discriminates patients with chronic obstructive pulmonary disease and healthy individuals. *PLoS one* **2013**, 8, (6), e65675.
54. Pelantová, H.; Bugáňová, M.; Anýž, J.; Železná, B.; Maletínská, L.; Novák, D.; Haluzík, M.; Kuzma, M., Strategy for NMR metabolomic analysis of urine in mouse models of obesity—from sample collection to interpretation of acquired data. *Journal of pharmaceutical and biomedical analysis* **2015**, 115, 225-235.

55. Wojtowicz, W.; Zabek, A.; Deja, S.; Dawiskiba, T.; Pawelka, D.; Glod, M.; Balcerzak, W.; Mlynarz, P., Serum and urine ^1H NMR-based metabolomics in the diagnosis of selected thyroid diseases. *Scientific reports* **2017**, *7*, (1), 9108.
56. Moore, G. J.; Sillerud, L. O., The pH dependence of chemical shift and spin-spin coupling for citrate. *Journal of Magnetic Resonance, Series B* **1994**, *103*, (1), 87-88.
57. Arito, M.; Nagai, K.; Ooka, S.; Sato, T.; Takakuwa, Y.; Kurokawa, M. S.; Sase, T.; Okamoto, K.; Suematsu, N.; Kato, T., Altered acetylation of proteins in patients with rheumatoid arthritis revealed by acetyl-proteomics. *Clinical and experimental rheumatology* **2015**, *33*, (6), 877-886.
58. Ahn, J. K.; Kim, S.; Kim, J.; Hwang, J.; Kim, K. H.; Cha, H.-S., A comparative metabolomic evaluation of Behcet's disease with arthritis and seronegative arthritis using synovial fluid. *PloS one* **2015**, *10*, (8), e0135856.

Chapter-4

NMR based serum metabolomics revealed distinctive metabolic patterns in Reactive Arthritis compared to Rheumatoid Arthritis

Durgesh Dubey, Sandeep Kumar, Smriti Chaurasia, Anupam Guleria, Sakir Ahmed, Rajeev Singh, Reena Kumari, Dinesh Raj Modi, Ramnath Misra, and Dinesh Kumar

J. Proteome Res., 2019, 18 (1), pp 130–146

CONTENTS-

3.1 Abstract

3.2 Introduction

3.3 Materials and Method

3.3.1 Sample Collection and preparation

3.3.2 NMR Measurements

3.3.3 Spectral Assignment

3.3.4 Data Pre-processing

3.3.5 Multivariate Statistical analysis

3.4 Results

3.4.1 Patient characteristics

3.4.2 ¹H NMR Spectral assignment

3.4.3 Multivariate Pattern Recognition analysis

3.4.4 Discovery of distinctive metabolic signatures of ReA compared to non-ReA groups

3.4.5 ROC curve analysis for Biomarker Discovery

3.5 Discussion

3.6 Concluding Remarks

3.7 Acknowledgment

3.8 References

3.1 Abstract:

Reactive arthritis (ReA) is a member of seronegative spondyloarthropathy (SSA) which involves an acute/subacute onset of asymmetrical lower limb joint inflammation following weeks after a genitourinary/gastrointestinal infection. The diagnosis is clinical as it is difficult to culture the microbes from synovial fluid. Arthritis patients with similar clinical picture, but, lapsed history of immediate preceding infection and do not fulfill the diagnostic criteria of other members of SSA such as ankylosing-spondylitis, psoriatic-arthritis and arthritis associated with inflammatory-bowel-disease, are labeled as peripheral undifferentiated spondyloarthropathy (uSpA). Both ReA and uSpA patients show a strong association with Class-I major-histocompatibility-complex (MHC) allele, HLA-B27 and a clear association with an infectious trigger, however, the disease mechanism is far from clear. As the clinical picture is largely dominated by Rheumatoid arthritis (RA) like features including elevated levels of inflammatory markers (such as ESR, CRP, etc.), these overlapping symptoms often confound the clinical diagnosis and represent a clinical dilemma making treatment choice more generalized. Therefore, there is a compelling need to identify biomarkers that can support the diagnosis of ReA/uSpA . In present study, we performed NMR based serum-metabolomics analysis and demonstrated that ReA/uSpA patients are clearly distinguishable from controls and further these patients can also be distinguished from the RA patients based on the metabolic profiles, both with high sensitivity and specificity. The discriminatory metabolites were further subjected to area under receiver operating characteristic (AUROC) curve analysis and led to the identification of four metabolic entities (i.e. valine, leucine, arginine/lysine and phenylalanine) which could differentiate ReA/uSpA from RA.

Keywords: Reactive Arthritis, Rheumatoid Arthritis, NMR, Metabolic signatures, Differential diagnosis

3.2 Introduction:

Reactive arthritis (ReA) is an autoimmune condition that typically, follows weeks after a genitourinary or gastrointestinal infection (predominantly in males).¹ The clinical symptoms include an acute or subacute onset of asymmetrical lower limb joint inflammation, however, sometimes other articular and extra-articular manifestations may also be seen such as dactylitis, enthesitis, conjunctivitis and unilateral sacroiliitis.¹⁻³ As such, ReA is a member of heterogeneous group called seronegative spondyloarthropathy (SSA). However, a substantial proportion of SSA patients who have similar clinical picture like ReA, but, do not confer history of preceding infection and do not fulfill diagnostic criteria of other members of SSA (such as Ankylosing spondylitis, Psoriatic arthritis and Arthritis associated with inflammatory bowel disease) are appropriately labeled as peripheral undifferentiated spondyloarthropathy (uSpA).⁴ In previous studies from our group,^{5,6} we have shown that both ReA and uSpA have similar levels of pro-inflammatory cytokines such as IL-17 and IL-6 in the sera and synovial fluid, sera antibodies to enteric organisms and recently expansion of antigen specific T-cell response to salmonella outer membrane protein A in enterically acquired ReA/uSpA. Both ReA and uSpA show a strong association with Class-I major-histocompatibility-complex (MHC) allele, HLA-B27 and a clear association with microbial trigger, however, the disease mechanism is still not clear. It is assumed that the components of bacteria persist *in vivo* (i.e. antigenic persistence, usually in the synovium and synovial fluid) and trigger immune reactions (molecular cross-reactivity).¹ Microbiological confirmation is the gold standard to support the diagnosis of ReA, but it is not practical since by the time the patient presents, organisms cannot be isolated or cultured from synovial fluid. Therefore, the diagnosis is largely empirical based on few clinical symptoms (including positive serological demonstration of antibodies directed against specific bacteria).⁷ However for majority of patients, the clinical picture is largely dominated by Rheumatoid arthritis (RA) like features which is another autoimmune, but, seropositive inflammatory arthritis condition. The laboratory parameters for instance acute-phase reactants, such as C-reactive protein (CRP)⁸ and erythrocyte sedimentation rate (ESR) are usually elevated significantly (e.g. ESR of 50-70 mm/hr) but does not distinguish ReA/uSpA from other inflammatory arthritis including RA. Therefore, there is an unmet need to identify distinctive biomarkers that can support the diagnosis of ReA/uSpA and its discrimination from other inflammatory arthritis conditions.

Metabolomics –an analytical approach to metabolism- involves quantitative and comparative analysis of metabolic profiles in affected biological systems and provides relevant biomarkers to improve diagnostic accuracy, define prognosis and predict and monitor treatment efficacy. So far, no serum based metabolomics studies have been attempted to identify distinctive serum metabolic patterns of ReA and metabolic biomarkers to facilitate the differential diagnosis of ReA from RA. Compared to gene and protein levels, the metabolic profiles are highly dynamic and may change even when the genes and protein levels do not change significantly. Thus the metabolite profiling has huge potential to facilitate early diagnosis, predicting disease course and improving the treatment. The present study intends to investigate the altered metabolic patterns in the sera of ReA/uSpA and RA patients. For this, we used the NMR based metabolomics approach in combination with multivariate statistical analysis tools and sought to identify the markers for early and reliable differential diagnosis of ReA and RA. The serum metabolic profiles of 52 ReA /uSpA patients were measured and compared to those of 29 RA patients. Important to mention here is that the ReA/uSpA condition is predominantly found in young adults in the age group 20–40 years, where it affects men more so than women (ratio 3:1),^{2,9} whereas RA condition predominantly affects old population with age ranging from 30-50 years and the prevalence of RA is higher in females than males, the incidence is 4-5 times higher below the age of 50, but above 60-70 years the female/male ratio is only about 2.¹⁰ Owing to different age groups and male to female ratios involved with these two immune mediated inflammatory arthritis conditions, we selected large sample size for normal control group with age ranging from 20 to 60 so that the metabolic changes due to confounding factors (i.e. age and sex-ratio) can be nullified as much as possible. In a preliminary study from our group,¹¹ we have found that the serum metabolic profiles of ReA and uSpA are almost similar i.e. the ReA and uSpA patients lack metabolomic discrimination (see **Figure 3.1**). Further, as ReA and uSpA patients are present with the same clinical picture, we have now used the notion ReA for combined ReA/uSpA group in rest of the manuscript to keep the graphics and related discussion simple. Accordingly, **Figure 3.2** shows the strategical protocol used in this study to compare the serum metabolic profiles of ReA and non-ReA groups.

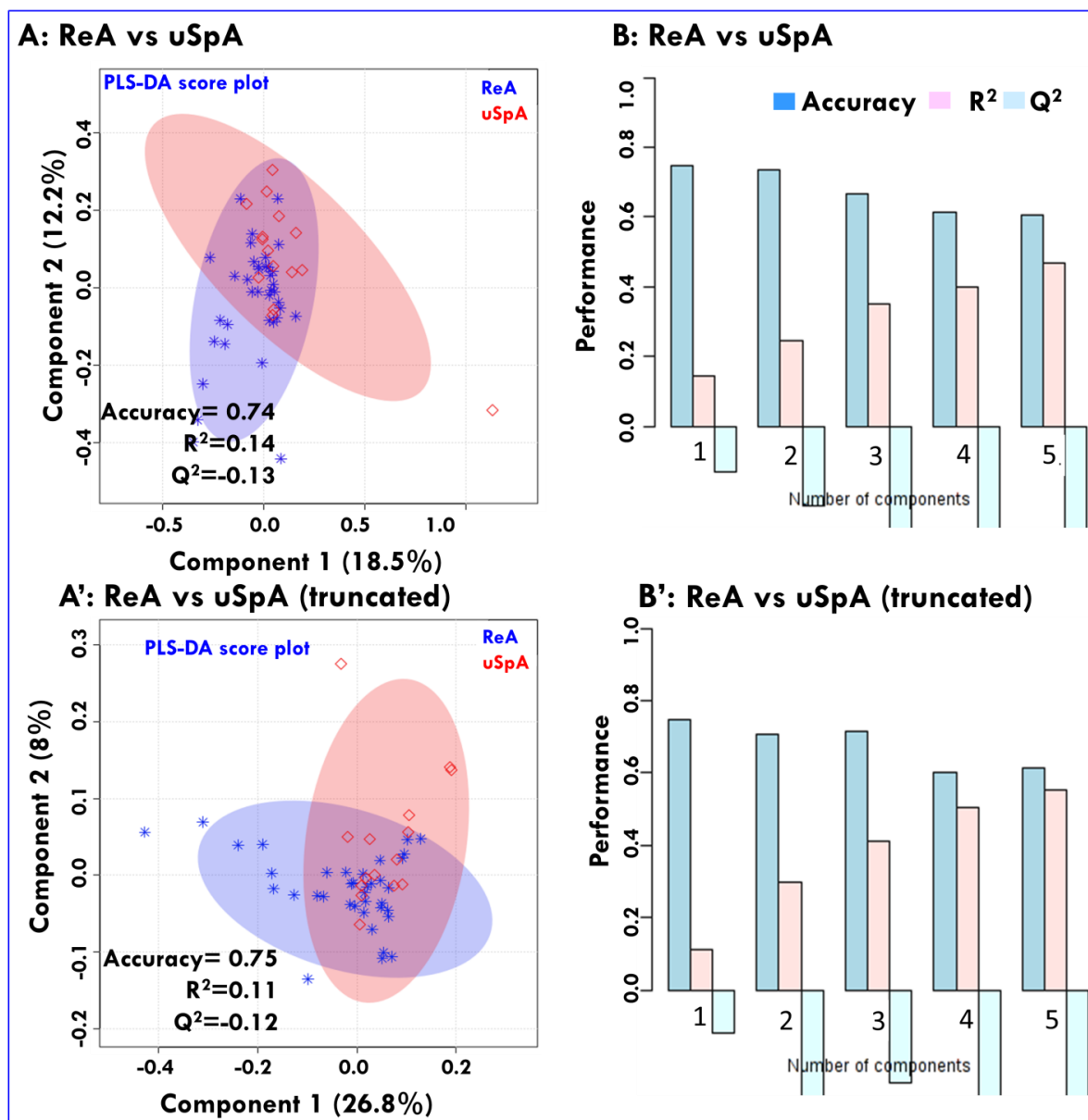


Figure 3.1: (A,A') The 2D score plots derived from pairwise PLS-DA analysis of 1D ¹H CPMG NMR spectra of serum samples obtained from ReA and uSpA patients. (A) represents the analysis of complete data matrix generated from 1D ¹H CPMG NMR spectra, whereas (A') represent the analysis of truncated data matrix i.e. CPMG data matrix with excluded spectral regions corresponding to glucose (3.21 to 6.0) and lipid metabolites (0.6 to 0.96, 1.2 to 1.36, 1.92 to 2.04, 2.9 to 3.02). The shaded or semi-transparent areas represent the 95% confidence regions of each group as depicted by their respective colors. (B,B') represent the bar plots showing the three performance measures (prediction accuracy, multiple correlation coefficient R² and the explained variance in prediction Q²) obtained after 10 fold Cross Validation analysis of complete (B) and truncated (B') CPMG data matrix, respectively. The negative Q² values clearly indicated that the ReA and uSpA patients lack metabolic discrimination i.e. the serum metabolic profiles of ReA and uSpA are almost similar.

As shown in **Figure 3.2**, the study protocol involves four types of discriminatory analysis: (a) first the serum metabolic profiles of ReA patients were compared to age and sex matched young normal controls (YNC), (b) second the serum metabolic profiles of RA patients were compared to age and sex matched elderly normal controls (ENC), (c) third, the serum metabolic profiles of ReA patients were compared to non-ReA groups (RA and NC, pairwise as well as combined) and finally (d) the serum metabolic profiles of ReA and RA patients were compared. The aim of this study was to explore whether NMR-based serum metabolomics would reveal a distinctive metabolic signature of ReA which are not influenced by age and sex; thereby, to appraise its utility in clinical screening of ReA patients presenting with RA disease like features. In addition, the study would also provide novel insights into the metabolic disturbances underlying ReA.

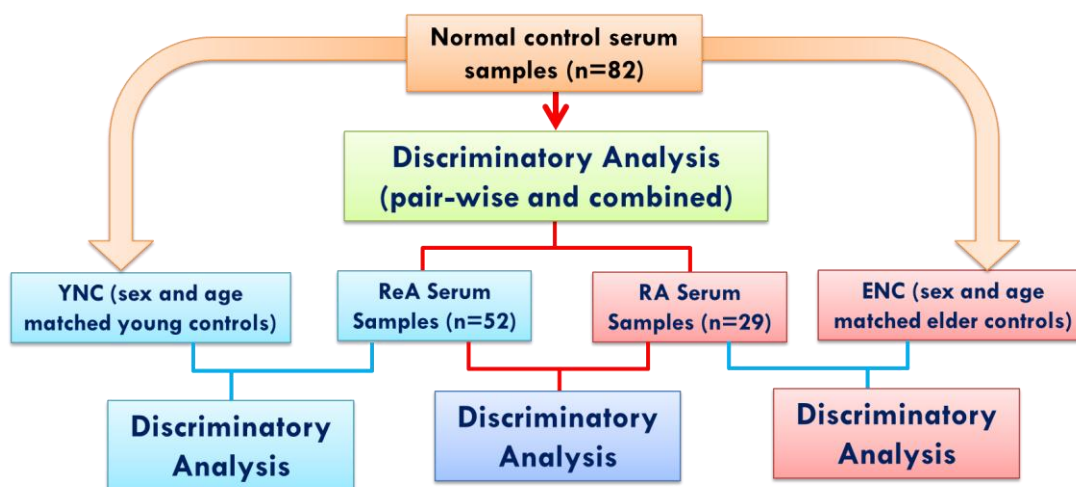


Figure 3.2: The schematic showing the study protocol used to compare the metabolic profiles of ReA and RA with respect to normal controls.

3.3 Material and methods

3.3.1 Sample collection and preparation:

Sera were obtained from 52 patients with ReA (n=52, confirmed ReA=37 and uSpA=15) and 29 patients with RA and 82 normal controls and informed consents were obtained from all the patients before their enrolment in the study after informed consent. The patients for the study were recruited from the outpatient and indoors of the department of Clinical Immunology, SGPGIMS Lucknow, Uttar Pradesh, India between July 2014 and September 2017. The patients satisfying the Braun's criteria for Reactive Arthritis are labelled as ReA patients,¹² whereas patients with undifferentiated

spondyloarthritis (uSpA) were selected if they fulfilled the ASAS criteria for pSpA¹³ but who did not fulfil criteria for psoriatic arthritis, inflammatory bowel disease associated arthritis. Patients with RA were selected if they fulfilled the ACR Criteria.¹⁴ The study protocol was approved by the Institutional Research Ethics Committee, SGPGIMS, Lucknow. Sera were stored at -80 °C, until the NMR measurements were performed. Cell free Synovial fluid (SF) from inflamed knee joints of 41 patients with ReA/uSpA were collected at the time of joint aspiration for local corticosteroid injections in whom sera was also collected (for paired analysis). For NMR investigations, the 300 µL SF samples were separately aliquoted in 1.5 ml micro-centrifuge tubes (MCT) and frozen immediately using liquid Nitrogen (N₂) and stored at a temperature of -80 °C. The demographics and clinical characteristics of ReA and RA patients are tabulated in **Table 3 (See, Appendix)**.

Prior to NMR experiments, the stored serum samples were thawed at room temperature, vortexed and centrifuged at relative centrifugal force (rcf) of 16278 for 5 minutes at 4 °C to remove precipitates if any. The aliquots of 300 µL of serum were then added with additional 300 µL of 0.9% saline sodium phosphate buffer (of strength 50 mM and pH 7.4 prepared in 100% D₂O) to minimise the variation in pH. The buffer also contained 1.0 mM DSS-d6 (i.e. 2,2-Dimethyl- 2-silapentane- 5-sulfonate sodium salt) which served as an internal standard reference for chemical shift to aid NMR identification of metabolites based on their specific chemical shift pattern in CHENOMX. The deuterium oxide (D-99%) was purchased from Cambridge Isotop Laboratories (Tewksbury, MA, USA); whereas all other buffer reagents (of analytical grade) as well as DSS-d6 were purchased from Sigma-Aldrich (St. Louis, MI, USA). Buffer mixed serum samples were vortexed and a 600 µL of sample was transferred into a 5 mm NMR tube (Wilma Glass, USA). For accurate concentration profiling of marker metabolites, the paired (n=41) serum and synovial fluid (SF) samples were subjected to ultra-centrifugation to remove protein and lipid metabolites as described previously.¹⁵ Briefly, the samples were filtered using 3 kDa molecular-weight-cut-off (MWCO) centrifugal filters (Amicon Ultra 0.5 Centrifugal filter; Merck USA). For filtered serum/SF samples, the 300µL serum/SF was mixed with 300 µL of 0.9% saline sodium phosphate buffer, transferred to the filter units and centrifuged for 30 min at 14000 rcf. After ultracentrifugation, the 500 µL of filtrate obtained in each case was collected in a 1.5 ml of MCT and transferred to 5 mm NMR tubes (Wilma Glass, USA) for NMR experiments.

3.3.2 NMR Measurements

The serum and SF metabolic profiles were measured using high-resolution 1D ^1H CPMG (Carr–Purcell–Meiboom–Gill) NMR spectra recorded at 800 MHz NMR spectrometer (Bruker, Avance III, equipped with Cryoprobe).^{16,17} All the spectra were recorded at 300 K using the Bruker’s standard pulse program library sequence (cpmgpr1d) with pre-saturation of the water peak during recycle delay (RD) of 5.0 sec. Other acquisition parameters used for 1D ^1H CPMG pulse sequence were as follows: number of scans: 128; number of dummy scans: 8; spectral sweep width: 12 ppm; and sampling data points: 32 K. For suppressing the signals of proteins and higher MW lipid or lipoprotein metabolites, the T_2 filtering was obtained with an echo time of 200 μs repeated 300 times, resulting in a total duration of effective echo time of 60 ms. The raw NMR data were processed using standard Fourier Transformation (FT) procedure in Bruker software Topspin-v2.1 (Bruker-BioSpin GmbH, Silberstreifen 4 76287 Rheinstetten, Germany). Prior to FT, each free induction decay (FID) was zero-filled to 64 k data points, multiplied by an exponential window function and a line broadening function of 0.3 Hz was applied.

3.3.3 Spectral Assignment:

The metabolite resonances in 1D ^1H CPMG NMR spectra were assigned as much as possible using commercial software Chenomx NMR Suite (form Chenomx Inc., Edmonton, AB, Canada containing 800 MHz chemical shift database). The left over peaks were assigned by comparing them with the metabolite assignments reported previously¹⁷⁻¹⁹ or those available with BMRB database (Biological Magnetic Resonance Data Bank) and HMDB (The Human Metabolome Database).^{20,21} The obtained resonance assignments were further validated based on their specific CH correlations and ^1H - ^1H scalar coupling patterns, respectively, in the 2D ^1H - ^{13}C HSQC spectra and 2D J-resolved NMR spectra (recorded for some of the serum samples selected randomly). Similarly, the marker metabolites in filtered serum samples were identified and validated through comparing with previous report.²² The metabolite assignment of filtered SF has recently been reported by our group¹⁵ and the same information has been extended here for spectral identification marker metabolites. The concentrations of marker metabolites in the 1D ^1H CPMG NMR spectra of filtered serum and SF samples have been measured using profiler module of CHENOMX NMR Suite using 0.5 mM DSS-d6 as an internal reference for all the samples.

3.3.4 Data Pre-processing:

Prior to multivariate data analysis, all the 1D ^1H CPMG NMR spectra were manually phased, baseline corrected and referenced internally to the methyl resonance of lactate at δ 1.3102. The CPMG spectra in the chemical shift region δ (0.7-8.5) ppm were binned into 0.02 ppm spectral buckets and automatically integrated using AMIX software (version 3.8.7, Bruker GmbH, Germany). The chemical shift region δ (4.6-5.1) distorted due to water suppression was excluded from the CPMG data matrix to avoid the effects of imperfect water suppression. The integrated spectral bins were further normalized to the total intensity of the spectrum. The resulted data matrix generated with AMIX software was then exported into Microsoft Office Excel 2010, converted into CSV (comma-separated values) format, added with sample and class information and finally imported into MetaboAnalyst 3.0 for multivariate analysis in which the data matrix was scaled to Pareto variance.^{23,24} Metaboanalyst is a freely available, user-friendly, web-based analytical platform for high-throughput metabolomics studies (opened for academic users from the University of Alberta, Canada).^{23,25}

3.3.5 Multivariate Statistical analysis:

The spectral features were first analyzed by principal component analysis (PCA) to detect intrinsic clusters and outliers within the data set. To maximize separation between samples, partial least-squares discriminant analysis (PLS-DA) was applied. As PLS-DA mainly focuses on to maximize the covariance between the predictor space and the response space, thus may overfit the data to separate classes of observations even there is no apparent difference between them, therefore discriminatory performance of the PLS-DA model needs to be validated rigourosuly.²⁶ The model validation was performed using first two latent variables via repeated 10-fold internal cross validation (CV) and the quality of model was accessed based on validation parameters: R^2 (which represents explained variation) and Q^2 (which represents predictive capability). To further verify the robustness of PLS-DA models in discriminating the different cohorts, the receiver operating characteristic (ROC) analysis was perfromed. The area under the ROC curve (AUROC) was computed to evaluate the effectiveness of PLS-DA model in discriminating ReA from non-ReA groups. The AUROC reveals excellent discriminatory potential if the value is close to one (>0.9 to 1.0), moderate discriminatory ability if value is between 0.6 to 0.9 and if it is less than 0.6, it represents almost no discriminatory ability. ROC curves are generated in Metaboanalyst using

Monte-Carlo cross validation algorithm based on balanced subsampling.²⁴ PLS-DA algorithm was selected as classification and feature ranking method. The metabolites of discriminatory significance were screened out based on the variable importance on projection score (VIP) statistics analysis using VIP score >1.0 as the criterion of discriminatory significance.^{23,27} The metabolites of discriminatory significance between two study groups (according to strategy described in **Fig. 2**) were further tested for statistical significance (i.e. to evaluate if the change is statistically significant or not) via nonparametric Wilcoxon-Mann-Whitney test and p-value <0.05 was used as the criterion for statistical significance.

The variations in the levels of significant metabolites in ReA and non-ReA samples were visualized using the boxplot representation with the error bars representing standard error of the mean. For each suggestive biomarker metabolite, the ROC curve analysis was also performed and the most sensitive and specific diagnostic panel of biomarkers was identified as described previously.^{25,28} The area under the ROC curve (AUROC), 95% confidence interval (CI) and p-values were computed to evaluate the effectiveness of panel metabolites in discriminating ReA from non-ReA groups.²⁹ To establish the impact of synovial inflammation on serum metabolic perturbations, we also performed correlation analysis between concentration levels of marker metabolites in serum and those in synovial fluid (SF). The correlation analysis was performed using software program SPSS (v11.2, IBM) and evaluated based on Spearman rank correlation coefficient (r). A p-value <0.05 was considered for a statistically significance.

3.4 Results

3.4.1 Patient characteristics

Demographic and clinical characteristics of 52 patients with ReA, 29 patients with RA and 82 normal control subjects are shown in **Table 3 (See, Appendix)**. The ReA patients were selected from more than 300 patients with post-infection arthritis and were not receiving prior antibiotic treatment; whereas the RA patients were selected from more than 200 patients who were not receiving any disease-modifying anti-rheumatic drug (DMARD) and had enrolled during the initial presentation of RA. The normal controls were randomly selected and further divided into two groups: (a) young normal control group (YNC, n=55) with age and sex matched to ReA patients and (b) elder normal control group (ENC, n=33) with age and sex matched to RA patients. As shown **Table 3**, overall there were 82 normal control samples with male: female ratio equal to 57:25 and age ranging from 21-57 years (mean age =36.38±9.25).

3.4.2 ^1H NMR Spectral assignment:

The representative 1D ^1H CPMG NMR spectra of serum samples obtained from ReA and non-ReA groups are shown in **Figure 3.3**. The ^1H NMR signals assigned for various metabolites are also annotated in the Figure.

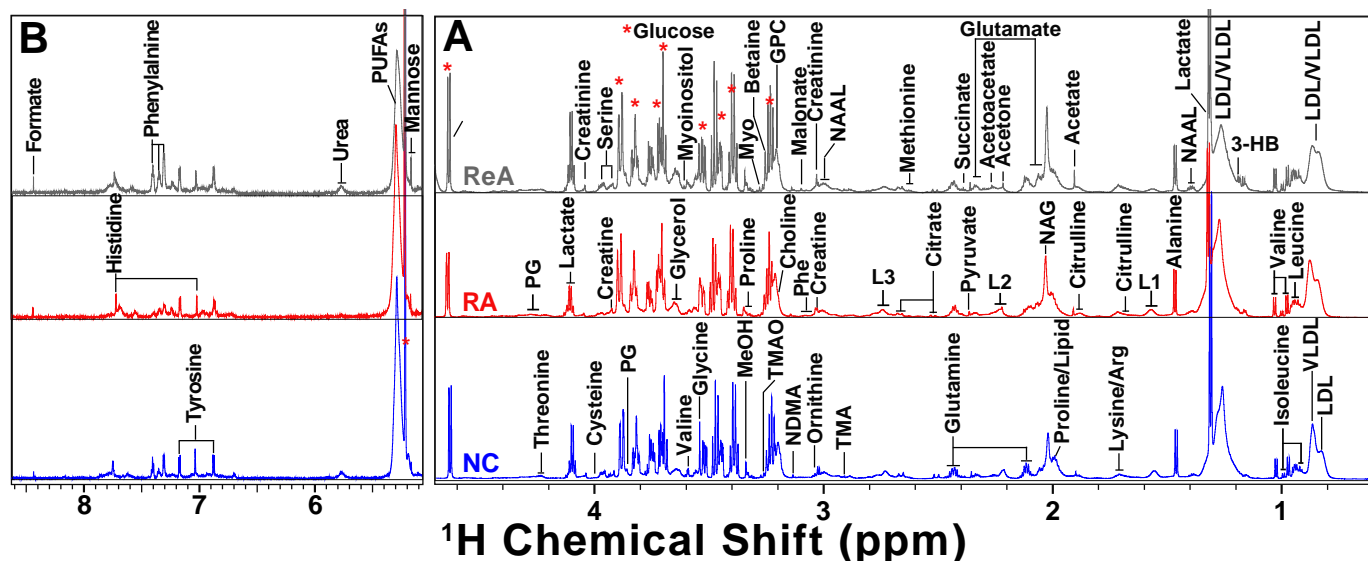


Figure 3.3: Representative 800 MHz 1D ^1H CPMG NMR spectra of serum samples selected from NC, RA and ReA study groups: (A) $\delta(0.75\text{-}4.65)$ and (B) $\delta(5.2\text{-}8.6)$. The spectral region $\delta(5.2\text{-}8.5)$ in (B) is magnified 8 times compared to spectral region $\delta(0.5\text{-}4.7)$ in (B) for the purpose of clarity. Abbreviations and notions used are: BCAA: Branched Chain Amino Acid (Isoleucine and Leucine); 3-HB: 3-Hydroxybutyrate; TMA: Trimethylamine; Lysine(P): Lysine side chains from proteins; TMA: Trimethylamine; PG: Phosphoglyceride; NDMA: N-nitroso-dimethylamine; NAG: N-acetylated glycoprotein; NAAL: N-alpha acetyl lysine; GPC: Glycerophosphocholine; LDL: Low Density Lipoprotein; VLDL: Very Low Density Lipoprotein; PUFA: Polyunsaturated Fatty Acid $-\text{CH}=\text{CH}-$; L1: $-\text{CH}_2-\text{CH}_2-\text{C}=\text{O}-$; L2: $-\text{CH}_2-\text{C}=\text{O}-$; L3: $=\text{CH}-\text{CH}_2-\text{CH}=\text{C}-$.

As evident, the serum spectra showed signals mainly from (a) lipid and membrane metabolites e.g. choline, Glycerophosphocholine (GPC), betaine, triglycerides (i.e. fatty acid chains annotated here as L1, L2 and L3) and polyunsaturated fatty acids (PUFAs), (b) lipoproteins e.g. low-density lipoprotein (LDL) and very low-density lipoprotein (VLDL), (c) amino acids e.g. alanine, valine, leucine, isoleucine, phenylalanine, histidine, tyrosine, glutamine, glutamate and proline etc., (d) energy metabolites e.g. glucose, lactate, creatine, creatinine, pyruvate, and citrate and (e) some other metabolites like acetate, acetoacetate, acetone, trimethylamine (TMA), trimethylamine-oxide (TMAO), N-acetyl-glycoproteins (NAG), myoinositol, malonate, and N-nitroso-dimethylamine (NDMA).

3.4.3 Multivariate Pattern Recognition analysis:

Multivariate Statistical analysis is performed to compare the metabolic profiles of ReA and non-ReA groups. The principal component analysis (PCA) and partial least-squares discriminant analysis (PLS-DA) are the two most commonly used multivariate data analysis tools in metabolomics studies of biofluids seeking metabolic differences between study groups.²³ Both PCA and PLS-DA facilitate researchers to interpret a vast amount of data easily and rapidly through reducing the hundreds of variables into few linearly uncorrelated components³⁰ represented in the form of score plots and loading plots. Of two, PCA is an unsupervised approach used to get an initial overview of intrinsic clustering or grouping trends and to identify outliers within the data set, whereas, PLS-DA is a supervised approach (requires class information) which minimizes the possible contribution of intergroup variability and further increases the discrimination between two or more groups compared to the results obtained by the PCA. For present study, the normalized CPMG data matrix was initially subjected to PCA analysis to examine inherent clustering and to identify outliers; however no markedly evident outlier found in the present study samples. Further, the PCA score plots showed only slight discrimination between ReA and non-ReA groups (results not shown), therefore PLS-DA is mainly used to demonstrate the discrimination/classification between ReA and non-ReA groups as it makes it possible to rotate the projection to latent variables that focus on class separation. Following the study protocol shown in [Figure 3.2](#), five distinct types of discriminatory analysis were performed to evaluate the metabolic disturbances associated with ReA compared to non-ReA groups ([Figure 3.4](#)): (a) ReA vs YNC, (b) RA vs ENC, (c) ReA vs NC, (d) RA vs NC and (e) ReA vs RA. As shown in [Figure 3.4](#), the clusters of ReA and RA patients were distinctively separated on the score plot of PLS-DA from YNC, ENC and NC clusters and were also well discriminated from each other indicating that the metabolic profiles of ReA and RA patients are quite different. Here, the purpose of comparing ReA and RA groups to NC group (involving 57 males and 25 females in the age group ranging from 21-57 years) is to rule out (or randomize) the effect of confounding factors like age and sex on the serum metabolic profiles. As shown in [Figure 3.4D](#) and [3.4E](#), the metabolic profiles of combined NC group are well clustered together and distinctively separated from arthritis patients (ReA and RA, respectively in [Figure 3.4D](#) and [3.4E](#)) suggesting that the metabolic changes associated with arthritis condition are of higher discriminatory significance than the metabolic changes associated with age and sex difference. In each case, the PLS-DA model validation parameters, R^2 (which indicates goodness of

fit) and Q^2 (which signifies the predictive capability) were significantly higher ($R^2 > 0.8$, $Q^2 > 0.6$, see **Figure 3.4**), indicating that the models possessed a satisfactory fit with good predictive power without overfitting of the original model.

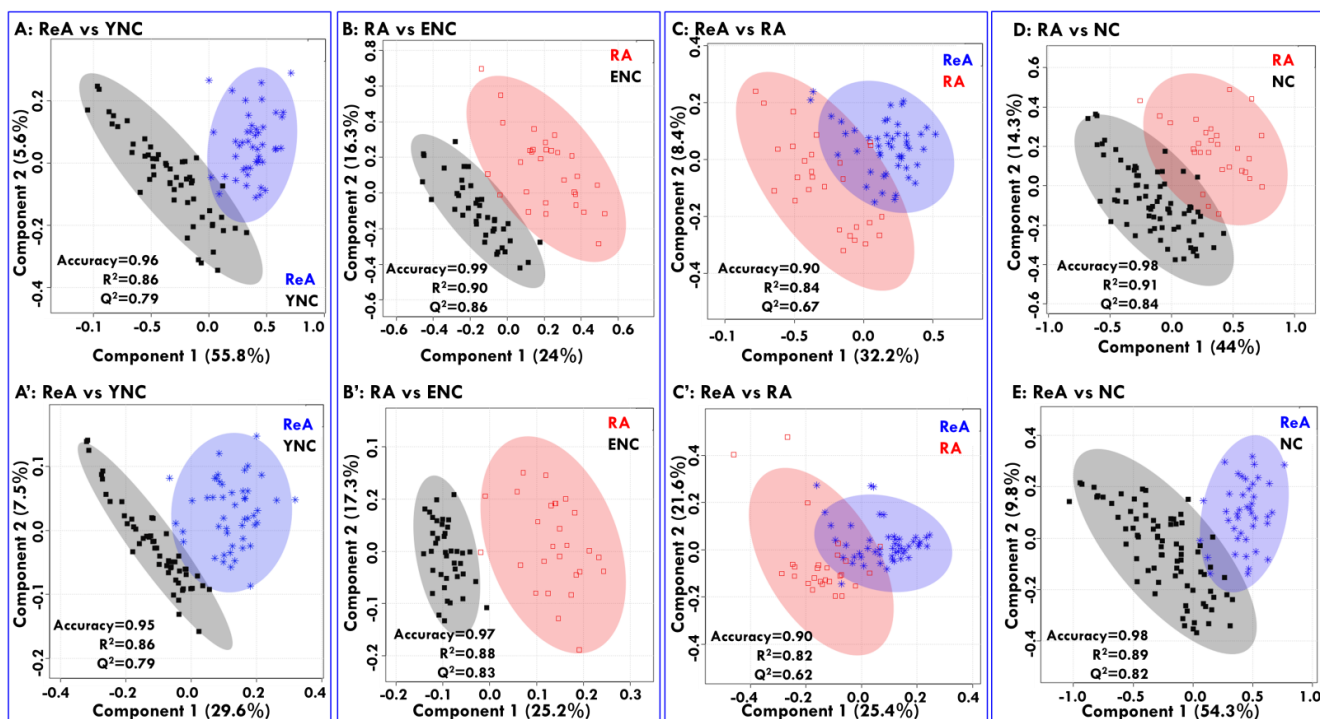


Figure 3.4: The 2D score plots derived from pairwise PLS-DA analysis of 1D ^1H CPMG NMR spectra of serum samples: **(A,A')** ReA vs YNC, **(B,B')** RA vs ENC, **(C)** ReA vs NC and **(D)** RA vs NC **(E,E')** ReA vs RA. **(A, B, C, D and E)** represent the 2D score plots obtained from pairwise PLS-DA analysis of complete data matrix generated from 1D ^1H CPMG NMR spectra, whereas **(A', B' and E')** represent the 2D score plots obtained from PLS-DA analysis of truncated data matrix generated from 1D ^1H CPMG NMR spectra. For score plots shown in **(A', B' and E')**, mainly the spectral regions corresponding to glucose (3.21 to 6.0) and lipid metabolites (0.6 to 0.96, 1.2 to 1.36, 1.92 to 2.04, 2.9 to 3.02) have been excluded owing to their higher serum concentration levels and thus to reveal the group discrimination based on serum metabolites present in low abundance and exhibiting relatively small difference in their quantitative profiles. The shaded or semi-transparent areas represent the 95% confidence regions of each group as depicted by their respective colors. Abbreviations used here are as per **Table 3** i.e. YNC: Young normal control; ENC: Elderly normal control; RA: Rheumatoid Arthritis; ReA: Reactive Arthritis.

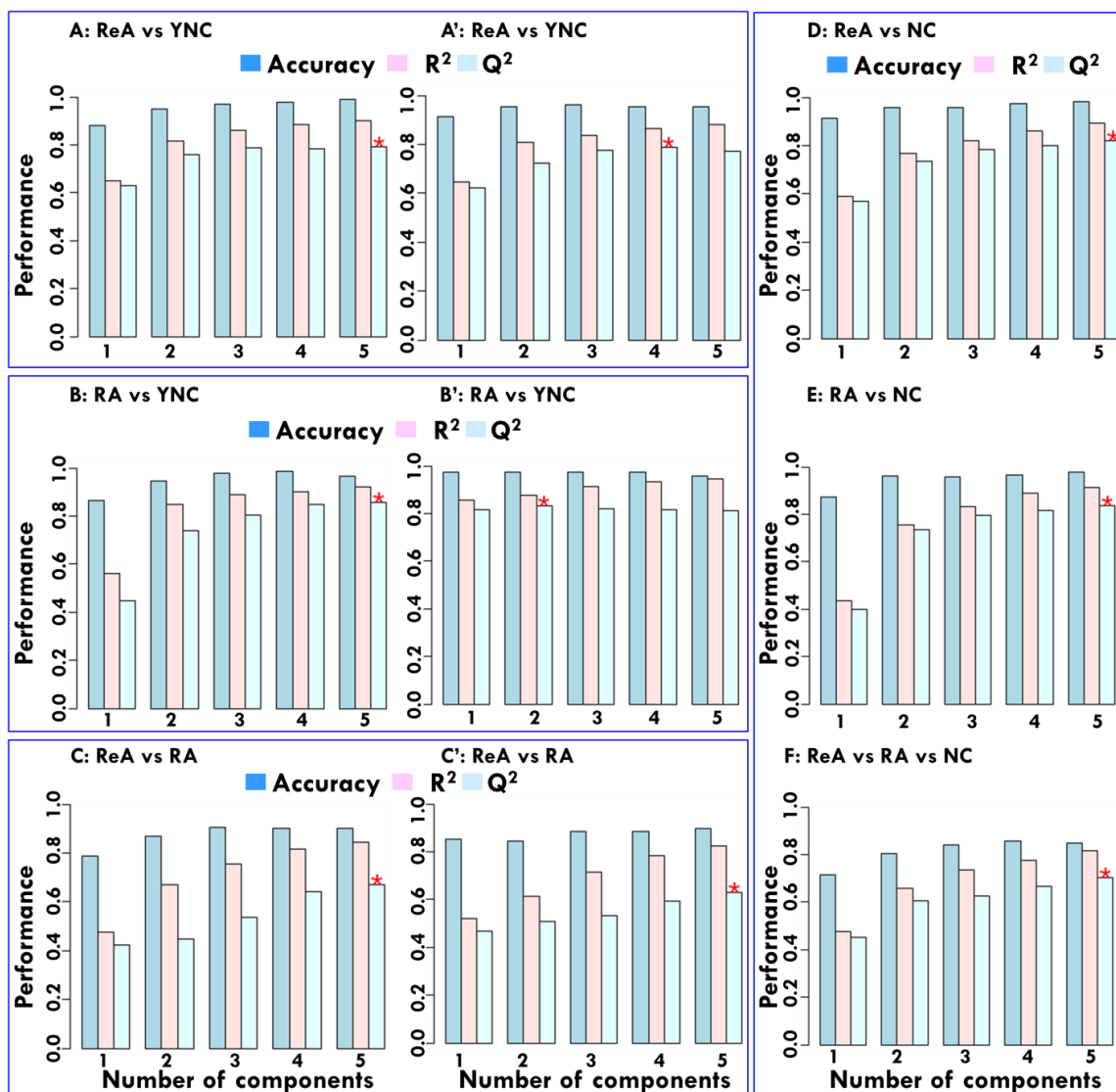


Figure 3.5: The 10 fold Cross Validation of pairwise PLS-DA models performed using different number of components: (A,A') ReA vs YNC, (B,B') RA vs ENC, and (C,C') ReA vs RA. The subsets (A, B and C) and (A', B' and C') represent the bar plots obtained from the analysis of complete and truncated CPMG data matrix, respectively and are showing quantitative measures of model performance for different number of components. Bar plots showing the three performance measures (prediction accuracy, multiple correlation coefficient R^2 and the explained variance in prediction Q^2) using different number of components. The red '*' indicates the best values of the currently selected measures (Q^2).

Important to mention here is that, we also performed additional PLS-DA model based analyses between patient (ReA and RA) groups and normal controls including samples from both YNC and ENC groups (Figure 3.6). The analysis revealed that the ReA samples are well separated from NC samples compared to RA samples suggesting that the metabolic disturbances are more aberrant in ReA compared to RA w.r.t NC.

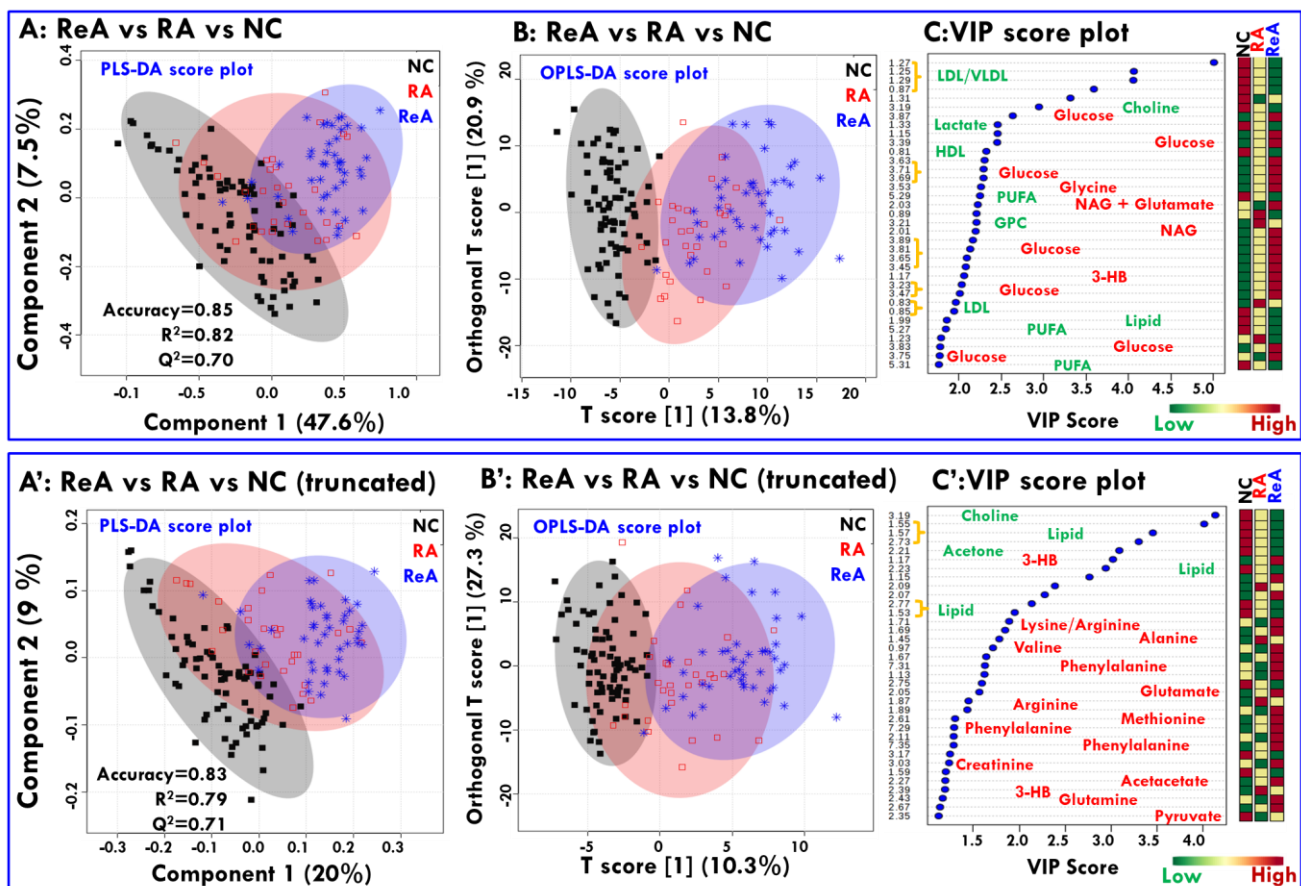


Figure 3.6: The 2D score plots derived from combined PLS-DA (**A, A'**) and OPLS-DA (**B, B'**) analysis of 1D ^1H CPMG NMR spectra of all the study groups: ReA, RA and NC and the corresponding VIP score plots derived from PLS-DA modelling are shown in (**C, C'**) for screening metabolite entities of discriminatory significance. The subsets (**A, B** and **C**) and (**A', B'** and **C'**) represent the score plots obtained from the analysis of complete and truncated CPMG data matrix, respectively. The truncated CPMG data matrix has been generated by excluding the lipid regions (0.6 to 0.96, 1.2 to 1.36, 1.92 to 2.04, 2.9 to 3.02) and the glucose regions (3.21 to 6.0) to reveal the discriminatory importance of serum metabolites present in low abundance and exhibiting relatively small change in metabolic concentration. The colored boxes present on the right side of each VIP score plot indicate the relative concentrations of the corresponding metabolite in each group under study.

3.4.4 Discovery of distinctive metabolic signatures of ReA compared to non-ReA groups:

The PLS-DA model based analysis was further used to identify the metabolites of potential discriminatory significance. As such, loading plots disclose the variables that are responsible for discrimination through situating them far from the origin, however, the plot is often very complex with many variables.²⁵ Therefore, the important variables responsible for group separation in PLS-DA model were identified based on the magnitude (score) of the variable influence on projection (VIP); the VIP score >1.0 was considered as the criterion for significant contribution to the discriminatory model. The VIP score plots derived from PLS-DA analysis of complete CPMG data

matrix showed a higher degree of metabolic redundancy (**Figure 3.4A, 3.4B, 3.4C**). Mainly, the resonances of lactate, glucose and lipid metabolites were dominating the VIP score plots (**Figure 3.7A, 3.7B, 3.7C**). Therefore, to minimize the redundancy in metabolic entities and to allow screening of additional metabolites of discriminatory significance, the spectral bins dominated by lactate, glucose, and lipid regions [i.e. δ (0.6 to 0.96, 1.2 to 1.36, 1.92 to 2.04, 2.9 to 3.02, 3.21 to 6.0) ppm] were excluded from the CPMG binned data matrix and discriminatory analysis (PLS-DA) was performed again. The spectral exclusion and repeating the PLS-DA resulted in no significant changes in grouping patterns on the 2D PLS-DA score plot (as well evident from **Figure 3.4A', 3.4B'** and **3.4C'** and **Figure 3.5**), however, this small exercise resulted in the identification of several other metabolite entities of discriminatory significance as evident from the VIP score plots generated for various discriminatory models (**Figure 3.7(A', B' and C')** and **Figure 3.6**). Similarly, the discriminatory analysis was also performed with CPMG data matrix containing bins from down-field spectral regions only (from 6.1 to 8.6 ppm for PLS-DA modelling, See **Figure 3.7(A'', B'' and C'')**) to reveal the alterations in serum metabolic profiles of format, histidine, tyrosine and phenylalanine (detectable in this region of the ^1H NMR spectrum, See **Figure 3.3**).

The metabolite entities of discriminatory potential (identified based on their VIP score value >1.0) were further evaluated for statistical significance. The metabolite entities were selected as candidate biomarkers if the p-value was ≤ 0.05 (the criterion used here for statistical significance) and the mean value difference between the groups was at 99% of significance level. The selected panel of biomarker metabolites responsible for discrimination between various groups and their relative changes are summarized in **Table 5 (See the Appendix)**. The distinctive metabolic signatures of ReA compared to non-ReA groups and those of RA compared to normal controls are described below.

ReA vs YNC: Compared to age and sex matched normal controls (referred here as group “YNC”), the sera of ReA patients were characterised by (a) elevated levels of glucose, creatinine, 3-HB, NAG, acetate, acetoacetate, citrulline, and various amino acids (such as valine, leucine, isoleucine, lysine, glutamate, glutamine, glycine, methionine, histidine, and phenylalanine), and (b) decreased levels of lipoproteins (LDL and VLDL), PUFA, choline, pyruvate and acetone (**Figure 3.7A, 3.7A' and Table 5, See the Appendix**).

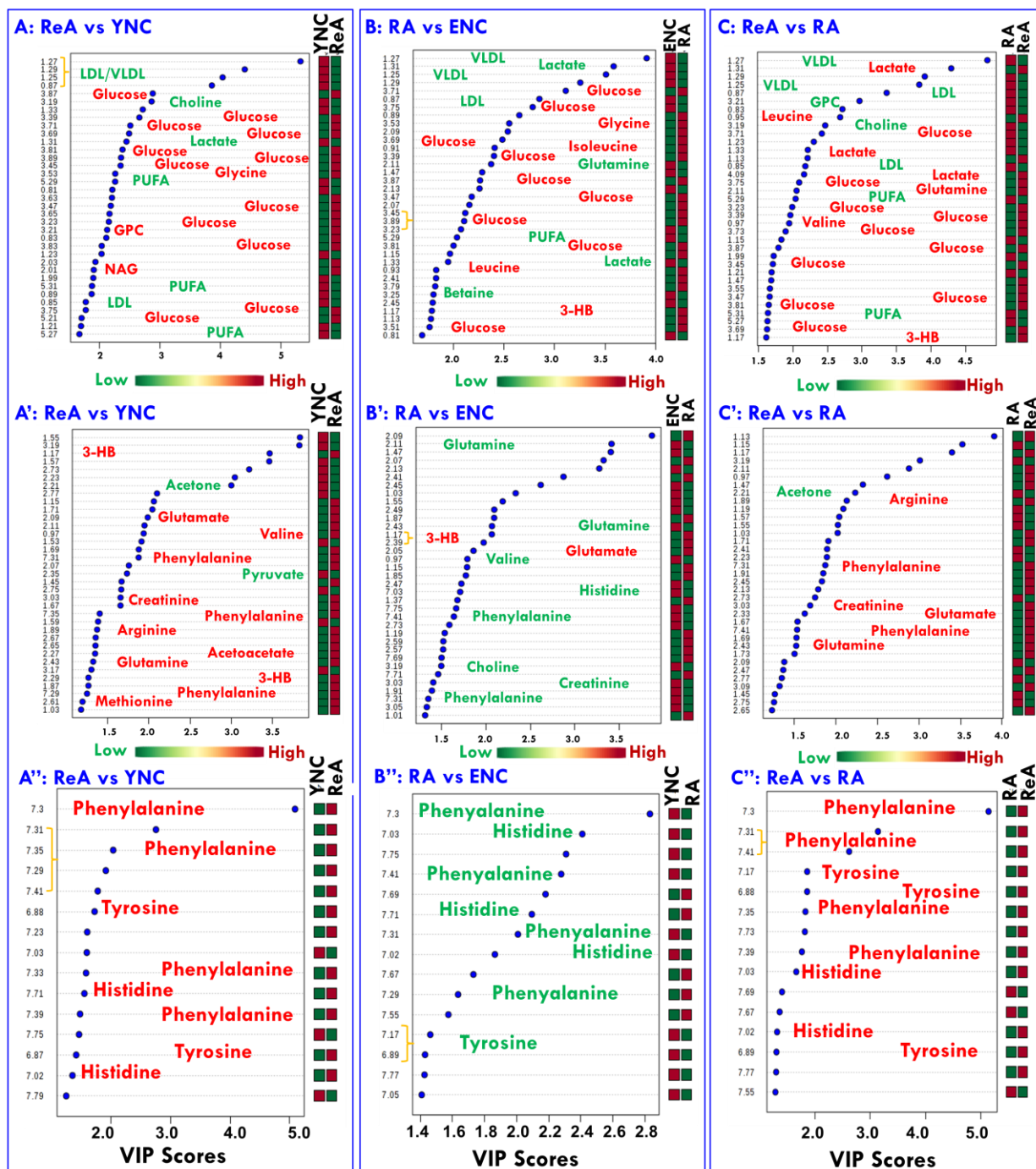


Figure 3.7: The potential discriminatory metabolite entities identified from VIP statistics based on paired PLS-DA models. The VIP score plots show the metabolite entities in decreasing order of their VIP score value. In (A, B and C), the complete NMR data matrix was used for PLS-DA modelling and resulted VIP scores for top 35 metabolite entities are shown. Most of these metabolite entities correspond to glucose, lactate and membrane/lipid metabolites. In (A', B' and C'), the truncated CPMG data matrix with excluded glucose and lipid regions (0.6 to 0.96, 1.2 to 1.36, 1.92 to 2.04, 2.9 to 3.02, 3.21 to 6.0) to reveal the discriminatory importance of serum metabolites present in low abundance and exhibiting relatively small change in metabolic concentration. In (A'', B'' and C''), the down-field spectral region from 6.1 to 8.6 ppm was used for PLS-DA modelling and revealed the discriminatory importance of aromatic amino acids like Histidine, Tyrosine and phenylalanine.

Alternatively, when the same ReA group was compared with normal control (NC) group, the aforementioned metabolic alterations were well consistent (See Figures 3.8 and 3.9) suggesting that the disease related metabolic changes are more prominent than age and sex related metabolic changes.

RA vs ENC: Compared to age and sex matched normal controls (referred here as ENC group), the sera of RA patients were characterised by (a) elevated levels of glucose, 3-HB, and various amino acids (such as isoleucine, leucine, glutamate, histidine, and glycine), and (b) decreased levels of lipoproteins (LDL and VLDL), PUFA, choline, lactate, creatinine and various amino acids (such as valine, glutamine, and phenylalanine) (Figure 3.7B, 3.7B' and Table 5, See the Appendix). These metabolic changes were well consistent when RA group was compared with normal control group (See Table 5, See the Appendix and Supplementary Figure 3.8B), however, for four metabolite entities (i.e. Acetone, pyruvate, GPC, tyrosine), these metabolic changes were found insignificant.

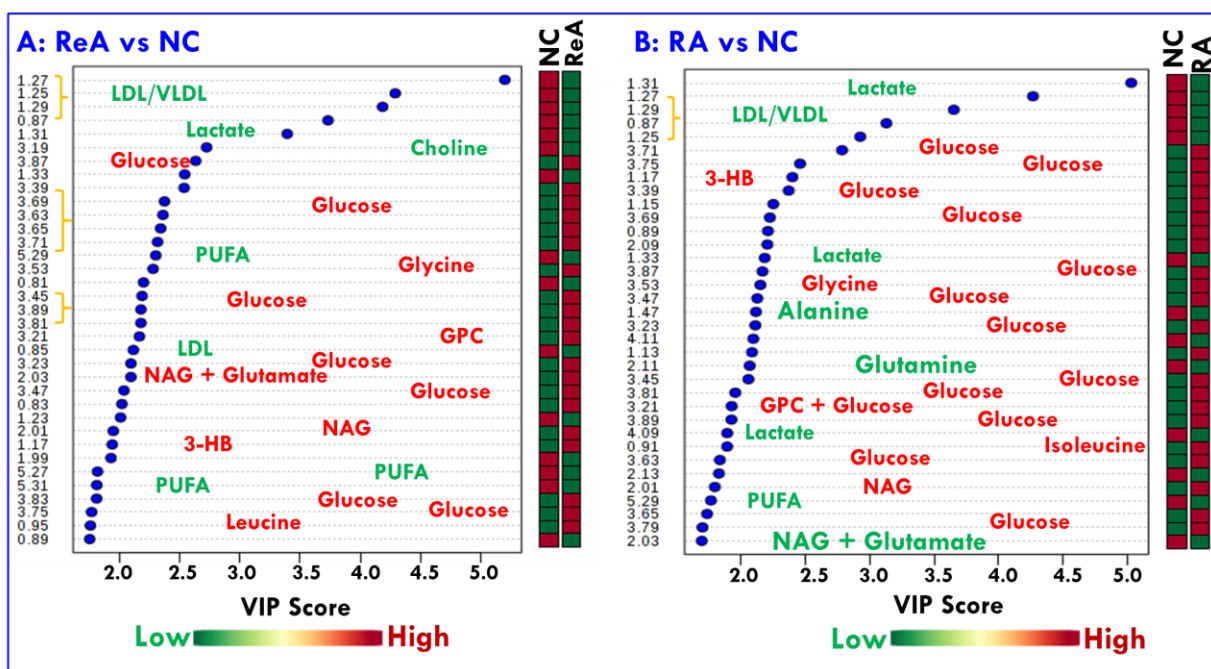


Figure 3.8: VIP score plot analysis used to identify metabolite entities of discriminatory significance for PLS-DA analysis between (A) ReA vs NC and (B) RA vs NC. The colored boxes present on the right side of each VIP score plot indicate the relative concentrations of the corresponding metabolite in each group under study.

ReA vs RA: Compared to RA patients, the sera of ReA patients were characterized by (a) elevated levels of glucose, lactate, acetate, acetoacetate, pyruvate, creatinine, 3-HB and various amino acids (such as valine, leucine, lysine/arginine, glutamate, glutamine, methionine, tyrosine, histidine and

phenylalanine) and (b) decreased levels of lipoproteins (LDL and VLDL), PUFA, choline, GPC and acetone (Figure 3.7C, 3.7C' and Table 5, See the Appendix).

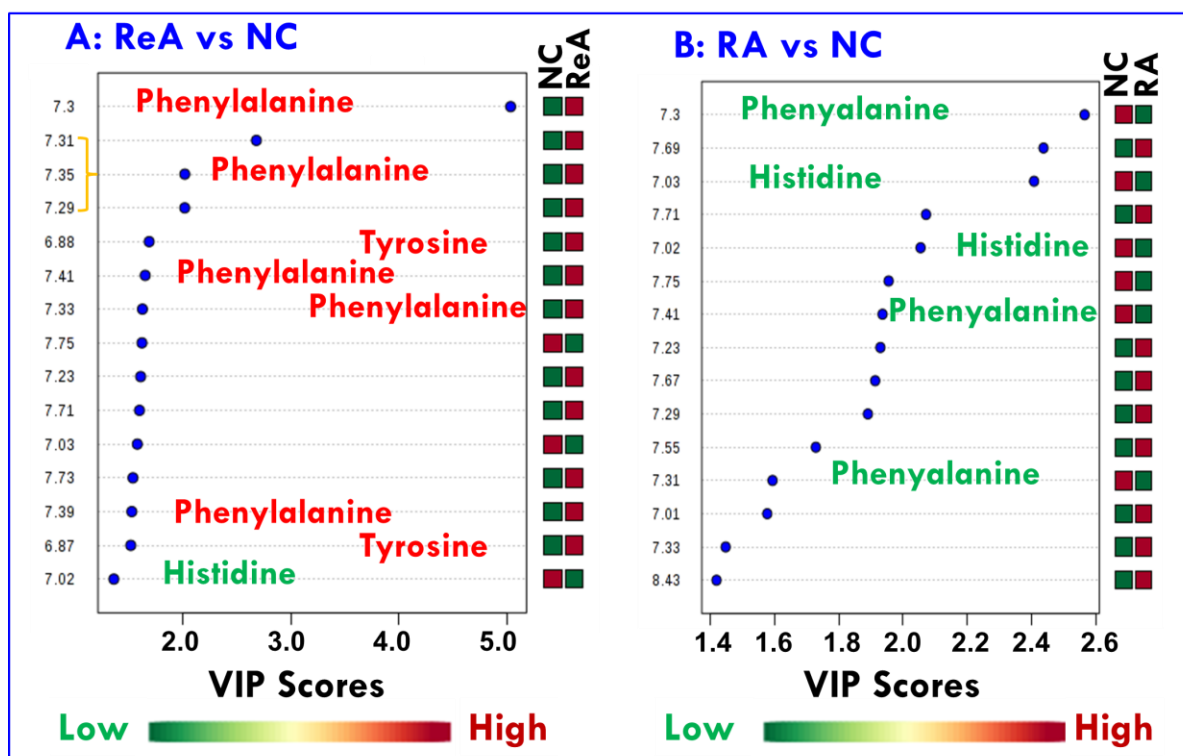


Figure 3.9: VIP score plot analysis used to identify metabolite entities of discriminatory significance for PLS-DA analysis involving truncated CPMG data matrices. The plots **A-B** represent the discriminatory analysis between: **(A)** ReA vs NC and **(B)** RA vs NC. The colored boxes present on the right side of each VIP score plot indicate the relative concentrations of the corresponding metabolite in each group under study.

3.4.5 Receiver operating characteristic (ROC) curve analysis for Biomarker Discovery:

Following identification of metabolite entities (NMR variables) differentiating ReA from non-ReA groups, the ROC analysis was performed as a quantitative measure for discriminatory potential (i.e. specificity and sensitivity) (Figure 3.10). The ROC curves were computed for each metabolite by classic univariate analysis in MetaboAnalyst followed by evaluation of diagnostic accuracy based on area under the ROC curve (AUC); $0.5 < AUC < 0.7$, $0.7 < AUC < 0.9$, $AUC > 0.9$ explain a low, fair, and superior accuracy of diagnosis, respectively. In our study, a marker was considered significant if AUC value is in excess of 0.9.

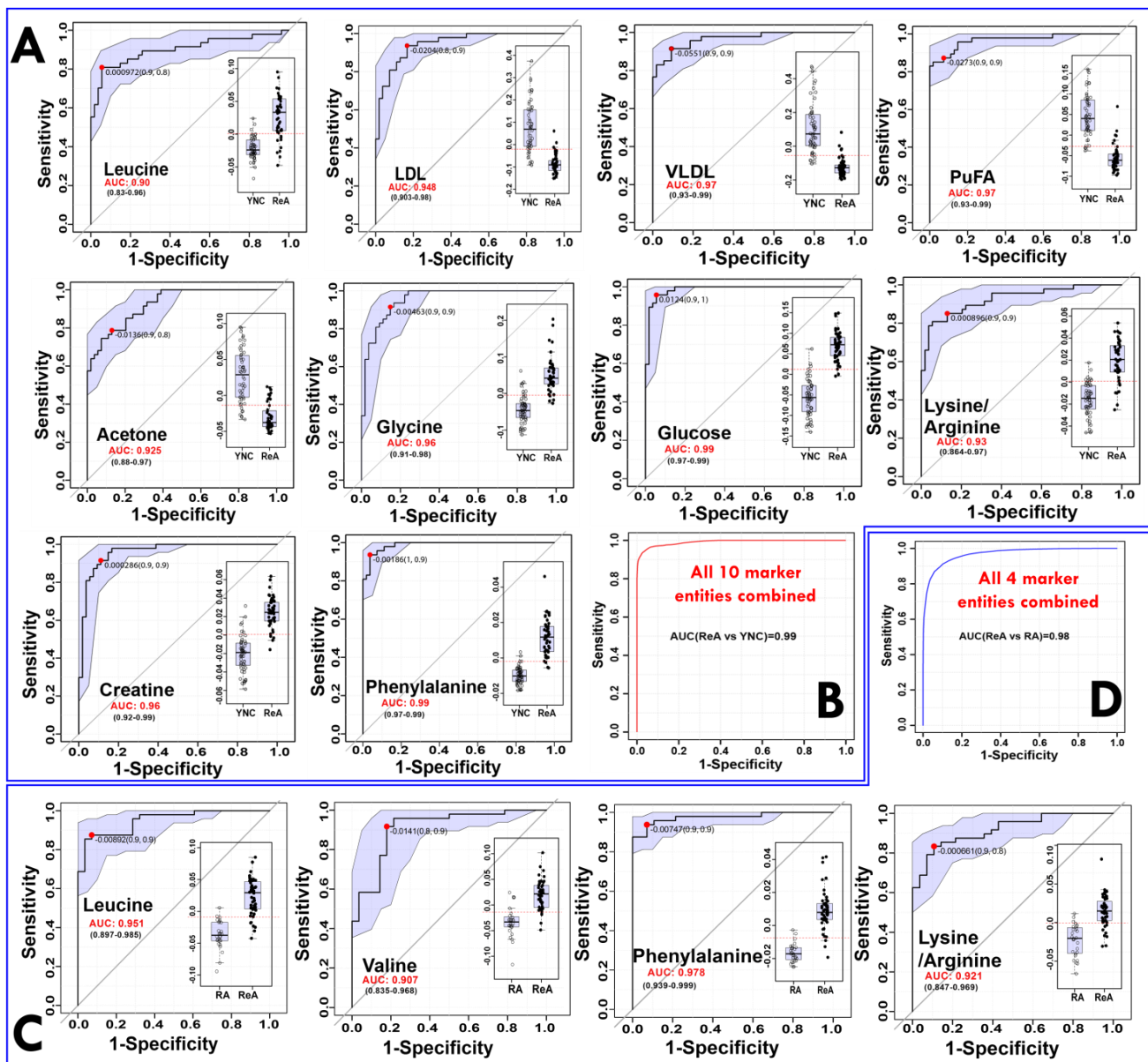


Figure 3.10: (A) Ten biomarker candidate metabolites identified after ROC curve analysis performed with all key discriminatory metabolites responsible for separation between ReA and YNC groups as tabulated in [Table 5, See the Appendix](#). These curve plots have been generated using binned spectral features normalized with respect to the total spectral intensity (also referred here as relative signal integrals). (B) Area under the receiver operating characteristic curve (AUC of ROC) calculated to find accuracy of the model by selecting all the 10 potential biomarkers metabolites. (C) Four biomarker candidate metabolites identified after ROC curve analysis performed with all key discriminatory metabolites responsible for separation between ReA and RA groups. (D) The area under the ROC curve (AUROC) calculated to find accuracy of the model by selecting all the 4 potential biomarker candidates. The computed 95 % confidence interval (CI) for individual marker metabolites is highlighted in faint blue background over the ROC curve. The insets within ROC plots represent the box-cum-whisker plots showing significantly elevated serum levels of these metabolites in the ReA patients. For each box plot showing quantitative variations of relative NMR signal integrals, the boxes denote interquartile ranges, horizontal red line inside the box denote the median, and bottom and top boundaries of boxes are 25th and 75th percentiles, respectively. Lower and upper whiskers are 5th and 95th percentiles, respectively.

Out of various discriminatory metabolites, ten metabolite entities (LDL, leucine, VLDL, lysine/arginine, acetone, glycine, glucose, creatine, PUFA and phenylalanine) achieved good AUC values in the discrimination of ReA from normal controls (YNC) (**Figure 3.10**) and four metabolites (valine, leucine, lysine/arginine, and phenylalanine) achieved good AUC values (>0.9) in the discrimination of ReA from RA patients (**Figure 3.10B**), which could be screened as robust predictors of ReA.

Depending upon the clinical condition, the individual metabolites may fail to predict a disease accurately. Therefore to assess the integrated predictive power for discriminating ReA patients from non-ReA groups, the ROC analyses were also performed for the combination of discriminatory metabolites (10 in case of ReA vs YNC model and 4 in case of ReA vs RA model). The resulted AUC values for both: ReA vs YNC model (0.99 with CI 0.975–1.00) and for ReA vs RA model (0.98 with CI 0.948–1.00) were found to be very close to one (**Figure 3.10B** and **3.10D**) indicating higher predictive power of biomarker panel than individual markers. Additionally, the ROC curves were also computed to evaluate the diagnostic potential of various discriminatory models by selecting different combinations of discriminatory metabolites (up to top 100 NMR variables with AUC value >0.8). The resulted ROC curves for different combinations (involving top 5, 10, 15, 25, 50 and 100 discriminatory metabolites) are shown in the **Figure 3.11** and the corresponding AUC values are shown in **Table 4 (See the Appendix)**. As evident, the AUC values were increasing progressively towards a value of one as the numbers of variables in the combination panel were increased; again suggesting that NMR based metabolic profiles has definite potential to screen ReA patients from normal controls as well as from RA patients. The metabolic alterations contributing to the development and progression of a disease often show correlation (positive or negative) depending upon the disease mechanism. Therefore, to evaluate if the metabolic profiles discriminating ReA from non-ReA groups are correlated as well, the correlation analysis was further performed on these discriminatory metabolites and the results are shown in **Figure 3.12** and **3.13**.

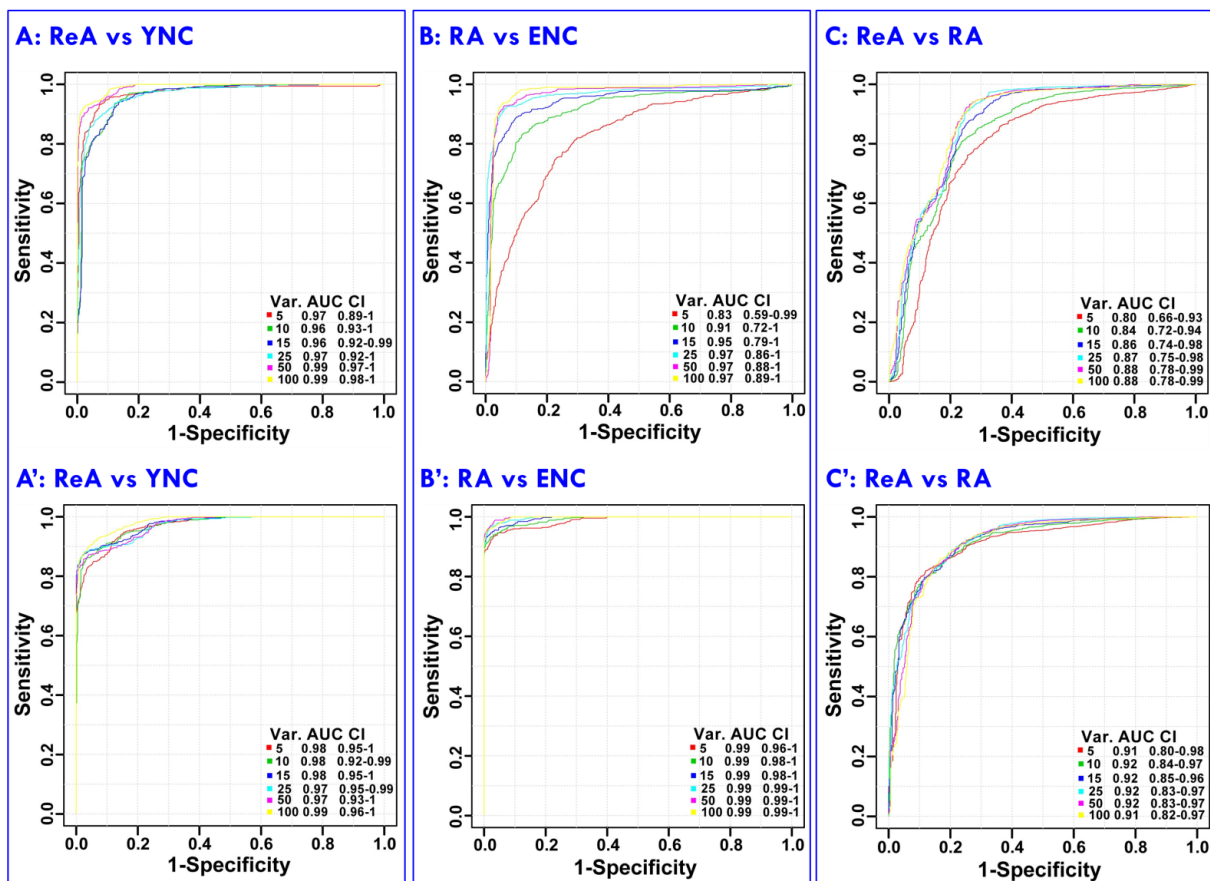


Figure 3.11: The ROC curves generated for six different PLS-DA models: (A,A') ReA vs YNC, (B,B') RA vs ENC, and (C,C') ReA vs RA. For ROC analysis, the predictive models were generated using top 100 features of discriminatory significance.

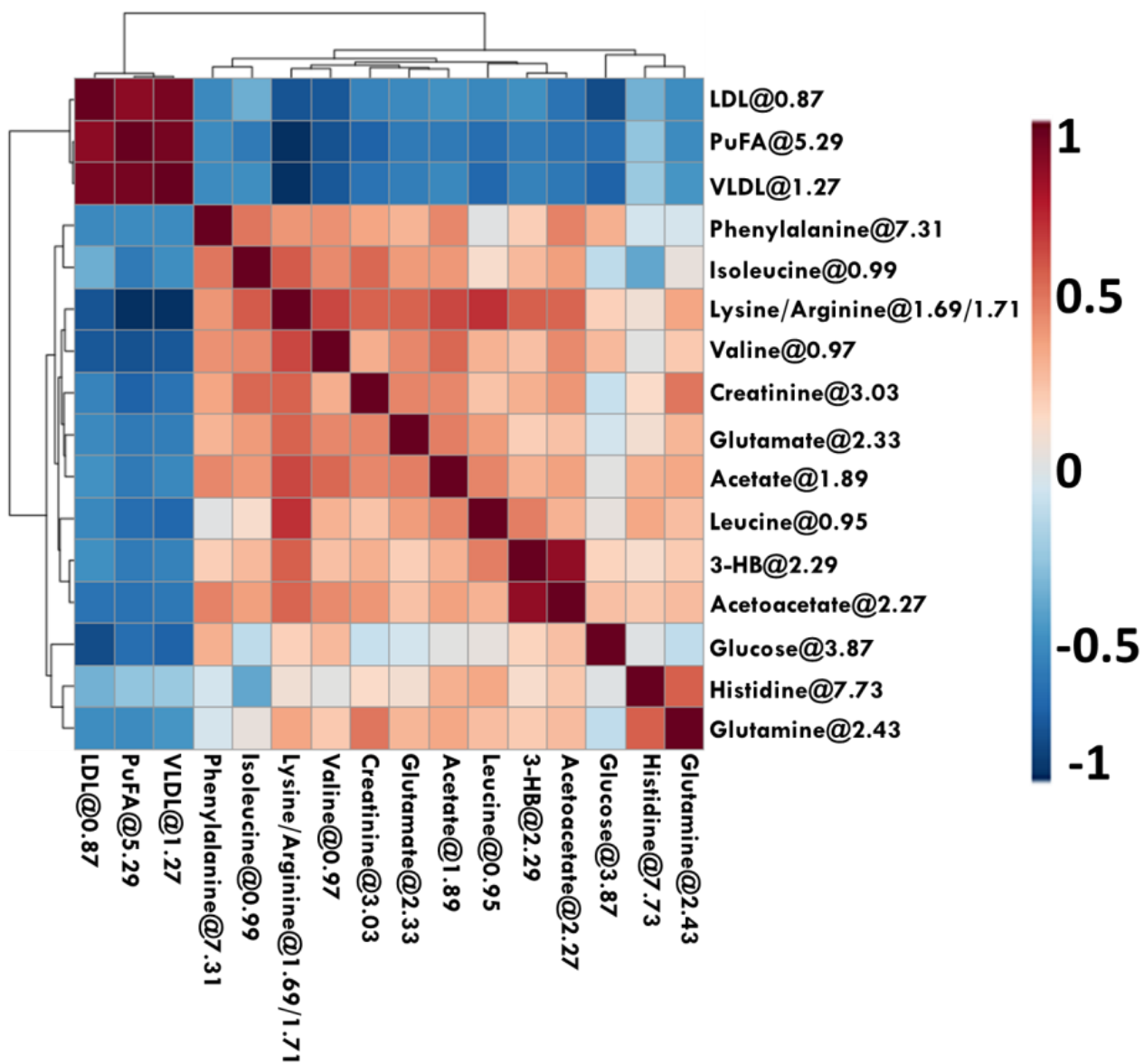


Figure 3.12: Pearson’s correlation analysis performed for serum metabolites responsible for discrimination between ReA and RA patients. Only metabolite correlations with $|R| \geq 0.6$ and $p < 0.05$ were considered.

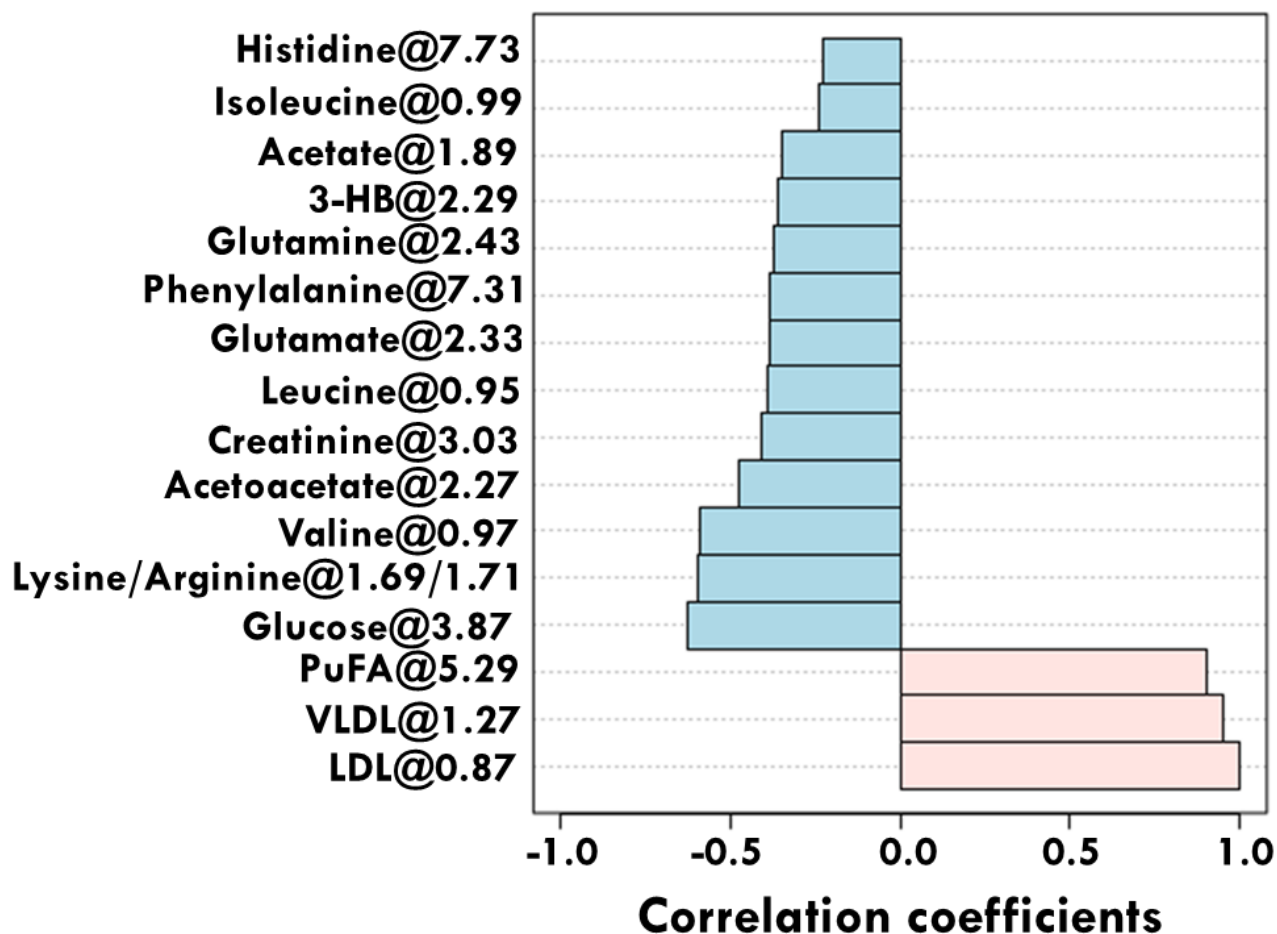


Figure 3.13: Pearson correlation coefficient (R) presented as bar plot showing top 16 metabolite entities (among the selected metabolite entities responsible for discrimination between ReA and RA) correlated with LDL bin at 0.87 ppm

The significant positive and negative correlations were observed between these metabolic profiles among the ReA patients suggesting that these alterations might be related to development and progression of ReA (however, further studies are required to validate these findings).

3.5 Discussion

To elucidate the differential pathogenesis of ReA and RA is imperative to aid a better understanding of the biochemical mechanisms involved in disease progression and to further improve its clinical management. Reactive arthritis is a disease affecting mostly young adults and causes systemic inflammation associated with joint lesions, leading to an uncomfortable life style for patients. It is well established that ReA is caused by an infection, mostly in genetically susceptible individuals. The pathogenetic mechanisms are still poorly understood, and the treatment rests mainly on

nonsteroidal anti-inflammatory drugs (NSAIDs), sulfasalazine, and sometimes drugs that suppress the immune system (such as azathioprine or methotrexate). The purpose of this study was to reveal the serum metabolic alterations underlying ReA and thus to improve the current understanding about this post-infection arthritis condition and to use the information further in its efficient clinical management. The application of multivariate pattern recognition analysis allowed not only the extraction of relevant discriminate information from the NMR spectral data, but also an effective sample classification. Our results clearly showed those ReA/RA patients exhibit significant metabolic disturbances that clearly distinguished them from normal controls and RA patients. The AUC of the biomarker panel containing 10 and 4 metabolites, respectively, for (ReA vs YNC) and (ReA vs RA) models indicated the highest predictive ability and these changes were also found to be in good agreement with the disease pathophysiology as discussed further.

The distinctive metabolic patterns of ReA compared to non-ReA groups were identified on the basis of VIP score values greater than one for the PLS-DA models (**Figure 3.7**). A total of 25 significantly altered serum metabolites with the VIP threshold ($VIP > 1$) in the above-mentioned PLS-DA model as well as the Student's t test ($p < 0.05$) were selected and their variations are summarized in **Table 5 (See the Appendix)**. With respect to normal controls, the serum metabolic profiles of ReA patients were found to be disturbed more compared to RA patients as inferred by the close proximity and overlap of NC and RA groups in the 2D PLS-DA score plots (See **Figure 3.6**). In serum of ReA patients, 23 metabolites showed significant changes in concentration versus control cohort subjects i.e. YNC while serum from RA patients revealed significant changes of concentrations in 19 metabolites. The representative box plots to highlight the observed metabolic alterations have been shown in **Figure 3.14**. Compared to normal control cohort, the circulatory metabolites altered both in ReA and RA patients were 3-HB, glucose, citrulline, isoleucine, leucine, glutamate, glycine, histidine) or decreased (LDL, VLDL, choline, PUFA); whereas, the circulatory levels of metabolites -such as valine, lysine/arginine, acetate, glutamine, NAG, acetone, acetoacetate, pyruvate, citrate, methionine, creatinine, GPC, lactate, tyrosine and phenylalanine- were differentially altered in ReA and RA cohorts as tabulated in **Table 5 (See the Appendix)**. Similar metabolic alterations were also observed when patient (ReA and RA) groups were compared to NC (YNC+ENC) group except NAG, acetone, pyruvate, citrate, choline, lactate and tyrosine suggesting that the serum levels of these metabolites may have been influenced by factor like age and sex. Overall, seventeen metabolic features met the selection criteria of VIP-score > 1.0 ,

statistical p -value < 0.05 and exclusion of metabolites influenced by age/sex, which denoted that their levels in the ReA patients were significantly different from those in the RA patients. Compared to NC, the akin pattern of serum metabolic changes were observed in ReA and RA patients for several metabolites (as evident from Table 5, See the Appendix and Figure 3.14) suggested that both these immune-mediated inflammatory conditions partly share the same metabolic pathway alterations (Figure 3.15). The implications of these metabolic changes (i.e. similarities or differences) in the pathogenesis of ReA/RA have been discussed in detail below.

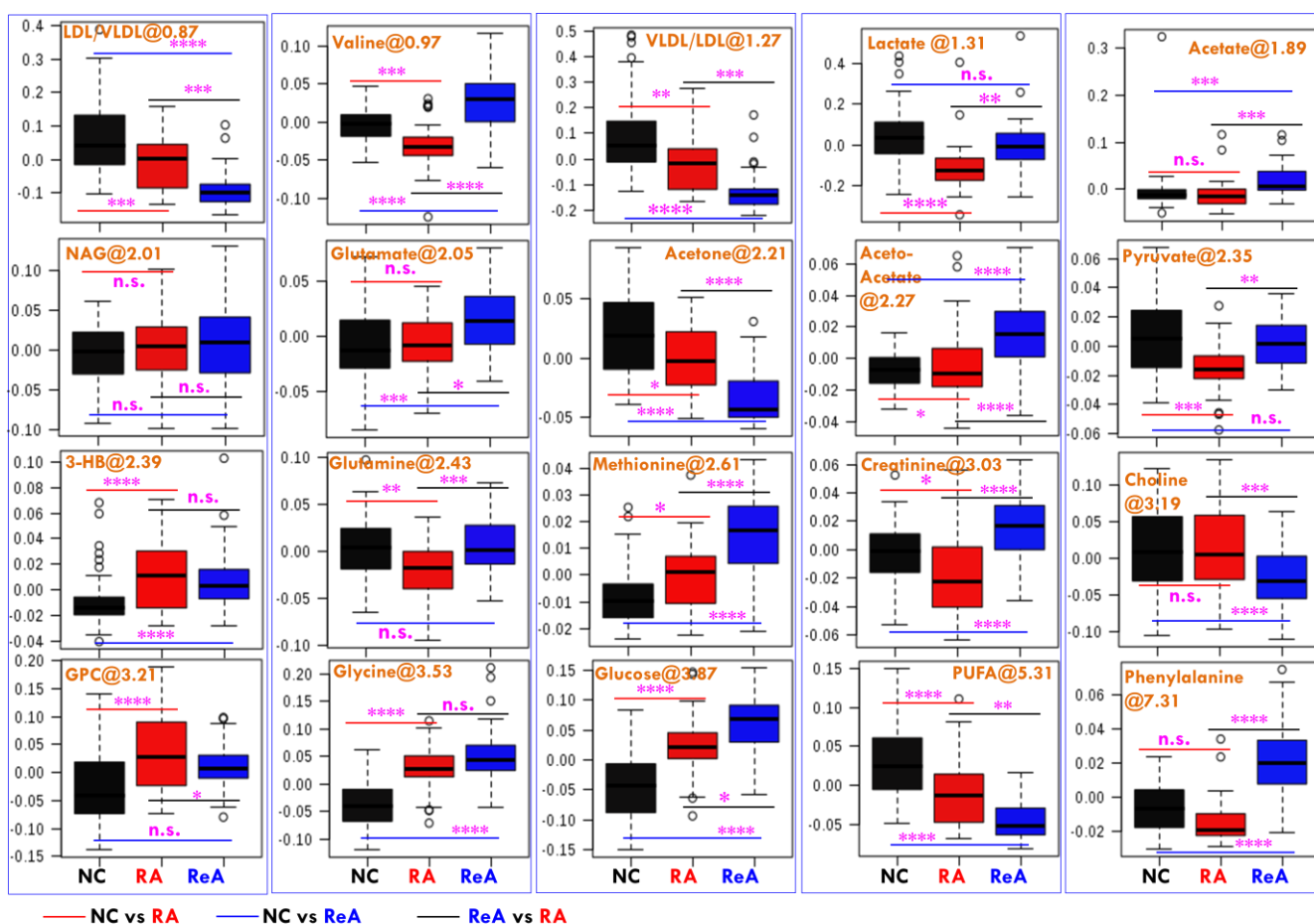


Figure 3.14: Representative box-cum-whisker plots showing quantitative variations for serum metabolites. These plots have been generated using binned spectral features normalized with respect to the total spectral intensity (also referred here as relative signal integrals). For presented metabolite entities, the VIP score >1 and statistical significance is at the level of $p \leq 0.05$. In the box plots, the boxes denote interquartile ranges, horizontal line inside the box denote the median, and bottom and top boundaries of boxes are 25th and 75th percentiles, respectively. Lower and upper whiskers are 5th and 95th percentiles, respectively.

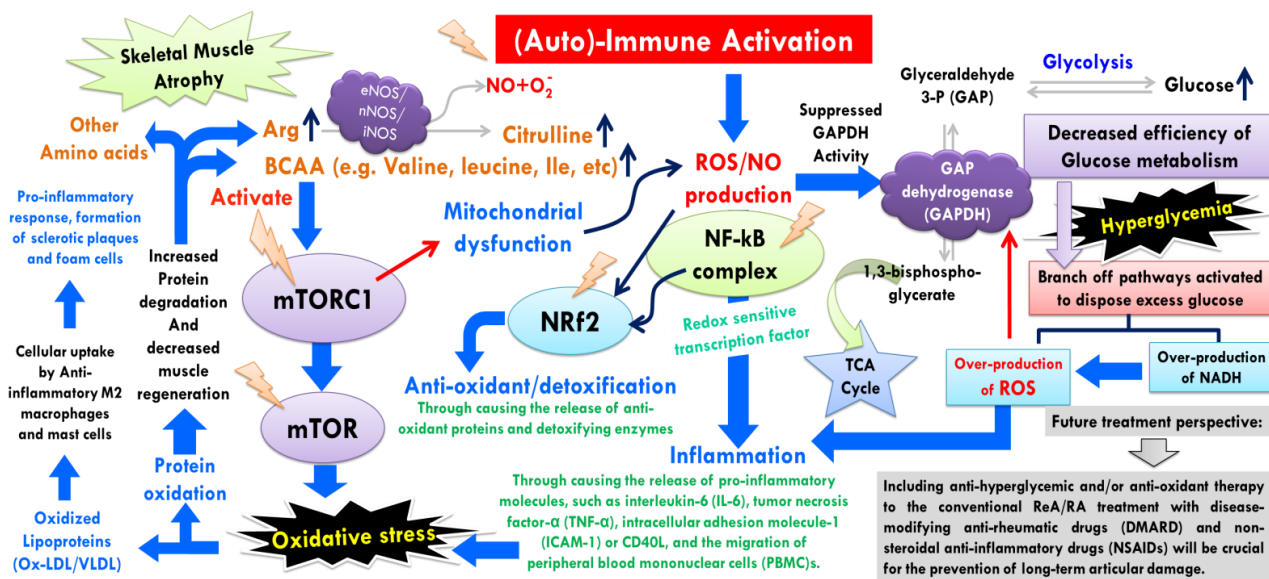


Figure 3.15: The possible disease mechanism in ReA patients illustrated based on current metabolic disturbances and previous pathophysiological mechanistic studies.^{54,56,61,62}

3.5.1 Glucose -energy and amino-acid metabolism:

General comparison with respect to normal controls showed a significant increase of glucose accompanied by a decrease in lactate in the sera of ReA and RA patients which clearly suggest that the glycolysis is dampened in RA patients (partially may be because of hypoxia). The similar elevated serum levels of glucose have also been seen previously in RA patients.^{31,32} The elevated glucose levels in patients suffering from chronic inflammatory conditions (i.e. hyperglycemia) have been related to dampened aerobic glycolytic activity^{17,33} to perpetuate the inflammatory condition through inducing conditions like oxidative stress as discussed previously.^{34,35} Some previous studies also show that hyperglycemia elevates the levels of inflammatory cytokines to stimulate inflammatory reaction; thus the condition serve as a pro-inflammatory which may suggest reason behind the inflammatory condition of RA and so in case of ReA patients.³⁶⁻⁴¹

The rheumatic conditions manifested with immuno-inflammatory dysregulation are characterized by elevated levels of several cytokines and factors, including TNF α , IL-1 β , IL-6, IFN γ , and reactive oxygen species (ROS) in addition, NF- κ B activation is increased.⁴²⁻⁴⁴ In addition to the well-characterized immuno-inflammatory dysregulation in ReA/RA, muscle wasting and energy expenditure are also common features linked to the production of cytokines. The proinflammatory

status of muscle cells can then dysregulate the protein degradation pathway (negative protein turnover) leading to perturbed metabolic processes. Under systemic inflammatory conditions, muscles along with liver are also known to release high quantity of amino acids in the circulation to maintain the cellular homeostasis.⁴⁵ Consistent with such pathophysiological activities and as reported in previous clinical profiling studies,^{46,47} the circulatory levels of several amino acids have been found to be elevated in RA patients such as glutamate, isoleucine, leucine, histidine and citrulline. These changes may indicate that proteins are degraded to amino acids partly to replenish the required energy demand and further to regulate biological functions such as gene transcription, cell-cycle progression, and immuno-inflammatory responses.

Contrary to such elevations, the serum levels of glutamine, phenylalanine, and valine were found to be decreased in RA patients. Glutamine is a substrate highly consumed by inflammatory cells such as macrophages and converted to glutamate.⁴⁸ The elevated glutamate levels and decreased glutamine levels in the sera of RA patients are found well consistent with previous metabolomics studies involving RA patients^{46,49-51} suggesting that the glutaminolysis is eminently active in these patients. The changes observed in the serum metabolic profiles of RA have also been compared symbolically to that of ReA in **Table 5 (See the Appendix)**. Compared to normal controls, the ReA and RA patients shared several common metabolic perturbations like (a) increased serum levels of leucine, isoleucine, citrulline, glutamate, 3-HB, glycine, glucose, creatine and histidine; whereas (b) the serum levels of lipid and membrane metabolites are decreased in these rheumatic conditions. The shared metabolic patterns suggested that both ReA and RA partly share the same the immuno-inflammatory dysregulation. Despite both ReA and RA are inflammatory conditions sharing the clinical symptoms with several similar metabolic profiles as evident from the present study, a prominent separation between the serum samples of ReA and RA patients were observed suggesting that these two autoimmune inflammatory conditions may involve different biochemical activities. Compared to RA, the serum levels of phenylalanine and valine were found to be elevated in ReA patients suggesting differential immune-metabolic activities present in ReA and RA patients. The branched chain amino acids (BCAAs) have been implicated in the production of IL-1, IL-2 and/or TNF- α and studies have identified changes in BCAA levels with inflammatory states such as sepsis and RA.^{47,52,53} BCAAs are involved in modulating immune properties and in several pathological and physiological conditions increased BCAA plasma concentrations have been described promotes oxidative stress, inflammation and migration of human peripheral blood mononuclear cells via

mTORC1 activation.⁵⁴ BCAAs have also been found to be elevated in the synovial fluid (SF) of the articular joints affected in rheumatic conditions such as RA.⁵³ The decreased serum levels of valine in RA patients may indicate its use as an alternative substrate donor for TCA cycle to meet the energy demand under conditions of suppressed activity of Glyceraldehyde 3-phosphate dehydrogenase (GAPDH) rendering dampened glycolytic activity.^{55,56} However, the observed increased serum levels of valine in ReA patients compared to RA may be attributed to dominance of protein degradation in ReA. Compared to RA, the serum levels of all the three BCAAs are elevated in ReA patients. Phenylalanine is an essential amino acid and under normal aerobic conditions is converted into tyrosine for downstream phenylalanine. Previous serum based biochemical profiling studies have shown the correlation between inflammation and reduced phenylalanine turnover resulting in increased serum levels of phenylalanine.⁵⁷ The underlying mechanism for this change has been attributed to the reduced activity of enzyme named phenyl-4-hydroxylase (PAH) due to oxidative stress under conditions of immune activation and inflammation.⁵⁸ The significantly elevated serum levels of phenylalanine (hyperphenylalaninemia) have also been seen under septic inflammatory conditions.⁵⁹ The reduced serum level of phenylalanine has been seen previously in RA patients⁶⁰ suggesting its negative metabolic turnover in infection induced inflammatory conditions. Compared to RA, the concomitantly elevated serum levels of BCAAs, glucose and phenylalanine in ReA clearly suggested aberrant immune activation and dominance of protein degradation in this post-infection inflammatory arthritis (underlying antigenic cross-reactivity). The possible disease mechanism of ReA ensuing from this comparative metabolomics analysis and previous mechanistic pathophysiological studies.^{54,56,61-63}

As evident from **Table 5**, the serum metabolic changes observed in RA patients have also been compared to three previous metabolomics studies involving RA patients.^{31,32,64} Both, consistencies as well as discrepancies have been seen e.g. the decreased serum levels of valine and glutamine in the sera of RA patients were consistent with study by Ouyang *et. al*,³² whereas, the serum levels of histidine are increased when compared to the same study. Similarly, depleted serum levels of several amino acids including valine have also been observed in a recent GC-MS based study.⁶⁵ The observed such inconsistent results might be partly explained by clinical RA condition or blood sample management between the present and other studies. Regardless of the underlying mechanism, these results suggest that a special consideration of amino acid balance should be made for patients with ReA and RA.

3.5.2 Disturbed lipid and membrane metabolism:

Dyslipidemia is a significant comorbidity of RA with multiple negative effects in the long term.^{66,67} Systemic chronic inflammation has a general effect in lowering circulating lipid levels.^{66,68} Consistent the serum levels of membrane and lipid metabolites (such as LDL/VLDL, PUFA, Choline, Glycerophosphocholine, etc.) were found to be significantly decreased in both RA as well as in ReA patients compared to NC (**Figure 3.8**). Similar “dyslipidemic/ dyslipoproteinemia pattern” characterized by decreased serum levels of LDL and VLDL have also been observed clinical studies on RA patients⁶⁹ as well as in NMR based serum metabolomics studies with previous metabolomics studies on patients with RA,^{31,64} Takayasu arteritis (TA),¹⁸ and lupus (non-renal).¹⁷ As both RA and ReA patients share common pro-inflammatory and inflammatory mediators, the observed dyslipidemic pattern can be attributed to (a) the augmented utilization of lipid/membrane metabolites in the synthesis of pro-inflammatory and inflammatory mediators for perpetuating immuno-metabolic response (b) the β -oxidation of the fatty acids to meet the energy demand under conditions of systemic inflammation accompanied by a state of hyperglycemia and (c) their augmented utilization in repairing membranes of affected cells and organelles due to inflammation and oxidative stress. Another reason for decreased serum levels of lipid/membrane metabolites may be attributed to their oxidative damage or adulterant transformations under systemic inflammatory conditions.^{70,71}

3.5.3 Suggested panel of Biomarkers for clinical diagnosis:

As purposed, the aim of current study is to test the utility of NMR based serum metabolomics in the diagnostic screening of ReA from non-ReA individuals. Therefore, ROC curve analysis was performed to evaluate the diagnostic potential of discriminatory metabolites between ReA and non-ReA groups. Considering AUC value >0.9 as the criterion for diagnostic potential; ten key metabolite entities (LDL, leucine, VLDL, lysine/arginine, acetone, glycine, glucose, creatine, PUFA and phenylalanine) have been suggested as biomarkers for discriminatory model between ReA vs YNC groups (**Fig 10A**), whereas four serum metabolic entities (valine, leucine, lysine/arginine, and phenylalanine) have been suggested as biomarkers for discriminatory model between ReA vs RA. When analyzed collectively, the AUC of the biomarker panel reached 0.99 and 0.98 by combination of ten (ReA:YNC) and four (ReA:RA) biomarker candidates, respectively, thus indicating the highest predictive ability. Point to be mentioned here is that the spectral features compared in this study are normalized w.r.t to total spectral intensity; therefore, the observed metabolic changes may

be different compared to the change in actual concentration levels in the serum. Further, from the CPMG NMR spectra of normal serum samples, the precise quantitative information about metabolites cannot be discerned owing to contribution from overlapping residual signals of proteins and other higher MW biomolecules. In order to rule out any such possibility, the collected serum samples were ultra-filtered as described previously¹⁵ for reliable concentration profiling and collected 1D ¹H CPMG spectra were analyzed using commercial software CHENOMX. The representative spectra of ultra-filtered serum samples selected from NC, RA and ReA study groups are shown in **Figure 3.16**.

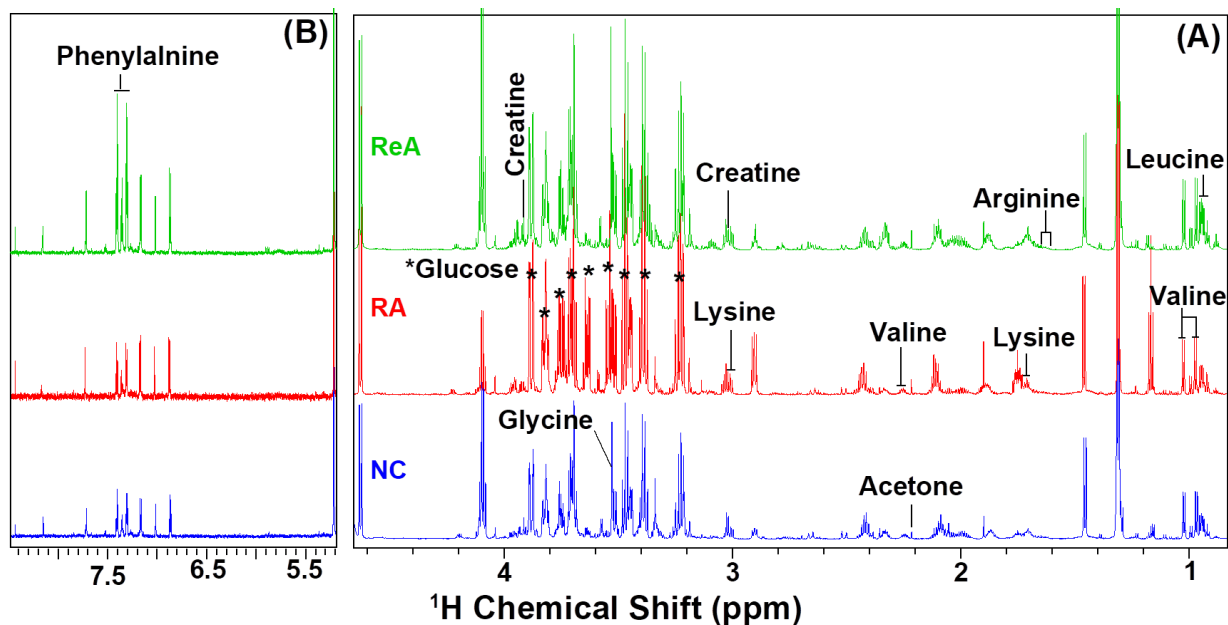


Figure 3.16: Representative 800 MHz 1D ¹H CPMG NMR spectra of ultra-filtered serum samples selected from NC, RA and ReA study groups: (A) $\delta(0.75-4.65)$ and (B) $\delta(5.2-8.6)$. The spectral region $\delta(5.2-8.5)$ in (B) is magnified 8 times compared to spectral region $\delta(0.5-4.7)$ in (B) for the purpose of clarity. The spectral peaks corresponding to marker metabolites are labelled and also re-validated using CHENOMX software as well.

As clearly evident, the protein filtering has greatly alleviated the peak attenuation problem; thus rendering improved and reliable metabolic profiling. The absolute concentrations of marker metabolites were compared using univariate statistics and the resulted box-cum-whisker plots with corresponding p-value are shown in above **Figure 3.17**; whereas other parameters such as fold change and mean values are shown in **Table 6 (See the Appendix)**. Consistent to above results based on normalized spectral features, the measured absolute concentrations of serum metabolites (valine, leucine, lysine, arginine, and phenylalanine) were found significantly higher in ReA compared to RA. However, when compared between ReA and YNC, the concentration levels of four metabolites –namely creatine, acetone, leucine, and lysine- were found to be contradictory compared to results discussed above. This inconsistency in part can be explained based on the fact that the

NMR signals of all these four metabolites are overlapped by other serum metabolites e.g. creatine signal at 3.91ppm is overlapped by signals of serine and fatty acid chains; similarly acetone signal at 2.21 ppm is overlapped by signals of valine and lipid metabolites (including FA chains).

Further, to evaluate if the suggested panel of serum markers correlate with the synovial joint inflammation, the quantitative concentration profiles of marker metabolites were measured for paired serum and synovial fluid (SF) samples obtained from ReA patients. Point to be mentioned here is that ReA patients often involve joint inflammation and the extraction of SF remains a part of clinical procedure due to SF accumulation in the joints. The paired serum and SF samples for RA patients were not obtained owing to heterogeneous representation of joint inflammation in RA.

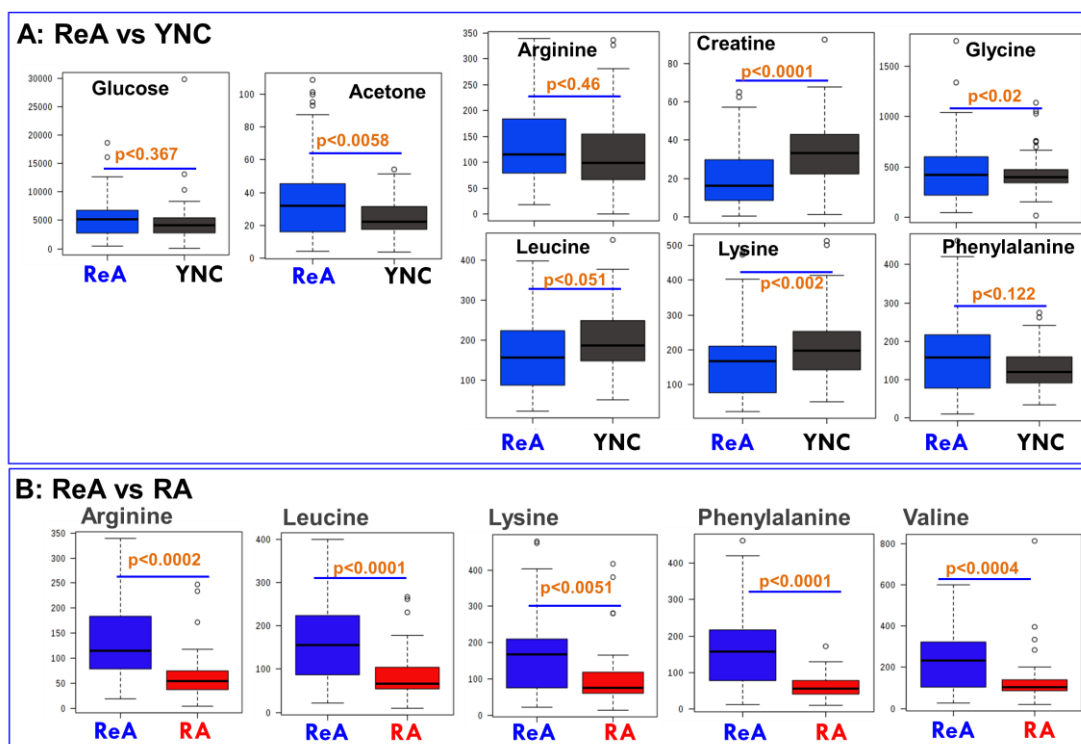


Figure 3.17: The box-cum-whisker plots for marker metabolites derived from their absolute concentrations determined using ultra-filtered serum samples to achieve reliable quantitative profiling. For each shown univariate analysis, the resulted p-values are shown in orange brown text to assess the statistical significance and other parameters such as fold change and mean values are shown in [Table 6, See the Appendix](#). For shown box-plots, the boxes denote interquartile ranges, horizontal line inside the box denote the median, and bottom and top boundaries of boxes are 25th and 75th percentiles, respectively. Lower and upper whiskers are 5th and 95th percentiles, respectively.

As SF remains in direct contact with the cartilage and other connective tissues affected in RDs, therefore, it is very likely that the pathophysiological changes will first accumulate in the SF before they can be detected in serum. In other words, the metabolic profiling of SF reflects directly what is

happening in a joint and under this assumption we intended to investigate the metabolic profiles of identified biomarkers between the paired serum and synovial fluids. Out of 53 ReA patients, the synovial fluid samples paired to serum samples were obtained for only 41 patients (n=41). For reliable concentration profiling, the 1D ^1H CPMG spectra were recorded on ultra-filtered serum and SF samples and analyzed using CHENOMX (for details, see the Materials and Method section). The concentrations of five selected marker metabolites (namely, arginine, leucine, lysine, phenylalanine, and valine) were determined using CHENOMX profiler module (in software *version 8.1*) and normalized w.r.t pyruvate concentration (within the sample for each marker metabolite). The correlation analysis between serum and SF metabolite concentrations was performed using Pearson correlation (ρ) method and the resulted correlation plots are shown in **Figure 3.18**.

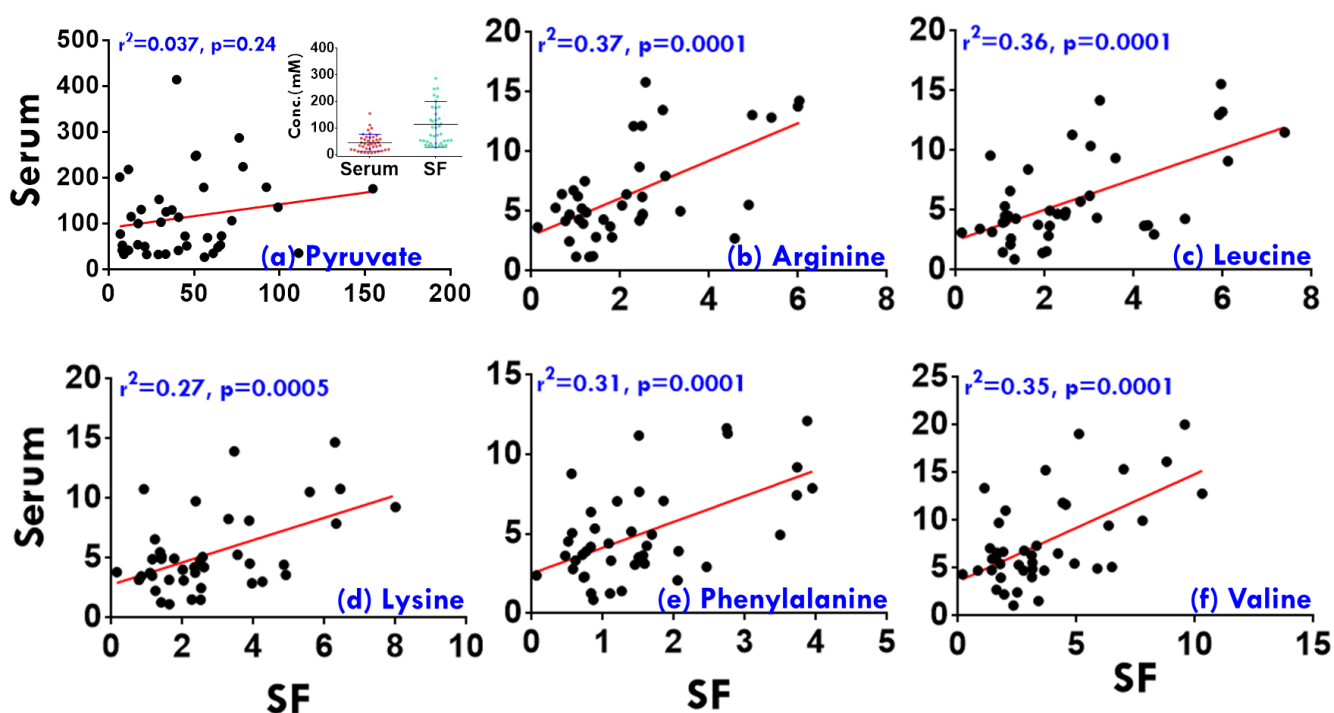


Figure 3.18: Serum marker metabolite except pyruvate showing correlation with Synovial fluid for ReA group.

The first graph in **Figure 3.18** shows the correlation between the concentration of pyruvate in serum and that in SF (inset showing the corresponding box plot). The resulted regression coefficient (r^2) of 0.037 and p value of 0.24 clearly suggested that pyruvate levels are not significantly different in serum and SF and thus may serve as a good internal reference for normalizing the concentrations for selected marker metabolites. Having done so, the concentration profiles of marker metabolites in serum of ReA patients showed a positive correlation with that in SF (the Pearson rank coefficients calculated for each correlation ranged from 0.27 to 0.37) suggesting that the observed changes in

serum biomarkers are reflecting the synovial inflammation. However, additional studies such as this one are required to establish the clinical relevance of these biomarkers and to explore their utility in early diagnosis and differentiation from other rheumatic inflammatory conditions and thus improve the clinical management.

3.6 Concluding Remarks

Identification of metabolic signatures that account for the differentiation of diseases not only helps to improve the diagnosis but further improve the understanding of disease mechanism. The present study provided proof of concept that NMR-based serum metabolomics coupled with pattern recognition methods can precisely discriminate not only ReA and RA from NC subjects but can also distinguish ReA from RA patients. The PLS-DA score plots not only achieved exquisite intra-group sample clustering, but also a good separation between ReA and non-ReA (i.e. RA and NC) subjects. The considerably high Q^2 values for the PLS-DA models (ReA vs. controls and RA vs. controls) support the hypothesis that the serum metabolic profiling could be employed to discriminate ReA and RA patients from normal controls. ROC analysis revealed ten serum biomarker metabolites of diagnostic potential for screening ReA patients from NC and four serum biomarker metabolites for differential diagnosis of ReA and RA patients. The potential metabolic hallmark discovered in this study is the elevated serum levels of leucine, valine, phenylalanine and arginine/lysine in ReA patients compared to RA patients and these changes were also found to be in good agreement with the disease pathophysiology as discussed in this paper. The concentration profiles of these markers metabolites in serum showed moderate positive correlation with the SF samples obtained from same ReA patients (paired study) (**Fig. 3.18**) reflecting possible impact of synovial inflammation on serum metabolic profiles. Though, we have identified relevant disease-specific metabolite profiles, however, further studies like this one are warranted to establish the clinical utility of suggested panel(s) of serum biomarker metabolites as a biochemical determinant of disease diagnosis, progression and prognosis. Overall, the study underscores the power of NMR coupled with multivariate pattern recognition analysis in identifying novel diagnostic and prognostic biomarkers of ReA and its potential to improve the clinical management.

The caveats associated with this study include (a) first, the accuracy of disease-specific metabolic profiles may be affected by inherent inaccuracies in clinical diagnosis, and co-morbidities such as the possible coexistence of ReA and RA, (b) second, the spectral features compared in this study are

normalized w.r.t to total spectral intensity, therefore, the observed metabolic perturbations may differ from actual levels of perturbations and (c) there may be detectable metabolic changes between the active and remission stages of ReA.

3.7 Acknowledgement

DK acknowledges the Department of Science and Technology for financial assistance under SERB EMR Scheme (**Ref. No.:** EMR/2016/001756). AG acknowledges the Department of Science and Technology (DST), Government of India for financial assistance under DST INSPIRE Faculty Award (**Ref. No.** DST/Inspire Faculty Award 2014/LSBM-120). We would also like to acknowledge the Department of Medical Education, Govt. of Uttar Pradesh for supporting the High Field NMR Facility at Centre of Biomedical Research, Lucknow, India. DD acknowledges receipt of a JRF/SRF fellowship from The Indian Council of Medical Research (ICMR), New Delhi, India.

3.8 References

- (1) Sieper, J. Disease mechanisms in reactive arthritis. *Current rheumatology reports* **2004**, 6, 110-116.
- (2) Kingsley, G.; Sieper, J. Current perspectives in reactive arthritis. *Immunology today* **1993**, 14, 387-391.
- (3) Kvien, T. K.; Glennas, A.; Melby, K.; Granfors, K.; Andrup, O.; Karstensen, B.; Thoen, J. E. Reactive arthritis: incidence, triggering agents and clinical presentation. *The Journal of rheumatology* **1994**, 21, 115-122.
- (4) Aggarwal, A.; Misra, R.; Chandrasekhar, S.; Prasad, K. N.; Dayal, R.; Ayyagari, A. Is undifferentiated seronegative spondyloarthropathy a forme fruste of reactive arthritis? *British journal of rheumatology* **1997**, 36, 1001-1004.
- (5) Singh, A. K.; Misra, R.; Aggarwal, A. Th-17 associated cytokines in patients with reactive arthritis/undifferentiated spondyloarthropathy. *Clinical rheumatology* **2011**, 30, 771-776.
- (6) Singh, R.; Aggarwal, A.; Misra, R. Th1/Th17 cytokine profiles in patients with reactive arthritis/undifferentiated spondyloarthropathy. *The Journal of rheumatology* **2007**, 34, 2285-2290.
- (7) Zeidler, H.; Hudson, A. P. Coinfection of Chlamydiae and other bacteria in reactive arthritis and spondyloarthritis: need for future research. *Microorganisms* **2016**, 4, 30.
- (8) Shadick, N. A.; Cook, N. R.; Karlson, E. W.; Ridker, P. M.; Maher, N. E.; Manson, J. E.; Buring, J. E.; Lee, I. M. C-reactive protein in the prediction of rheumatoid arthritis in women. *Archives of Internal Medicine* **2006**, 166, 2490-2494.
- (9) Hamdulay, S. S.; Glynn, S. J.; Keat, A. When is arthritis reactive? *Postgraduate medical journal* **2006**, 82, 446-453.
- (10) Kvien, T. K.; Uhlig, T.; Ødegård, S.; Heiberg, M. S. Epidemiological aspects of rheumatoid arthritis. *Annals of the New York Academy of Sciences* **2006**, 1069, 212-222.
- (11) Dubey, D.; Kumar, S.; Ahmed, S.; Chaudhary, A.; Chaurasia, S.; Guleria, A.; Kumar, D.; Misra, R. NMR based serum and synovial fluid metabolomics reveal similar metabolomic profile in patients with reactive arthritis and undifferentiated spondyloarthropathy. *Indian Journal of Rheumatology* **2017**, 12, S24.
- (12) Sieper, J.; Braun, J. Problems and advances in the diagnosis of reactive arthritis. *The Journal of rheumatology* **1999**, 26, 1222.
- (13) Taylor, W. J.; Robinson, P. C. Classification criteria: peripheral spondyloarthropathy and psoriatic arthritis. *Current rheumatology reports* **2013**, 15, 317.
- (14) Aletaha, D.; Neogi, T.; Silman, A. J.; Funovits, J.; Felson, D. T.; Bingham, C. O.; Birnbaum, N. S.; Burmester, G. R.; Bykerk, V. P.; Cohen, M. D. 2010 rheumatoid arthritis classification criteria: an American College of Rheumatology/European League Against Rheumatism collaborative initiative. *Arthritis & Rheumatology* **2010**, 62, 2569-2581.

- (15) Dubey, D.; Chaurasia, S.; Guleria, A.; Kumar, S.; Modi, D. R.; Misra, R.; Kumar, D. Metabolite assignment of Ultra-Filtered Synovial Fluid extracted from knee joints of Reactive Arthritis patients using High-Resolution NMR spectroscopy. *Magnetic Resonance in Chemistry* **2018**,
- (16) Wishart, D. S. Quantitative metabolomics using NMR. *TrAC Trends in Analytical Chemistry* **2008**, 27, 228-237.
- (17) Guleria, A.; Pratap, A.; Dubey, D.; Rawat, A.; Chaurasia, S.; Sukesh, E.; Phatak, S.; Ajmani, S.; Kumar, U.; Khetrpal, C. L.; Bacon, P.; Misra, R.; Kumar, D. NMR based serum metabolomics reveals a distinctive signature in patients with Lupus Nephritis. *Sci Rep.* **2016**, 6, 35309.
- (18) Guleria, A.; Misra, D. P.; Rawat, A.; Dubey, D.; Khetrpal, C. L.; Bacon, P.; Misra, R.; Kumar, D. NMR-Based Serum Metabolomics Discriminates Takayasu Arteritis from Healthy Individuals: A Proof-of-Principle Study. *J Proteome Res* **2015**, 14, 3372-3381.
- (19) Nicholson, J. K.; Foxall, P. J.; Spraul, M.; Farrant, R. D.; Lindon, J. C. 750 MHz ¹H and ¹H-¹³C NMR spectroscopy of human blood plasma. *Analytical chemistry* **1995**, 67, 793-811.
- (20) Wishart, D. S.; Jewison, T.; Guo, A. C.; Wilson, M.; Knox, C.; Liu, Y.; Djoumbou, Y.; Mandal, R.; Aziat, F.; Dong, E.; Bouatra, S.; Sinelnikov, I.; Arndt, D.; Xia, J.; Liu, P.; Yallou, F.; Bjorndahl, T.; Perez-Pineiro, R.; Eisner, R.; Allen, F.; Neveu, V.; Greiner, R.; Scalbert, A. HMDB 3.0--The Human Metabolome Database in 2013. *Nucleic Acids Res.* **2013**, 41, D801-D807.
- (21) Xia, J.; Bjorndahl, T. C.; Tang, P.; Wishart, D. S. MetaboMiner-semi-automated identification of metabolites from 2D NMR spectra of complex biofluids. *BMC Bioinformatics* **2008**, 9, 507.
- (22) Gowda, G. A. N.; Raftery, D. Quantitating Metabolites in Protein Precipitated Serum Using NMR Spectroscopy. *Analytical chemistry* **2014**, 86, 5433-5440.
- (23) Xia, J.; Psychogios, N.; Young, N.; Wishart, D. S. MetaboAnalyst: a web server for metabolomic data analysis and interpretation. *Nucleic acids research* **2009**, 37, W652-W660.
- (24) Xia, J.; Sinelnikov, I. V.; Han, B.; Wishart, D. S. MetaboAnalyst 3.0-making metabolomics more meaningful. *Nucleic acids research* **2015**, 43, W251-W257.
- (25) Xia, J.; Wishart, D. S. Using MetaboAnalyst 3.0 for comprehensive metabolomics data analysis. *Current protocols in bioinformatics* **2016**, 14-10.
- (26) Westerhuis, J. A.; Hoefsloot, H. C.; Smit, S.; Vis, D. J.; Smilde, A. K.; van Velzen, E. J.; van Duijnoven, J. P.; van Dorsten, F. A. Assessment of PLS-DA cross validation. *Metabolomics* **2008**, 4, 81-89.
- (27) Xia, J.; Wishart, D. S. Web-based inference of biological patterns, functions and pathways from metabolomic data using MetaboAnalyst. *Nature protocols* **2011**, 6, 743.
- (28) Greiner, M.; Pfeiffer, D.; Smith, R. D. Principles and practical application of the receiver-operating characteristic analysis for diagnostic tests. *Preventive veterinary medicine* **2000**, 45, 23-41.

- (29) Hajian-Tilaki, K. Receiver operating characteristic (ROC) curve analysis for medical diagnostic test evaluation. *Caspian journal of internal medicine* **2013**, 4, 627.
- (30) Worley, B.; Powers, R. Multivariate analysis in metabolomics. *Current Metabolomics* **2013**, 1, 92-107.
- (31) Young, S. P.; Kapoor, S. R.; Viant, M. R.; Byrne, J. J.; Filer, A.; Buckley, C. D.; Kitas, G. D.; Raza, K. The impact of inflammation on metabolomic profiles in patients with arthritis. *Arthritis & Rheumatism* **2013**, 65, 2015-2023.
- (32) Ouyang, X.; Dai, Y.; Wen, J. L.; Wang, L. X. ¹H NMR-based metabolomic study of metabolic profiling for systemic lupus erythematosus. *Lupus* **2011**, 20, 1411-1420.
- (33) Wu, T.; Xie, C.; Han, J.; Ye, Y.; Weiel, J.; Li, Q.; Blanco, I.; Ahn, C.; Olsen, N.; Putterman, C.; Saxena, R.; Mohan, C. Metabolic disturbances associated with systemic lupus erythematosus. *PLoS One* **2012**, 7, e37210.
- (34) Schulze, P. C.; Yoshioka, J.; Takahashi, T.; He, Z.; King, G. L.; Lee, R. T. Hyperglycemia promotes oxidative stress through inhibition of thioredoxin function by thioredoxin-interacting protein. *Journal of Biological Chemistry* **2004**, 279, 30369-30374.
- (35) Chang, S. C.; Yang, W. C. V. Hyperglycemia, tumorigenesis, and chronic inflammation. *Critical reviews in oncology/hematology* **2016**, 108, 146-153.
- (36) Tsan, M. F.; Gao, B. Endogenous ligands of Toll-like receptors. *Journal of leukocyte biology* **2004**, 76, 514-519.
- (37) Mohammad, M. K.; Morran, M.; Slotterbeck, B.; Leaman, D. W.; Sun, Y.; von Grafenstein, H.; Hong, S. C.; McInerney, M. F. Dysregulated Toll-like receptor expression and signaling in bone marrow-derived macrophages at the onset of diabetes in the non-obese diabetic mouse. *International immunology* **2006**, 18, 1101-1113.
- (38) Jiang, S. Y.; Wei, C. C.; Shang, T. T.; Lian, Q.; Wu, C. X.; Deng, J. Y. High glucose induces inflammatory cytokine through protein kinase C-induced toll-like receptor 2 pathway in gingival fibroblasts. *Biochemical and biophysical research communications* **2012**, 427, 666-670.
- (39) Devaraj, S.; Dasu, M. R.; Rockwood, J.; Winter, W.; Griffen, S. C.; Jialal, I. Increased toll-like receptor (TLR) 2 and TLR4 expression in monocytes from patients with type 1 diabetes: further evidence of a proinflammatory state. *The Journal of Clinical Endocrinology & Metabolism* **2008**, 93, 578-583.
- (40) Creely, S. J.; McTernan, P. G.; Kusminski, C. M.; Da Silva, N. F.; Khanolkar, M.; Evans, M.; Harte, A. L.; Kumar, S. Lipopolysaccharide activates an innate immune system response in human adipose tissue in obesity and type 2 diabetes. *American Journal of Physiology-Endocrinology And Metabolism* **2007**, 292, E740-E747.
- (41) Caricilli, A. M.; Nascimento, P. H.; Pauli, J. R.; Tsukumo, D. M.; Velloso, L. A.; Carvalheira, J. B.; Saad, M. J. Inhibition of toll-like receptor 2 expression improves insulin sensitivity and signaling in

- muscle and white adipose tissue of mice fed a high-fat diet. *Journal of Endocrinology* **2008**, 199, 399-406.
- (42) He, M.; Harms, A. C.; Wijk, E.; Wang, M.; Berger, R.; Koval, S.; Hankemeier, T.; Greef, J. Role of amino acids in rheumatoid arthritis studied by metabolomics. *International journal of rheumatic diseases* **2017**,
- (43) Simmonds, R. E.; Foxwell, B. M. Signalling, inflammation and arthritis: NF- κ B and its relevance to arthritis and inflammation. *Rheumatology* **2008**, 47, 584-590.
- (44) Morgan, M. J.; Liu, Z. g. Crosstalk of reactive oxygen species and NF- κ B signaling. *Cell research* **2011**, 21, 103.
- (45) Schutz, Y. Protein turnover, ureagenesis and gluconeogenesis. *International Journal for Vitamin and Nutrition Research* **2011**, 81, 101.
- (46) Kobayashi, T.; Okada, M.; Ito, S.; Kobayashi, D.; Shinhara, A.; Muramatsu, T.; Kobayashi, T.; Narita, I.; Nakazono, K.; Murasawa, A. Amino acid profiles in relation to chronic periodontitis and rheumatoid arthritis. *Open Journal of Stomatology* **2014**, 4, 49.
- (47) Trang, L. E.; Fürst, P.; Odeback, A. C.; Lövgren, O. Plasma amino acids in rheumatoid arthritis. *Scandinavian journal of rheumatology* **1985**, 14, 393-402.
- (48) Olkku, A.; Bodine, P. V. N.; Linnala-Kankkunen, A.; Mahonen, A. Glucocorticoids induce glutamine synthetase expression in human osteoblastic cells: a novel observation in bone. *Bone* **2004**, 34, 320-329.
- (49) Guma, M.; Tiziani, S.; Firestein, G. S. Metabolomics in rheumatic diseases: desperately seeking biomarkers. *Nature Reviews Rheumatology* **2016**, 12, 269.
- (50) Nicastro, H.; Da Luz, C. R.; Chaves, D. F. S.; Bechara, L. R. G.; Voltarelli, V. A.; Rogero, M. M.; Lancha, A. H. Does branched-chain amino acids supplementation modulate skeletal muscle remodeling through inflammation modulation? Possible mechanisms of action. *Journal of nutrition and metabolism* **2012**, Article ID 136937, 1-10.
- (51) Nettelbladt, E.; Sandell, B. M. Amino-acid content of serum in rheumatoid arthritis. *Annals of the Rheumatic Diseases* **1963**, 22, 269.
- (52) Freund, H. R.; Ryan Jr, J. A.; Fischer, J. E. Amino acid derangements in patients with sepsis: treatment with branched chain amino acid rich infusions. *Annals of surgery* **1978**, 188, 423.
- (53) Ahn, J. K.; Kim, S.; Kim, J.; Hwang, J.; Kim, K. H.; Cha, H. S. A comparative metabolomic evaluation of Behcet's disease with arthritis and seronegative arthritis using synovial fluid. *PLoS One* **2015**, 10, e0135856.
- (54) Zhenyukh, O.; Civantos, E.; Ruiz-Ortega, M.; Sánchez, M. S.; Vázquez, C.; Peiró, C.; Egido, J.; Mas, S. High concentration of branched-chain amino acids promotes oxidative stress, inflammation and

- migration of human peripheral blood mononuclear cells via mTORC1 activation. *Free Radical Biology and Medicine* **2017**, 104, 165-177.
- (55) Yang, X. Y.; Di Zheng, K.; Lin, K.; Zheng, G.; Zou, H.; Wang, J. M.; Lin, Y. Y.; Chuka, C. M.; Ge, R. S.; Zhai, W. Energy metabolism disorder as a contributing factor of rheumatoid arthritis: a comparative proteomic and metabolomic study. *PLoS One* **2015**, 10, e0132695.
- (56) Yan, L. J. Pathogenesis of chronic hyperglycemia: from reductive stress to oxidative stress. *Journal of diabetes research* **2014**, Article ID 137919, 1-11.
- (57) Neurauter, G.; Schrocksnadel, K.; Scholl-Burgi, S.; Sperner-Unterweger, B.; Schubert, C.; Ledochowski, M.; Fuchs, D. Chronic immune stimulation correlates with reduced phenylalanine turnover. *Current drug metabolism* **2008**, 9, 622-627.
- (58) Ploder, M.; Neurauter, G.; Spittler, A.; Schroecksnadel, K.; Roth, E.; Fuchs, D. Serum phenylalanine in patients post trauma and with sepsis correlate to neopterin concentrations. *Amino Acids* **2008**, 35, 303-307.
- (59) Wannemacher Jr, R. W.; Klainer, A. S.; Dinterman, R. E.; Beisel, W. R. The significance and mechanism of an increased serum phenylalanine-tyrosine ratio during infection. *The American journal of clinical nutrition* **1976**, 29, 997-1006.
- (60) Borden, A. L.; Brodie, E. C.; Wallraff, E. B.; Holbrook, W. P.; Hill, D. F.; Stephens, C. A. L.; Johnson, R. B.; Kemmerer, A. R. Amino acid studies and clinical findings in normal adults and rheumatoid arthritis patients treated with ACTH. *The Journal of clinical investigation* **1952**, 31, 375-379.
- (61) Van Tits, L. J. H.; Stienstra, R.; Van Lent, P. L.; Netea, M. G.; Stalenhoef, A. F. H. Oxidized LDL enhances pro-inflammatory responses of alternatively activated M2 macrophages: a crucial role for Krüppel-like factor 2. *Atherosclerosis* **2011**, 214, 345-349.
- (62) Cuzzocrea, S. Role of nitric oxide and reactive oxygen species in arthritis. *Current pharmaceutical design* **2006**, 12, 3551-3570.
- (63) Boger, R. H. The pharmacodynamics of L-arginine. *The Journal of nutrition* **2007**, 137, 1650S-1655S.
- (64) Zabek, A.; Swierkot, J.; Malak, A.; Zawadzka, I.; Deja, S.; Bogunia-Kubik, K.; Mlynarz, P. Application of ¹H NMR-based serum metabolomic studies for monitoring female patients with rheumatoid arthritis. *Journal of Pharmaceutical and Biomedical Analysis* **2016**, 117, 544-550.
- (65) Zhou, J.; Chen, J.; Hu, C.; Xie, Z.; Li, H.; Wei, S.; Wang, D.; Wen, C.; Xu, G. Exploration of the serum metabolite signature in patients with rheumatoid arthritis using gas chromatography-mass spectrometry. *Journal of Pharmaceutical and Biomedical Analysis* **2016**, 127, 60-67.
- (66) Erum, U.; Ahsan, T.; Khowaja, D. Lipid abnormalities in patients with Rheumatoid Arthritis. *Pakistan journal of medical sciences* **2017**, 33, 227.
- (67) Tselios, K.; Koumaras, C.; Gladman, D. D.; Urowitz, M. B. Dyslipidemia in systemic lupus erythematosus: just another comorbidity? *Seminars in arthritis and rheumatism* **2016**, 45, 604-610.

- (68) Ahmad, W. N. H. W.; Sakri, F.; Mokhsin, A.; Rahman, T.; Nasir, N. M.; Abdul-Razak, S.; Yasin, M. M.; Ismail, A. M.; Ismail, Z.; Nawawi, H. Low serum high density lipoprotein cholesterol concentration is an independent predictor for enhanced inflammation and endothelial activation. *PLoS One* **2015**, *10*, e0116867.
- (69) García-Gómez, C.; Nolla, J. M.; Valverde, J.; Gómez-Gerique, J. A.; Castro, M. J.; Pintó, X. Conventional lipid profile and lipoprotein (a) concentrations in treated patients with rheumatoid arthritis. *The Journal of rheumatology* **2009**, *36*, 1365-1370.
- (70) Bhakdi, S.; Dorweiler, B.; Kirchmann, R.; Torzewski, J.; Weise, E.; Trantum-Jensen, J.; Walev, I.; Wieland, E. On the pathogenesis of atherosclerosis: enzymatic transformation of human low density lipoprotein to an atherogenic moiety. *Journal of Experimental Medicine* **1995**, *182*, 1959-1971.
- (71) Rawat, A.; Srivastava, R. K.; Dubey, D.; Guleria, A.; Singh, S.; Prakash, A.; Modi, D. R.; Khetrapal, C. L.; Tiwari, S.; Kumar, D. Serum Metabolic Disturbances Hailing in Initial Hours of Acute Myocardial Infarction Elucidated by NMR based Metabolomics. *Current Metabolomics* **2017**, *5*, 55-67.

Chapter-5

Conclusion and Future Prospects

5.1 Conclusion

The primary abnormality in reactive arthritis is synovitis (inflammation of the synovial membrane), which is followed by erosion, exposition of cartilage antigens, and autoimmunity. Systemic inflammation has an enormous impact on metabolism; thus, subsequently, metabolomics have been utilised to study human and animal models of inflammation. These studies have shown that metabolite levels are modified by inflammation, which has offered valuable insights into the pathophysiology of these conditions and exposed numerous possible biomarkers for disease assessment. In recent years, metabolomics has emerged as a high-throughput technique particularly feasible for the study of complex biological samples. By the study of the overall low molecular weight metabolites (metabolome), synthesized in relation to genetic alterations and/or external stimuli, it provides comprehensive insights into the pathophysiological state of an organism. The great versatility of NMR spectroscopy has enabled this analytical technique to be a useful tool for the identification and quantification of a wide range of cellular metabolites in biological samples. In particular, when combined with pattern recognition methods, it provides important contributions to the characterization of the phenotype of an organism, offering metabolomic research great possibilities in several scientific areas.

In this Ph.D. thesis, NMR-based metabolomics was applied for metabolic profiling to find possible distinctive metabolic patterns and biomarker candidates for ReA where unexpected changes in metabolite levels can be exploited to uncover novel mechanistic knowledge in health as well as disease. The two studies included in this thesis mirror this development in the field, starting from paper I. Here, we describe protocols for human SF sampling and processing and present a novel approach of metabolite characterization on both normal and ultra-filtered (deproteinized) SF samples of ReA patients. The ultrafiltration and high-resolution ^1H NMR analysis is a particularly powerful combining method for concentration profiling of low molecular weight metabolites. The removal of proteins from serum/SF by ultrafiltration using low molecular weight cutoff filters serves to free metabolic components which significantly alleviates the peak attenuation problem and offers an avenue for absolute metabolite quantitation. The intact SF, however, has been used previously in many NMR-based metabolomics studies and they have faced numerous challenges such as the limited resolution, low metabolite identification, and the adverse effects of ample proteins. We were able to recognise a total of 64 small endogenous metabolites (including many complex coupled spin systems) using ultra-filtered SF which probably representing several metabolic pathways including

those relevant in the context of energy metabolism, amino acid metabolism, lipid metabolism, inflammation, and oxidative stress conditions. Thus, this study will serve to lead future metabolomics studies directing to identify/evaluate the SF based metabolic biomarkers of diagnostic/prognostic potential or searching biochemical insights into disease mechanisms from a clinical perspective.

In paper II, Using serum samples, we have shown that two different inflammatory conditions (ReA and RA) can be distinguished using NMR spectroscopy and our work also demonstrates that patients with ReA can be differentiated from healthy controls. The potential metabolic signature discovered in this study is the elevated serum levels of leucine, valine, phenylalanine and arginine/lysine in ReA patients compared to RA patients and these alterations were also found to be in good agreement with the disease pathophysiology. The literature also suggests that there are a number of such metabolites which are common to several inflammatory conditions and thus markers of inflammation. In this study, we also demonstrated the relationship between the serum and synovial fluid concentrations of individual biomarkers to determine whether measurements made in the serum reflect the concentrations observed within the signal knee which suggests that NMR may be a promising tool for predicting specific pathogenic pathways in the inflammatory condition of ReA patients.

5.2 Future Prospects

Recent technological advances have boosted the capacity to mine the metabolite composition of biological samples associated with different diseases. This new layer of information strongly complements the previously established genomic, transcriptomic and proteomic technologies. In the near future, studies integrating these different layers of biological information will provide essential knowledge for the identification of the biological mechanisms that operate in each disease and will provide an accurate molecular profile of each patient. This individual profiles will have a high translational potential in the rheumatic disease since it could help to advance the time of diagnosis as well as help medical specialists to perform more guided therapeutic decisions. Metabolomics analysis technologies must improve in sensitivity and be less time consuming and costly, and the associated analysis algorithms must improve their accuracy. Also, if large cohort analyses are to be performed, there is a clear need for improvement in the throughput of most metabolomics platforms. Additionally, sample and clinical collection procedures must be standardized to ensure the quality of

the results and the minimization of technical and biological confounders. Although metabolomics is an emergent discipline, it is rapidly evolving and, in the next years, new findings will clearly increase our knowledge of the molecular basis of rheumatic diseases and contribute to improve the prognosis of these patients.

5.3 Future Works Plan

Conventional treatments target established ReA late on in disease and in a non personalised manner. For the first time, we have demonstrated the serum metabolic profiling of ReA patient using NMR base metabolomics approaches and identify the potential biomarkers for the diagnosis of ReA distinguished from other inflammatory arthritis such as RA. We also demonstrated that the relationship between potential serum biomarker and synovial metabolites suggests that NMR may be a promising tool for predicting specific pathogenic pathways in the inflamed synovium of patients with ReA. There is a pressing need to confirm and extend this finding in a larger cohort of patients, combining metabolomic with cytokine and autoantibody analyses to develop tests that can predict response without the need for empirical treatment, bringing closer the era of individually tailored therapy.

In the next future, we will also try to go through the actions of the different drugs on the cellular metabolite, unequivocally assigning the metabolite NMR signals responsible for the differentiation among the treatments through advanced multivariate data analysis for biomarker profiling.

Appendix I:**Table 1:** ^1H and ^{13}C chemical shift assignments of the metabolites observed in the NMR spectra of pooled Synovial Fluid samples.

S. No.	Name of metabolites	Assignment	$\delta^1\text{H}$ (multiplicity)	$\delta^{13}\text{C}$	J-Coupling (Hz)	Methods
1	2-Hydroxybutyric acid	$\gamma\text{-CH}_3$ $\frac{1}{2}\beta\text{-CH}_2$ $\frac{1}{2}\beta\text{-CH}_2$	0.88 (t) 1.63 (m) 1.73 (m)	- - 29.62	7.46	1D, JRES, HSQC, TOCSY, Chenomx
2	2-Hydroxyisovaleric acid	$\gamma\text{-CH}_3$	0.82(d)	-	6.80	1D, JRES, Chenomx
3	2-Hydroxyphenylacetate [#]	C4,3H	7.19(m)	130.9	-	1D, HSQC, JRES, Chenomx
4	3-Methyl-2-oxovaleric acid	$\alpha'\text{-CH}_3$	1.11(d)	-	7.03	1D, JRES, Chenomx
5	2-Oxoisocaproic acid	$\gamma\beta'\text{-CH}_3$ $\alpha\text{-CH}_2$	0.92(d) 2.60(d)	- -	6.58 7.01	1D, JRES,Cheno mx
6	3-Methyladipic acid	$\alpha'\text{-CH}_3$	0.91(d)	-	6.74	1D, JRES, Chenomx
7	3-Hydroxybutyric Acid	$\gamma\text{-CH}_3$ $\frac{1}{2}\alpha\text{-CH}_2$ $\frac{1}{2}\alpha\text{-CH}_2$ $\beta\text{-CH}$	1.18 (d) 2.28 (m) 2.39 (m) 4.14(m)	24.44 49.23 49.23 68.5	6.27 - - -	1D, JRES, HSQC, TOCSY, Chenomx
8	4-Hydroxyphenylacetate [#]	C5,3H	7.14(d)	-	8.68	1D, JRES, Chenomx
9	6-Hydroxynicotinic acid [#]	C3H ₂	6.66(d)	-	9.2	1D, JRES, Chenomx
10	Acetate	CH ₃	1.90 (s)	-	-	1D, JRES, Chenomx
11	Acetone	CH ₃	2.21(s)	32.91	-	1D, JRES, HSQC, Chenomx
12	Acetylcarnitine	CH ₃ N+(CH ₃) ₃	2.13(s) 3.19(s)	- 56.46	- -	1D, JRES, HSQC, Chenomx
13	Alanine	$\beta\text{-CH}_3$ $\alpha\text{-CH}$	1.44 (d) 3.73 (q)	19.06 53.5	7.13 -	1D, JRES, HSQC, TOCSY, Chenomx
14	Arginine	$\gamma\text{-CH}_2$ $\delta\text{-CH}_2$ $\alpha\text{-CH}$	1.69 (m) 3.23 (t) 3.76 (t)	26.48 43.32 57.26	- - -	1D, JRES, HSQC, TOCSY
15	Aspartic acid	$\frac{1}{2}\beta\text{-CH}_2$ $\frac{1}{2}\beta\text{-CH}_2$	2.65(dd) 2.80(dd)	- -	15.85,8.37 15.85,4.28	1D, JRES, TOCSY, Chenomx
16	Betaine	N+(CH ₃) ₃ $\alpha\text{-CH}_2$	3.25 (s) 3.88 (s)	55.85 68.64	- -	1D, JRES, HSQC, Chenomx
17	Butyrate [#]	$\alpha\text{-CH}_3$	0.86(t)	-	7.37	1D, JRES, Chenomx

18	Carnitine	α -CH ₂ N+(CH ₃) ₃ γ -CH ₂	2.41(m) 3.21(s) 3.41(m)	45.7 56.91 72.87	- - -	1D, JRES, HSQC, TOCSY, Chenomx
19	Choline	N+(CH ₃) ₃	3.19 (s)	56.69	-	1D, JRES, HSQC, TOCSY, Chenomx
20	Citric acid	$\frac{1}{2}$ γ -CH ₂ $\frac{1}{2}$ γ -CH ₂	2.51 (d) 2.66 (d)	48.71 48.71	15.4 -	1D, JRES, HSQC, TOCSY, Chenomx
21	Citrulline [#]	γ -CH ₂ β -CH ₂ γ -CH ₂	1.56(m) 1.86 (m) 3.13 (q)	27.58 30.72 42.05	- - -	1D, JRES, HSQC, TOCSY
22	Creatine	CH ₃ CH ₂	3.01 (s) 3.91 (s)	39.44 56.45	- -	1D, JRES, HSQC, Chenomx
23	Creatinine	CH ₃ CH ₂	3.03 (s) 4.04 (s)	32.97 59.23	- -	1D, JRES, HSQC, Chenomx
24	Ethanol	CH ₃ CH ₂	1.16 (t) 3.63(q)	19.42 -	7.07 -	1D, JRES, HSQC, TOCSY, Chenomx
25	Formate	C2H	8.44 (s)	-	-	1D, JRES, Chenomx
26	Fucose	C22H ₃ C11H ₃ C2H	1.22(d) 1.25(d) 4.54(d)	- - -	6.68 6.9 7.93	1D, JRES, Chenomx
27	α -Glucose	C4H C2H C3H $\frac{1}{2}$ -C6H ₂ $\frac{1}{2}$ -C6H ₂ C1H	3.40 (m) 3.52 (dd) 3.70 (t) 3.82 (m) 3.81(m) 5.22 (d)	72.39 74.52 75.6 63.32 74.19 94.88	- - - - - 3.67	1D, JRES, HSQC, TOCSY, Che nomx
28	β -Glucose	C2H C5H C3H $\frac{1}{2}$ -C6H ₂ $\frac{1}{2}$ -C6H ₂ C1H	3.23 (dd) 3.45 (m) 3.47 (m) 3.72 (m) 3.88 (dd) 4.64 (d)	77.01 78.64 78.51 63.53 63.39 98.72	- - - - - 7.95	1D, JRES, HSQC, TOCSY, Che nomx
29	Glutamate	$\frac{1}{2}$ β -CH ₂ $\frac{1}{2}$ γ -CH ₂	2.04 (m) 2.34 (m)	29.98 36.35	- -	1D, JRES, HSQC, TOCSY, Chenomx
30	Glutamine	$\frac{1}{2}$ β -CH ₂ $\frac{1}{2}$ γ -CH ₂	2.06(m) 2.42(m)	- 33.92	- -	1D, JRES, HSQC, TOCSY, Chenomx
31	Glycerol	$\frac{1}{2}$ CH ₂ $\frac{1}{2}$ CH ₂ C2H	3.54 (dd) 3.64 (dd) 3.77	65.4 65.49 74.97	6.64 4.33 -	1D, JRES, HSQC, TOCSY
32	Glycolate	α -CH ₂	3.92 (s)	64.05	-	1D, HSQC
33	Glycine	α -CH ₂	3.51 (s)	44.53	-	1D, JRES, HSQC, Chenomx
34	Histidine	C ₄ H-ring C ₂ H-ring	7.00 (d) 7.71(d)	119.99 -	- 1.4	1D, JRES, HSQC,

						Chenomx
35	Hydroxyacetone [#]	α -CH ₃	2.15(s)	25.36	-	1D, JRES, HSQC, Chenomx
36	Isobutyric Acid [#]	CH ₃	1.06 (d)	-	7.01	1D, JRES, Chenomx
37	Isopropanol	CH ₃	1.18(d)	-	6.22	1D, JRES, Chenomx
38	Isovaleric acid	CH ₃	0.90(d)	-	6.61	1D, JRES, Chenomx
39	Isoleucine	γ -CH ₃ δ -CH ₃ $\frac{1}{2}$ γ -CH ₂ $\frac{1}{2}$ γ -CH ₂ β -CH α -CH	0.92 (t) 0.99 (d) 1.24 1.46 1.94 3.65 (d)	13.98 17.36 - 26.99 38.77 -	7.41 7.05 - - - -	1D, JRES, HSQC, TOCSY, Chenomx
40	Lactate	β -CH ₃ α -CH	1.31 (d) 4.11 (q)	22.9 71.11	6.95 6.93	1D, JRES, HSQC, TOCSY, Chenomx
41	Leucine	δ -CH ₃ δ -CH ₃ β -CH γ -CH	0.93 (d) 0.95 (d) 1.70 (m) 1.70 (m)	23.57 24.79 26.77 42.82	6.44 6.46 - -	1D, JRES, HSQC, TOCSY, Chenomx
42	Lysine	γ -CH ₂ γ -CH ₂ δ -CH ₂ ϵ -CH ₂ α -CH	1.43 (m) 1.49(m) 1.71 (m) 3.01 (t) 3.74 (t)	24.04 24.04 29.51 42.11 -	- - - - -	1D, JRES, HSQC, TOCSY, Chenomx
43	α -Mannose	C11H C1H	3.37(dd) 5.17(d)	78.93 96.8	-	1D, JRES, HSQC, Chenomx
44	β -Mannose	C8H C7H C4H C2H	3.65(m) 3.80(m) 3.83(m) 4.90(d)	69.72 75.26 73.12 96.4	- - - -	1D, JRES, HSQC, Chenomx
45	Methionine	δ -CH ₃ γ -CH	2.12(s) 2.61(t)	- -	- 7.58	1D, JRES, HSQC, Chenomx
46	Methylsuccinic acid	β' -CH ₃	1.08(d)	-	7.01	1D, JRES, Chenomx
47	Myo-Inositol	C5H C1H & C3H C4H & C6H C2H	3.27 (t) 3.52 (dd) 3.62 (t) 4.05 (t)	77.15 73.95 75.13 74.95	10.27 - 9.3 -	1D, JRES, HSQC, TOCSY, Chenomx
48	Melatonin	C7H	7.44(d)	-	8.68	1D, JRES, Chenomx
49	N-Acetyltyrosine [#]	C2,6H C3,5H	6.82(d) 7.12(d)	- -	8.5 8.48	1D, JRES, Chenomx
50	N-Nitrosodimethylamine (NDMA) [#]	CH ₃ CH ₃	3.15(s) 3.79(s)	32.3 -	- -	1D, JRES, HSQC, Chenomx
51	Phenylalanine	$\frac{1}{2}$ β -CH ₂ C2H & C6H C4H C3H & C5H	3.11(m) 7.30 (d) 7.35 (m) 7.42 (t)	39.09 132.11 130.37 131.84	- - - -	1D, HSQC, TOCSY, Chenomx

52	Propylene glycol	α -CH ₃	1.13(d)	-	6.45	1D, JRES, Chenomx
53	Proline	γ -CH ₂ $\frac{1}{2}$ β -CH ₂ $\frac{1}{2}$ β -CH ₂ $\frac{1}{2}$ δ -CH ₂ $\frac{1}{2}$ δ -CH ₂ α -CH	1.99 (m) 2.05 (m) 2.34 (m) 3.32(dt) 3.41(dt) 4.12	26.46 31.84 31.72 48.95 48.95 64.03	- - - - - -	1D, JRES, HSQC, TOCSY, Chenomx
54	Pyroglutamic acid	C5H	4.16(dd)	60.98	5.86,9.00	1D, JRES, HSQC, Chenomx
55	Pyruvate	CH ₃	2.38(s)	-	-	1D, JRES, Chenomx
56	Succinylacetone [#]	α -CH ₂	2.42(t)	33.67	6.48	1D, JRES, HSQC, Chenomx
57	Sucrose [#]	C7H	5.40(d)	94.8	3.89	1D, JRES, HSQC, Chenomx
58	Threonine	γ -CH ₃ α -CH	1.27 (d) 3.57 (d)	22.3 -	6.58 4.83	1D, JRES, HSQC, Chenomx
59	Trimethylamin-N-oxide (TMAO) [#]	N-CH ₃	3.25(s)	62.22	-	1D, JRES, Chenomx
60	Tyrosine	α -CH C2H & C6H C3H & C5H	3.93(dd) 6.84 (d) 7.15 (d)	58.98 118.88 133.56	- 8.52 8.53	1D, JRES, HSQC, Chenomx
61	Valine	γ -CH ₃ γ -CH ₃ β -CH	0.96 (d) 1.01 (d) 2.23 (m)	19.4 20.75 31.9	7.00 7.05 -	1D, JRES, HSQC, TOCSY, Chenomx
62	Xylose	C4H	3.43(t)	78.66	9.27	1D, JRES, HSQC
63	Serine	β -CH ₂	3.96(m)	-	-	Spiking
64	Cysteine	β -CH	4.00(dd)	-	-	Spiking

(s) Singlet; (d) doublet; (t) triplet; (q) quartet; (dd) doublet of doublets; (m) multiplet.

[#]Represent the metabolite was not found in the 1D 1H CPMG NMR spectrum of individual filtered SF.

Table 2: The ^1H and ^{13}C chemical shift assignments of the metabolites observed in various NMR spectra of normal Synovial Fluid

S. No.	Name of metabolites	Assignment	$\delta^1\text{H}$ (multiplicity)	$\delta^{13}\text{C}$	Methods
1	2-Hydroxybutyric acid	CH_3 $\frac{1}{2}\text{CH}_2$ $\frac{1}{2}\text{CH}_2$ $\alpha\text{-CH}$	0.87 (t) 1.63 (m) 1.73 (m) 3.98(dd)	29.62 76.26	1D, JRES, HSQC,
2	3-Hydroxybutyric acid	$\gamma\text{-CH}_3$ $\frac{1}{2}\alpha\text{-CH}_2$ $\frac{1}{2}\alpha\text{-CH}_2$ $\beta\text{-CH}$	1.18 (d) 2.31 (m) 2.41 (m) 4.16		1D, JRES
3	Acetate	CH_3	1.90 (s)	26.08	1D, JRES, HSQC
4	Acetoacetic acid	CH_3 CH_2	2.29 (s) 3.42 (s)	32.24	1D, JRES, HSQC
5	Acetone	CH_3	2.22 (s)	32.91	1D, JRES, HSQC
6	Alanine	$\beta\text{-CH}_3$ $\alpha\text{-CH}$	1.46 (d) 3.77 (q)	19.06 53.55	1D, JRES, HSQC
7	Albumin lysyl	$\epsilon\text{-CH}_2$	2.88(t)		1D, JRES
8	Arginine	$\gamma\text{-CH}_2$ $\beta\text{-CH}_2$ $\delta\text{-CH}_2$ $\alpha\text{-CH}$	1.68 (m) 1.87 (m) 3.23 (t) 3.75 (t)	26.86 30.49 43.3	1D, JRES, HSQC
9	Betaine	$\text{N}+(\text{CH}_3)_3$ CH	3.25 (s) 3.88 (s)	55.84	1D, JRES, HSQC
10	Cholesterol	C6 C27	0.86(t)	23.3	HSQC
11	Choline	$\text{N}+(\text{CH}_3)_3$ $\beta\text{-CH}_3$ $\alpha\text{-CH}_2$	3.19 (s) 3.50 (m) 4.05 (m)	56.69	1D, HSQC
12	Citric acid	$\frac{1}{2}\gamma\text{-CH}_2$ $\frac{1}{2}\gamma\text{-CH}_2$	2.52 (d) 2.69 (d)		1D, JRES,
13	Citrulline	$\beta\text{-CH}_2$ $\frac{1}{2}\gamma\text{-CH}_2$ $\frac{1}{2}\gamma\text{-CH}_2$ $\alpha\text{-CH}$	1.56 (m) 1.86 (m) 3.13 (q) 3.69 (dd)	27.46 30.72 42.05 57.35	1D, JRES, HSQC

14	Creatine	CH ₃ CH ₂	3.01 (s) 3.91 (s)	39.44 56.45	1D, JRES, HSQC
15	Creatinine	CH ₃ CH ₂	3.02 (s) 4.04 (s)	32.66 59.04	1D, JRES, HSQC
16	Ethanol	CH ₃ CH ₂	1.19 (t) 3.65(q)	19.42	1D,JRES, HSQC
17	Formate	CH	8.44 (s)		1D, JRES
18	α -Glucose	C4H C2H C3H $\frac{1}{2}$ -C6H ₂ $\frac{1}{2}$ -C6H ₂ C5H C1H	3.39 (m) 3.52 (dd) 3.70 (t) 3.82 (m) 3.82 (m) 5.22 (d)	72.39 74.19 75.45 63.41 63.41 94.87	1D,JRES, HSQC
19	β -Glucose	C2H C5H C3H $\frac{1}{2}$ -C6H ₂ $\frac{1}{2}$ -C6H ₂ C1H	3.23 (dd) 3.45 (m) 3.47 (m) 3.71 (m) 3.89 (dd) 4.63 (dd)	76.95 78.69 78.51 63.51 63.47 98.71	1D,JRES, HSQC
20	Glutamate	β -CH ₂ γ -CH ₂ α -CH	2.08 (m) 2.33 (m) 3.75 (t)	29.91 36.35	1D,JRES, HSQC
21	Glutamine	β -CH ₂ γ -CH ₂ α -CH	2.12 (m) 2.43(m) 3.74 (t)	29.88 33.92 57.26	1D,JRES, HSQC
22	Glycerol	$\frac{1}{2}$ -CH ₂ $\frac{1}{2}$ -CH ₂ CH	3.54 (m) 3.64 (m) 3.77 (tt)	65.66 65.49 74.97	1D,JRES, HSQC
23	Glycerophosphocholine	N+(CH ₃) ₃ C5H ₂ C4H ₂ C3H ₂ *C3H ₂ C2H C1H ₂ *C1H ₂	3.21 (s) 3.66 (m) 4.32 (m) 3.89 (m) 3.94 (m) 3.90 (m) 3.67 3.62	56.64 68.6 62.06 69.14 64.67	1D, HSQC
24	Glycolate	α -CH ₂	3.92 (s)	64.05	1D, HSQC, JRES

25	Glycine	α -CH ₂		44.45	1D, HSQC, JRES
26	Histidine	$\frac{1}{2}$ CH ₂ $\frac{1}{2}$ CH ₂ α -CH C ₄ H-ring C ₂ H-ring	3.09 (dd) 3.20 (d) 3.94 (dd) 7.71(d) 7.00 (d)		1D, JRES
27	Isobutyric Acid	γ -CH ₃	1.06 (d)		1D, JRES
28	Isoleucine	γ -CH ₃ δ -CH ₃ $\frac{1}{2}$ γ -CH ₂ $\frac{1}{2}$ γ -CH ₂ β -CH α -CH	0.93 (t) 0.98 (d) 1.13 1.46 1.94 3.61 (d)	13.6	1D,JRES, HSQC
29	Lactate	β -CH ₃ α -CH	1.31 (d) 4.11 (q)	22.9 71.11	1D,JRES, HSQC
30	Leucine	δ -CH ₃ δ -CH ₃ β -CH ₂ γ -CH α -CH	0.94 (d) 0.95 (d) 1.69 (m) 1.70 (m) 3.74	23.56 24.84 26.83 42.59	1D,JRES, HSQC
31	Lipids	CH ₃ (CH ₂) _n CH ₂ CH ₂ C=C CH ₂ CH=CH CH ₂ CO CH=CH-CH ₂ -CH=CH CH=CH -CH ₂ -CH ₂ -CO-	0.86 1.24 1.67 2.04 2.21 2.66 5.32 1.38	24.76 32.47 27.07 27.2 24.6	1D, HSQC
32	Lysine	γ -CH ₂ δ -CH ₂ β -CH ₂ ϵ -CH ₂ α -CH	1.43 (m) 1.49 1.69 (m) 1.88 (m) 3.01 (t) 3.74 (t)	24.53 24.53 29.15 32.88 42.11 57.45	1D,JRES, HSQC,
33	Mannose	C2H	5.17(s)	96.8	1D, JRES,

					HSQC
34	Methanol	CH ₃	3.34(s)		1D, JRES
35	Methionine	S-CH ₃ S-CH ₂	2.06(s) 2.17(m) 2.61(t)	16.83	1D,JRES, HSQC
36	<i>Myo</i> -Inositol	C5H C1H & C3H C6H C2H	3.30 (t) 3.52 (dd) 3.62 (t) 4.04 (t)	77.15 75.13 74.93	1D,JRES, HSQC
37	N-Nitrosodimethylamine	NCH ₃	3.15(s)		1D, JRES
38	N-Acetylglycoproteins	NHCOCH ₃	2.04 (s)	24.95	1D,JRES, HSQC
39	Phenylalanine	½ β-CH ₂ ½ β-CH ₂ α-CH C2H & C6H C4H C3H & C5H	3.07(m) 3.22 (dd) 3.96(dd) 7.31 (d) 7.37 (m) 7.43 (m)	39.17 131.31	1D,JRES, HSQC
40	Proline	γ-CH ₂ ½ β-CH ₂ ½ β-CH ₂ ½ δ-CH ₂ ½ δ-CH ₂ α-CH	1.99 (m) 2.06 (m) 2.34 (m) 3.32(dt) 3.41(dt) 4.12	26.95 48.78 48.87 63.03	1D,JRES, HSQC
41	Pyruvate	γ -CH ₃	2.38(S)		1D, JRES
42	Succinic acid	α, β-CH ₂	2.39 (s)	36.44	JRES, HSQC
43	Threonine	γ-CH ₃ α-CH β-CH	1.30 (d) 3.59 (d) 4.24 (m)	22.3 63.45	1D, JRES, HSQC
44	Tyrosine	½ β-CH ₂ α-CH C2H & C6H C3H & C5H	3.21 (dd) 3.92 6.87 (d) 7.17 (d)	58.96 118.86	1D, JRES, HSQC

45	Valine	γ -CH ₃ γ -CH ₃ β -CH α -CH	0.97 (d) 1.03 (d) 2.25 (m) 3.57(d)	19.4 20.75 31.89 63.34	1D, JRES, HSQC
46	Unsaturated Fatty Acid	CH=CHCH ₂ CH=CH CH=CHCH ₂ CH=CH CH=CHCH ₂ CH=CH =CHCH ₂ CH ₂ =CHCH ₂ CH ₂	5.26 5.28 5.29 5.32 5.32	130.29 130.29 130.29 132.1	1D, JRES, HSQC
47	N- α -acetyl-L-Lysine (NAAL)	γ -CH ₂ β, δ -CH ₂ β -CH ₂ ϵ -CH ₂ -CH ₃	1.39(dq) 1.67(m) 1.80(m) 2.99(t) 2.02 (s)	--	Spiking
48	Serine	β -CH ₂	3.96(m)	--	Spiking

(s) Singlet; (d) doublet; (t) triplet; (q) quartet; (dd) doublet of doublets; (m) multiplet.

Table 3: Demographics and clinical characteristics of patients and normal control subjects included in the study.

	Reactive Arthritis (ReA*, n=52)	Young Normal controls (YNC,n=55)	Rheumatoid Arthritis (RA, n=29)	Elderly normal controls (ENC, n=33)	Normal Control (NC) (n=82)
Gender (M:F)	44:8	43:12	02:27	08:33	57:25
Age (years)	29.00 ± 10.88 (range; 16-49)	32.72± 7.57 (range; 21-52)	40.10±11.75 (range; 18-61)	41.20± 9.20 (range; 21-57)	36.38±9.25 (range; 21-57)
CRP, mg/dl	7.42± 7.80 (range; 0.40-44.5)	-	4.17±5.00 (range; 0.33-19.8)	-	-
ESR, mm/h	77.82± 37.56 (range; 12-135)	-	55.67± 33.63 (range; 12-130)	-	-

Table 4: Cross validation parameters for various PLS-DA models obtained from analysis of serum samples showing the goodness-of-fit and its statistical significance.

S.No.		Accuracy	R²	Q²	p-value(100 permutations)	Model AUROC	
1	ReA vs YNC	Complete data	0.96	0.86	0.79	<0.001	0.99
		Truncated data	0.95	0.86	0.79	<0.001	0.99
2	RA vs ENC	Complete data	0.99	0.90	0.86	<0.001	0.97
		Truncated data	0.97	0.88	0.83	<0.001	0.99
3	ReA vs RA	Complete data	0.90	0.84	0.67	<0.001	0.88
		Truncated data	0.90	0.82	0.62	<0.001	0.91
4	ReA vs NC	Complete data	0.98	0.89	0.82	<0.001	0.99
		Truncated data	0.97	0.88	0.77	<0.001	0.99
5	RA vs NC	Complete data	0.98	0.91	0.84	<0.001	0.99
		Truncated data	0.96	0.86	0.79	<0.001	0.99
6	ReA vs RA vs NC	Complete data	0.85	0.82	0.70	<0.001	--
		Truncated data	0.83	0.79	0.71	<0.001	--

--ROC analysis cannot be performed for discriminatory models involving more than two groups; therefore AUROC values cannot be evaluated.

Table 5: The identified discriminating metabolites responsible for class separation between ReA and non ReA groups. The metabolic biomarkers were screened based on VIP score values > 1.0 (derived from PLS-DA modelling, showing discrimination significance) and then tested (using univariate and student t-test) for statistical significance based on p-value < 0.05. The up (↑) and down (↓) arrows represent, respectively, increased and decreased metabolite levels in ReA and RA groups compared to controls. The metabolite levels here represent binned spectral features normalized with respect to the total spectral intensity.

S.No	Metabolite	ppm	ReA vs YNC (NC)	RA vs ENC (NC)	ReA vs RA	RA vs NC in		
						Study 1	Study 2	Study 3
1	LDL	0.87	↓(↓)	↓(↓)	↓	↑ ^{\$}	↑ ^{\$}	↓
2	Isoleucine	0.91	↑(↑)	↑(↑)	↑	↓ ^{\$}	↓ ^{\$}	-
3	Leucine	0.95	↑(↑)	↑(↑)	↑	-	↓ ^{\$}	-
4 [#]	Valine	0.97	↑(↑)	↓(↓)	↑	↓	↓	-
5	VLDL	1.27	↓(↓)	↓(↓)	↓	↑ ^{\$}	↓	↓
6 [#]	Lysine/Arginine	1.71/1.69	↑(↑)	--	↑	↓ ^{\$}	↓ ^{\$}	--
7 [#]	Citrulline	1.87	↑(↑)	↑(↑)	--	--	--	--
8 [#]	Acetate	1.89	↑(↑)	↓(↓)	↑	-	↑ ^{\$}	-
9	NAG	2.01	↑* (↑)	↑ (-)	--	↑	↑	↑
10 [#]	Glutamate	2.05/2.07/2.33	↑(↑)	↑(↑)	↑	↓ ^{\$}	-	-
11	Acetone	2.21	↓(↓)	- (↓)	↓&	-	↑ ^{\$}	-
12 [#]	Acetoacetate	2.27	↑(↑)	--	↑	-	↑	-
13	Pyruvate	2.35	↓ (-)	- (↓)	↑&	↓	-	-
14 [#]	3-HB	2.29/2.39	↑(↑)	↑(↑)	↑	-	↓ ^{\$}	↑
15 [#]	Glutamine	2.43/2.11	↑(↑)	↓(↓)	↑	↓	-	-
16	Citrate	2.51	--	↓ (-)	-	↓	↓	-
17 [#]	Methionine	2.61/2.63	↑(↑)	--	↑	-	-	-
18 [#]	Creatinine	3.03	↑(↑)	↓(↓)	↑	↓	↓	-
19	Choline	3.19	↓(↓)	↓ (-)	↓&	-	↓	-
20	GPC	3.21	↑(↑)	- (↑)	↓&	-	↓ ^{\$}	-
21	Glycine	3.53	↑(↑)	↑(↑)	-	-	-	-
22	Glucose	3.87	↑(↑)	↑(↑)	↑	↑	↑	↑
23	Creatine	3.91	↑(↑)	↑(↑)	-	-	↓	-
24	Lactate	4.09/4.11	- (↑)	↓(↓)	↑&	↑ ^{\$}	↓	↑ ^{\$}
25	PUFA	5.29/5.31	↓(↓)	↓(↓)	↓	-	↓	↓
26	Tyrosine	7.17	--	↓ (-)	↑&	↓	↓	-
27	Phenylalanine	7.31	↑(↑)	↓(↓)	↑	↓	↑ ^{\$}	-
25 [#]	Histidine	7.73	↑(↑)	↑(↑)	↑	↓	↓ ^{\$}	-

Note: *p-value > 0.05

Represent the marker metabolites identified from truncated data matrix analysis (excluding the glucose and lipid regions)

^{\$} - Serum levels contradictory as reported in previous studies (1-3) with references ^{31,32,64}




&- not considered as significant metabolite

Table 6: Univariate statistics performed on marker metabolites using their concentration measured on ultra-filtered serum samples with the help of commercial software CHENOMX.

S.No.	Metabolite	ReA vs YNC			ReA vs RA		
		Mean \pm SD (ReA)	Mean \pm SD (YNC)	FC	Mean value (ReA)	Mean value (RA)	FC
1	Creatine	21.70 \pm 16.53	33.89 \pm 19.23	0.63* [#]	--	--	--
2	Acetone	36.38 \pm 27.25	23.65 \pm 11.98	1.54 [#]	--	--	--
3	Phenylalanine	163.99 \pm 106.63	124.29 \pm 57	1.33	163.99 \pm 106.63	73.3 \pm 69.06	2.56*
4	Lysine	162.33 \pm 103.40	208.36 \pm 101.48	0.78* [#]	162.33 \pm 103.40	121.06 \pm 118.4	1.46*
5	Arginine	138.94 \pm 90.12	117.7 \pm 69.9	1.21	138.94 \pm 90.12	89.57 \pm 117.4	2.07*
6	Leucine	165.55 \pm 97.74	200.64 \pm 89.7	0.83 [#]	165.55 \pm 97.74	97.30 \pm 93.6	1.88*
7	Glucose	5391.5 \pm 3678.6	4839.65 \pm 4178	1.12	--	--	--
8	Glycine	459.76 \pm 317.08	446.66 \pm 215.9	1.03*	--	--	--
9	Valine	--	--	--	231.92 \pm 138.6	147.81 \pm 138.4	1.57*

Note: SD: Standard Deviation; FC: Fold change; * is used when p-value < 0.05; [#] Signifies if relative change is different compared to normalized spectral features

Metabolite assignment of ultrafiltered synovial fluid extracted from knee joints of reactive arthritis patients using high resolution NMR spectroscopy

Durgesh Dubey^{1,2} | Smriti Chaurasia³ | Anupam Guleria¹  | Sandeep Kumar³ |
Dinesh Raj Modi² | Ramnath Misra³  | Dinesh Kumar¹ 

¹ Centre of Biomedical Research, Sanjay Gandhi Postgraduate Institute of Medical Sciences, Lucknow, India

² Babasaheb Bhimrao Ambedkar University, Lucknow, India

³ Department of Clinical Immunology, Sanjay Gandhi Postgraduate Institute of Medical Sciences, Lucknow, India

Correspondence

Ramnath Misra, Department of Clinical Immunology, Sanjay Gandhi Postgraduate Institute of Medical Sciences, Raibareli Road, Lucknow 226014, India.
Email: rnmisra2000@gmail.com

Dinesh Kumar, Centre of Biomedical Research (CBMR), Sanjay Gandhi Postgraduate Institute of Medical Sciences, Raibareli Road, Lucknow 226014, India.
Email: dineshcbmr@gmail.com

Funding information

Science and Engineering Research Board, Grant/Award Number: EMR/2016/001756

Abstract

Currently, there are no reliable biomarkers available that can aid early differential diagnosis of reactive arthritis (ReA) from other inflammatory joint diseases. Metabolic profiling of synovial fluid (SF)—obtained from joints affected in ReA—holds great promise in this regard and will further aid monitoring treatment and improving our understanding about disease mechanism. As a first step in this direction, we report here the metabolite specific assignment of ¹H and ¹³C resonances detected in the NMR spectra of SF samples extracted from human patients with established ReA. The metabolite characterization has been carried out on both normal and ultrafiltered (deproteinized) SF samples of eight ReA patients (*n* = 8) using high-resolution (800 MHz) ¹H and ¹H–¹³C NMR spectroscopy methods such as one-dimensional ¹H CPMG and two-dimensional J-resolved ¹H NMR and homonuclear ¹H–¹H TOCSY and heteronuclear ¹H–¹³C HSQC correlation spectra. Compared with normal SF samples, several distinctive ¹H NMR signals were identified and assigned to metabolites in the ¹H NMR spectra of ultrafiltered SF samples. Overall, we assigned 53 metabolites in normal filtered SF and 64 metabolites in filtered pooled SF sample compared with nonfiltered SF samples for which only 48 metabolites (including lipid/membrane metabolites as well) have been identified. The established NMR characterization of SF metabolites will serve to guide future metabolomics studies aiming to identify/evaluate the SF-based metabolic biomarkers of diagnostic/prognostic potential or seeking biochemical insights into disease mechanisms in a clinical perspective.

KEYWORDS

biomarkers, metabolomics, NMR, reactive arthritis, rheumatic diseases (RD), rheumatoid arthritis, synovial fluid

Abbreviations: CPMG, Car–Purcell–Meiboom–Gill sequence; DSS, 2, 2-Dimethyl-2-silapentane-5-sulfonate; HSQC, heteronuclear single quantum correlation; JRES, J-resolved; NMR, nuclear magnetic resonance; RA, rheumatoid arthritis; RD, rheumatic disease; ReA, reactive arthritis; TOCSY, total correlation spectroscopy

1 | INTRODUCTION

Differential biomarkers are becoming clinically essential for timely diagnosis and predicting prognosis of rheumatic diseases (RDs) and subsequent treatment

NMR-Based Serum Metabolomics Revealed Distinctive Metabolic Patterns in Reactive Arthritis Compared with Rheumatoid Arthritis

Durgesh Dubey,^{†,§} Sandeep Kumar,[‡] Smriti Chaurasia,[‡] Anupam Guleria,[†] Sakir Ahmed,[‡] Rajeev Singh,^{||,⊥} Reena Kumari,[⊥] Dinesh Raj Modi,[§] Ramnath Misra,^{*,‡,||} and Dinesh Kumar^{*,†,||}

[†]Centre of Biomedical Research and [‡]Department of Clinical Immunology, SGPGIMS, Raibareilly Road, Lucknow 226014, India

[§]Babasaheb Bhimrao Ambedkar University, Lucknow 226025, India

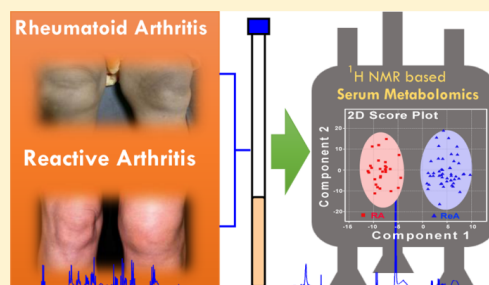
^{||}National Institute of Virology, Gorkhpur Unit, BRD Medical College Campus, Gorakhpur 273013, India

[⊥]Department of Biochemistry, KGMU, Lucknow 226003, India

Supporting Information

ABSTRACT: Reactive arthritis (ReA) is a member of seronegative spondyloarthropathy (SSA), which involves an acute/subacute onset of asymmetrical lower limb joint inflammation weeks after a genitourinary/gastrointestinal infection. The diagnosis is clinical because it is difficult to culture the microbes from synovial fluid. Arthritis patients with a similar clinical picture but lapsed history of an immediate preceding infection that do not fulfill the diagnostic criteria of other members of SSA, such as ankylosing spondylitis, psoriatic arthritis, and arthritis associated with inflammatory bowel disease, are labeled as peripheral undifferentiated spondyloarthropathy (uSpA). Both ReA and uSpA patients show a strong association with class I major histocompatibility complex allele, HLA-B27, and a clear association with an infectious trigger; however, the disease mechanism is far from clear. Because the clinical picture is largely dominated by rheumatoid-arthritis (RA)-like features including elevated levels of inflammatory markers (such as ESR, CRP, etc.), these overlapping symptoms often confound the clinical diagnosis and represent a clinical dilemma, making treatment choice more generalized. Therefore, there is a compelling need to identify biomarkers that can support the diagnosis of ReA/uSpA. In the present study, we performed NMR-based serum metabolomics analysis and demonstrated that ReA/uSpA patients are clearly distinguishable from controls and further that these patients can also be distinguished from the RA patients based on the metabolic profiles, with high sensitivity and specificity. The discriminatory metabolites were further subjected to area under receiver operating characteristic curve analysis, which led to the identification of four metabolic entities (i.e., valine, leucine, arginine/lysine, and phenylalanine) that could differentiate ReA/uSpA from RA.

KEYWORDS: reactive arthritis, rheumatoid arthritis, NMR, metabolic signatures, differential diagnosis



INTRODUCTION

Reactive arthritis (ReA) is an autoimmune condition that typically follows weeks after a genitourinary or gastrointestinal infection (predominantly in males).¹ The clinical symptoms include an acute or subacute onset of asymmetrical lower limb joint inflammation; however, sometimes other articular and extra-articular manifestations may also be seen such as dactylitis, enthesitis, conjunctivitis, and unilateral sacroiliitis.^{1–3} As such, ReA is a member of the heterogeneous group called seronegative spondyloarthropathy (SSA). However, a substantial proportion of SSA patients who have a similar clinical picture as ReA but do not confer a history of preceding infection and do not fulfill the diagnostic criteria of other members of SSA (such as ankylosing spondylitis, psoriatic arthritis, and arthritis associated with inflammatory bowel disease) are appropriately labeled as peripheral undifferentiated

spondyloarthropathy (uSpA).⁴ In previous studies from our group,^{5,6} we have shown that both ReA and uSpA have similar levels of proinflammatory cytokines such as IL-17 and IL-6 in the sera and synovial fluid (SF), sera antibodies to enteric organisms, and recently expansion of antigen-specific T-cell response to *Salmonella* outer membrane protein A in enterically acquired ReA/uSpA. Both ReA and uSpA show a strong association with class I major histocompatibility complex (MHC) allele, HLA-B27, and a clear association with microbial trigger; however, the disease mechanism is still not clear. It is assumed that the components of bacteria persist *in vivo* (i.e., antigenic persistence, usually in the synovium and SF) and trigger immune reactions (molecular cross-reactiv-

Received: June 11, 2018

Published: October 17, 2018



NMR-Based Metabolomic Approach To Elucidate the Differential Cellular Responses during Mitigation of Arsenic(III, V) in a Green Microalga

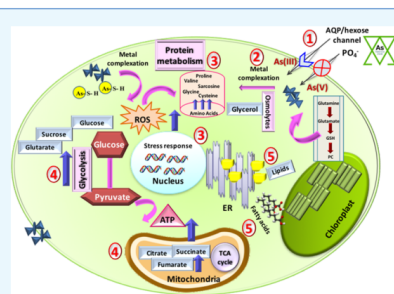
Neha Arora,^{†,||} Durgesh Dubey,^{§,||} Meenakshi Sharma,[†] Alok Patel,[†] Anupam Guleria,[§] Parul A. Pruthi,[†] Dinesh Kumar,^{*,§} Vikas Pruthi,^{*,†,‡} and Krishna Mohan Poluri^{*,†,‡}

[†]Department of Biotechnology and [‡]Centre for Transportation Systems, Indian Institute of Technology Roorkee, Roorkee 247667, Uttarakhand, India

[§]Centre of Biomedical Research, SGPGIMS, Lucknow 226014, Uttar Pradesh, India

Supporting Information

ABSTRACT: Nuclear magnetic resonance (NMR)-based metabolomic approach is a high-throughput fingerprinting technique that allows a rapid snapshot of metabolites without any prior knowledge of the organism. To demonstrate the applicability of NMR-based metabolomics in the field of microalgal-based bioremediation, novel freshwater microalga *Scenedesmus* sp. IITRIND2 that showed hypertolerance to As(III, V) was chosen for evaluating the metabolic perturbations during arsenic stress in both its oxidation states As(III) and As(V). Using NMR spectroscopy, we were able to identify and quantify an array of ~45 metabolites, including amino acids, sugars, organic acids, phosphagens, osmolytes, nucleotides, etc. The NMR metabolomic experiments were complemented with various biophysical techniques to establish that the microalga tolerated the arsenic stress using a complex interplay of metabolites. The two different arsenic states distinctly influenced the microalgal cellular mechanisms due to their altered physicochemical properties. Eighteen differentially identified metabolites related to bioremediation of arsenic were then correlated to the major metabolic pathways to delineate the variable stress responses of microalga in the presence of As(III, V).



1. INTRODUCTION

Metabolomics is the end point of omics cascade that represents an array of metabolites, including amino acids, carbohydrates, organic acids, nucleotides, etc.¹ Metabolic profiling can be performed using nuclear magnetic resonance (NMR) spectroscopy and/or with setup of gas/liquid chromatography/capillary electrophoresis (GC/LC/CE) coupled with mass spectrometry (MS) (examples: GC-MS, LC-MS, CE-MS, etc.).^{2,3} The key parameters required for developing a robust metabolomics platform include reproducibility, easy and rapid quantification, and identification of large number of metabolites with minimal sample preparation steps.⁴ NMR spectroscopy metabolomic approach is a nondestructive and non-discriminating technique, thus making it an ideal tool for metabolomic profiling for any chosen organism.^{1,5} Given the above advantages of ¹H NMR metabolomics, it has been widely applied to diverse fields, including understanding of drug metabolism, disease progression, biomarker discovery, nutritional research, effects of xenobiotics on plants, photochemistry, food adulterations, etc.^{4,6–8}

Among the above mentioned applications, environmental metabolomics is an effective tool for analyzing the changes in complex biochemical mechanisms/pathways against the stress-generating agents, such as toxic chemicals, heavy metals, and

extreme pH/temperature conditions.^{3,9} Rapid industrialization and urbanization has led to escalation in levels of heavy metals in aquatic ecosystems, thus posing a greater threat to plant, animal, and human life.^{10,11} Among the heavy metals, arsenic (As) has been reported to cause high incidence of arsenicosis in more than 20 countries across the globe, thereby listing it as a category 1 and class A carcinogen by the U.S. Environmental Protection Agency.^{11,12} High levels of arsenic in potable water sources have been reported in various countries, including southwest Finland (17–980 mg/L), western United States (1–48 000 mg/L), and Inner Mongolia, China (1354 mg/L).¹³ Arsenic has a complex physicochemistry as it exists in two interchangeable forms, anoxic trivalent As(III) and oxo pentavalent As(V) in the aquatic ecosystems.¹⁴

The conventional techniques deployed for the removal of arsenic from contaminated water bodies are biased toward one form of arsenic species, pH dependent, and require high maintenance and expensive mineral adsorbents making the overall process costly and less efficient.^{15,16} In this regard, microalgae have emerged as budding vectors for green

Received: July 18, 2018

Accepted: September 11, 2018

Published: September 25, 2018

Nuclear magnetic resonance-based metabolomics reveals similar metabolomics profiles in undifferentiated peripheral spondyloarthritis and reactive arthritis

Sakir Ahmed¹  | Durgesh Dubey² | Abhra Chowdhury¹  | Smriti Chaurasia¹ | Anupam Guleria² | Sandeep Kumar¹ | Rajeev Singh¹ | Dinesh Kumar²  | Ramnath Misra¹ 

¹Department of Clinical Immunology, Sanjay Gandhi Postgraduate Institute of Medical Sciences, Lucknow, India

²Centre of Biomedical Research, Sanjay Gandhi Postgraduate Institute of Medical Sciences, Lucknow, India

Correspondence

Ramnath Misra, Department of Clinical Immunology, Sanjay Gandhi Postgraduate Institute of Medical Sciences, Lucknow, India.
Email: rnmisra2000@gmail.com

Funding information

Overhead research fund of Ramanth Misra

Abstract

Introduction: After exclusion of reactive, psoriatic and enteritis-associated arthritis, a group of “undifferentiated” peripheral spondyloarthritis (pSpA) remains. This group shares genetics, T-cell repertoire, and cytokines with reactive arthritis (ReA). ReA is preceded by gut or urogenital infection. Otherwise the two may be similar. We know little of the metabolic pathways driving undifferentiated pSpA or ReA. Nuclear magnetic resonance (NMR)-based metabolomics presents a hypothesis-free approach to study and compare metabolic pathways driving undifferentiated pSpA and ReA.

Methods: Serum and synovial fluid metabolomes of 19 ReA and 13 undifferentiated pSpA, and serum metabolome of 18 controls were profiled using ¹H-based NMR. Partial least square-discriminant analysis (PLS-DA) identified metabolites different in patients as compared to controls. Multivariate analysis confirmed these. Altered metabolic pathways were identified using metabolites set enrichment analysis (MSEA). The serum and synovial fluid metabolomes of ReA and undifferentiated pSpA were compared.

Results: Ten serum metabolites of ReA/undifferentiated pSpA were different from those of controls. Six metabolites were different between serum and synovial fluid of these patients. MSEA identified five pathways different between patients and controls, and five pathways different between serum and synovial fluid of patients. PLS-DA showed no difference between the metabolomes of serum or of synovial fluid between ReA and undifferentiated pSpA.

Discussion: Identified metabolic pathways may be explored further to understand the pathogenesis and to target therapeutics. The similar immuno-metabolic pathways suggest similar pathogenesis of ReA and undifferentiated pSpA. Thus, they should be studied as a single disease entity.

KEYWORDS

biomarkers, immunometabolism, inflammatory arthritis, metabolomics, nuclear magnetic resonance, reactive arthritis, spondyloarthritis, synovial fluid

¹H NMR-based serum metabolomics reveals erythromycin-induced liver toxicity in albino Wistar rats

Atul Rawat^{1,2}, Durgesh Dubey^{1,2}, Anupam Guleria², Umesh Kumar², Amit K. Keshari³, Swati Chaturvedi³, Anand Prakash¹, Sudipta Saha³, Dinesh Kumar²

Departments of
¹Biotechnology and
³Pharmaceutical Sciences,
Babasaheb Bhimrao
Ambedkar University,
²Centre of Biomedical
Research, Sanjay Gandhi
Post Graduate Institute
of Medical Sciences
Campus, Lucknow,
Uttar Pradesh, India

Address for correspondence:
Dr. Dinesh Kumar,
E-mail: dineshcbmr@gmail.com

Received : 12-07-16
Review completed : 28-08-16
Accepted : 31-08-16

ABSTRACT

Introduction: Erythromycin (ERY) is known to induce hepatic toxicity which mimics other liver diseases. Thus, ERY is often used to produce experimental models of drug-induced liver-toxicity. The serum metabolic profiles can be used to evaluate the liver-toxicity and to further improve the understanding of underlying mechanism. **Objective:** To establish the serum metabolic patterns of Erythromycin induced hepatotoxicity in albino wistar rats using ¹H NMR based serum metabolomics. **Experimental:** Fourteen male rats were randomly divided into two groups (*n* = 7 in each group): control and ERY treated. After 28 days of intervention, the metabolic profiles of sera obtained from ERY and control groups were analyzed using high-resolution 1D ¹H CPMG and diffusion-edited nuclear magnetic resonance (NMR) spectra. The histopathological and SEM examinations were employed to evaluate the liver toxicity in ERY treated group. **Results:** The serum metabolic profiles of control and ERY treated rats were compared using multivariate statistical analysis and the metabolic patterns specific to ERY-induced liver toxicity were established. The toxic response of ERY was characterized with: (a) increased serum levels of Glucose, glutamine, dimethylamine, malonate, choline, phosphocholine and phospholipids and (b) decreased levels of isoleucine, leucine, valine, alanine, glutamate, citrate, glycerol, lactate, threonine, circulating lipoproteins, N-acetyl glycoproteins, and poly-unsaturated lipids. These metabolic alterations were found to be associated with (a) decreased TCA cycle activity and enhanced fatty acid oxidation, (b) dysfunction of lipid and amino acid metabolism and (c) oxidative stress. **Conclusion and Recommendations:** Erythromycin is often used to produce experimental models of liver toxicity; therefore, the established NMR-based metabolic patterns will form the basis for future studies aiming to evaluate the efficacy of anti-hepatotoxic agents or the hepatotoxicity of new drug-formulations.

KEY WORDS: Erythromycin, metabolomics, multivariate data analysis, nuclear magnetic resonance, rats, liver-toxicity

Erythromycin (ERY) belongs to a group of drugs called macrolide antibiotics and is widely used to treat or prevent different types of bacterial infections.^[1,2] However, ERY has been found to induce certain side effects and may produce allergic reactions like hives, difficult breathing, swelling of face, lips, tongue, or throat. Further, the continuous use of ERY can also alter the gut flora;^[3] thus additionally producing gastrointestinal disorders like abdominal pain, nausea, and diarrhea, but are

rarely severe. However, the most adverse side-effect of frequent use of ERY have been linked to the instances of hepatotoxicity manifested as disturbances in liver function and jaundice.^[4,5] ERY-induced hepatotoxicity likely arises from a combination of intrinsic hepatotoxic effects and the hypersensitivity reactions that characterize most cases with evidence of hepatocellular

Access this article online	
Quick Response Code: 	Website: www.jpbsonline.org
	DOI: 10.4103/0975-7406.199339

This is an open access article distributed under the terms of the Creative Commons Attribution-NonCommercial-ShareAlike 3.0 License, which allows others to remix, tweak, and build upon the work non-commercially, as long as the author is credited and the new creations are licensed under the identical terms.

For reprints contact: reprints@medknow.com

How to cite this article: Rawat A, Dubey D, Guleria A, Kumar U, Keshari AK, Chaturvedi S, et al. ¹H NMR-based serum metabolomics reveals erythromycin-induced liver toxicity in albino Wistar rats. J Pharm Bioall Sci 2016;8:327-34.

SCIENTIFIC REPORTS

OPEN

NMR based serum metabolomics reveals a distinctive signature in patients with Lupus Nephritis

Received: 20 April 2016
Accepted: 27 September 2016
Published: 14 October 2016

Anupam Guleria¹, Avadhesh Pratap², Durgesh Dubey^{1,3}, Atul Rawat^{1,3}, Smriti Chaurasia², Edavalath Suresh², Sanat Phatak², Sajal Ajmani², Umesh Kumar¹, Chunni Lal Khetrpal¹, Paul Bacon⁴, Ramnath Misra² & Dinesh Kumar¹

Management of patient with Lupus Nephritis (LN) continues to remain a challenge for the treating physicians because of considerable morbidity and even mortality. The search of biomarkers in serum and urine is a focus of researchers to unravel new targets for therapy. In the present study, the utility of NMR-based serum metabolomics has been evaluated for the first time in discriminating LN patients from non-nephritis lupus patients (SLE) and further to get new insights into the underlying disease processes for better clinical management. Metabolic profiling of sera obtained from 22 SLE patients, 40 LN patients and 30 healthy controls (HC) were performed using high resolution 1D ¹H-CPMG and diffusion edited NMR spectra to identify the potential molecular biomarkers. Using multivariate analysis, we could distinguish SLE and LN patients from HC and LN from SLE patients. Compared to SLE patients, the LN patients had increased serum levels of lipid metabolites (including LDL/VLDL lipoproteins), creatinine and decreased levels of acetate. Our results revealed that metabolic markers especially lipids and acetate derived from NMR spectroscopy has high sensitivity and specificity to distinguish LN among SLE patients and has the potential to be a useful adjunctive tool in diagnosis and clinical management of LN.

Systemic lupus erythematosus (SLE) is a complex autoimmune disease characterized by diverse clinical manifestations which affect multiple end organs including joints, skin, heart, lungs, blood vessels and kidneys^{1,2}. The most severe manifestation of SLE is renal involvement, the condition known as lupus nephritis (LN)³. About 50–60% of patients with SLE have nephritis with combinations of oedema, proteinuria, hypertension, urinary sediment abnormalities, hypocomplementemia and impaired renal function^{4–6}. It may develop early in the course of SLE⁷, but in about 5–10% of cases, it becomes clinically apparent several years after the onset of SLE^{5,6,8}. Despite advances in effective immunosuppressive therapies, the treatment of LN remains a challenge with considerable morbidity and progressive end stage renal disease requiring renal replacement therapy^{1,3}. Renal biopsy is the gold standard for documenting histological class of nephritis and ascribing activity and damage features to guide the treatment⁹. However, being invasive, there are limitations on performing it serially for monitoring patients with LN. Thus there is an unmet need of biomarkers specific to nephritis among patients with SLE.

Metabolomics, the analysis of concentration profiles of low molecular weight metabolites present in biological fluids, has immense potential in identifying new biomarkers that are highly discriminatory for biological perturbations or diseased states^{10–13}. Nuclear Magnetic Resonance (NMR) spectroscopy and mass spectrometry (MS) are the most widely used analytical techniques for metabolomics studies; the former being preferred as it is rapid, requires minimal sample preparation and provides highly reproducible results. Previous metabolomics studies have shown the potential of metabolic profiling in the diagnosis of many inflammatory and rheumatic diseases such as ulcerative colitis, Crohn's disease, inflammatory bowel disease, osteoarthritis and rheumatoid arthritis^{12,14–22}. Metabolic disturbances associated with SLE have also been reported in urine and serum using NMR spectroscopy and LC/MS and GC/MS-based approaches^{23–25}. However, serum metabolomics of LN has not been studied so far to identify the metabolic changes to differentiate it from SLE. The aim of this study was to explore

¹Centre of Biomedical Research, SGPGIMS Campus, Lucknow-226014, India. ²Department of Immunology, SGPGIMS Campus, Lucknow-226014, India. ³Department of Biotechnology, Babasaheb Bhimrao Ambedkar University, Lucknow-226025, India. ⁴Rheumatology Research Group, Division of Immunity and Infection, Birmingham University, UK. Correspondence and requests for materials should be addressed to A.G. (email: anuguleriaphy@gmail.com) or R.M. (email: rnmisra2000@gmail.com) or D.K. (email: dineshcbmr@gmail.com)

NMR-Based Serum Metabolomics Reveals Reprogramming of Lipid Dysregulation Following Cyclophosphamide-Based Induction Therapy in Lupus Nephritis

Anupam Guleria,^{*,†} Sanat Phatak,[‡] Durgesh Dubey,[†] Sandeep Kumar,[‡] Abhishek Zanwar,[‡] Smriti Chaurasia,[‡] Umesh Kumar,[†] Ranjan Gupta,[‡] Amita Aggarwal,[‡] Dinesh Kumar,^{*,†} and Ramnath Misra^{*,†}

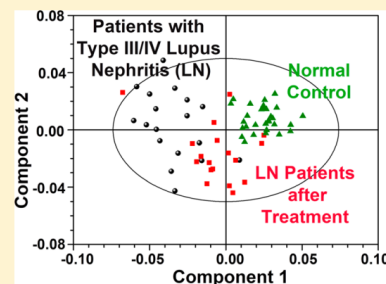
[†]Centre of Biomedical Research, SGPGIMS Campus, Lucknow 226014, India

[‡]Department of Clinical Immunology, SGPGIMS, Lucknow 226014, India

Supporting Information

ABSTRACT: Lupus nephritis (LN) is a major cause of morbidity and mortality in lupus. Renal biopsy is the gold standard for classification of nephritis, but because of its impracticality, new approaches for improving patient prognostication and monitoring treatment efficacy are needed. We aimed to evaluate the potential of metabolic profiling in identifying biomarkers to distinguish disease and monitor treatment efficacy in patients with LN. Serum samples from patients with LN ($n = 18$) were profiled on NMR-based metabolomics platforms at diagnosis and after 6 months of treatment. LN patients had a different metabolomic fingerprint as compared with healthy controls, with increased lipoproteins and lipids and reduced acetate and amino acids. Using multivariate statistical analysis, we found that the metabolic changes observed in naïve LN patients at diagnosis displayed a variation in the opposite direction upon responding to treatment. Increased levels of lipid metabolites including low- and very-low-density lipoproteins (LDL/VLDL) in LN patients significantly decreased after 6 months of treatment, whereas the serum levels of acetate increased. These levels correlated significantly with SLE Disease Activity Index (SLEDAI 2K), renal SLEDAI, and serum C3 and C4 levels. The result presented in this pilot longitudinal study revealed the reprogramming of metabolome in LN patients on immunosuppressive therapy using NMR-based metabolomics, and thus this approach may be used to monitor the response to treatment.

KEYWORDS: NMR-based metabolomics, systemic lupus erythematosus, lupus nephritis, serum metabolites



INTRODUCTION

Systemic lupus erythematosus (SLE) is a multisystem autoimmune disorder. Renal involvement in the form of glomerulonephritis remains a significant cause of significant morbidity and mortality in patients with SLE.¹ A major challenge in the management of LN is the assessment of disease activity and monitoring of treatment response; currently used biomarkers like 24 h proteinuria, anti-dsDNA antibody, and complement levels are far from perfect to differentiate disease activity from damage.^{2,3} Treatment of lupus nephritis is guided by histological classification of disease activity and damage on kidney biopsy.⁴ The severe LN conditions are generally treated with induction therapy comprising corticosteroids and immunosuppressive agents such as cyclophosphamide, mycophenolate mofetil, and azathioprine, with the aim to normalize renal function or, at least, to prevent progressive loss of renal function.⁵ Renal biopsy is impractical in monitoring treatment efficacy because it is unduly invasive. Therefore, there is an unmet need for biomarkers that will accurately reflect the efficacy of the

treatment protocol and thus could avoid the need for serial renal biopsies and provide a basis of an alternative treatment protocol.

Metabolomics is the analysis of global changes in a complete set of metabolites present in biological fluids and has increasingly been exploited for the discovery of disease biomarkers in recent times in various diseases.^{6,7} In our previous nuclear magnetic resonance (NMR)-based serum metabolomics study,⁸ we have shown that the LN patients, compared with lupus patients, exhibit distinctive metabolic profiles characterized by raised serum levels of lipid metabolites including low- and very-low-density lipoproteins (LDL/VLDL), triglycerides, and fatty acids and decreased levels of acetate in LN patients, and these metabolites discriminated LN from nonrenal SLE patients with high sensitivity and specificity.⁸ In this study, we sought to investigate whether the deranged metabolic profile was

Received: March 22, 2018

Published: June 7, 2018

RESEARCH ARTICLE

Serum Metabolic Disturbances Hailing in Initial Hours of Acute Myocardial Infarction Elucidated by NMR based Metabolomics

Atul Rawat^{1,2*}, Rohit K. Srivastava³, Durgesh Dubey^{1,2}, Anupam Guleria¹, Sanjay Singh², Anand Prakash², Dinesh R. Modi², C. L. Khetrpal¹, Sunita Tiwari³ and Dinesh Kumar^{1*}

¹Centre of Biomedical Research, SGPGIMS Campus Lucknow, ²Department of Biotechnology, Babasaheb Bhimrao Ambedkar University, and ³Department of Physiology, King George's Medical University, Lucknow, India

Abstract: Background: Acute myocardial infarction (AMI) is a serious medical emergency and leading cause of cardiac-related deaths worldwide. The devastating outcome is sudden death of the patient within first few hours from the onset of symptoms. The rapid detection of physiological transformations associated with AMI coupled with instant treatment to reset these changes and monitoring response to treatment can greatly decrease the mortality and morbidity of patients.

Objective: To establish the early hour metabolomic signatures in the sera of AMI patients.

Methodology: Metabolic profiles of sera collected from 42 AMI patients (immediately after the myocardial infarction) and 38 age/sex matched normal controls were obtained using high-resolution 1D ¹H CPMG and diffusion edited NMR spectra. The metabolic profiles were compared using multivariate statistical analysis to identify the disease specific metabolic disturbances associated with AMI and, therefore, the perturbed biochemical pathways in this condition.

Results: Our results revealed significant metabolic perturbations in AMI compared to control cohorts. The upregulated metabolites in AMI condition include arginine, glycine, tyrosine, phenylalanine, glucose, creatine, creatinine, lactate, N-acetyl glycoproteins and phospholipids, while the levels of amino acids (such as valine, alanine, glutamate, glutamine, threonine and methionine), citrate, acetone, choline, glycerophosphocholine, trimethylamine-N-oxide and lipids/fatty acids were decreased. Receiver operating curve characteristics (ROC) confirmed the robustness and validity of these metabolic markers.

Conclusion: The resulted metabolic profiling provided new insights into the metabolic processes involved in acute myocardial infarction. Further, we foresee that these changes would aid rapid clinical evaluation of myocardial infarction in emergency and its timely management.

ARTICLE HISTORY

Received: July 11, 2016
Revised: July 31, 2016
Accepted: August 03, 2016

DOI:
10.2174/2213235X04666160809123
143



Keywords: Acute Myocardial Infarction, ¹H NMR, Serum Metabolomics, Metabolic signatures.

INTRODUCTION

Acute myocardial infarction (AMI) -also known as heart attack- is a catastrophic event and the devastating outcome is sudden death of the patient within first few hours from the onset of symptoms. It is also the leading cause of cardiac-related hospitalizations and disabilities worldwide [1]. The majority of AMI-related deaths and disability episodes are the result of inappropriate diagnosis or delayed treatment given to such patients presenting to the emergency departments with sudden acute chest pain [2, 3]. Statistics have shown that death victims usually die in less than 6 hours

after AMI occurs and the current diagnostic approaches are not sensitive enough to make such an early and rapid diagnosis of AMI [4]. Traditionally, the predictive diagnosis of AMI is based on 3 criteria [5]: (a) severe chest pain, (b) characteristic changes it produces on the electrocardiogram (ECG), imaging and morphological studies and (c) rise and fall of serological biomarkers such as troponin I and T, creatine kinase (CK), an isoenzyme of creatine kinase (CK-MB), myoglobinglutamic oxaloacetic transaminase (GOT), and lactate dehydrogenase (LDH) [6, 7]. However, these traditional indicators are not very successful in timely diagnosis of AMI owing to the procedural complexity and low sensitivity [6, 8]. Further, the aforementioned serological markers lack sufficient specificity and therefore, are limited to provide a reliable diagnosis of AMI or predicting its risk. Particularly, the predictive diagnosis of AMI in patients with

*Author correspondence to these authors at the Centre of Biomedical Research, SGPGIMS Campus Lucknow, India; Tel: +91-8953261506; Fax: +91-522-2668215; E-mails: dineshcbmr@gmail.com; atulcbmr@gmail.com

NMR-Based Serum Metabolomics Discriminates Takayasu Arteritis from Healthy Individuals: A Proof-of-Principle Study

Anupam Guleria,^{*,†} Durga Prasanna Misra,^{‡,||} Atul Rawat,^{†,||} Durgesh Dubey,[†] Chunni Lal Khetrapal,[†] Paul Bacon,[§] Ramnath Misra,^{*,‡} and Dinesh Kumar^{*,†}

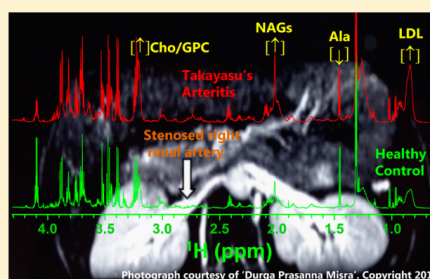
[†]Centre of Biomedical Research and [‡]Department of Immunology, SGPGIMS, Lucknow, 226014 Uttar Pradesh, India

[§]Rheumatology Research Group, Division of Immunity and Infection, University of Birmingham, Birmingham B15 2TT, United Kingdom

Supporting Information

ABSTRACT: Takayasu arteritis (TA) is a debilitating, systemic disease that involves the aorta and large arteries in a chronic inflammatory process that leads to vessel stenosis. Initially, the disease remains clinically silent (or remains undetected) until the patients present with vascular occlusion. Therefore, new methods for appropriate and timely diagnosis of TA cases are needed to start proper therapy on time and also to monitor the patient's response to the given treatment. In this context, NMR-based serum metabolomic profiling has been explored in this proof-of-principle study for the first time to determine characteristic metabolites that could be potentially helpful for diagnosis and prognosis of TA. Serum metabolic profiling of TA patients ($n = 29$) and healthy controls ($n = 30$) was performed using 1D ^1H NMR spectroscopy, and possible biomarker metabolites were identified. Using projection to least-squares discriminant analysis, we could distinguish TA patients from healthy controls. Compared to healthy controls, TA patients had (a) increased serum levels of choline metabolites, LDL cholesterol, N-acetyl glycoproteins (NAGs), and glucose and (b) decreased serum levels of lactate, lipids, HDL cholesterol, and glucogenic amino acids. The results of this study are preliminary and need to be confirmed in a prospective study.

KEYWORDS: NMR-based metabolomics, Takayasu arteritis, large vessel vasculitis, serum metabolites



INTRODUCTION

Takayasu arteritis (TA) is a rare but serious form of large vessel vasculitis and adversely affects the quality of life.^{1–6} It involves the aorta and large arteries in a chronic inflammatory process that leads to wall thickening and vessel stenosis.^{5,7–9} Initially, the disease may be clinically silent or may remain undetected until the patient presents with a complete occlusion of at least one vessel.^{10,11} This contrasts with the overt systemic illness seen in small vessel vasculitis such as antineutrophil cytoplasmic antibody (ANCA)-associated vasculitis (AAV),¹² suggesting that TA not only involves different arteries than those in AAV but also appears to be a very different form of vascular inflammation with a different disease mechanism. However, there is a considerable lack of understanding of TA's disease mechanism owing to the inability to biopsy large arteries. A basic understanding of this process is required, but the immediate clinical challenge is the early appropriate diagnosis of TA, as no specific autoantibodies have been identified for the disease so far and even nonspecific tests for inflammation, such as acute-phase response, often do not help with diagnosis. Therefore, early stage molecular markers of subclinical processes are needed to allow initiation of therapy to control the disease, to avoid further

progression, and to alleviate complications. The pertinent recent advance in this area is PET (positron emission tomography) scanning, using fluorine-18-labeled 2-fluoro-2-deoxy-D-glucose.^{13–16} However, the procedure can be time-consuming and costly. The use of high-dose radiation would further prohibit its routine clinical utility to scan possible cases. Therefore, cost-effective and less invasive methods for diagnosis, such as determination of clinical markers from serum, would be a significant advantage and potentially useful as an adjunct to conventional diagnostics for primary diagnosis, surveillance, and early detection of relapses.

Metabolomics, a systematic approach focusing on the quantitative analysis of endogenous metabolites,^{17–20} may significantly help to address this issue, i.e., understanding multiplex molecular events regulating the onset and progression of the disease. Quantitative analysis of metabolites, the final downstream product of the whole biosystem, helps to identify metabolic perturbations in biofluids, and metabolites that are significantly altered under pathological conditions can be used as

Received: May 18, 2015

Published: June 17, 2015



Contents lists available at ScienceDirect

Diabetes & Metabolic Syndrome: Clinical Research & Reviews

journal homepage: www.elsevier.com/locate/dsx

Original Article

¹H NMR based serum metabolic profiling reveals differentiating biomarkers in patients with diabetes and diabetes-related complication



Atul Rawat ^{a, b, **}, Gunjan Misra ^{b, e, 1}, Madhukar Saxena ^{b, 1}, Sukanya Tripathi ^c,
Durgesh Dubey ^{a, b}, Sulekha Saxena ^d, Avinash Aggarwal ^d, Varsha Gupta ^e, M.Y. Khan ^b,
Anand Prakash ^{b, f, *}

^a Centre of Biomedical Research, Lucknow, India^b Department of Biotechnology, Babasaheb Bhimrao Ambedkar University, Lucknow, India^c Department of Zoology, Lucknow University, Lucknow, India^d Department of Critical Care Medicine, King George Medical University, Lucknow, India^e Department of Biotechnology, CSJMU, Kanpur, India^f Department of Biotechnology, Mahatma Gandhi Central University, Motihari, India

ARTICLE INFO

Article history:

Received 20 August 2018

Accepted 11 September 2018

Keywords:

Nuclear magnetic resonance spectroscopy
Metabolomics
Biomarker
Random forest

ABSTRACT

Background: Diabetes is among the most prevalent diseases worldwide, of all the affected individuals a significant proportion of the population remains undiagnosed due to lack of specific symptoms early in this disorder and inadequate diagnostics. Diabetes and its associated sequela, i.e., comorbidity are associated with microvascular and macrovascular complications. As diabetes is characterized by an altered metabolism of key metabolites and regulatory pathways. Metabolic phenotyping can provide us with a better understanding of the unique set of regulatory perturbations that predispose to diabetes and its associated complication/comorbidities.

Methodology: The present study utilizes the analytical platform NMR spectroscopy coupled with Random Forest statistical analysis to identify the discriminatory metabolites in diabetes (DB = 38) vs. diabetes-related complication (DC = 35) along with the healthy control (HC = 50) subjects. A combined and pairwise analysis was performed to identify the discriminatory metabolites responsible for class separation. The perturbed metabolites were further rigorously validated using *t*-test, AUROC analysis to examine the statistical significance of the identified metabolites.

Results: The DB and DC patients were well discriminated from HC. However, 15 metabolites were found to be significantly perturbed in DC patients compared to DB, the identified panel of metabolites are TCA cycle (succinate, citrate), methylamine metabolism (trimethylamine, methylamine, betaine), -in-termediates; energy metabolites (glucose, lactate, pyruvate); and amino acids (valine, arginine, glutamate, methionine, proline, and threonine).

Conclusion: The ¹H NMR metabolomics may prove a promising technique to differentiate and predict diabetes and its complication on their onset or progression by determining the altered levels of the metabolites in serum.

© 2018 Published by Elsevier Ltd on behalf of Diabetes India.

Abbreviations: NMR, Nuclear Magnetic Resonance; CPMG, Carr–Purcell–Meiboom–Gill; DB, Diabetes; DC, Diabetes-related Complication/Comorbidity; ROC, Receiver operating characteristic; AUROC, area under the ROC curve; RF, Random Forest; ESM, Electronic Supplementary Material.

* Corresponding author. Centre of Biomedical Research, Lucknow, India.

** Corresponding author. Department of Biotechnology, Mahatma Gandhi Central University, Bihar, India.

E-mail address: anandprakash@mngcub.ac.in (A. Prakash).¹ Author's Contributed Equally.<https://doi.org/10.1016/j.dsx.2018.09.009>

1871–4021/© 2018 Published by Elsevier Ltd on behalf of Diabetes India.

1. Introduction

Diabetes is an enigmatic, genetically inherited, primarily a metabolic disorder characterized by multifaceted perturbation in metabolism mainly glucose and lipid [1] in both -type 1 (insulin deficiency due to autoimmune destruction of the pancreatic β-cells) [2] and -type 2 (insulin resistance or reduced insulin secretion due to islet cell dysfunction) [3] diabetes. From being

Metabolomics approach discriminates toxicity index of pyrazinamide and its metabolic products, pyrazinoic acid and 5-hydroxy pyrazinoic acid

A Rawat^{1,2}, S Chaturvedi^{3,4}, AK Singh³, A Guleria², D Dubey^{1,2},
AK Keshari³, V Raj³, A Rai³, A Prakash¹, U Kumar²,
D Kumar² and S Saha³

Abstract

Pyrazinamide (PYZ)—an essential component of primary drug regimen used for the treatment and management of multidrug resistant or latent tuberculosis—is well known for its hepatotoxicity. However, the mechanism of PYZ-induced hepatotoxicity is still unknown to researchers. Studies have shown that the drug is metabolized in the liver to pyrazinoic acid (PA) and 5-hydroxy pyrazinoic acid (5-OHPA) which individually may cause different degrees of hepatotoxicity. To evaluate this hypothesis, PYZ, PA, and 5-OHPA were administered to albino Wistar rats orally (respectively, at 250, 125, and 125 mg kg⁻¹ for 28 days). Compared to normal rats, PYZ and its metabolic products decreased the weights of dosed rats and induced liver injury and a status of oxidative stress as assessed by combined histopathological and biochemical analysis. Compared to normal controls, the biochemical and morphological changes were more aberrant in PA- and 5-OHPA-dosed rats with respect to those dosed with PYZ. Finally, the serum metabolic profiles of rats dosed with PYZ, PA, and 5-OHPA were measured and compared with those of normal control rats. With respect to normal control rats, the rats dosed with PYZ and 5-OHPA showed most aberrant metabolic perturbations in their sera as compared to those dosed with PA. Altogether, the study suggests that PYZ-induced hepatotoxicity might be associated with its metabolized products, where 5-OHPA contributes to a higher degree in its overall toxicity than PA.

Keywords

Pyrazinamide, 5-hydroxy pyrazinoic acid, hepatotoxicity, NMR, metabolomics

Introduction

Drug-induced hepatotoxicity is a crucial healthcare issue and one of the leading causes of morbidity and mortality around the world.¹ Individuals suffering from drug-induced liver injury exhibit a wide range of manifestations clinically, biochemically, and histologically including acute liver failure with severe encephalopathy, acute hepatitis with or without jaundice, and so on.² Therefore, it is necessary to assess drug-induced hepatotoxicity for the design of safer and better therapeutic agents. Within this framework, the recent study was performed to evaluate the mechanism of toxicity of pyrazinamide (PYZ) using albino Wistar rats.

PYZ, an amide derivative of pyrazine-2-carboxylic acid, is an essential component of the first-line drug

¹Department of Biotechnology, Babasaheb Bhimrao Ambedkar University, Vidya Vihar, Lucknow, Uttar Pradesh, India

²Centre of Biomedical Research (CBMR), Sanjay Gandhi Post-Graduate Institute of Medical Sciences Campus, Lucknow, Uttar Pradesh, India

³Department of Pharmaceutical Sciences, Babasaheb Bhimrao Ambedkar University, Vidya Vihar, Lucknow, Uttar Pradesh, India

⁴Division of Pharmacokinetics and Metabolism (PKMD), CSIR-Central Drug Research Institute, Lucknow, Uttar Pradesh, India

Corresponding authors:

D Kumar, Centre of Biomedical Research (CBMR), Sanjay Gandhi Post-Graduate Institute of Medical Sciences Campus, Raebareli Road, Lucknow 226014, Uttar Pradesh, India.

S Saha, Department of Pharmaceutical Sciences, Babasaheb Bhimrao Ambedkar University, VidyaVihar, Raebareli Road, Lucknow 226025, Uttar Pradesh, India.

Emails: dineshcbmr@gmail.com; sudiptapharm@gmail.com

NMR-based urinary profiling of lactulose/mannitol ratio used to assess the altered intestinal permeability in acute on chronic liver failure (ACLF) patients

Dinesh Kumar,^{a*} Gaurav Pandey,^{b*} Deepak Bansal,^{b†} Atul Rawat,^{a,c†} Umesh Kumar,^a Durgesh Dubey,^{a,c} Anupam Guleria^a and Vivek Anand Saraswat^b

ABSTRACT The article presents a simplified NMR-based protocol for urinary profiling of lactulose/mannitol ratio (LMR) and demonstrates here its utility to assess increased intestinal permeability (IP) in patients with acute on chronic liver failure (ACLF). ACLF is a serious clinical complication associated with chronic liver disease (cirrhosis). The major risk factor in its development is increased IP ('leaky gut'), which has been linked to disease progression and to infectious complications. However, IP has seldom been investigated in patients with ACLF, even though patients frequently report gastrointestinal disorders and associated complications. To this end, we first optimized the NMR-based targeted profiling of urinary metabolites (i.e. actulose, mannitol, and creatinine) and subsequently used this resulted protocol (a) first to evaluate the altered IP in ACLF patients and then (b) to explore its utility for monitoring the treatment response in these patients. The normal profiles were obtained for 7 age and sex matched healthy volunteers. The results revealed that the urinary LMR excretion was significantly higher in ACLF patients compared to normal controls (median ~0.7, range (0.12–2.84), vs median ~0.11, range (0.02–0.28), $p < 0.001$) suggesting that the ACLF patients exhibit altered IP. However, the LMR excretion in six clinically improved follow-up ACLF patients was comparable to normal controls indicating restored IP after the treatment. The protocol—as demonstrated here with ACLF—is equally applicable for evaluating IP or mucosal barrier function in other intestinal disorders with reasonable sensitivity and specificity, highlighting its general utility. Copyright © 2016 John Wiley & Sons, Ltd.

Keywords: ¹H NMR; urinary profiling; lactulose–mannitol ratio test; intestinal permeability; acute-on-chronic liver failure (ACLF)

Introduction

The intestinal mucosa uniquely functions as a digestive-cum-absorptive organ for nutrients and allows passage of digested nutrients into the bloodstream.^[1] It also acts as a powerful immunological and mechanical barrier against invasion of harmful substances like bacteria, food antigens and other undigested food macromolecules. These functions of the intestinal mucosa are regarded as intestinal permeability (IP). Several intestinal diseases including celiac disease, gluten-sensitive enteropathy and inflammatory bowel diseases (e.g. Crohn's disease and ulcerative colitis) are associated with malabsorption or abnormally increased permeability ('leaky gut').^[2–5] Leaky gut is common manifestation in acute on chronic liver failure (ACLF) patients as well, and its timely resolution is crucial to save life of these patients in critical care.

Regarding ACLF, it is a newly recognized form of liver failure characterized by an acute deterioration of liver function in the background of a pre-existing well compensated or even decompensated cirrhosis or chronic liver disease.^[6–8] Particularly, it differs from acute liver failure and decompensated cirrhosis in timing, presence of acute precipitant, course of disease and one or more extra-hepatic organ failure(s); thus, it is often associated with a high risk of short-term mortality (~≥15% at 28 days).^[6,8] The

deterioration of intestinal epithelial barrier integrity in cirrhotic patients and the resulting altered IP plays a major pathophysiological role in the development of this medical emergency.^[9,10] However so far, there are no prospective follow-up studies showing altered IP in patients with ACLF and if this altered IP resets back to

* Correspondence to: Dinesh Kumar, Centre of Biomedical Research (CBMR), SGPGIMS Campus, Raibareli Road, Lucknow 226014, Uttar Pradesh, India. E-mail: dineshcbmr@gmail.com
Gaurav Pandey, Department of Gastroenterology, SGPGIMS, Lucknow 226014, Uttar Pradesh, India. E-mail: drgauravpandey@yahoo.com.

† Authors contributed equally

a Centre of Biomedical Research, Sanjay Gandhi Post Graduate Institute of Medical Science, Lucknow, India

b Department of Gastroenterology, Sanjay Gandhi Post Graduate Institute of Medical Science, Lucknow, India

c Department of Biotechnology, Babasaheb Bhimrao Ambedkar University, Lucknow, India

Abbreviations: ACLF, acute-on-chronic liver failure; IP, intestinal permeability; L/M test, lactulose–mannitol test; LMR, lactulose/mannitol ratio



NMR Based Metabolomics: An Emerging Tool for Therapeutic Evaluation of Traditional Herbal Medicines

Dinesh Kumar^{1*}, Atul Rawat^{1,2}, Durgesh Dubey^{1,2}, Umesh Kumar¹, Amit K Keshari³, Sudipta Saha³ and Anupam Guleria^{1*}

¹Centre of Biomedical Research, India

²Department of Biotechnology, Babasaheb Bhimrao Ambedkar University, India

³Pharmaceutical Sciences, Babasaheb Bhimrao Ambedkar University, India

***Corresponding author(s):** Dinesh Kumar, Centre of Biomedical Research (CBMR), SGPGIMS Campus, Lucknow-226014, Uttar Pradesh, India. Tel: +91-8953261506; Email: dineshcbmr@gmail.com

Anupam Guleria, Centre of Biomedical Research (CBMR), SGPGIMS Campus, Lucknow-226014, Uttar Pradesh, India. Tel: +91-9918004592; Email: anuguleriaphy@gmail.com

Published Date: June 10, 2016

ABSTRACT

Traditional Herbal Medicines (**THMs**) and Chinese herbal medicines have been used in the treatment of variety of diseases for thousands of years because of their natural origin and lesser side effects. However, the safety and efficacy data (including dose and quality parameters) on most of these traditional medicines are far from sufficient to meet the criteria needed to support their world-wide therapeutic use. Also, the mechanistic understanding of most of these herbal medicines is still lacking. Metabolomics -a novel approach to reveal altered metabolism (biochemical effects) produced in response to a disease or its therapeutic intervention- has huge potential to assess the pharmacology and toxicology of THMs. Therefore, it is gradually becoming a mutually complementary technique to genomics, transcriptomics and proteomics for therapeutic evaluation of pharmaceutical products (including THMs); the approach is so called metabolomics or pharmaco-metabolomics in the present context. Nuclear Magnetic Resonance

Nuclear Magnetic Resonance Spectroscopy | www.smgebooks.com

1

Copyright © Kumar D and Guleria A. This book chapter is open access distributed under the Creative Commons Attribution 4.0 International License, which allows users to download, copy and build upon published articles even for commercial purposes, as long as the author and publisher are properly credited.

**JOHN WILEY AND SONS LICENSE
TERMS AND CONDITIONS**

Jan 17, 2019

This Agreement between Mr. Durgesh Dubey ("You") and John Wiley and Sons ("John Wiley and Sons") consists of your license details and the terms and conditions provided by John Wiley and Sons and Copyright Clearance Center.

License Number	4511200938237
License date	Jan 17, 2019
Licensed Content Publisher	John Wiley and Sons
Licensed Content Publication	Magnetic Resonance in Chemistry
Licensed Content Title	Metabolite assignment of ultrafiltered synovial fluid extracted from knee joints of reactive arthritis patients using high resolution NMR spectroscopy
Licensed Content Author	Durgesh Dubey, Smriti Chaurasia, Anupam Guleria, et al
Licensed Content Date	Jul 10, 2018
Licensed Content Volume	57
Licensed Content Issue	1
Licensed Content Pages	14
Type of use	Dissertation/Thesis
Requestor type	Author of this Wiley article
Format	Print and electronic
Portion	Full article
Will you be translating?	No
Title of your thesis / dissertation	NMR based Metabolomics of Synovial Fluid from patient with Reactive Arthritis (ReA) for Identifying abnormal metabolic status
Expected completion date	Mar 2019
Expected size (number of pages)	200
Requestor Location	Mr. Durgesh Dubey CBMR Lucknow, Uttar Pradesh 226014 India Attn: Mr. Durgesh Dubey
Publisher Tax ID	EU826007151
Total	0.00 USD
Terms and Conditions	

TERMS AND CONDITIONS

This copyrighted material is owned by or exclusively licensed to John Wiley & Sons, Inc. or one of its group companies (each a "Wiley Company") or handled on behalf of a society with which a Wiley Company has exclusive publishing rights in relation to a particular work (collectively "WILEY"). By clicking "accept" in connection with completing this licensing transaction, you agree that the following terms and conditions apply to this transaction

**RightsLink®**[Home](#)[Create Account](#)[Help](#)**Title:**

NMR-Based Serum Metabolomics Revealed Distinctive Metabolic Patterns in Reactive Arthritis Compared with Rheumatoid Arthritis

Author:

Durgesh Dubey, Sandeep Kumar, Smriti Chaurasia, et al

Publication:

Journal of Proteome Research

Publisher:

American Chemical Society

Date:

Jan 1, 2019

Copyright © 2019, American Chemical Society

LOGIN

If you're a **copyright.com user**, you can login to RightsLink using your copyright.com credentials.

Already a **RightsLink user** or want to [learn more?](#)

PERMISSION/LICENSE IS GRANTED FOR YOUR ORDER AT NO CHARGE

This type of permission/license, instead of the standard Terms & Conditions, is sent to you because no fee is being charged for your order. Please note the following:

- Permission is granted for your request in both print and electronic formats, and translations.
- If figures and/or tables were requested, they may be adapted or used in part.
- Please print this page for your records and send a copy of it to your publisher/graduate school.
- Appropriate credit for the requested material should be given as follows: "Reprinted (adapted) with permission from (COMPLETE REFERENCE CITATION). Copyright (YEAR) American Chemical Society." Insert appropriate information in place of the capitalized words.
- One-time permission is granted only for the use specified in your request. No additional uses are granted (such as derivative works or other editions). For any other uses, please submit a new request.

[BACK](#)[CLOSE WINDOW](#)

Copyright © 2019 [Copyright Clearance Center, Inc.](#) All Rights Reserved. [Privacy statement](#). [Terms and Conditions](#). Comments? We would like to hear from you. E-mail us at customercare@copyright.com